Thermal Transformation of Organoboranes: Applicability of ^{11}B NMR Spectroscopy and Supporting Molecular Modelling

by

Andile Bulelani Mzinyati

Submitted in fulfillment of the academic requirements for the degree of

Doctor of Philosophy

in the

School of Chemistry

Faculty of Science & Agriculture

University of KwaZulu-Natal

Pietermaritzburg

April 2008

Declaration

I, Andile Bulelani Mzinyati, hereby declare that the experimental work and discussion thereof presented in this thesis have been conducted by me in the School of Chemistry of the University of KwaZulu-Natal (Pietermaritzburg) under the supervision of Professor D. Jaganyi.

The work presented here is original and has not otherwise been submitted in any form for any degree or diploma to any University. Where use of others' work has been made, it has been duly accredited in the work.

……..

A. B. Mzinyati

I hereby certify that the above statement is correct.

……..

Professor D. Jaganyi (Supervisor)

Thermal Transformation of Organoboranes: Applicability of ^{11}B NMR Spectroscopy and Supporting Molecular Modelling

Abstract

The high temperature transformations of trialkylboranes were investigated in the range: 50-200 ºC. The extent of dealkylation was found to be linked to temperature with *ca.* 10% octene liberation from tri-*n*-octylborane at 150 ºC in the absence of bulk solvent. Analysis of the oxidised samples from the dealkylation investigation shows that, whereas the control experiment shows no back-isomerisation of tri-*n*-octylborane at 150 ºC, the addition of 10 mol% of DMF, DMSO, HMPA and trimethoxyphosphate results in back-isomerisation of the alkyl chain. In general, the addition of Lewis base catalyst was found to enhance the extent of dealkylation.

In a supporting ^{11}B NMR spectroscopy study to understand the interaction of trialkylboranes and Lewis bases, the interactions of a series of oxygen and phosphorous donor Lewis bases with tri-*n*-butylborane were found to be favourable, as indicated by large negative binding enthalpy (ΔH_{BIND}) and entropy (ΔS_{BIND}) values. Only the trialkylamine Lewis bases were found to have unfavourable interactions with tri-*n*-butylborane, as indicated by positive ΔH_{BIND} and ΔS_{BIND} values. The results also show that the chemical shift of the adduct at infinite dilution ($\Delta\delta^{11}B_{\infty}$) is not as reliable a measure of the interaction between the two species and that correlation of binding constant ($\log K_{BIND}$) at 25.0 ºC to ΔG_{BIND} defines a linear trend that orders the Lewis bases according to spontaneity of the interaction with the strength of the dative bond formed.

The applicability of ^{11}B NMR spectroscopy to the study of the reactions of boranes and alkylboranes was extended to the investigation of the reduction of nitriles by $BH_3.SMe_2$ in dichloromethane (15-30 ºC). Results from the kinetic study indicate that the overall reduction with $BH_3.SMe_2$ is associative ($\Delta S_{activation}$ = -71 ± 10 J K^{-1} mol^{-1}), with the dependence of k_{obs} data on SMe_2 concentration highlighting the importance of the dissociation of the SMe_2 from BH_3 to the reduction process. The lack of reaction with propionitrile and benzonitrile at 25 ºC can be attributed to lack of stability of their adducts with BH_3 as demonstrated by the small equilibrium constants for the formation of their adducts with borane; as determined by ^1H NMR spectroscopy and further illustrated by computational calculation of their energies at the B3LYP/6-31G* level of theory.

Table of Contents

List of Figures

List of Tables

List of Abbreviations

9-BBN	9-borabicyclo[3.3.1]nonane
B3LYP	Becke, three-parameter, Lee-Yang-Parr
BACH-EI™	*N*-ethyl-*N*-isopropylaniline-borane
BF_3:OEt_2	borane trifluoride-etherate
BH_3:THF	borane-tetrahydrofuran complex
BH_3:SMe_2	borane-dimethyl sulfide complex
BMS	borane-dimethyl sulfide complex
Bu	butyl
Cp	cyclopentadiene
diglyme	*bis*-(2-methoxyethyl)-ether
DMF	dimethyl formamide
DMSO	dimethyl sulfoxide
$\Delta H^{\neq}$	enthalpy of formation
$\Delta S^{\neq}$	entropy of formation
Et	ethyl
GC	gas chromatography
HMPA	hexamethyl phosphoric triamide
HMPT	hexamethyl phosphoric amine
HOMO	highest occupied molecular orbital
hrs/hr	hour(s)
IR	infrared (spectroscopy)
$J_{B\text{-}H}$	coupling constant between the boron nucleus and a neighbouring proton
k_{obs}	observed rate constant
K	equilibrium constant
LUMO	lowest unoccupied molecular orbital
LAO	linear-α-olefin
LIO	linear internal olefin
Me	methyl
MO	molecular orbital
MNDO	Modified Neglect of Diatomic Overlap
NEt_3	triethyl amine

NMR	nuclear magnetic resonance
Orange-CRET	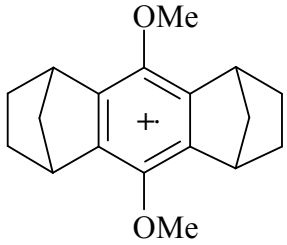
PEG	polyethylene glycol
Ph	phenyl
Pr	propyl
PE	poleethylene
PP	polypropylene
PRDDO	Partial Retention Diatomic Difference Overlap
R_2BH	dialkylborane (generic)
R_3B	trialkylborane (generic)
rt	room temperature
SMe_2	dimethyl sulfide
THF	tetrahydrofuran
TME	tetramethylethene
UV/Vis	ultraviolet-visible (spectroscopy)
VT	variable temperatureLUMO, B3LYP

1. INTRODUCTION

1.1. α-Olefins in the Sasol Context

Higher olefins can be divided into two classes: internal and α-olefins. The linear α-olefins (LAOs), especially up to C_{18}, are the more industrially important class. By far the biggest consumer of LAOs is the co-monomer industry, which accounts for over 50% of LAO consumption.[1] This industry generally uses 1-butene, 1-hexene and 1-octene to engineer a host of characteristics in a variety of polyethylene (PE) and polypropylene (PP) plastics. The more important characteristics imparted by LAOs to plastics are strength, thinness, elasticity and puncture resistance. Thus, plastics found in wire coatings, car interiors, raincoats, garbage bags, shopping bags, cling-wrap film and various plastic food containers have properties imparted by LAOs. **Figure 1.1** gives a view of the complexity of the α-olefin business.

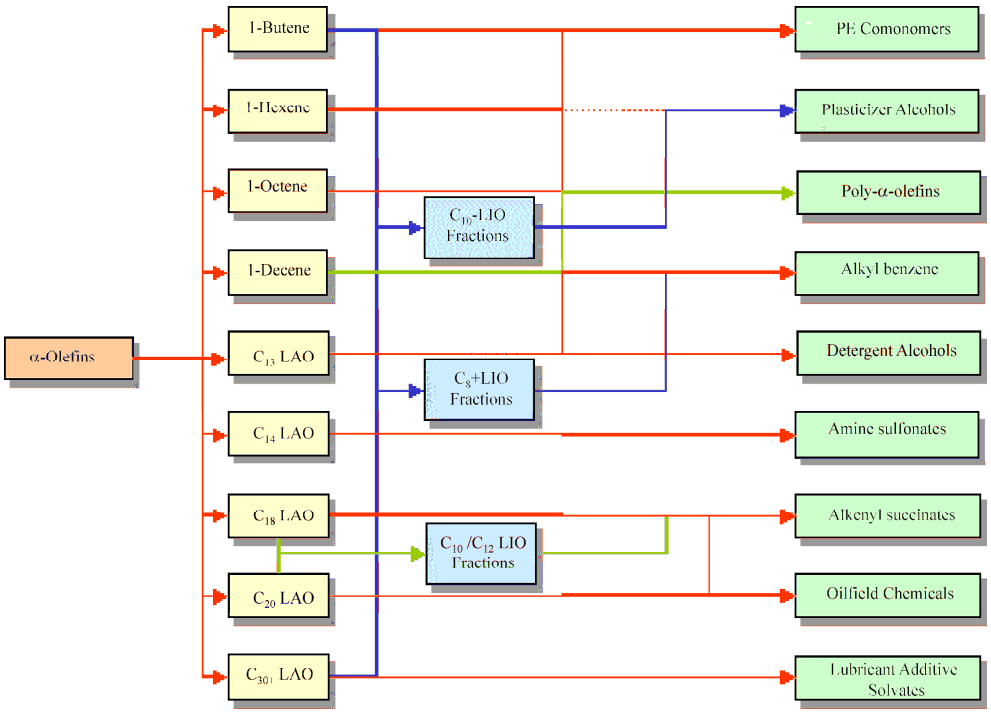

Figure 1.1 - Breakdown of typical end-uses of linear-α-olefins [2]

By far the largest producer geographically of LAOs in 2003[2] was North America with 68% of the market share (up 5% from the 1994 figure[3]); followed by Western Europe, South Africa, Japan and Russia in terms of production capacity. **Figure 1.2** gives a company breakdown of world capacity for LAO in 2003.

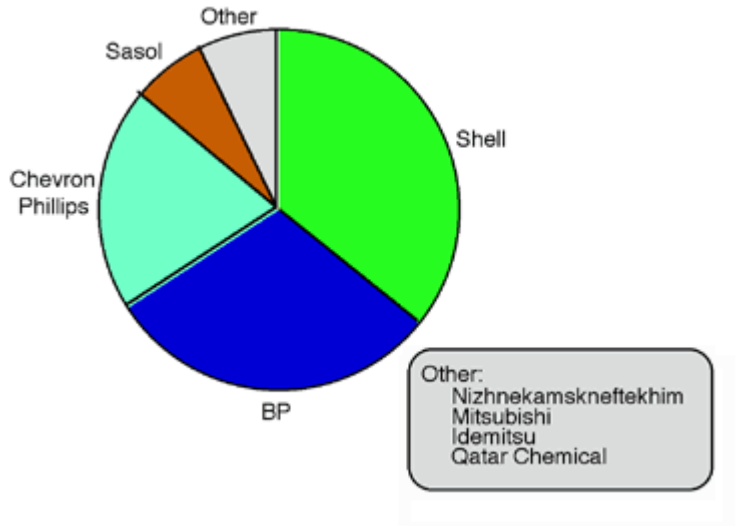

Figure 1.2 - World capacity for linear-α-olefin production in 2003 by producer[1]

Producers of LAOs can be divided by whether they produce the full spectrum of LAOs (C_4-C_{20+}) mainly through Ziegler-based/derived chemistry or whether they produce specific α-olefins. The former group (full range producers) include major multinational companies such as BP, Shell and Chevron-Phillips. Sasol, South Africa's only olefin producer, is a typical on-purpose producer of LAOs. This is done by recovering olefins from its Advanced Synthol Process (proprietary and unique technology). **Figure 1.3** illustrates the distribution of α-olefins produced by Sasol's Advanced Synthol Process. Since Ziegler-based ethylene oligomerisation does not allow for the production of odd-numbered olefins. Sasol is unique in that it is the world's only producer of 1-pentene. Further to extraction of olefins from Fischer-Tropsch streams, the area of chromium-based chemistry is actively researched at Sasol such that the company can selectively produce LAOs by the chromium catalysed trimerisation and tetramerisation of ethylene to afford 1-hexene[b-d] and 1-octene,[d-e] respectively.

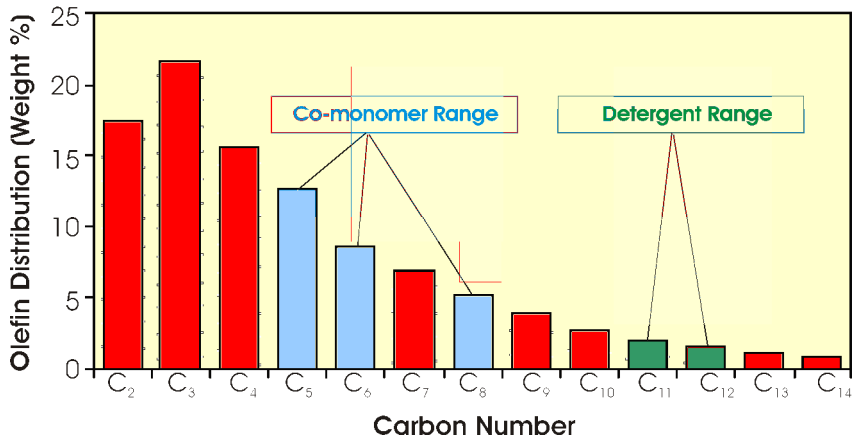

Figure 1.3 - Sasol α-olefin distribution from the Advanced Synthol® Process[2a]

The demand for co-monomer grade LAOs is forecast to grow by 5-8% per annum up to 2010. Demand for LAOs by year-end 2003 was estimated at 3.5-million metric tonnes, with production reaching only 2.5-million metric tonnes (a market worth $2.5-billion at 2003 prices).[1] The production of 1-octene, in particular, has not kept up with demand. This has prompted a number of companies to step up production.

The construction by Sasol of a R3.1-billion 1-octene plant to be operational in the second half of 2007 (see **Table 1.1**) is set to give the company a stake of over a third in the global 1-octene markets.[5,6,7]

Table 1.1 - Recent ventures to increase α-olefin production

New Capacity (tonnes per year)	Target α-olefin	Location	Company	Commencement Date
340 000[4]	Various	Texas	Chevron-Phillips	2002
250 000[4]	Various	Alberta	BP	2002
318 000[4]	Various	Louisiana	Shell	2002
100 000[4]	1-Hexene	Texas	Phillips	2002
47 000[4]	1-Hexene	Qatar	Q-Chem*	2003
150 000[4]	Various	Al-Jubail	SABIC	2004
2100 000[4]	1-Hexene	Secunda	Sasol	2000
196 000[5,6,7]	1-Octene	Secunda	Sasol	2007

* Joint venture between Chevron-Phillips and Qatar General Petroleum Company

The increased demands for 1-octene and higher carbon number α-olefins (C_{12}-C_{14} olefins for detergent alcohols and C_{16}-C_{18} olefins for oilfield chemicals) have necessitated the oligomerisation of C_4-C_6 olefins with higher fractions to produce longer olefin chains.

Apart from Ziegler-based oligomerisation, cracking and subsequent dehydrogenation of *n*-paraffins and recovery of α-olefins from naphtha streams, metathesis presents the only other viable method for further production of longer chain olefins. Thus, the metathesis of hard-to-sell 1-pentene (of which Sasol is the only producer) [8] or 1-butene (of which Sasol has 40% of the global market share)[8] would be valuable beneficiation of Sasol's by-product streams (see **Scheme 1.1**).

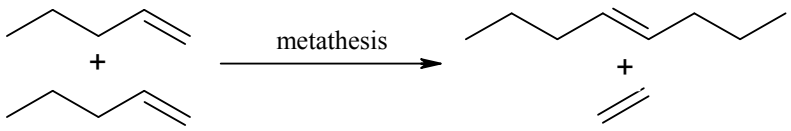

Scheme 1.1

The major problem with the metathesis route is that it ultimately produces an internal olefin, which then requires isomerisation to the terminal position. Thus, such an isomerisation would be contra-thermodynamic.

Means of olefin isomerisation, as investigated through the Sasol National Double Isomerisation Project (SNDBIP), include hydroboration-isomerisation, hydrozirconation-isomerisation, hydrosilylation-isomerisation, as well as transition metal-mediated olefin isomerisation. The universities taking part in the SNDBIP explored three of these:[9]

a) Organometallic chemistry

Zirconium chemistry – University of the Witwatersrand,

Palladium chemistry – Rand Afrikaans University and University of Cape Town

Rhodium chemistry – Rand Afrikaans University

Ruthenium chemistry – Potchefstroom University for Christian Higher Education

b) Boron chemistry

University of KwaZulu-Natal (Pietermaritzburg)

Potchefstroom University for Christian Higher Education

c) Silicon chemistry (PU for CHE).

The findings of the SNDBIP on these projects are summarised in SNDBIP 2: Bulletin 7. But of interest to the current study is boron-mediated isomerisation of internal olefins to linear-α-olefins. The boron-mediated contra-thermodynamic isomerisation of olefins is desirable in that it allows for the concurrent running of two olefin streams as shown in **Scheme 1.2**.

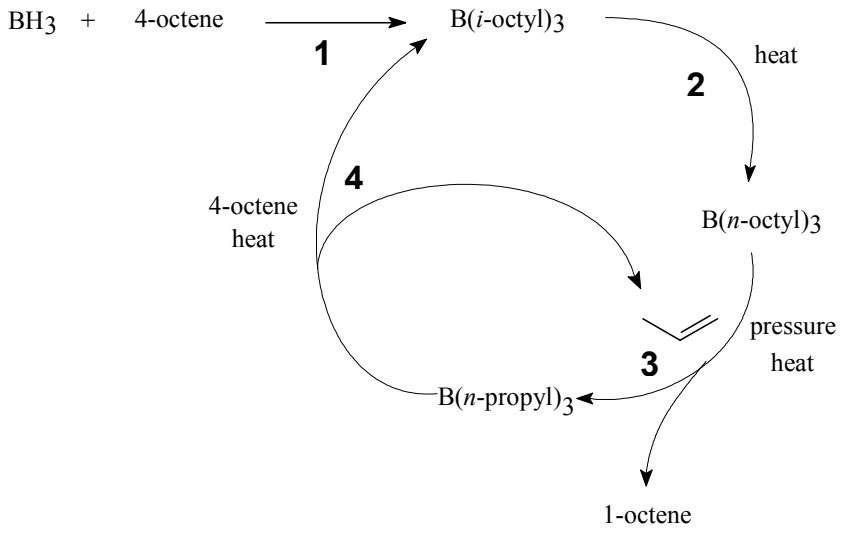

Scheme 1.2

1.2. General Aspects of Hydroboration

The term hydroboration refers to the addition of a B-H bond across carbon-carbon,[10,11] carbon-oxygen[12] and carbon-nitrogen[13] unsaturated bonds bonds, as shown in **Scheme 1.3**. In the mid-1950s Brown and Subba Rao[10,11] introduced a reaction converting alkenes to organoboranes.

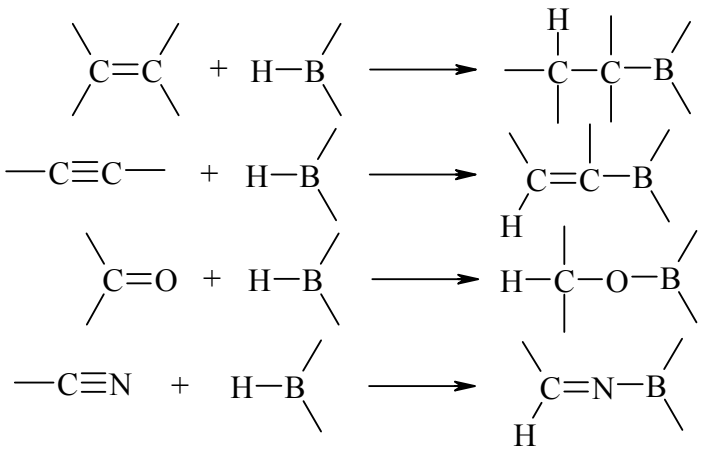

Scheme 1.3

The great significance of their work was that it offered a convenient route towards organoboranes under mild experimental conditions. Prior to this synthetic route, organoboranes had been synthesised through reaction of an organometallic compound with a boron ester or halide.[14] By 1948 Hurd[15] had already reported the sluggish reaction of diborane with alkenes, but it was Brown's observation that the use of ethereal solvents speeded up the reaction and substantially lowered the reaction temperature that was critical.[16]

The great majority of alkenes undergo complete hydroboration to the trialkylborane stage (i.e., they initially react to form monoalkylboranes, then dialkylboranes and finally trialkylboranes). Alkenes with a larger degree of steric hindrance about the alkene bond react to form only monoalkylboranes and dialkylboranes.[17,18,19]

The characteristic features of the hydroboration reaction are as follows:[16,20]

- The hydroboration reaction proceeds rapidly and quantitatively in an anti-Markovnikov manner (i.e., to place the boron atom preferentially on the least hindered side of an asymmetrically substituted double bond).
- This regioselectivity is a result of steric factors rather than electronic ones. A study of directive effects in the hydroboration reaction revealed that terminal (straight-chain) alkenes react to add 94% of the boron reagents to the terminal position in a terminal alkene.[21]
- The same study showed that alkyl substituents on the 2-position of a terminal alkene direct the attachment of the boron atom to the terminal position because of steric crowding on the 2-position. Aryl substituents on the 2-position (e.g., styrenes) show increased influence of the electronic effect, causing increased boron addition to the non-terminal position.[22]
- Preferential addition of boron atoms to the least sterically hindered carbon atom extends to internal alkenes.
- The hydroboration reaction is a controlled *cis* addition of the boron-hydride bond to an alkene. This addition takes place on the least sterically crowded face of the double bond.[23]

1.3. Hydroborating Agents

1.3.1. Diborane and its Lewis Base Derivatives

Diborane (B_2H_6) is the simplest reagent for hydroboration. As already stated, the rate of hydroboration is significantly increased by the use of ethereal solvents; the most commonly used of these being tetrahydrofuran (THF) and *bis*-(2-methoxyethyl)-ether (diglyme). The role of these donor solvents is to dissociate diborane into borane-solvent complex molecules. The maximum solubility of diborane in THF is approximately 2.2 M, while its solubility in diglyme is about 0.2 M.[24] Diborane is not very soluble in diethyl ether or hydrocarbon solvents, which has limited the use of these solvents in hydroboration reactions except for cases where retardation of the reaction is desirable. While ethereal solvents have, historically, been the preferred solvents for the hydroboration reaction, very recent developments have shown chlorohydrocarbon solvents such as dichloromethane, 1,2-dichloroethane and 1,1,2,2-tetrachloroethane to be just as effective as hydroboration solvents.[16] These solvents were shown to dissolve diborane to form 0.5 M solutions, with diborane existing as a 90% diborane and 10% solvent:BH_3 adduct. Rates of hydroboration in these solvents were found to be similar to those of hydroboration in diethyl ether, with regioselectivities comparable to those of BH_3.THF and $BH_3.SMe_2$ (BMS).[25] It was

observed that dichloromethane retards the hydroboration of alkenes with amine-borane adducts, possibly through the formation of dipolar interactions between the dichloromethane and the amine-borane adduct.[25] Another promising method for the enhancement of the rate of hydroboration reaction in traditionally "slow" solvents has been the use of ultrasound irradiation.[26]

The air and moisture sensitivity of diborane requires that it be generated *in situ* for reactions, making it an inconvenient hydroborating agent to handle. While commercially available diborane-solvent complexes (e.g., BH_3.THF) solved the handling problem, the expensive nature of ethereal solvents detracted from their usefulness. In addition to this, reductive-cleavage of THF and diglyme by the hydride has been shown to take place at room temperature.[27] This reductive cleavage process ultimately results in the loss of hydride activity (i.e., hydroborating ability). The solution to this problem came with the use of a borane-dimethyl sulfide complex (BMS) in hydroboration reactions. First reported by Burg and Wagner[28] in 1954 and later studied by Stone and co-workers,[29] this complex has numerous advantages over the available BH_3.THF reagent.[30,31] These include the facts that:

- BMS is stable for an indefinite duration when refrigerated.
- It is available commercially in a molar concentration ten times that of the BH_3.THF reagent.
- BMS is soluble in a number of aprotic solvents (most of which could not previously be used in hydroboration reactions), with which it does not react.

Although very widely used, the malodorous, water-immiscible, volatile and highly flammable nature of dimethyl sulfide makes it an unfriendly reagent by creating environmental and safety problems. Brown and co-workers[32] proposed the use of borane-1,4-dioxothiane as an alternative hydroborating agents because of lower odour, volatility and increased stability. However, the much higher cost of this reagent has limited its use. Zaidlewicz *et al.*[33] have made use of the fact that diisoamyl sulfide has a more pleasant aroma than dimethyl sulfide to create a friendlier hydroborating agent. They also studied a range of isoamyl sulfide derivatives, whose borane adducts they found to be more reactive towards 1-octene. The problem with these isoamyl sulfide-borane adducts was that the majority were found to be immiscible with water, thereby causing problems in product isolation. The use of hydroxydialkyl sulfides as borane carriers has been a welcome development. These hydroxydialkyl sulfides react with diborane to form borates. The

borates then form 1:1 adducts with borane, which can then react with three molecules of olefin. The reaction scheme is shown in equation *1.1* and *1.2*.

$$6\ CH_3SCH_2CH_2OH + B_2H_6 \rightarrow 2\ (CH_3SCH_2CH_2O)_3B + 3\ H_2 \qquad 1.1$$

$$3\ (1\text{-Octene}) + (CH_3SCH_2CH_2O)_3B{:}BH_3 \rightarrow (n\text{-Octyl})_3B + (CH_3SCH_2CH_2O)_3B \qquad 1.2$$

These borane-borate adducts were found to be similar to BMS in terms of reactivity and stability during storage. Most importantly, these adducts were found to have less obnoxious odours (with some even being found to have agreeable smells) and much more water-soluble. This is especially important for larger-scale operations where odour would be a critical concern. The improved water-solubility would aid in the separation of the trialkylborane products from the borane carrier.[34] A more recent addition to the compendium of sulfide borane carriers is fluorous dimethyl sulfide ($H_3B.S(CH3)CH_2C_8H_{17}$) which associates with borane to form a 1:1 adduct fluorous BMS.[35] Fluorous dimethyl sulfide is formed by the reaction of diborane with 2-(perfluorooctyl)ethyl methyl sulfide. Like the hydroxydialkyl sulfide borane adduct, fluorous BMS is odourless. Furthermore, the fluorous dimethyl sulfide can be recovered and recycled from solution.

Borane also forms complexes readily with amines (e.g., $BH_3.NEt_3$). Due to the higher basicity of amines, they form more stable borane complexes than dimethyl sulfide, thereby lowering the reactivity of these adducts towards alkenes. This lower reactivity requires the use of higher hydroboration temperatures, which can cause unwanted isomerisation of the alkene.[36] Even at high temperatures, long reaction times are required to achieve complete hydroboration of even the simplest alkenes. Until recently, amine-boranes have not found wide applicability in the hydroboration reaction, though their distinctive reducing ability has found use in the reduction of other functional groups.[36] In the case of phosphine-boranes, which form even more stable complexes to borane than amines, no hydroboration had been observed.[37] Yet, the inclusion of methyl iodide in the reactions of trimethylamine-borane and triphenylphosphine-borane with 1-octene resulted in 93% and 88% yields, respectively, after six hours of reaction time in refluxing THF.[37]

Further attempts at the activation of amine-boranes towards hydroboration have taken into cognisance the fact that steric bulk and reduced basicity in the amine will result in

improved reactivity in amine-borane adducts. Reagents such as *N*-phenylmorpholine-borane and *N,N*-diethylaniline-borane[38] have been surpassed by very new reagents such as *N*-ethyl-*N*-isopropylaniline-borane (BACH-EI™).[39] These compounds are shown in **Scheme 1.4**.

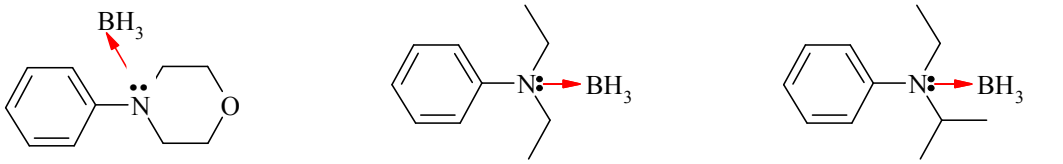

N-phenylmorpholine-BH_3 *N,N*-diethylaniline-BH_3 *N*-ethyl-N-isopropylaniline-BH_3

Scheme 1.4

BACH-EI™ has been shown to have similar hydroboration characteristics to BH_3.THF and BMS, and has even been used in the synthesis of representative classical dialkylborane hydroborating agents.[40]

Even more recent investigations into enhancing the reactivity of amine-boranes towards hydroboration have led to the use of aliphatic (medium chain length) amines as borane carriers. In these studies, the steric bulk around the amine was increased in order to raise the reactivity of the borane adducts of the compounds towards hydroboration. Hence, a series of highly sterical *tert*-butyldialkylamine-borane adducts have been shown to have comparable hydroboration characteristics to BH_3.THF and BMS.[41,42] Work done on new and more reactive amines for hydroboration has been reviewed by Kanth.[43]

Another class of borane adducts that has recently received interest is that of the silylamine-boranes (equation *1.3*). Silylamines can be viewed as amines with much reduced basicity because of the electron-withdrawing nature of the silicon atom. Researchers in this area have cited the instability of BH_3.THF,[44] the contamination of reaction solvents and the interference caused by BMS in the isolation of products,[45] as well as isolation problems encountered with some aryl- and bulky tertiary amine-borane adducts[46] as enhancing the desirability of silylamine-boranes as hydroborating agents.[47] Primary and secondary silylated amines form stable yet reactive borane adducts.

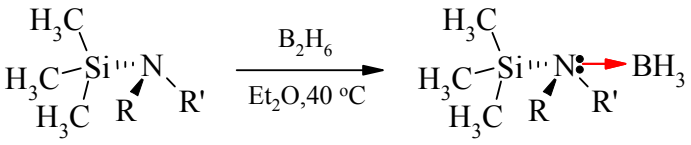

1.3

These silylated amines are easily hydrolysed to their amine precursors and volatile silicon by-products. Silylamine-boranes have also been employed in the synthesis of representative classical dialkylborane hydroborating agents.[48]

While some might dismiss the convenience of these latter-day hydroborating agents owing to their lack of commercial availability, it cannot be disputed that some of these hydroborating agents have physical properties that make them desirable for large-scale applications. Many of the more sterically hindered amine-borane adducts, as well as some silylamine-borane adducts and triphenylphosphine-borane, are solids with high melting points. An example of this is triphenylphosphine-borane, which has a melting point of 189 ^{o}C.[37] Furthermore, triphenylphosphine-borane was found to be resistant to air oxidation even after six months of being left open to the atmosphere. Even more impressive was the fact that the compound was not affected by alkaline hydrogen peroxide, yet the use of methyl iodide achieves near-quantitative hydroboration from this seemingly inert compound.[37] In addition to their physical properties, the fact that most of the compounds discussed are possible alternatives to BH_3:THF and BMS make them very desirable for both lab-scale and plant-scale operations.

1.3.2. Metal Borohydrides as Sources of Diborane

A very different approach to Lewis base borane carriers is the *in situ* generation of diborane. Classically, $NaBH_4$ was used to generate diborane. Other hydrides such as KBH_4, $LiBH_4$ and $LiAlH_4$ are also discussed in the very early literature.[49] The improvement in the reactivity and selectivity of $NaBH_4$ towards the hydroboration reaction has been the subject of a recent review by Periasamy and Thirumalaikunar.[50]

The first reaction employing $NaBH_4$ to generate diborane was reported in 1950.[51]

$$12\,RCH=CH_2 + 3\,NaBH_4 + 4\,BF_3 \xrightarrow{\text{diglyme}} 4\,(RCH_2CH_2)_3B + 3\,NaBF_4 \qquad 1.4$$

The discovery was that a 1:1 mixture of $NaBH_4$ with acetic acid led not only to improved hydroboration yields, but also to the reduction of other functional groups.[52,53]

Metal salts have also been enlisted to improve the reactivity of metal hydrides towards alkenes. The reaction of $CoCl_2$ with two equivalents of $NaBH_4$ in THF has been used to generate borane.[54]

$$CoCl_2 + 2\,NaBH_4 \rightarrow "CoH_2" + 2\,BH_3 + 2\,NaCl \qquad 1.5$$

This reaction has been found to both hydroborate and/or hydrocobaltate (and subsequently hydrogenate) alkenes. Stirring of the $CoCl_2$-$NaBH_4$ mixture in THF for two hours at room temperature prior to addition of the alkene has been found to result in hydroboration.

$$CoCl_2 + 2\,NaBH_4 \xrightarrow{2hrs,\,RT} \xrightarrow{1-Decene,3hrs,\,RT} \xrightarrow{NaOH,\,H_2O_2} \underset{\mathbf{30\%}}{1-decanol} \qquad 1.6$$

Titanium complexes have also been shown to aid hydroboration by borohydrides. Catalytic amounts of Cp_2TiCl_2 and 18-crown-6 have been found to be particularly useful in this regard.[55]

$$Cp_2TiCl_2 + NaBH_4 \xrightarrow[65^oC,1hr]{18-Crown-6,THF} \xrightarrow[65^oC,24hrs]{1-Octene} \xrightarrow[H_2O_2]{NaOH} \underset{\mathbf{72\%}}{1-Octanol} + \underset{\mathbf{5\%}}{2-Octanol} \qquad 1.7$$

The Cp_2TiCl_2/18-crown-6 system was also shown to be compatible with $LiBH_4$, $NaBH_4$ and KBH_4. Interestingly, substitution of titanium with zirconium, which is in the same group in the periodic table, resulted in no hydroboration. The type of ligand in the titanium catalyst was also shown to be influential (see **Table 1.2**).[55]

Table 1.2 - Catalyst Effects on the Hydroboration-Oxidation of Styrene with the Cp_2TiCl_2/ 18-Crown-6/$NaBH_4$ System[55]

Catalyst	Temp (^oC)	Time (hrs)	PhEtOH yield (%)	PhEt-1-OH/PhEt-2-OH
Cp_2TiCl_2	65	5	70	69/31
Cp_2ZrCl_2	65	24	0	-
$TiCl_3$	30	3	90	80/20
$TiCl_4$	65	5	33	72/28

*Styrene:$NaBH_4$:Catalyst:18-Crown-6 Ratio = 5:5:1:1

From **Table 1.2** it is evident that $TiCl_3$ is the best catalyst for the 18-crown-6/$NaBH_4$ system. Not only did it employ the lowest temperature, but also the shortest reaction time. The $TiCl_3$/18-crown-6/$NaBH_4$ system has been shown to hydroborate 1-octene (under similar conditions as in **Table 1.2**) to afford a 92% yield of octanol after oxidation, with a 95:5 ratio between 1- and 2-octanol.[56]

A very simple procedure for the generation of borane is the direct reaction of two equivalents of $NaBH_4$ with I_2 in THF.[57] This method has been shown to afford 1-decanol in a 92% yield after hydroboration oxidation.[58] The iodide anion, present in catalytic amounts as NaI, has also been reported to be effective in improving hydroboration of alkenes by $NaBH_4$ in diglyme.[59] Diborane, in this instance, is generated *via* the anodic oxidation of $NaBH_4$. The cyclic voltammetry of $NaBH_4$ in diglyme revealed an oxidation peak of –0.045 V (with the saturated calomel electrode as the reference electrode). This was an indicator that $NaBH_4$ is easily oxidisable to afford diborane and hydrogen in diglyme. The role of the NaI is believed to be that of a supporting electrolyte.[59]

$$2\,BH_4^- \xrightarrow{\text{electrolysis}} B_2H_6 + H_2 + 2e^-$$

$$1-\text{Octene} \xrightarrow[NaBH_4,NaI]{} \xrightarrow[NaOH,H_2O_2]{} \underset{\textbf{81 \%}}{1-\text{Octanol}} \qquad \textit{1.8}$$

An interesting development that occurred around the same time was the use of polyethylene glycol (PEG) and $NaBH_4$ for the synthesis of extra long-chain 1-alkanols from extra long-chain symmetrical *trans* alkenes.[60] Since the general formula for PEG is $HO(CH_2CH_2O)_nH$, it acts as an open-chain crown ether that reacts with $NaBH_4$ to form a dialkoxyborohydride.

$$NaBH_4 + 2\,HO(CH_2CH_2O)_nH \xrightarrow{65\text{–}80^oC} NaBH_2[(OCH_2CH_2)_nOH]_2 + H_2 \qquad 1.9$$

While a $PdCl_2/NaBH_4$/PEG system had previously been reported for the synthesis of *cis* alkenes *via* the hydroboration of carbon-carbon triple bonds,[60] the $BF_3.OEt_2/NaBH_4$/PEG system has been successfully shown to hydroborate internal alkenes.[61] Isomerisation of the product and subsequent oxidation afforded the alcohol in greater than 90% yield (equation *1.10*).

$$C_{30},\ C_{34},\ C_{38}\ \text{symmetrical}\ \textit{trans}\ \text{alkene} \xrightarrow[BF_3.OEt_2,\text{diglyme}]{NaBH_4/\text{PEG-400}} \xrightarrow[160\ ^oC,\ 4\ \text{hrs}]{\text{isomerisation}} \xrightarrow[H_2O_2]{NaOH} \underset{>\mathbf{90\ \%}}{\text{R-OH}} \qquad 1.10$$

$Me_3SiCl/PhCH_2N^+(Et)_3BH_4^-$ has also been reported to cause the hydroboration of alkenes to produce the corresponding alcohols after oxidation.[62] A similar system involving $TiCl_4/PhCH_2N^+(Et)_3BH_4^-$ system has also been shown to hydroborate alkenes.[63] More recently, $Bu_4N^+BH_4^-$ has been reported to hydroborate terminal alkenes (equation *1.11*).[64] The $Bu_4N^+BH_4^-$ system essentially liberates diborane in solvents such as CH_2Cl_2, $CHCl_3$ and CCl_4. The same study revealed that 1-alkynes can also be dihydroborated by this route to afford the terminal alcohols. Disubstituted alkynes generally undergo monohydroboration to produce vinyl boranes that are oxidised to ketones after oxidation.

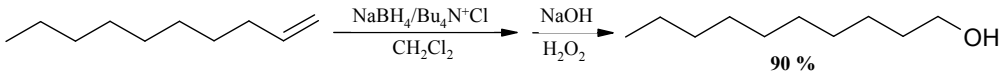

1.11

A very important development in the hydroboration chemistry of $NaBH_4$ has been the adaptation of the reaction for liquid-liquid phase transfer catalysis conditions.[65] The best results for this investigation were obtained by stirring an *n*-butylbromide-alkene solution with a mixture of saturated aqueous solution of $NaBH_4$ and quaternary onium salt (Q^+X^-) at room temperature under nitrogen. The best onium salts were found to be the more lipophilic ones such as methyltricaprylammonium chloride and hexadecylphosphonium bromide. The BH_4^- anion is extracted from the aqueous phase to the organic phase as $Q^+BH_4^-$, which reacts with the alkyl bromide to generate BH_3 for the hydroboration of the alkene (equation *1.12*).

$$NaBH_4(aq) \xrightarrow{Q^+X^-cat} Q^+BH_4^-(org) + NaX(aq)$$
$$Q^+BH_4^-(org) + R'Br(org) \rightarrow Q^+Br^-(org) + R'H(org) + BH_3(org) \qquad 1.12$$
$$3\ RCH=CH_2(org) + BH_3(org) \rightarrow [(RCH_2CH_2)_{n=1-2}B(OH)_{3-n}](org)$$

Under optimal conditions, the reaction was found to be complete in 12-16 hours with yields all above 90%. The process is effective for both terminal and internal alkenes.

Finally, an interesting recent development is the use of mechanochemistry for the synthesis of diborane and borane-Lewis base adducts from the metal borohydrides. Volkov and Myakishev's review on the subject notes that the major advantages of such a strategy include the absence of solvent in the reactions and the synthesis of products in highly pure states.[66] The field of mechanochemistry is the meeting of chemistry and mechanical engineering where mechanical energy is applied to molecules such that they break apart in a precise manner to afford desired products.

1.3.3. Mono-, Dialkylborane and Heterosubstituted Hydroborating Agents

Figure 1.4 provides a list of the more commonly used hydroborating agents. Their chemistry has been detailed extensively in many texts.[8,10,67-71] Hydroborating agents derived from α-pinene have been used extensively in the asymmetric synthesis of various compounds. The synthesis of these compounds, as well as their chemistry, has been the subject of a comprehensive review by Brown and Ramachandran.[69] Other akylboranes used in asymmetric synthesis have been discussed by Ramachandran and Srebnik.[70]

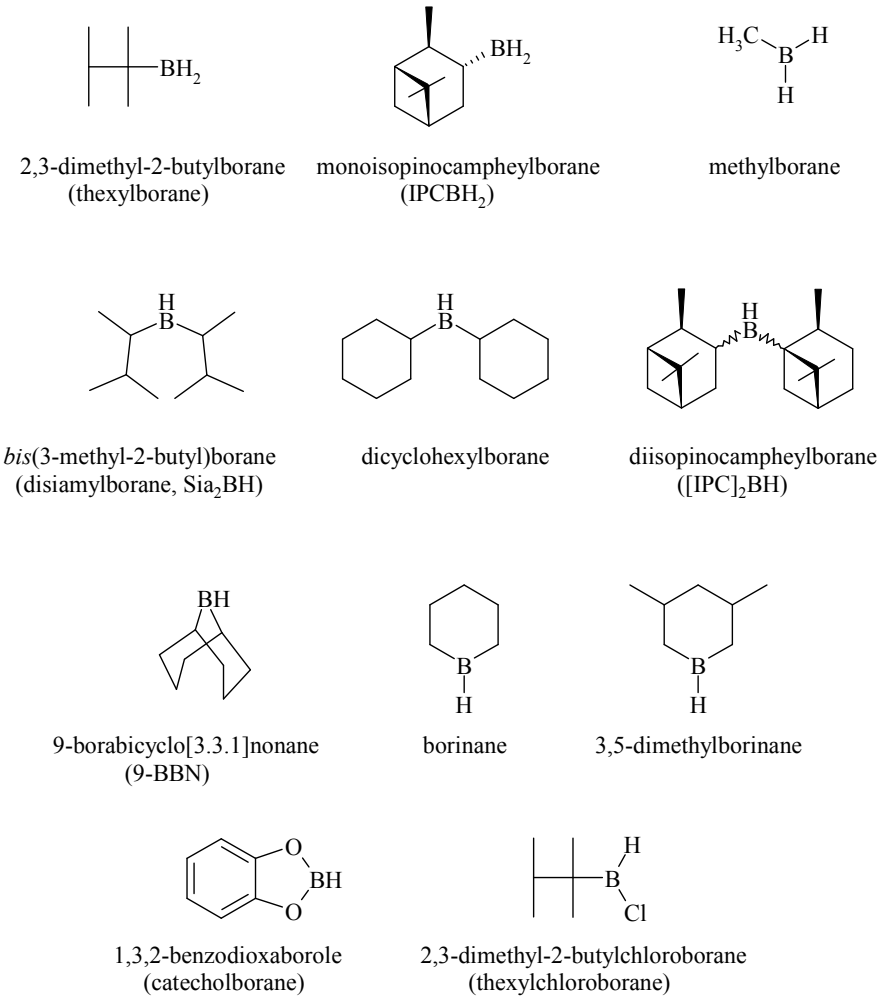

Figure 1.4 - Commonly used alkyl- and heterosubstituted boranes

1.4. Kinetic Aspects of the Hydroboration Reaction

The hydroboration reaction using BH_3 can essentially be viewed as three addition reactions (**Scheme 1.5**), if it is assumed that there is no reverse reaction.

$$\text{alkene} + BH_3 \xrightarrow{k_1} RBH_2$$

$$RBH_2 + BH_3 \xrightarrow{k_2} R_2BH$$

$$R_2BH + BH_3 \xrightarrow{k_3} R_3B$$

Scheme 1.5

Monomer-dimer equilibria (**Scheme 1.6**) and redistribution equilibria (**Scheme 1.7**) hamper kinetic studies on the hydroboration reaction. As a result, there have not been many kinetic studies on the reaction of borane with alkenes reported in the literature.[24]

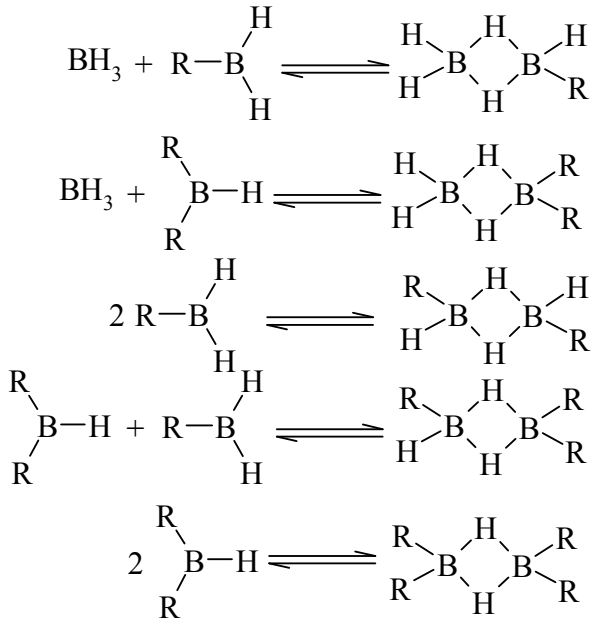

Scheme 1.6

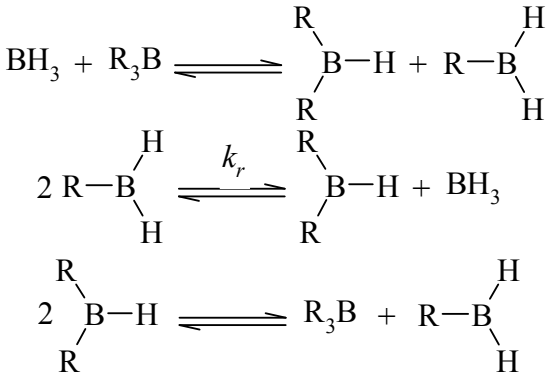

Scheme 1.7

Attempts to measure k_1 and k_2 by fast-flow quenching techniques failed due to the inability to quench the reaction of monoalkylboranes with amine bases.[72] The purpose of the study had been to explain the observation made by Brown and co-workers in the hydroboration of 1-pentene. They found that the dialkylborane was initially formed in greater quantity than the monoalkylborane.[73] Pasto rationalised these findings by suggesting that k_2 was larger than k_1 and that the rate constant for the redistribution of the monoalkylborane to

form dialkylborane, k_r, was larger than k_1.[73] A study into the hydroboration of alkenes with methylborane found that the rate constant for the formation of dialkylborane was larger than that for the formation of the monoalkylborane.[74] The higher reactivity of the monoalkylborane (when compared with borane) was attributed to the weaker complexing interaction in the RBH_2-THF complex than the BH_3-THF complex.[75]

Investigations by Whatley and Pease on the high temperature gas phase hydroboration of ethene with diborane found that the rate was given by equation *1.13*, where *p* defines the total pressure (mm) of the B_2H_6/C_2H_4 mixture, while *k* is the experimental rate constant :[76]

$$-\frac{dp}{dt} = \frac{k[B_2H_6]^{3/2}}{\left(1-2\frac{[B_2H_6]}{[C_2H_4]}\right)} \qquad 1.13$$

This equation indicated that the reaction became explosive when the B_2H_6/C_2H_4 ratio exceeded 0.5. Fehlner's study on the same system (450 ^oC/4.7 Torr) found the absolute bimolecular rate constant to be defined by equation *1.14*, where k_1 is the absolute bimolecular rate constant and T defines the temperature in Kelvin: [77]

$$\log k_1 = 10.2 - (2000/4.757\ T)\ L.mol^{-1}.s^{-1} \qquad 1.14$$

The study also found that the rate of dimerisation of two ethylborane molecules was one order of magnitude less than the rate of dimerisation of two borane molecules to form diborane. The implication was that the ethyl substituent either sterically hinders or inductively lowers the reactivity of the free valence bond. The same reasoning was used to explain why the reaction of ethylborane with ethene was about twenty times slower than that of borane with ethene. The activation energy for the hydroboration of tetramethylethene (TME) with borane has been reported to be 38.5 ± 1.7 kJ/mol.[72] The

reaction is first order in both borane and TME. The bimolecular rate constants for the forward and reverse redistribution equilibria for the system have been shown to be considerably smaller than those of the reaction rate constant in the *n*-propylborane system.[75]

1.4.1. Kinetics of Hydroboration with Dialkylboranes and their Dimers

The kinetics of the hydroboration of alkenes with 9-BBN dimer in both non-complexing and complexing solvents have been reported, thereby elucidating the role of the complexing solvent in the hydroboration reaction.[78] The hydroboration of alkenes with 9-BBN dimer is envisaged as consisting of two steps as shown in equation *1.15*. The rates of reaction of 9-BBN and 1-hexene in various solvents are shown in **Table 1.3**.

$$(\text{9-BBN})_2 \underset{k_{-1}}{\overset{k_1}{\rightleftharpoons}} 2(\text{9-BBN})$$
$$\text{9-BBN} + \text{alkene} \underset{k_{-2}}{\overset{k_2}{\rightleftharpoons}} \text{B-alkyl-9-BBN} \qquad 1.15$$

Table 1.3 - First Order Rate Constants (k_1) for the Hydroboration of 1-Hexene by 9-BBN in Various Solvents at 25 °C[78]

Solvent	$10^4 \times k_1$ (s^{-1})
Cyclohexane	1.45
CCl_4	1.54
Benzene	2.05
Diethyl Ether	2.83
THF	14.2

Table 1.3 shows a large increase in k_1 when THF is used as a solvent. The value is almost ten-fold when comparing THF and cyclohexane. In the case of the reaction of 9-BBN dimer with unhindered amines (e.g., pyridine) the authors observed second order kinetics for the reaction (first order in both the dimer and the pyridine), suggesting direct attack of the amine on the 9-BBN dimer, as is shown in equation *1.16*.

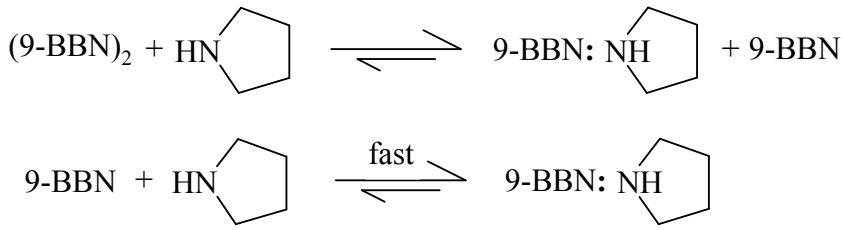

1.16

It was, therefore, concluded that it is not unlikely that the reaction of THF with the 9-BBN dimer also occurs through direct attack of THF on the dimer. This process breaks up the dimer, increasing the hydroboration process in return. In the case of diethyl ether, which shows only a slight increase in k_1, the large steric requirements and lower Lewis acidity are cited as the limiting factors. Hydrocarbon solvents lack a donor atom with which to attack and break up dialkylborane dimers, consequently hydroboration has to occur *via* the much slower dissociation of the dimer prior to hydroboration. Hydroboration reactions in these solvents are, therefore, slower than those in ethereal solvents.

It has also been observed that dimethyl sulfide is much more efficient than THF at breaking up the dimer. This is explained by the much larger equilibrium constant found in the case of dimethyl sulfide ($K = 2.1 \times 10^{-3}\ M^{-1}$) when compared to THF ($K = 8.05 \times 10^{-5}\ M^{-1}$), as defined in equation *1.17*.

$$K = \frac{[9-BBN.THF]^2}{[(9-BBN)_2][THF]^2} \qquad K = \frac{[9-BBN.SMe_2]^2}{[(9-BBN)_2][SMe_2]^2} \qquad 1.17$$

However, hydroboration with 9-BBN-amine complexes was found to be substantially slower because of the much higher stability of the 9-BBN-amine complexes.

1.4.2. Kinetic Effects of Alkene and Hydroborating Agent Structure

The most commonly applied method for the investigation of alkene structural effects on the rates of hydroboration is that of competitive hydroboration. In this method the relative

rate of hydroboration between two alkenes is determined using an expression derived by Ingold and Shaw:[79]

$$Relative\ Rate = k_x/k_y = (\ln x_0 - \ln x)/(\ln y_0 - \ln y) \qquad 1.18$$

In this expression, x_0 and y_0 are the initial concentrations of the alkenes, while x and y represent the respective alkene concentrations at the end of the reaction. Work on the hydroboration of representative alkenes by 9-BBN at 25 ^oC, and disiamylborane at 0 ^oC has been reported in the literature.[80,81] The rate constants for the hydroboration of various alkenes by 9-BBN and disiamylborane were compared to the hydroboration of 1-hexene by these two hydroborating agents and are reported as relative rates in **Table 1.4**.

Table 1.4 - Relative Reactivities of Representative Alkenes Toward 9-BBN (25 ^{o}C, THF) and Disiamylborane (0 ^{o}C, Diglyme) as Measured Against 1-Hexene[80,81]

Alkene	Relative Rate	
	9-BBN	*Disiamylborane*
1-Hexene	100	100
1-Octene	110	108
3-Methyl-1-butene	50	57
2-Methyl-1-pentene	194	4.9
Cyclopentene	7.2	1.4
Cyclohexene	0.067	0.01
Cycloheptene	7.6	7
Cyclooctene	6.9	26
trans-3-Hexene	1.2	0.2
cis-3-Hexene	0.56	2

Note: All relative rates reported in this table are relative to 1-hexene; hence its relative rate of reaction is 100.

The results in **Table 1.4** indicate that there is no appreciable difference in the relative rate of hydroboration of straight-chain alkenes. In both cases a methyl substituent attached on C_3 resulted in a 50% decrease in the reactivity, while one at C_2 caused a decrease in the relative reactivity of the alkene towards disiamylborane and a marked increase in the reactivity towards 9-BBN. The increase in reactivity for 2-substituted alkenes can be explained by general chemistry in terms of the inductive effect of the C_2 alkyl substituent, which is expected to increase the electron availability at the double bond and favouring hydroboration.[80,81] Accordingly, a reactivity increase was observed in the relatively

unhindered 9-BBN in contrast to the decrease in the much more sterically crowded disiamylborane.

The higher reactivity of cyclopentene towards both 9-BBN and disiamylborane, when compared to cyclohexene, has been explained in terms of differences in ring strain causing strain in the double bonds. The higher strain on the double bond of cyclopentene is responsible for the higher reactivity.[82,83] Cycloheptene and cyclooctene both have highly strained double bonds because of their unorthodox shapes and accordingly react faster than cyclohexene, which can adopt the more stable boat or chair configurations. Disiamylborane clearly distinguishes between cyclopentene, cycloheptene and cyclohexene. 9-BBN shows no distinction between cyclopentene and cycloheptene, but differentiates cyclohexene from these two.

The higher reactivity of disiamylborane towards *cis*-3-hexene when compared to *trans*-3-hexene was attributed to the higher strain on the *cis* double bond.[83] 9-BBN shows a reversal of this trend.

1.5. Mechanistic Aspects of the Hydroboration Reaction

Brown originally proposed that the mechanism of hydroboration involved a four-centre transition state shown in **Figure 1.5**.[84] In this transition state the alkene donates electrons, through its more electronegative sp^2 carbon, to the vacant $2p$ orbital on the boron atom. The borane hydrogen donates electrons to the more electropositive sp^2 carbon of the alkene. This charge redistribution weakens the alkene π-bond and the boron hydrogen σ-bond while forming bonds between boron and carbon and carbon and hydrogen.[84]

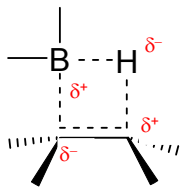

Figure 1.5 - Four-centre transition state proposed by Brown *et al.*[84]

This mechanism is consistent with hydroboration being a *cis* addition reaction. This was seen in the hydroboration-oxidation of 1-methylcyclopentenes and 1-methylcyclohexenes that afforded *trans*-2-alkanols (equation *1.19*).[85]

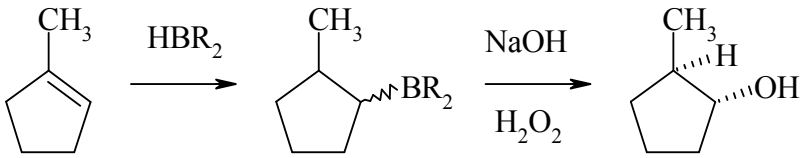

1.19

Extended Hückel calculations on propene showed that C_1 (the terminal carbon atom in an alkene) possessed a higher electron density than C_2, thereby explaining the *anti*-Markovnikov regioselectivity of the hydroboration reaction.[24]

This mechanism was also applicable to the hydroboration of cycloalkenes.[83] This was despite the fact that monoalkylboranes and dialkylboranes are known to exist as dimers in solution.[23] The proposed intermediate is as shown in equation *1.20*.

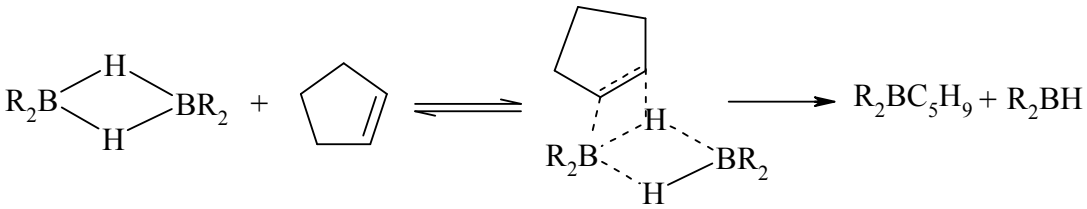

1.20

Streitwieser and co-workers proposed an alternative mechanism involving a three-centre π-transition state, shown in **Figure 1.6**, when Brown's model could not explain the stereochemistry of product from the hydroboration of *cis*-1-butene with diisocamphenylborane.[86] The π-complex is formed because of attractive forces between

the alkene π cloud and the vacant 2*p* orbital on the borane. The borane is thought to form a continuous distortion of orbitals in the π-complex into those of the product.[86]

Figure 1.6 - Three-centre π-complex proposed by Streiwieser *et al.*[86]

This model was also able to explain the *cis* stereochemistry of hydroboration reactions. In addition, it was maintained that there was little perturbation from this triangular transition state. Objections to this model were raised because of stereochemical reasons based on a study evaluating steric effects in the hydroboration of substituted cyclohexenes.[87] In support of Streitwieser *et al.*,[86] Jones[88] suggested that Brown's four-centred complex had symmetry restrictions. Jones also added that, on the basis of orbital symmetry of the three-centre molecular orbitals (MOs) of the π-complex, the rate-determining conversion of the π-complex to the product was a concerted process. Contrary to Jones's exclusion of Brown's four-centre complex on symmetry grounds, it has been reported that involvement of the boron atom's vacant 2*p* orbital in a four-centre process did in fact make it a feasible model.[69] A*b initio* MO calculations by Clark and Schleyer indicated that the gas phase reaction of ethene and borane proceeds exothermically *via* an intermediate π-complex without an overall activation barrier.[89] This lack of overall activation energy was in contrast with the observed selectivity of the hydroboration reaction. Clark and Schleyer agreed with Dewar and McKee's MNDO (Modified Neglect of Diatomic Overlap) semi-empirical study stating that gas phase hydroboration with borane monomer (as opposed to diborane) had no selectivity. The reason given was that the activation barrier introduced by solvent–borane interaction caused the selectivity of the reaction in solution.[90] The three-centre π-complex was also supported by Fehlner's kinetic studies.[79]

Lipscomb and co-workers later suggested that Brown's four-centre complex was a description of a transition state,[85] with the three-centre π-complex being a description of a pre-transition state intermediate. The transition state would then be encountered at the last stage of the π-complex mechanism.[91] This PRDDO (Partial Retention Diatomic Difference Overlap) study by Lipscomb *et al.*[83] favoured the four-centre transition state

even though a weakly bound π-complex of borane and the alkene was found prior to the transition state. This study also stated that the alkene's two sp^2 carbon atoms acquire a substantial charge separation in the transition state, with the terminal carbon (closest to the boron atom in the transition state structure) getting more of the negative charge than the neighbouring carbon atom. This observation accounted for the *anti*-Markovnikov nature of the addition of boranes to alkenes. This description of the mechanism was supported by studies published by Nagase *et al.*[92] and further studies by Lipscomb *et al.*[93] It was further added that the observed reaction barrier to hydroboration and the observed regioselectivity of the reaction both arose from the internal barrier to the transition from π-complex to the transition state. The most accepted mechanism in support of the low activation barrier was summarised by Wang *et al.*,[94] stating that the gas phase reaction of borane and ethene proceeds through a π-complex formation then a four-centre transition state, as shown in **Figure 1.7**.

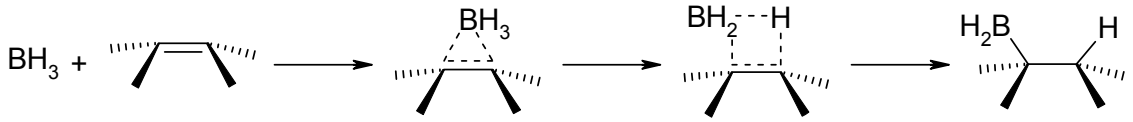

Figure 1.7 - Revised mechanism of the gas phase reaction of alkenes with borane

Three mechanistic possibilities exist in the reaction of borane-solvent complexes with alkenes:[24]

- The borane-solvent complex reacts directly with the alkene.
- The borane-solvent complex dissociates in a fast, reversible pre-rate-determining equilibrium, which is then followed by the rate-determining reaction of the free borane with the alkene.
- Rate-determining dissociation of the borane-solvent complex is followed by a fast reaction of the free borane and the alkene.

Work by Pasto *et al.*[72] for the hydroboration of tetramethyl ethylene (TME) with BH_3:THF revealed second order kinetics (first order in both the alkene and the hydroborating agent). Both direct attack of the free borane complex on the alkene and pre-rate-determining borane-solvent complex dissociation were first order in the borane-solvent complex and the alkene. It was only in the latter that the enthalpy of the transition

state complex was found to be insensitive to the nature of the donor solvent.[24] The observed entropies (in conjunction with those measured by Fehlner[77] in the gas phase hydroboration of TME with BH_3:THF) dictated that the reaction did involve direct attack of the borane-solvent complex on the alkene. This mode of hydroboration is further supported by kinetic studies conducted by Pasto and co-workers.[75]

Hydroboration of representative styrenes with the BH_3.THF complex by Klein *et al.*[91] also showed second order kinetics (first order in both styrene and hydroborating agent). The induction effect observed in this case supported the pre-rate-determining dissociation of the borane-solvent complex. Additional support for this mechanism is based on Brown and Wang's study of hydroboration using 9-BBN.THF complexes.[78]

Clark, Wilhelm and Schleyer's *ab initio* calculations suggests that the hydroboration with borane-solvent complex is similar to an S_N2 displacement of the solvent by the alkene with the solvent playing no role in the transition state and the borane never being free during the reaction.[95] This contradicted Brown and Wang's model,[78] especially as Clark and his co-workers did not envision the dissociation of the borane-solvent complex being a spontaneous process. Tocachini's *ab initio* calculations on the reaction of ethene with BH_3:OEt_2 slightly modified the observations of Clark *et al*.[96] In Tocachini's reaction the rate-determining step involved the complete displacement of the solvent prior to the formation of the three-centre borane-ethene π-complex intermediate. The second step was the formation of the transition state structure, through a low energy barrier, where the solvent interacted very weakly with the transition state complex. This weak interaction was found to be insignificant on both energetic and structural grounds. The direct reaction of the borane-solvent complex with the alkene was found to be more energetically favourable than the prior dissociation of the borane-solvent complex.

1.6. Thermal Transformations of Organoboranes

Organoboranes undergo four types of thermal reaction: redistribution, cyclisation, isomerisation and displacement. The discussion of these reactions in this section will be restricted to alkylboranes examples.

1.6.1. Redistribution

The redistribution reaction is facilitated by the empty *p*-orbital in trivalent alkylboranes. The reaction is essentially an exchange of alkyl side chains between alkylborane species and occurs *via* a bridged mechanism (**Scheme 1.8**).[97-101]

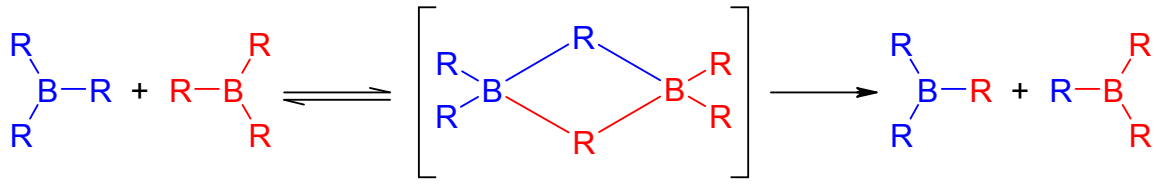

Scheme 1.8

The reaction is hampered by bulky groups attached to the boron atom and enhanced by the presence of B-H bonds.[102-104]

1.6.2. Cyclisation

The cyclisation of trialkylboranes occurs as a result of pyrolysis of these compounds when subjected to temperature ranges of 200-350 ºC for prolonged durations. Köster *et al.*[105] have published an extensive review on the decomposition and subsequent cyclisation of trialkylboranes, showing that 5- and 6-membered rings dominate the cyclic structures formed on the cyclisation of trialkylboranes (**Scheme 1.9**).[105-107]

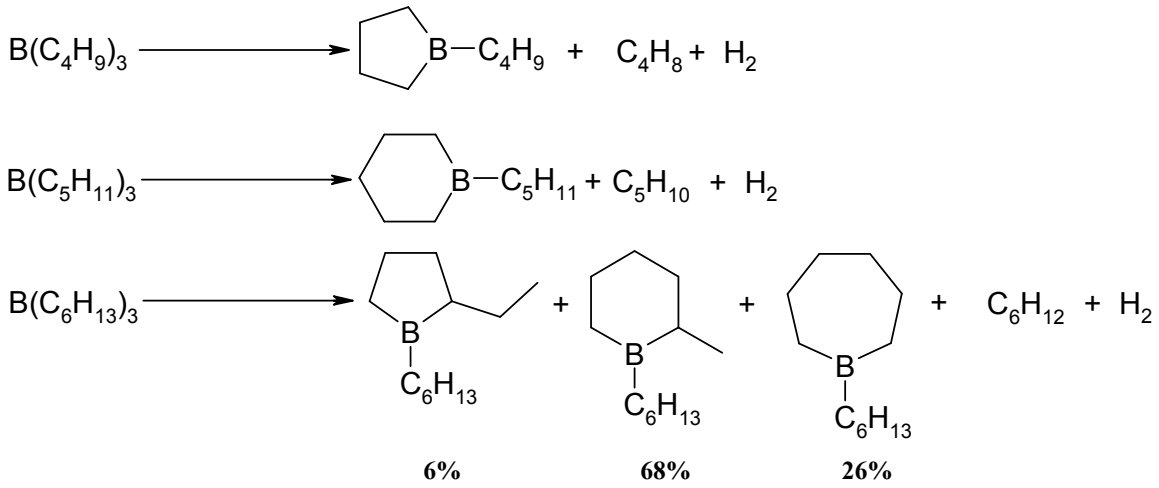

Scheme 1.9

For trialkylboranes with chain lengths greater than eight, bicyclic compounds are formed (**Scheme 1.10**).

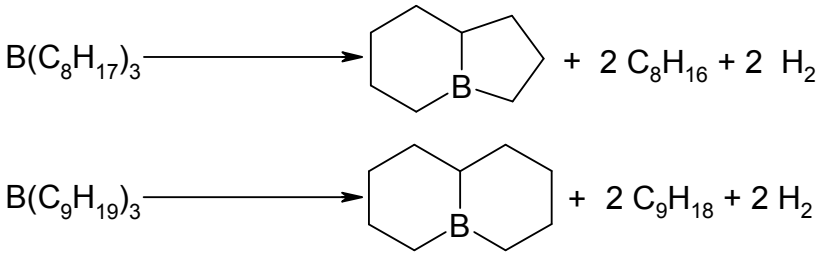

Scheme 1.10

All studies into the cyclisation of trialkylboranes found that the process follows *via* elimination of an olefin (generally as an internal alkene) to form a dialkylborane, as is evident from the IR data of Köster *et al.*[105] Cyclisation takes place in order to stabilize the alkylborane after elimination of hydrogen from the dialkylborane. Both Brown *et al.*[108] and Köster *et al.*[105] found that the presence of B-H bonds promotes the cyclisation process.

1.6.3. Isomerisation

The synthetic utility of the isomerisation reaction of trialkylboranes has been reviewed in the literature.[109]

The reaction can be classified into four types of isomerisation:[110]

- Isomerisation of branched chain acyclic compounds to straight chain acyclic compounds.
- Isomerisation of acyclic compounds to cyclic compounds.
- Isomerisation resulting in either ring contraction or expansion.
- Isomerisation of *cis* compounds to *trans* compounds.[111,112]

The discovery of organoborane isomerisation dates back to the 1950s when Henion and his co-workers observed that tri-*sec*-butylborane prepared *via* the Grignard procedure isomerised to tri-*n*-butylborane after refluxing for two days under a nitrogen atmosphere, followed by distillation (200-215 ºC) to obtain the pure trialkylborane product.[113] Brown and Subba Rao observed similar isomerisation at milder temperatures (100 ^{o}C) and shorter reaction times (2 hours) in their organoborane synthesis using sodium borohydride as a source of diborane.[111,114] Rosenblum's observation of the dealkylation of tri-*n*-butylborane during its distillation suggested that the hydroboration reaction was reversible at elevated temperatures.[106]

It has been observed that the presence of a small excess of borane enhances the rate of isomerisation, while the use of the stoichiometric quantity of alkene slowed the process down.[115,116] In the presence of excess alkene, the dialkylborane dimer reacts with new alkene instead of the previously liberated alkene.[108] The standard procedure for isomerisation employs a 10-20% excess of boron hydride to hydroborate the alkene in diglyme, after which the solution is refluxed at 160 ^{o}C with isomerisation being complete in most cases except where the alkyl chain is relatively long (equation *1.25*).[16]

The mechanism of the reaction is thought to involve a dehydroboration-rehydroboration equilibrium, depicted in equation *1.24*.[117]

1.24

$$B(C_4H_9)_3 \overset{\Delta}{\rightleftharpoons} HB(C_4H_9)_2 + C_4H_8$$

The mechanism is thought to involve a dimeric species (**Figure 1.8**), which reacts with the unsaturated alkene.[18] This dimeric dialkylborane species is formed through initial dehydroboration of the trialkylborane.[106]

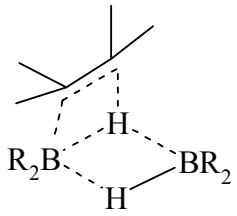

Figure 1.8 - Dialkylborane-alkene interaction during isomerisation

The dehydroboration step is probably rate-determining, with the dehydroboration being shown to actually take place.[118,108,139] Most investigations point towards complete dissociation of the alkyl chain from the boron atom as is evident from the large and positive entropy values observed for these reactions;[119,120] but some compounds, especially, tri-*sec*-alkylboranes exhibit only partial dissociation (smaller enthalpy values and negative entropy values).[119,120] There are also investigations that show that some alkylborane isomerisation reactions take place *via* a mechanism that does not involve dehydroboration, but one that involves bridging.[108,118,121]

The thermodynamic driving force for the isomerisation reaction is the formation of the tri-*n*-alkylborane, which is thermodynamically more stable than the internal isomers.[102,122] The results of work done by Brown and Subba Rao,[19] shown in **Table 1.5**, indicate that the isomerisation of alkylboranes involves a stepwise shift of the boron atom from the internal to the terminal position. This observation is in accord with the proposed elimination-addition mechanism. At the end of the reaction an equilibrium distribution of isomers is obtained, with alkylboranes with the boron atom attached to the terminal position being the dominant product.

Table 1.5 - Hydroboration Mediated Isomerisation of 3-Hexene at 125 °C[19]

Time (hours)	Yield (%)		
	3-Hexene	2-Hexene	1-Hexene
0	100	0	0
1	26	30	4
2	18	25	57
4	11	15	47
8	9	9	82
24	6	6	88

The isomerisation reaction is temperature dependent and can be shifted to completion by setting the reaction up as a distillation.[16]

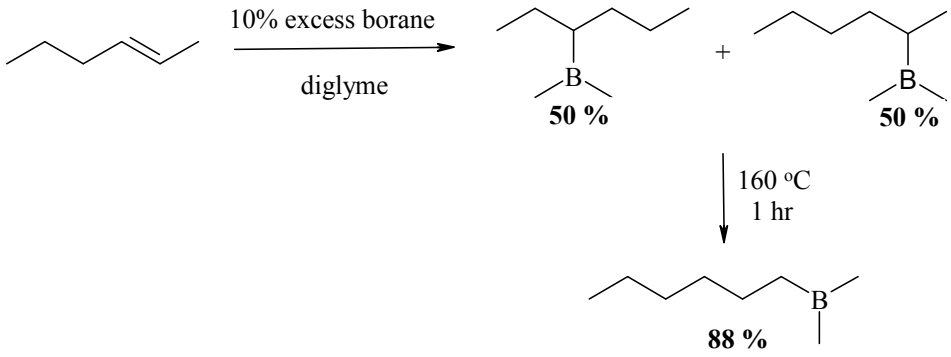

1.25

Arase *et al.*[123] investigated the effect of various high-boiling solvents on the isomerisation reaction (**Table 1.6**).

Table 1.6 - Conversion of tri-*s*-pentylborane to tri-*n*-pentylborane in different solvents

Solvent	Reaction Temp. (°C)	% Conversion
Anisole	160	92
	180	95
Diphenyl ether	160	80
	180	90
Cumene	160	75
	180	90

Ethereal solvents such as anisole and diphenyl ether accelerated the isomerisation process at lower temperatures (92 ºC), while those such as pyridine, its related compounds and cumene retarded isomerisation. Retardation of isomerisation by amines had been reported earlier in the literature.[124,125] It can be reasoned that this inhibitory effect of amines is probably due the strong complexes they form with alkylboranes, thereby preventing re-hydroboration from taking place.

It has also been demonstrated that boranes readily catalyse the migration of a double bond from an endocyclic to an exocyclic position (equation *1.26*).[126]

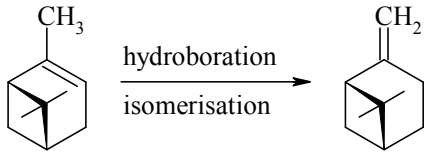

1.26

This, however, does depend on the size of the ring and steric interactions.[127,128]

The isomerisation of branched alkenes takes place much more easily than in unbranched alkenes, with 2,4,4-trimethyl-2-pentene showing a 75% yield of terminal isomer after borane mediated isomerisation at 75 ^{o}C.[16] In addition, certain cyclic and acyclic tetrasubstituted alkenes have been known to undergo isomerisation at 50 ^{o}C.[129,130] It is also possible to isomerise bulky tertiary organoboranes at 60 ^{o}C, as shown in equation *1.27*.[131]

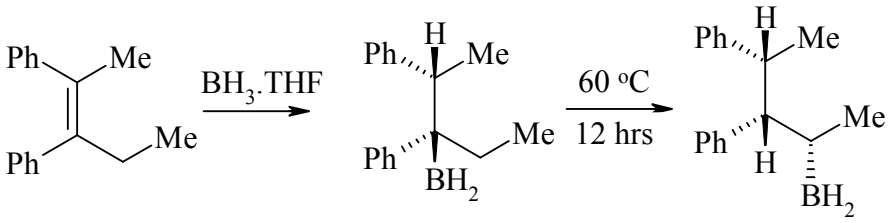

1.27

A patented procedure utilising a catalytic amount of tri-*n*-alkylborane to isomerise internal alkenes of equivalent chain length has been reported in the literature (equation *1.28*).[132]

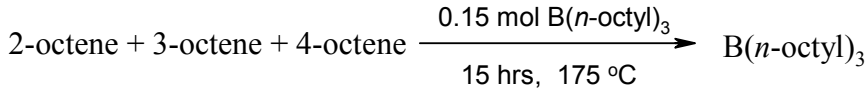

1.28

1.6.4. Displacement of Alkenes from Organoboranes

The contrathermodynamic isomerisation of internal alkenes by organoboranes presents a commercial opportunity because of the higher commercial value of terminal alkenes when compared to their internal isomers. It is possible to recover the terminal alkenes by setting up the isomerisation as a distillation, but continual removal of the isomerised alkene by this method will eventually result in the decomposition of the borane as was observed by Rosenblum.[106] A more commercially viable alternative would be the use of a less volatile (or more reactive) olefin to displace the more volatile olefin, therefore ensuring that the borane is recycled and not destroyed.

The synthetic utility of the isomerisation-displacement reaction of trialkylboranes was recognised early in the open and patent literature.[133-137,119]

The mechanism of the displacement reaction is also thought to proceed through a four-centre transition state (equation *1.29*) caused by the dissociation of the trialkylborane into dialkylborane and free alkene at isomerisation temperatures (100-160 °C).[16]

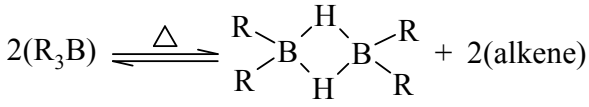

1.29

Mikhailov *et al.*[138] proposed a different mechanism for the displacement reaction, which involves a concerted cyclic process (**Scheme 1.11**).

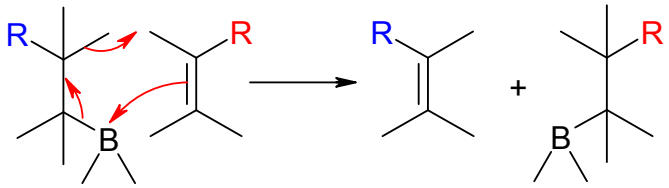

Scheme 1.11

The lack of dependence on olefin concentration of the displacement reaction[115,120] suggests that it is the dehydroboration mechanism that operates in the displacement reaction.

Since displacement is generally carried out over the same temperature ranges as the isomerisation, back-isomerisation of the alkene during the displacement reaction might be a concern. Fortunately, this is not a serious consideration in the case of terminal alkenes. The use of excess displacing alkene converts the catalytic excess (10-20 mol%) of borane used at the start of the isomerisation reaction into trialkylborane, thereby cancelling the possibility of back-isomerisation.

The process of displacing terminal alkenes requires approximately six to eight hours. The products obtained are typically made up of 90-95% pure terminal alkene, with the remaining 5-10% being 2-alkene. For example, 1-decene displaces 1-pentene from tri-*n*-pentylborane in five hours to a yield of 83%, of which 91% is 1-pentene with the remainder being 2-pentene.[19,106]

The ease of displacement of alkenes varies with the structure of the alkene. Cyclic and bicyclic alkenes undergo displacement from their corresponding organoboranes with remarkable ease when compared to straight-chain organoboranes.[126,139] This stability is correlated to the heat of hydrogenation of the alkene.[16] Thus, the rate of displacement of olefins from their corresponding organoboranes is as shown in equation *1.30*.

$$R_2C{=}CHR > R_2C{=}CH_2,\ RCH{=}CHR > RCH{=}CH_2 \qquad 1.30$$

Because the displacement reaction proceeds through equilibrium between the initial organoborane and the organoborane formed by the displacing alkene, it follows that the terminal alkenes should be the most efficient displacing agents. Consequently, the order of displacing efficiency is exactly opposite that of the rates of displacement listed above.

Investigations have found no effect of solvent on the displacement reaction.[140,141] Rousseau[141] notes that, while not actually affecting the rate of the displacement reaction,

diglyme affects chemical equilibrium. These findings are in contrast to Rutkowski's observation that several solvents chosen for their inertness were found to influence the displacement reaction rates of organoboranes by varying degrees.[134] Investigations by Rousseau[141] and Rutkowski[134] found activation energies of 122 and 118 kJ/mol for the displacement of decene from tridecylborane by 1-pentene and 1-octene, respectively. The inertness in displacing the respective alkenes from trinorbonylborane and triethylborane by 1-decene can be attributed to their higher heats of hydrogenation when compared to terminal alkenes.[142,143,144] This suggests that norbonene and ethene should be ideal displacing agents for other alkenes, including 1-decene. For industrial purposes however, where recycling of the borane would be desirable, these two alkenes would not be suitable as displacing agents because of their high stability.

From a commercial standpoint, the displacement reaction is slow even at high temperatures. A patent by Rutkowski and co-inventors introduced the possibility of using catalysts to accelerate the displacement process.[137] The catalyst should be aprotic, strongly basic, dipolar, non-hydroxylic and have a high dielectric constant. Examples of these are shown in **Figure 1.9**.

Table 1.7 - Kinetic data for the reaction of olefins with trialkylboranes at 125 ºC

Olefin	R_3B	$10^{-3}k$ (hr^{-1})
C_8	C_{10}	31.3
C_{10}	C_8	24.3
C_8	C_{12}	85.2
C_{12}	C_8	28.5
C_5	C_{10}	162
C_{10}	C_5	23.5

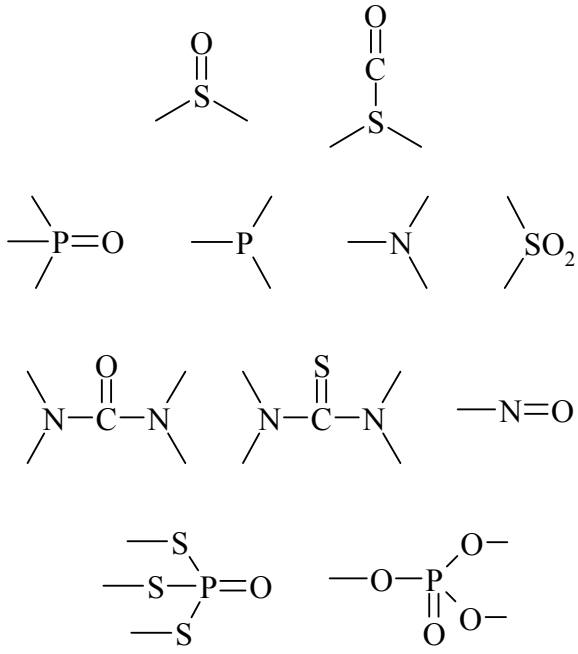

Figure 1.9 - Catalysts proposed by Rutkowski *et al.*[138] for the displacement of alkenes from organoboranes

1.7. Study Objectives

Sections 1.4 and **1.5** have, respectively, shown that considerable effort over the years has gone into explaining the reactivity of borane and its alkyl derivatives. However, given that the majority of the information available in the literature is obtained from experimental work carried out with gas chromatography as the sole means of analysis, it becomes interesting to consider whether the application of modern techniques does not provide more detailed information on the reactivity of borane and its derivatives. A part of this study therefore focuses on the use of ^{11}B NMR spectroscopy for delineating mechanistic aspects of boron chemistry.

Section 1.6 detailed the reaction by means of which internal olefins could be converted to linear-α-olefins. **Sections 1.6.1** and **1.6.2** specifically discussed the manner by which trialkylboranes may decompose under influence of extreme heating. No studies exist that shown the behaviour of trialkylboranes in the temperature range (typically 100-200 ºC) in which a boron-mediated cycle, as envisaged in **Scheme 1.2**, would be operated. Thus, the decomposition behaviour of trioctylborane in this temperature range is investigated. The

claims in the patent literature described in **Section 1.6.4** also warrant investigation to understand the fate of the borane species.

The scope of ^{11}B NMR spectroscopy as a technique can also be assessed by the investigation of the association of trialkylboranes to the compounds detailed in **Figure 1.9**. Where appropriate, molecular modelling has been used to rationalise the findings.

2. EXPERIMENTAL

The analysis of organoboranes by various modern instrumental investigations is comprehensively reviewed by Odom.[145]

2.1. Apparatus

Standard techniques for handling of air- and moisture-sensitive materials were used for handling syringes, needles, canulae, glassware, quartz NMR tubes and reagents. [146,147] Glassware was assembled and attached to a vacuum line. The glassware was then dried by heating with a heat gun under strong vacuum (0.5 mmHg) and cooled under a stream of dry nitrogen. Syringes, needles and canulae were stored overnight in an oven (110 ^{o}C) and cooled in a desiccator lined with silica gel prior to assembly.

NMR spectroscopy was used to identify hydroboration reaction products as well as carry out kinetic measurements and binding studies. NMR experiments were performed at appropriate temperatures on a Varian Unity Inova 500 spectrometer in 5 mm quartz tubes. These NMR tubes were oven-dried (110 ^{o}C) overnight, cooled in a desiccator, sealed with appropriate rubber septa, evacuated and flushed with dry nitrogen. Samples were introduced into the tube through syringe or canulae. ^{11}B NMR spectra were referenced externally against $BF_3.OEt_2$ (0 ppm).

2.2. Purification of Reagents

Table 2.1 - Details for drying of reagents and solvents

Reagent	Drying Agent	Purification
THF	Sodium Wire + 4 Å molecular sieve	Distillation
Diglyme	Sodium Wire + 4 Å molecular sieve	Distillation
1- and 4 -Octene	Sodium Wire + 4 Å molecular sieve	Distillation
Xylene	$MgSO_4$ + 4 Å molecular sieve	Distillation
Toluene	Sodium Wire + 4 Å molecular sieve	Distillation
HMPA	4 Å molecular sieve, stirring *in vacuo* for an hour to remove dimethyl amine	Degassed
HMPT	4 Å molecular sieve	Degassed
NBu_3	4 Å molecular sieve	Degassed
PBu_3	4 Å molecular sieve	Degassed
EtO_3PO	4 Å molecular sieve	Degassed
EtO_3P	4 Å molecular sieve	Degassed
DMF	4 Å molecular sieve	Degassed
DMSO	4 Å molecular sieve	Degassed

The nitrogen gas used for these studies was dried by passing the gas from the cylinder through a drying tube, containing 4 Å molecular sieves and $CaCl_2$, between the N_2 cylinder and the vacuum line. Self-indicating silica gel was placed at both ends of the drying tube as a wetness indicator.

2.3. Preparation of Samples for GC Analysis

Samples obtained from reaction mixtures (**Sections 3.4.2** and **3.5**) were quenched and oxidised prior to GC analysis. Samples were quenched with 3 M sodium hydroxide (0.5 mL) and oxidised by the addition of 50% aqueous hydrogen peroxide (0.5 mL). THF (1 mL) was added to the sample as a diluent. The organic layer was removed by Pasteur pipette and dried with anhydrous magnesium sulfate. The sample was filtered through cotton wool in a Pasteur pipette prior to GC.

2.4. Hydroboration of Alkenes

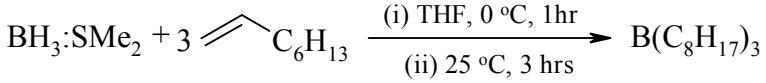

3.2

The hydroboration of alkenes prior to thermal dealkylation and alkene liberation studies was achieved as shown in equation *3.2*. In the reaction, three equivalents of 1-octene were dissolved in dry THF under dry N_2. The reaction mixture was then cooled to 0 ^oC in an ice-bath. Hydroboration was achieved by the dropwise addition of one equivalent of a solution of $BH_3.SMe_2$ in THF from a funnel reservoir into the reaction flask. The reaction was stirred at 0 ^oC for an hour and subsequently at 25 ^oC for a further three hours. Scrupulous attention was paid to the exclusion of moisture and air at all stages of the reaction. As such, all reagents and solvents were introduced into the glassware through syringes. Typical reagent quantities used in experiments were as follows:

- BH_3:SMe_2 (10 M): *5.98 g (7.00 mL, 78.7 mmol)*
- 1-Octene: *30.28 g (42.35 mL, 268.9 mmol)*
- *n*-Decane: *3.60 g (4.95 mL, 25.3 mmol)*
- THF: *250 mL*
- Reaction time: *1 hour (0 ^oC), 3 hours (25 ^oC)*
- Yield (GC) *95%*

Reaction progress was monitored by GC analysis for remaining number of moles of 1-octene with *n*-decane as internal standard. For these purposes, 2 mL aliquots were withdrawn from the reaction flask and quenched and oxidised as in **Section 2.3** prior to GC analysis. ^{11}B NMR was also used to confirm product distribution since hydroboration by borane does not afford trialkylboranes exclusively. Chemical shifts for the products and starting materials are as follows: $\delta^{11}B$ = +86.0 ppm [broad singlet, $B(C_8H_{17})_3$]; $\delta^{11}B$ = +53.8 ppm [broad singlet, $H_2B_2(C_8H_{17})_4$]; $\delta^{11}B$ = +1.1 ppm [quartet (J_{B-H} = 107 Hz), BH_3:THF]; $\delta^{11}B$ = -18.5 ppm [quartet (J_{B-H} = 106 Hz), BH_3:SMe_2]. A typical spectrum is shown in **Figure 2.1**.

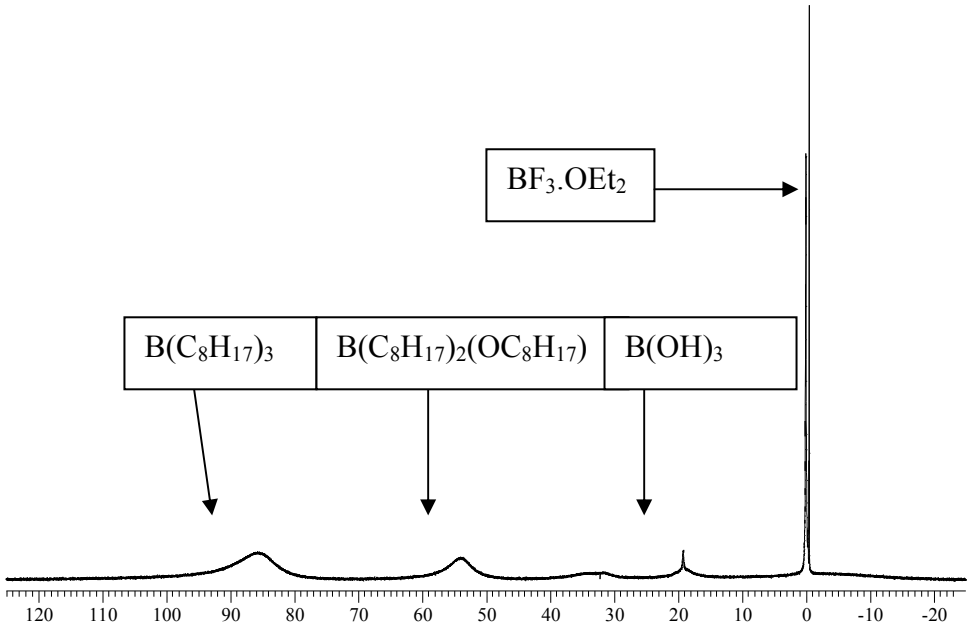

Figure 2.1 - Typical ^{11}B NMR spectrum from the hydroboration of 1-octene

2.5. Thermal Dealkylation Studies

2.5.1. Time Dependence

Time dependence studies were conducted on trioctylborane and tridecylborane. 1-Octene and 1-decene were respectively hydroborated as outlined in **Section 2.4**. Thereafter the trialkylboranes were placed in stainless steel reactors through the reagent interlock tube. The temperature was set at 100 ^{o}C over a period of ten minutes in the trioctylborane study. The temperature was set at 150 ^{o}C over a period of fifteen minutes in the tridecylborane study. The reactions were sampled at hourly intervals over a period of eight hours by collecting 2 mL samples through a liquid sampling valve. The samples were prepared for analysis as described in **Section 2.3** and analysed by GC-MS for alkene, alkane and alcohol content.

2.5.2. Temperature Dependence

Temperature dependence studies were conducted on tri-*n*-octylborane and tri-*n*-decylborane. 1-Octene and 1-decene were respectively hydroborated as outlined in **Section 2.4**. Thereafter the trialkylboranes were placed in stainless steel reactors. The temperature of the reactor was initially set at 50 ^{o}C for an hour and thereafter an hour each at 100, 150 and 200 ^{o}C. The reactions were sampled after an hour at each set temperature by collecting 2 mL samples through a liquid sampling valve. The samples were prepared for analysis as described in **Section 2.3** and analysed by GC-MS for alkene, alkane and alcohol content.

GC-MS analysis for the thermal dealkylation studies were performed at the Sasol Chemical Industries Routine Laboratories on a Hewlett Packard Agilent 6890 model fitted with a Hewlett Packard 5683A Mass sensitive Detector and a capillary PONA column (50 m × 0.5 mm × 0.2 μm). GC conditions were set as indicated in **Table 2.2.**

Table 2.2 - Operating conditions for GC-MS analyses

Initial Column Temperature (^{o}C)	50	Column Ramp Rate (^{o}C/min)	4
Final Column Temperature (^{o}C)	240	Split Ratio (mL/min)	200
Injector Port Temperature (^{o}C)	250	Split Flow Rate (mL/min)	20
Detector Temperature (^{o}C)	300		

2.5.3. Effect of Lewis base on Dealkylation

The effect of the Lewis base on the dealkylation on tri-*n*-octylborane reaction was investigated at 150 ºC. 1-Octene was hydroborated as outlined in **Section 2.4**. The volatile components were removed first *in vacuo* and then by distillation up to 80 ºC. 500 μL aliquots of the resulting neat trialkylborane (checked for purity by ^{11}B NMR) were injected into dry, nitrogen-flushed and septum-capped 5 mm glass NMR tubes. The required volumes of Lewis base (10 mol% based on the borane) were injected into the borane. In cases where the Lewis base was solid (tetramethylthiourea and tetramethylurea) the

required mass was placed into the NMR tube, which was then capped with a rubber septum, evacuated and then flushed with nitrogen prior to injection of the trialkylborane. The sample tubes were then placed in a stainless steel heating block equilibrated to 150 ºC for eight hours. The reaction was stopped by placing the sample tubes in ice/water and adding 250 μL of distilled water to quench any active boron-hydrogen bonds. The samples in the NMR tubes were oxidised by pouring into a 3 M aqueous solution of sodium perborate and left to stand at room temperature for two hours. 2 mL hexane was added to the quenched samples in order to extract the organic components of the sample, which were analysed by GC for alkene, alkane and alcohol content.

GC analysis for the thermal dealkylation samples was performed on a Varian GC (FID) 3800 model fitted with the following column:

- Teknokroma PONA column (50 m × 0.20 mm × 0.50 μm) for alkane and alkene analysis.
- Perkin-Elmer Elite Wax column (30 m × 0.53 mm × 0.20 μm) for alcohol analysis

GC conditions were set as indicated in **Table 2.3**. A representative chromatogram for alcohol analysis is shown in **Figure 2.3**.

Table 2.3 - Operating conditions for Varian 3800 GC for thermal dealkylation studies

Operating Parameters	Column	
	PONA	Elite Wax
Injection Volume (μL)	1.0	0.2
Initial Oven Temp (ºC)	40	40
Initial Hold Time (minutes)	0	0
Ramp Rate (ºC/min)	10	12
Final Oven Temp. (ºC)	250	240
Final Hold Time (minutes)	0	2
Flow Rate (mL/min)	1.0	1.0
Injector Temp (ºC)	200	200
Split Ratio	50	Splitless
FID Temp (ºC)	300	250

Figure 2.2 was used for the calibration of the Carbowax column for the detection of alcohols. Alcohol concentrations were obtained through peak areas relative to those of the internal standard (*n*-decane).

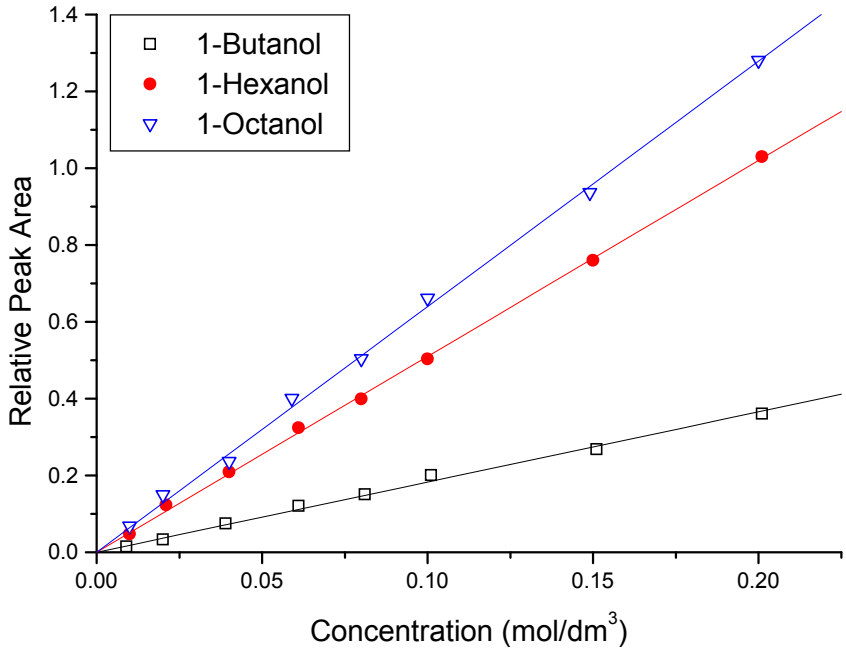

Figure 2.2 - Calibration of Perkin Elmer Elite Wax column for alcohol detection

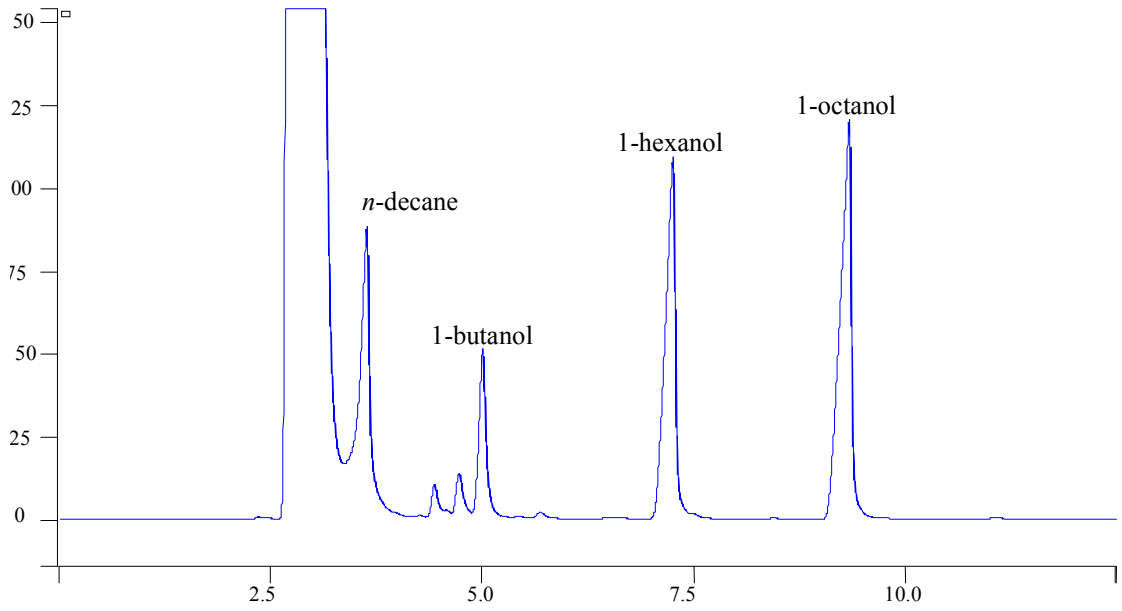

Figure 2.3 - Typical chromatogram from Perkin-Elmer Elite Wax column

Table 2.4 - Data for the calibration of Perkin Elmer Elite Wax column for alcohol determination

Analyte	Concentration (M)	Moles (mmol)	Area (Alcohol) / Area (n-Decane)	Response Factor	
				Octanol	Butanol
1-Butanol	0.009	0.045	0.015	0.735	3.000
1-Octanol	0.010	0.050	0.068		
1-Butanol	0.020	0.100	0.033	0.671	3.030
1-Octanol	0.020	0.100	0.149		
1-Butanol	0.039	0.195	0.075	0.847	2.600
1-Octanol	0.040	0.200	0.236		
1-Butanol	0.061	0.305	0.121	0.738	2.521
1-Octanol	0.059	0.295	0.400		
1-Butanol	0.081	0.405	0.151	0.795	2.682
1-Octanol	0.080	0.400	0.503		
1-Butanol	0.101	0.505	0.201	0.756	2.512
1-Octanol	0.100	0.500	0.661		
1-Butanol	0.151	0.755	0.268	0.796	2.817
1-Octanol	0.149	0.745	0.936		
1-Butanol	0.201	1.005	0.361	0.782	2.784
1-Octanol	0.200	1.000	1.278		
		Average Response Factors:		0.765 ± 0.053	2.74 ± 0.20

Calibration of the PONA GC column was conducted by determining a response factor for 1-octene. A representative chromatogram for alkene and alkane detection is shown in **Figure 2.4**. The number of moles of 1-octene in a sample could then be calculated from the response factor by using equation *3.1*. Data for the determination of the response factor for 1-octene are tabulated in **Table 2.5** and the chromatogram for identification shown in **Figure 2.4**.

$$\text{Response Factor} = \text{moles of } 1-\text{Octene} \div \frac{\text{Peak Area of 1 - Octene}}{\text{Peak Area of n - Decane}} \qquad 3.1$$

Table 2.5 - Data for the determination of the 1-octene response factor of Technokroma PONA column

Volume (µL)	Moles (mmol)	Area (1-Octene) / Area (n-Decane)	Response Factor
450	2.87	0.7923	3.62
900	5.73	1.5763	3.64
1350	8.60	2.4077	3.57
1800	11.47	3.2313	3.55
2250	14.34	4.1117	3.49
2700	17.20	5.0097	3.43
3250	20.07	5.9177	3.39
3600	22.94	6.9787	3.29
4050	25.80	8.000	3.23
4500	28.67	8.0510	3.56
4950	31.54	8.9610	3.52
5400	34.41	10.2980	3.34

Average response factor = 3.47 ± 0.13

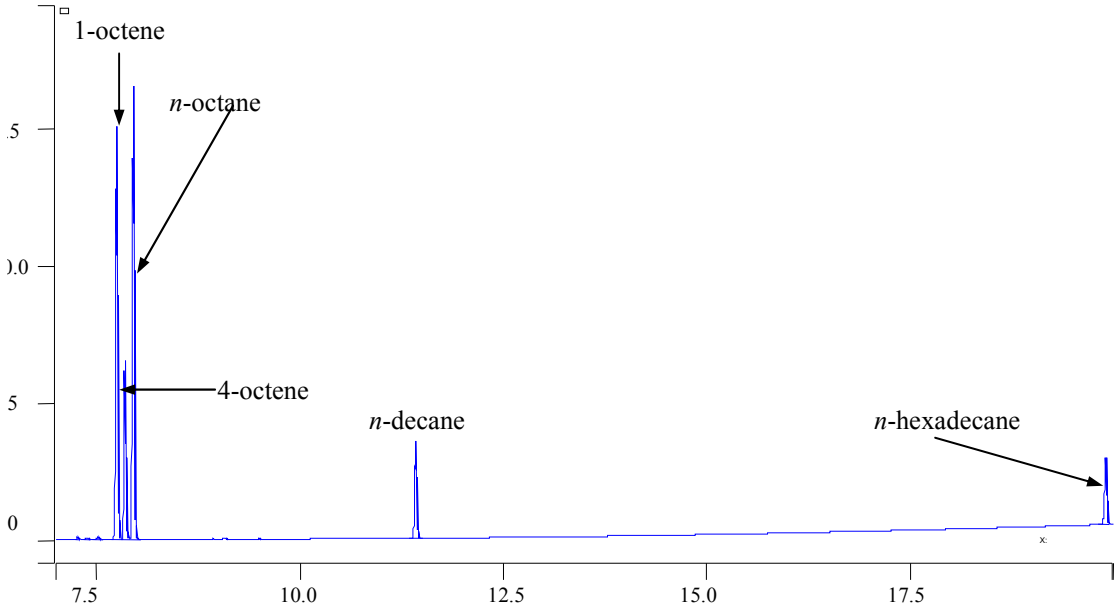

Figure 2.4 - Typical chromatogram from Teknokroma PONA column

2.6. ^{11}B NMR Spectroscopy Investigations

2.6.1. Kinetic Investigations: Reduction of Nitriles

Borane dimethyl sulfide (1M in dichloromethane, Sigma-Aldrich) was used without further purification. Acrylonitrile, propionitrile and benzonitrile (all Sigma-Aldrich) were dried by percolating over activated 3Å molecular sieve before use. Nitrile and borane dimethyl sulfide solutions were diluted to the relevant concentrations with dichloromethane (Merck) distilled over calcium hydride.

Standard techniques for handling of air- and moisture-sensitive materials were used for handling syringes, needles, canulae, glassware, quartz NMR tubes and reagents.

2.6.2. Kinetic Measurements

^{11}B NMR spectra were recorded at 160 MHz and referenced externally against $BF_3.OEt_2$ (0 ppm) on a Varian Unity Inova 500 spectrometer in 5 mm quartz tubes with proton decoupling (Waltz-16 sequence). A proton-coupled spectrum of the reaction was also recorded in order to identify reaction intermediates and products. A one-minute delay was allowed for mixing and temperature equilibration in the spectrometer, after which arrayed spectra were recorded at set time intervals. The temperature of the spectrometer was controlled to an accuracy of ± 0.5 °C. The kinetic data were obtained by monitoring the signal area of the borane dimethyl sulfide peak with time. The following peaks were identified over time in the ^{11}B NMR spectrum: $BH_3.SMe_2$ [quartet, $\delta^{11}B$ = -20.3 ppm, J_{B-H} = 110 Hz], CH_2=CH-C≡N.BH_3 [quartet, $\delta^{11}B$ = -25.7 ppm, J_{B-H} = 104 Hz] and vinylimino borane [triplet, $\delta^{11}B$ = -16.3 ppm, J_{B-H} = 111 Hz], EtC≡N.BH_3 [quartet, $\delta^{11}B$ = -26.2 ppm, J_{B-H} = 102 Hz] and C_6H_5C≡N.BH_3 [quartet, $\delta^{11}B$ = -25.8 ppm, J_{B-H} = 102 Hz]. Also identified in the spectrum were impurities in the $BH_3.SMe_2$ solution [singlet, $\delta^{11}B$ = -10.9 ppm; singlet, $\delta^{11}B$ = -13.5 ppm; singlet, $\delta^{11}B$ = -17.3 ppm; singlet, $\delta^{11}B$ = -15.4 ppm; singlet, singlet, $\delta^{11}B$ = -23.2 ppm; $\delta^{11}B$ = -29.2 ppm].

The concentration dependence study of the reduction of acrylonitrile was carried out under pseudo-first order conditions with the concentration of the nitrile in at least 10-fold excess over that of the borane. Pseudo-first order rate constants were calculated from single-exponential kinetic traces of integral data from arrayed NMR spectra on Origin 5.0 software. The activation parameters, $\Delta H^{\neq}$ and $\Delta S^{\neq}$, were determined from temperature studies of $k_2^{/}$ over the temperature range 15 – 30 °C.

2.6.3. Binding Studies

^{11}B NMR spectra of 500 μL samples of tri-*n*-butylborane (0.25 M) and respective Lewis bases (>2.5 M) in toluene (20% (v/v) Toluene-d_8) were recorded at 160 MHz and referenced externally against $BF_3.OEt_2$ (0 ppm) on a Varian Unity Inova 500 spectrometer in 5 mm quartz tubes with proton decoupling (Waltz-16 sequence). A ten-minute delay was allowed for temperature equilibration of the sample in the spectrometer, with the spectrometer controlled at an accuracy of ±0.5 °C. Changes in the shift of tri-*n*-butylborane were monitored over the temperature range 25 – 100 ºC relative to the internal standard, borane-triphenylphosphine (0.025 M). The following peaks were identified in the proton-decoupled ^{11}B NMR spectrum (**Figure 2.5**) at 25 ºC: B(*n*-C_4H_9)$_3$ [singlet, δ^{11}B = 84.3 ppm] and $BH_3.PPh_3$ [doublet, δ^{11}B = -39.8 and -39.9 ppm, $J_{B\text{-}H}$ = 46 Hz].

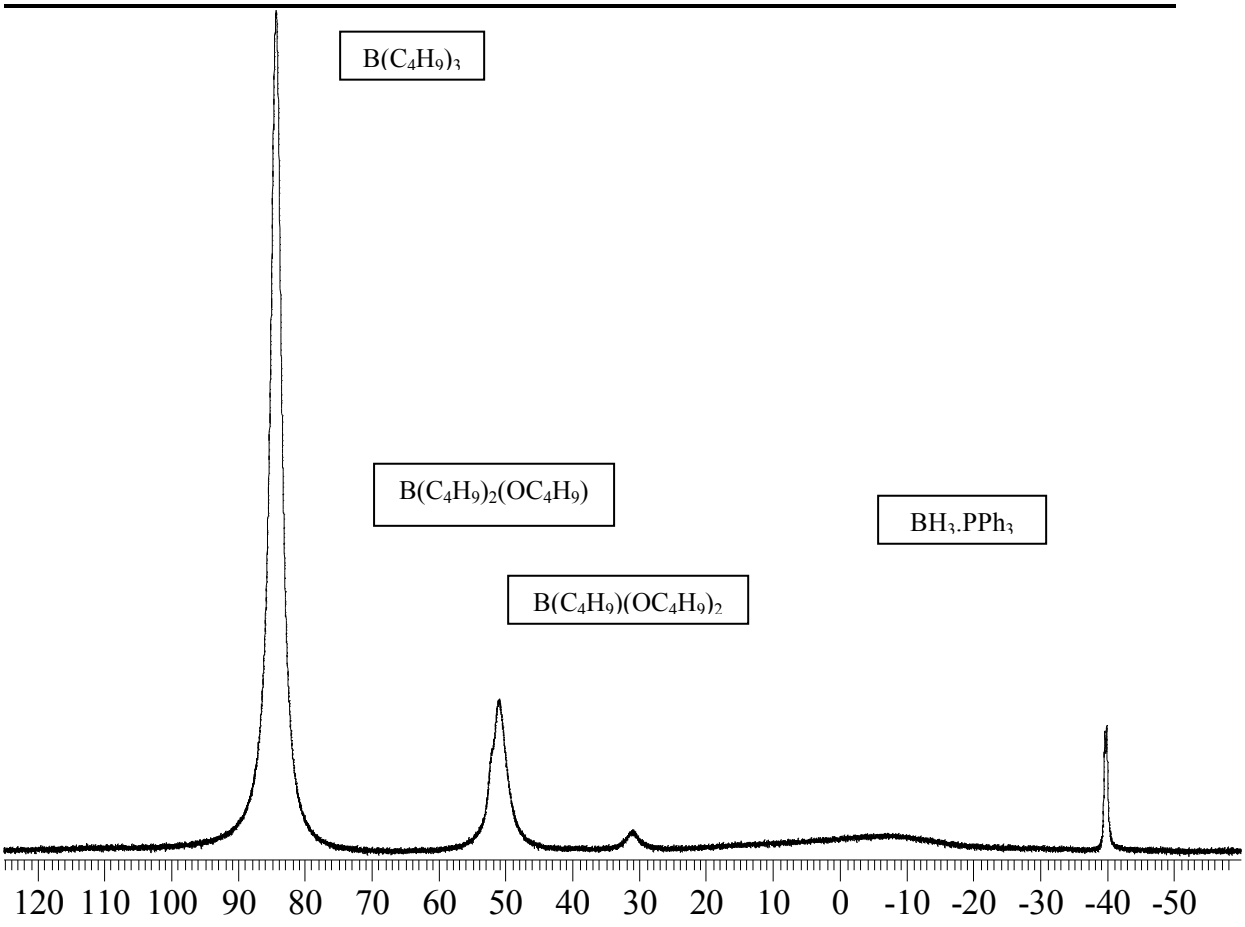

Figure 2.5 - Typical ^{11}B NMR spectrum from the binding studies of tributylborane with Lewis bases

2.7. Computational Modelling

Computational studies were performed on Spartan '04[148] computational software installed on a standard Windows 2000 operated PC (2.8 GHz Intel Pentium® IV processor with 512 MB RAM). The following procedure was adopted for generation of computational data:

- Generation of energy profile at SE/AM1 level
- Refinement of transition state and trialkylborane-Lewis base adduct structures at RHF/6-31G* level.[149,150]
- Optimisation of HF/6-31G* structure at B3LYP/6-13G* structures to afford single point energies, atomic charges and thermodynamic parameters.[151]

2.8. Kinetic Studies

2.8.1. Synthesis of Amine Boranes

The synthesis of amine boranes was achieved through a displacement synthesis based on that of Gatti and Wartik.[152] Borane-triethylamine (20 mmol) was dissolved in dry hexane (25 mL), stirred and cooled to 0 ºC using a dry nitrogen stream. The amine (20 mmol) or diamine (10 mmol), dissolved in dry THF (25 mL), was added dropwise to the borane solution through an addition funnel. The reaction was stirred at 0 ºC for an hour after which the ice-bath was removed and the reaction stirred at room temperature for a further three hours. The solvents were removed *in vacuo* (0.5 mmHg) and the resulting crystals washed with cold hexane over a filtration funnel to remove residual amine. The crystals were dried in an oven (60 ºC) for an hour and cooled in a silica-lined desiccator overnight.

2.8.2. GC studies

The concentration dependence study of the hydroboration of 1-octene with amine-boranes at 120 ºC was carried out under pseudo-first order conditions with the concentration of the 1-octene in at least 10-fold excess over that of the borane. 25 mL of a 1-octene solution in xylene was charged into a two-neck round bottom flask fitted with a rubber septum, a magnetic stirrer and a reflux condenser connected to a dry nitrogen stream. The octene was placed in an oil bath set at 120 ºC for half an hour to allow for equilibration. 25 mL of mixture of amine borane (0.04 M) and *n*-decane (0.04 M) in xylene were placed into pear-shaped flask fitted with a canula, a septum and a nitrogen inlet side arm. After equilibration for 30 minutes at 120 ºC, the nitrogen pressure was increased and the canula placed into the flask containing the 1-octene solution. Transfer of the borane of the borane solution into the 1-octene solution was achieved within 30 seconds. The reaction mixture was sampled by withdrawing 0.5 mL aliquots at 5, 10, 20, 30, 45, 60, 75, 90, 120, 150, 180, 240, 300, 360 and 480-minute intervals. A total of 7.5 mL was sampled from the reaction, representing 15% of the total reaction volume. The last two points of the data set were, therefore, ignored in the analysis of the data in order to counter the effects of

changing the reaction quotient by over-sampling. The aliquots withdrawn from the reaction flask were oxidised with sodium perborate and analysed as outlined in **Section 2.5.3**.

Pseudo-first order rate constants were calculated from single-exponential kinetic traces of octanol concentration data on Origin 5.0 software.

3. RESULTS AND DISCUSSION: DISPLACEMENT STUDIES

The cyclisation of trialkylboranes as discussed in **Section 1.6.2** presents an interesting field of study - the liberation of olefins from their trialkylboranes through dealkylation. The reactions discussed in **Section 1.6.2** typically take place at pyrolysis temperatures (> 200 ºC) *via* dealkylation of the trialkylborane and eventually lead to decomposition of the trialkylborane. An interesting opportunity to exploit is the tendency of trialkylboranes to undergo dealkylation at lower temperatures, especially isomerisation and displacement temperatures. For the purposes of this investigation, it becomes interesting and, indeed, important to consider the levels of dealkylation taking place at the temperatures employed for isomerisation and displacement reaction (100-200 ºC) as they (1) allow an insight into the rate-controlling reaction[16,126] during displacement and (2) give valuable information on the fate of trialkylboranes kept under the reaction conditions of isomerisation and displacement reactions. This chapter focuses mainly on the possibility of thermal dealkylation of trialkylboranes between 100 and 200 ºC and the consequences thereof. Specifically, the amount of octene liberated through this process and the placement of the boron atom along the alkyl chain, as a result of the application of heat, are of interest. Oxidation of the borane sample converts the alkyborane into an alcohol, with the placement of the alcohol indicating the placement of the boron atom along the alkyl chain. Such information allows for the determination of any isomerisation of the trialkylboranes having taken place; a process that would be counter-productive for the purposes of double bond isomerisation. Determination of the presence of *n*-alkanes in the reaction mixture was of particular interest as these would be indicative of decomposition taking place. Such a process has detrimental effects for an industrial process as it would result in a gradual loss of the borane that is meant to be recycled in the process. Decomposition of trialkylboranes to yield *n*-alkanes has been noted in pyrolysis studies,[105] and the possibility of its taking place in the 100-200 ºC temperature range is of interest.

The initial aim of the study was, therefore, to investigate the effects of temperature and time on the dealkylation process, with particular attention paid to the possibility of back-isomerisation and/or decomposition of the trialkylborane. The second aim of the study was to investigate the effect of a selected set of Lewis base compounds on the dealkylation reaction of trialkylboranes. Rutkowski and co-workers[137] have suggested the beneficial influence of Lewis base catalysts on the dealkylation reaction. Though the exact effect of these is not well understood, it can be surmised that the interaction is a Lewis acid-base one, which would allow for the stabilisation of the dialkylborane dimers formed through dealkylation. Examining the influence of Lewis bases on the extent of the dealkylation reaction would, therefore, provide insight into their action since the dealkylation step is thought to be the rate-controlling reaction of the displacement step.[16,126] The experimental details of the study are discussed in **Section 2.5**, with the primary data from these studies presented in **Appendix A**.

3.1. Thermal Dealkylation of Tri-*n*-Alkylboranes

Studies into the thermal dealkylation behaviour of trialkylboranes were conducted on tri-*n*-decylborane and tri-*n*-octylborane (**Section 2.5**). Emphasis was placed in identifying the oxidation products of the reactions. More importantly, the product distribution served as an indicator of the side reactions taking place during the thermal dealkylation process. The reactions of particular interest during the thermal dealkylation reaction were the back-isomerisation and decomposition of the trialkylborane. Investigating the relative distributions of alcohols after oxidation of the reaction mixtures revealed the existence of back-isomerisation. The alcohols obtained were the oxidation products of the alkyl chains of the alkylboranes and, therefore, served as indicators of the placement of the boron atom along a carbon chain.

Back-isomerisation is an expected process due to the presence of active boron-hydrogen bonds in a dealkylation reaction mixture. These bonds are generated at the high temperatures employed in the study and are expected to facilitate the isomerisation of the alkyl chains in alkylboranes. It has been shown in the literature that active boron-hydrogen bonds in the reaction mixture will facilitate isomerisation of the alkyl chain.[115,116]

Generally, the use of excess displacing agent has been effective in minimising back-isomerisation during displacement reaction.[16] The primary role of the excess displacing agent is to deactivate the boron-hydrogen bonds through hydroboration. In the current thermal dealkylation study, back-isomerisation was of concern since there is no displacing alkene added to the reaction to deactivate the boron-hydrogen bonds.

The other factor that needed to be taken into account in this study of the thermal dealkylation of trialkylboranes was the decomposition of the trialkylborane. Studies by various researchers have revealed that trialkylboranes undergo decomposition at high temperatures.[105-108] The process generally involves thermal dealkylation to liberate one molecule of alkene followed by decomposition of the dialkylborane. It has been shown in the literature that the alkene is liberated as an internal derivative;[105b] this suggests that back-isomerisation takes place prior to the decomposition process. This release of an internal alkene supports the proposed sequence[106,107] in which alkenes are liberated from trialkylboranes. The temperatures employed in this study were lower than those in literature examples (> 200 ºC),[105-108] and there are no studies in the literature that details the dealkylation reaction at the relatively mild temperature range of 100-200 ºC. However, dealkylation of the trialkylborane is expected at this temperature range as it is the mechanism by which displacement takes place. What is not clear is the possibility of reaction such as decomposition at the relatively mild conditions at which dealkylation is presumed to take place in this study.

3.1.1. Time Dependence in the Thermal Dealkylation of Tri-*n*-decylborane

The time dependence study on the thermal dealkylation of tri-*n*-decylborane at 150 ºC was conducted as outlined in **Section 2.51**. The temperature of 150 ºC was chosen because it is lower than the boiling point of 1-decene (boiling point = 168-170 ºC), in order to minimise evaporation of liberated 1-decene. The primary data from which the results in **Table 3.1** are obtained from is **Table 6.1** in **Section 6.1.1** of **Appendix A**. Other species identified in the product mixture were THF, 1-butanol and dihydro-2(3H)-furanone. These are not related to or do not originate from the hydroboration and dealkylation processes and were,

accordingly, not included in the mass balance. The mass percentages of the components were divided by the mass percentage of the internal standard (*n*-octane) to obtain relative mass percentages. The relative mass percentages were added to obtain a sum. Each relative mass percentage was then divided by this sum and converted into a percentage. A worked example of the manipulation of the primary data to obtain the presented results is provided in **Appendix A** (equation *6.1*).

The results of the thermal dealkylation study of tri-*n*-decylborane are presented in **Table 3.1** as relative percentages of the sample components at each hourly sampling point, with the internal pressure of the reactor at each sampling point indicated in the table. The results are also represented pictorially as in **Figure 3.1**, which shows the relative quantities of the oxidation products derived from the thermal dealkylation process and related reactions over a period of eight hours. **Table 3.2** shows the relative distribution of decanol.

Figure 3.1 reveals that there is no significant change in the product distribution of the system after an hour. This indeed seems to be a valid observation, when the pressure response of the system is taken into consideration. **Figure 3.2** shows the pressure response in a thermal dealkylation study on tri-*n*-decylborane at 150 ºC.

The main pointer towards this observation is the lack of change in the distribution of 1-decanol, the primary hydroboration-oxidation product, whose relative standard deviation is only 4% over the period of investigation. This is underpinned by the fact that the internal pressure of the reactor, mainly due to solvent volatilisation, is relatively constant at an average value of 750 kPa over the eight-hour period. On average the 2-decanol to 1-decanol ratio is 6:86. Products of particular interest in **Table 3.1** are 2-, 3- and 4-decanol. Their presence is an indication of back-isomerisation having taken place. It is also worth mentioning that the sum of the relative percentages of the 3- and 4-decanol isomers (**Table 3.1**) ranges from 4-9% of the decanol balance. Being that dealkylation is envisaged to occur *via* dealkylation, the total level of dealkylation can be estimated to be equal to the level of isomerisation and the free olefin. Re-hydroboration of the liberated isomers of decene in the presence of THF at 150 ºC and the pressure levels of the reactor must then be very rapid. The other products formed, *n*-decane and *n*-eicosane are also present in low levels and their formation will be discussed in **Sections 3.1.5** and **3.1.6**, respectively. The

results indicate clearly that the dominant product, with over 86 ± 3% distribution, is 1-decanol.

Table 3.1 - Product Distribution (Percentage) Results for the Time Effect Study of $B(decyl)_3$ at 150 ºC

Product	Product Distribution (%) at Time Interval (hours)							
	0*	1	2	3	4	6	7	8
1-Decene	0.53	0.38	0.18	0.28	0.16	0.21	0.16	0.08
n-Decane	4.68	6.65	3.09	3.94	1.45	2.04	2.18	1.33
n-Eicosane	1.28	0.67	0.71	0.84	0.48	0.54	0.62	0.39
1-Decanol	87.46	80.00	81.26	87.44	83.97	80.86	80.87	84.18
2-Decanol	5.85	5.80	6.72	3.23	5.96	6.97	7.09	5.96
3-Decanol	0.00	2.19	2.74	1.12	2.74	3.22	3.12	2.75
4-Decanol	0.00	4.18	5.31	2.95	2.82	6.11	5.90	5.41
5-Decanol	0.00	0.00	0.00	0.00	2.42	0.00	0.00	0.00
Σ(Decanol Isomers)	93.31	92.17	96.03	94.79	95.49	97.16	96.27	98.30
Internal Reactor Pressure (kPa)	0Ω	710	720	740	750	750	750	760

*Temperature = 29 °C

Ω Gauge pressure (internal reactor pressure)

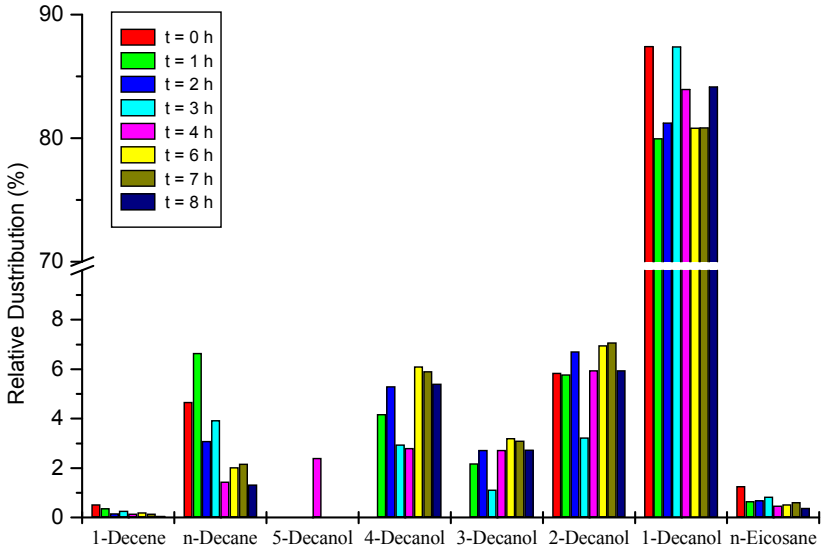

Figure 3.1 - Product distribution in the time dependence study on the thermal dealkylation of $B(decyl)_3$ at 150 ºC

The data in **Table 3.1** indicate that there is no change in the internal pressure of the reactor after the first hour. This is in accordance with the lack of change in the system over the eight-hour period of investigation. A study of the pressure response of tri-*n*-decylborane, whereby the internal pressure of the reactor was divided by the number of moles of trialkylborane, over an eight-hour period reveals an identical trend (see **Figure 3.2**).

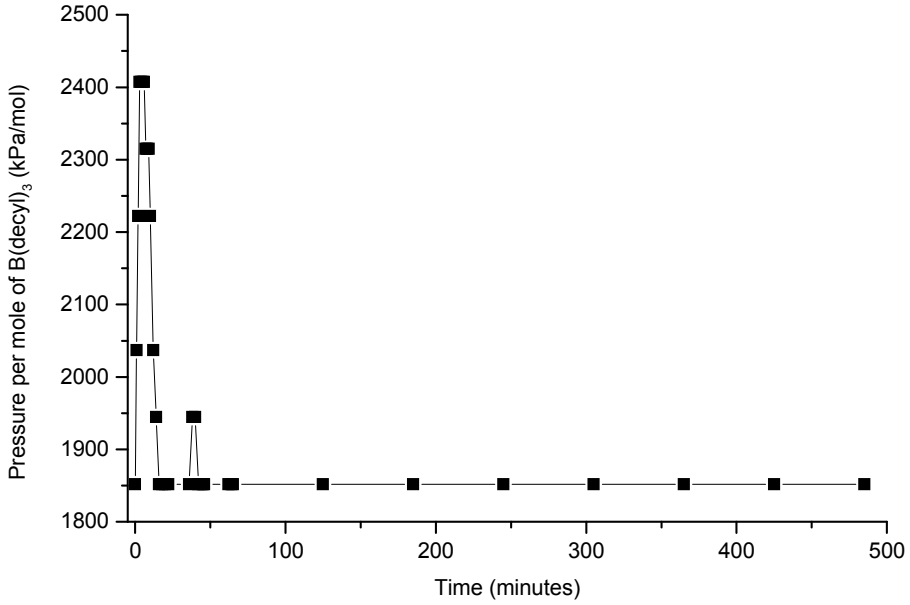

Figure 3.2 - Pressure response during a thermal dealkylation study on $B(decyl)_3$ at 150 ºC

Thus, as indicated by the trend in **Figure 3.2** there is no change in the pressure of the system after the first fifty minutes. This indicates that the system reaches equilibrium after fifty minutes, with most of the changes in the system occurring within the first five minutes. Accordingly, the results in **Table 3.1** indicate that the only observable change in the system occurs when the temperature of the system is changed from 29 ºC to 150 ºC. The decrease in the amount of 1-decene is due to the hydroboration process. The amount of 1-decanol decreases by 7% while the amounts of 3- and 4-decanol are observed to increase. To try to understand the distribution of decanol isomers in terms of the back-isomerisation process, the data in **Table 3.1** were re-analysed to reflect the selectivity of the decanol distribution for different decanol isomers. The results presented in **Table 3.2** indicate that back-isomerisation of the decyl chain of tri-*n*-decylborane does take place under the current experimental conditions. Most indicative of this is the change from the

typical 94:6 distribution of 1-decanol:2-decanol after hydroboration (0 hours) to a decrease in 1-decanol and a corresponding increase in 2-, 3- and 4-decanol isomers. This is an indication that back-isomerisation took place under these conditions. It can further be concluded that this is likely to be the case with all trialkylborane species when left at elevated temperature. Furthermore, it is worth noting that this equilibration of the alkyl chain distribution is complete within the first hour.

Table 3.2 - Distribution (Percentage) of Decanol Isomers During the Effect Study of $B(decyl)_3$ at 150 ºC

Time (hours)	Decanol Isomer Distribution (%)				
	1-Decanol	2-Decanol	3-Decanol	4-Decanol	5-Decanol
0*	93.7	6.3	0.0	0.0	0.0
1	86.8	6.3	2.4	4.5	0.0
2	84.6	7.0	2.9	5.5	0.0
3	92.3	3.4	1.2	3.1	0.0
4	85.8	6.1	2.8	2.9	2.5
6	83.2	7.2	3.3	6.3	0.0
7	83.4	7.3	3.2	6.1	0.0
8	85.6	6.1	2.8	5.5	0.0

*Temperature = 29 ºC, after hydroboration

3.1.2. Time Dependence in the Thermal Dealkylation of Tri-*n*-octylborane

The time dependence study on the thermal dealkylation of tri-*n*-octylborane at 100 ºC was conducted as outlined in **Section 2.5.1**. A temperature of 100 ºC was chosen as it is lower than the boiling point of 1-octene (boiling point = 122-123 ºC), and therefore evaporation of liberated 1-octene was minimsed. The results obtained are shown in **Table 3.3** as relative percentages. The results are also represented pictorially in **Figure 3.3**. The results were obtained from the primary data in **Table 6.3** in **Section 6.1.2** of **Appendix A** as explained in **Section 3.1.1**. The following species, not related to or originating from the hydroboration and dealkylation processes, were identified in the product mixture: THF, 1-butanol, dihydro-2(3H)-furanone, C_8H_{14}, octanal, $C_{16}H_{32}$ and dioctyl ether. These species

were, therefore, excluded from the mass balance. The data in **Table 3.3** and **Table 3.4** were obtained as described for tri-*n*-decylborane (**Table 3.1** in **Section 3.1.1**).

Table 3.3 - Product Distribution (Relative Mass Percentage) Results for the Time Dependence of $B(octyl)_3$ at 100 °C

Product	Product Distribution (%) at Time Interval (hours)								
	0*	1	2	3	4	5	6	7	8
1-Octene	0.00	5.75	3.70	-	8.79	1.86	11.91	4.92	8.72
C_8H_{16}	1.21	0.86	0.93	0.84	0.97	0.88	1.00	0.93	0.98
n-Octane	3.31	4.11	4.72	5.06	7.10	4.41	5.88	5.14	4.77
$C_{16}H_{34}$	0.40	0.37	0.47	0.62	0.55	0.47	0.50	0.55	0.39
n-Hexadecane	2.50	2.51	3.15	3.88	3.79	3.41	3.57	3.72	3.14
2-Butyl-THF	0.97	0.98	1.34	1.85	1.52	1.18	1.19	1.09	1.05
1-Octanol	86.37	81.25	81.75	84.19	74.57	84.21	73.06	80.73	78.11
2-Octanol	5.41	4.35	3.90	3.37	2.83	3.53	2.69	3.01	2.94
Σ(Octanol Isomers)	91.78	85.60	85.65	87.56	77.40	87.74	75.75	83.74	81.05
Internal Reactor Pressure (kPa)	0 Ω	190	190	190	190	190	180	180	180

*Temperature = 29 °C, after hydroboration

Ω Gauge pressure (internal reactor pressure)

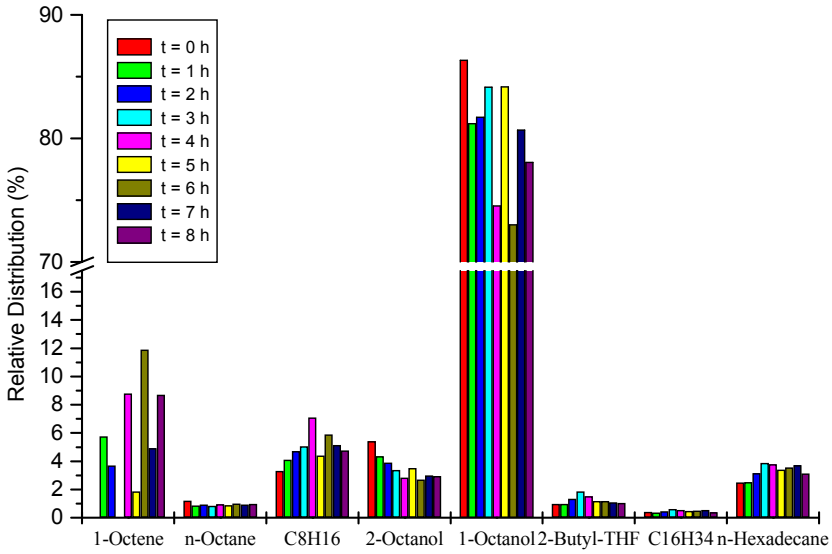

Figure 3.3 - Product distribution in the time dependence study on the thermal dealkylation of $B(octyl)_3$ at 100 °C

Table 3.4 - Distribution (Percentage) of Octanol Isomers During the Effect Study of $B(octyl)_3$ at 100 ºC

Time (hours)	Octanol Isomer Distribution (%)			
	1-Octanol	2-Octanol	3-Octanol	4-Octanol
0*	94.1	5.9	0.0	0.0
1	94.9	5.1	0.0	0.0
2	95.4	4.6	0.0	0.0
3	96.2	3.8	0.0	0.0
4	96.3	3.7	0.0	0.0
5	96.0	4.0	0.0	0.0
6	96.4	3.6	0.0	0.0
7	96.4	3.6	0.0	0.0
8	96.4	3.6	0.0	0.0

*Temperature = 29 ºC, after hydroboration

The most striking observation from the results presented in **Table 3.3** is the 6% increase on 1-octene in heating the system from 29 ºC to 100 ºC. This increase corresponds to a similar decrease in the distribution of 1-octanol, the primary hydroboration product. This observation is in contrast to the results obtained in the thermal dealkylation study of tri-*n*-decylborane, which was conducted at a higher temperature. Furthermore, the results do not show the presence of any other alcohol isomers besides 1-octanol and 2-octanol. The ratio of 1-octanol to 2-octanol remains constant at 96:4 throughout the eight-hour duration of the experiment (**Table 3.4**). This ratio is not markedly different from the literature value of 94:6.[21] This observation, coupled with the absence of other octanol isomers, precludes the possibility of back-isomerisation. This is in contrast to the emergence of 3- and 4-decanol isomers seen for tri-*n*-decylborane in **Table 3.1**. This may be explained by the difference in the temperature at which these studies were conducted. A temperature of 100 ºC is not expected to facilitate a rapid isomerisation rate, whereas a temperature of 150 ºC is close to the conventionally employed isomerisation temperature of 160 ºC.[16]

The trend for the thermal dealkylation of tri-*n*-octylborane is similar to that of tri-*n*-decylborane in that there is no significant change in the distribution of 1-alcohol after the first hour of reaction. The results for 1-octanol show only a 6% relative standard deviation. The constant pressure of the system within the reactor after the first hour underpins this constant distribution in the system. Accordingly, there is no further

liberation of 1-octene after the first hour. The reason behind the formation of *n*-octane and *n*-hexadecane is discussed in **Sections 3.1.5** and **3.1.6**, respectively.

An interesting development is the formation of 2-butyl-tetrahydrofuran, which increases to a level of 1% over the first three hours. Its presence seems to suggest that, rather than isomerise further, tri-*n*-octylborane undergoes decomposition *via* cyclisation. Studies by Köster *et al.*[105] reveal that when tri-*n*-octylborane decomposes it forms internal octenes and hydrogen as well as the formation of small amounts of 8-borahydrindane (equation *3.1*).[105a,b]

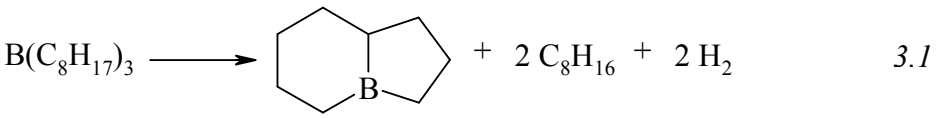

3.1

In general, tri-*n*-alkylboranes are converted into boron heterocycles (boracyclanes) at 150-200 ^{o}C.[105b] This process proceeds *via* dimeric dialkylborane intermediates (alkyldiboranes). This is in agreement with other decomposition studies on tributylborane, triamylborane and trihexylborane.[106,107] These studies have shown that alkene liberation (dealkylation) is the first step in the decomposition of trialkylboranes. This is then followed by the elimination of molecular hydrogen from the alkyldiborane. The cyclisation of the dehydrogenated dialkylborane product takes place in order to stabilise the alkylborane. It is therefore possible to propose a sequence for the formation of 2-butyl-THF through the decomposition of tri-*n*-octylborane. This is shown in **Scheme 3.1**.

One point of contention with the formation of 2-butyl-THF would be the ring size of the boracyclane. The five-membered boracyclane (borolane) formed is not consistent with literature precedents, where trialkylboranes with side chains that have more than six carbons form six-membered boracyclanes (borinanes).[107] Köster *et al.*[105b] have shown that the ring sizes are inter-convertible. At high temperatures, different-sized boracyclanes are in equilibrium with one another because of ring contraction or ring enlargement. Yet, the reaction temperatures employed in this study are not sufficiently high to cause decomposition of the trialkylborane. A more plausible explanation for the observed 2-butyl-tetrahydrofuran is the reductive cleavage of THF by the boron hydride.[27]

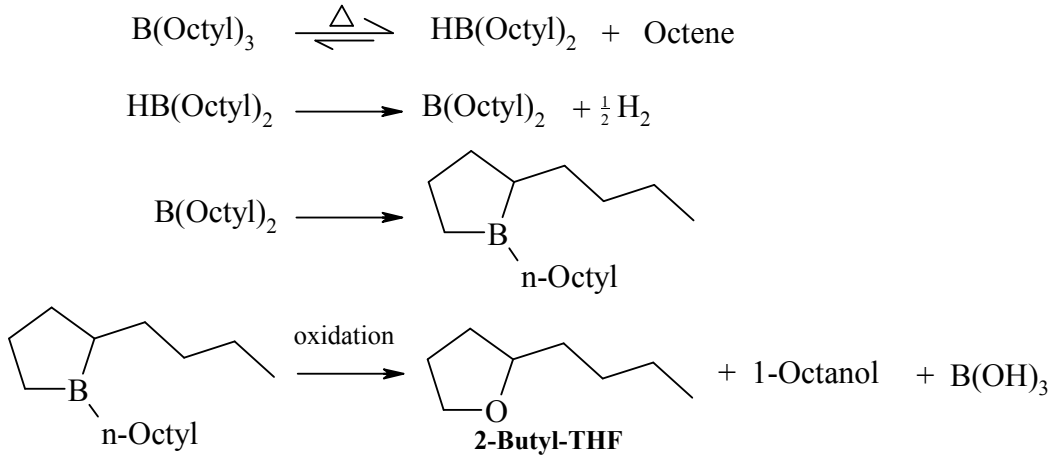

Scheme 3.1 - Decomposition and cyclisation of tri-*n*-octylborane[105]

Both the time dependence studies on tri-*n*-decylborane and tri-*n*-octylborane indicate that there is no change in product distribution after the first hour of the reaction. This is evident when looking at the sums of the alcohol isomers in **Table 3.1** and **Table 3.3**. These remain fairly constant after the first hour at the set temperatures. Thus any changes that do take place occur when heating the system from the room temperature to the set high temperature. While heating tri-*n*-octylborane from 29 ºC to 100 ºC resulted in a 6% liberation of 1-octene, no such alkene liberation was observed when heating tri-*n*-decylborane 29 ºC to 150 ºC. Furthermore, tri-*n*-octylborane does not undergo back-isomerisation beyond the second carbon of the alkene.

3.1.3. Temperature Dependence in the Thermal Dealkylation of Tri-*n*-decylborane

In order to understand the effect of temperature on the dealkylation process, the study was conducted at different temperatures and monitored within the first hour only as **Section 3.1.1**-**3.1.2** have shown that equilibration of the trialkylborane takes place within that time frame. The temperature dependence study on the thermal dealkylation of tri-*n*-decylborane was conducted as outlined in **Section 2.5.2**. The tri-*n*-decylborane solution used in the temperature dependence study was different from that used for the time dependence study

of the same compound since fresh batches of solution were made for each study. The solution was heated to the required temperature after which it was allowed to equilibrate at that temperature for an hour prior to sampling, quenching and analysis and heated to the next temperature in the experimental regime. The results are shown in **Table 3.5** as relative percentages of the product distribution at the investigated temperatures. These were extracted from the primary data as shown in **Table 6.5** of **Section 6.2.1** of **Appendix A**. The calculation and manipulation of the primary data is as explained in **Section 3.1.1**. The results in **Table 3.5** are represented pictorially in **Figure 3.4.**

Table 3.5 - Product Distribution (Relative Percentage) Results for the Temperature Dependence Study on $B(decyl)_3$

Product	Product Distribution (%) at Temperature (^oC)				
	50	100	150	200	28*
1-Decene	12.67	11.44	9.31	8.96	1.78
n-Decane	7.18	6.13	6.34	6.84	12.08
n-Eicosane	2.19	1.92	2.58	1.47	47.92
1-Decanol	73.25	76.81	80.00	81.94	37.82
2-Decanol	0.27	0.25	0.25	0.34	0.20
3-Decanol	4.33	3.34	1.44	0.40	0.20
4-Decanol	0.00	0.05	0.00	0.00	0.00
5-Decanol	0.11	0.05	0.08	0.06	0.00
Σ(Decanol Isomers)	77.96	80.50	81.77	82.74	38.22
Internal Reactor Pressure (kPa)	100	200	640	1510	0^{Ω}

*After cooling system from 200 ^oC

$^{\Omega}$ Pressure after reactor was cooled down to room temperature

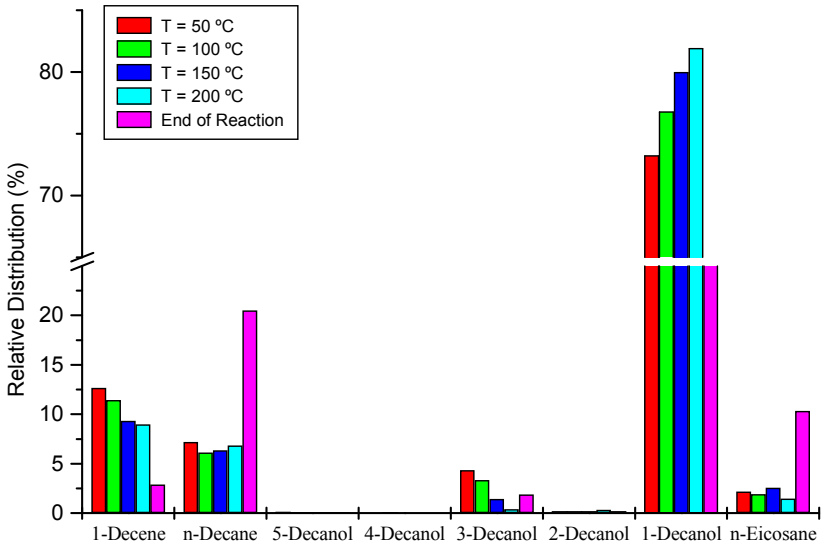

Figure 3.4 - Product distribution in the temperature dependence study on the thermal dealkylation of $B(decyl)_3$

The results shown in **Table 3.1** and **Figure 3.4** indicate that increasing temperature from 50 to 200 ºC does not have a marked effect on the product distribution of the thermal dealkylation results. This can be seen in the relatively constant value for the sum of the decanol isomers. The 9% increase in the amount of 1-decanol (50-200 ºC) corresponds to a 4% decrease in the amount of free 1-decene. The fact that hydroboration is still taking place implies that there are active boron-hydrogen bonds in the reaction mixture. This would be expected to facilitate the isomerisation of the decyl chain. Yet the distribution of 3-decanol, which is more prevalent in this study than the time dependence study, exhibits a decreasing trend as temperature is increased from 50 to 200 ^{o}C (**Table 3.5**). It would be expected that such an increase would contribute towards an increase in the distribution of 2-decanol. However, this is not the case as the relative distribution of 2-decanol remains constant and there are no noticeable changes in the distributions of 4- and 5-decanol. Thus, the decline in the distribution of 3-decanol may be accounted for in the increase in the distribution of 1-decanol. This suggests rapid movement of the boron atom from the third carbon to the terminal position.

The sample at the end of the reaction, when the reaction mixture had been allowed to cool to room temperature, provides one interesting observation: the distribution of 1-decanol

decreases by 44% as the temperature dropped from 200 °C to room temperature. This drop can be accounted for by the increases in the concentrations of *n*-decane and *n*-eicosane. Since these are derived from the quenching of alkylboranes, they offer indirect insight into the dealkylation process. When their relative percentages are added to those of the decanol isomers, the sum is 98%. Formation of *n*-decane and *n*-eicosane under these reaction conditions is discussed in **Sections 3.1.5-3.1.6**.

3.1.4. Temperature Dependence in the Thermal Dealkylation of Tri-*n*-octylborane

The temperature dependence study on the thermal dealkylation of tri-*n*-octylborane was conducted as outlined in **Section 2.5.2**. The tri-*n*-octylborane solution was heated to the required temperature after which it was allowed to equilibrate at that temperature for an hour prior to sampling, quenching and analysis. The results obtained from this study are shown in **Table 3.6** as relative percentages of the product distribution at the investigated temperatures. These were extracted from the primary data in **Table 6.7** of **Section 6.2.2** of **Appendix A**. The calculation and manipulation of the primary data is as explained in **Section 3.1.1**. The results in **Table 3.6** are represented pictorially in **Figure 3.5**.

Table 3.6 - Product Distribution (Relative Percentage) Results for the Temperature Dependence Study on $B(octyl)_3$

Product	Product Distribution (%) at Temperature (°C)				
	50	100	150	200	25*
1-Octene	4.43	2.78	1.50	1.40	7.30
C_8H_{16}	2.94	2.99	3.54	2.31	0.25
n-Octane	7.67	7.77	7.56	8.40	2.72
$C_{16}H_{34}$	0.41	0.38	0.58	0.32	0.58
n-Hexadecane	3.30	3.03	4.47	3.80	9.91
2-Butyl-THF	1.85	1.75	4.06	0.68	2.14
1-Octanol	79.25	81.25	78.19	75.15	76.79
2-Octanol	0.15	0.05	0.10	0.05	0.33
Σ(Octanol Isomers)	79.40	81.30	78.29	75.20	77.12
Internal Reactor Pressure (kPa)	150	300	600	860	0

*After cooling system from 200 °C

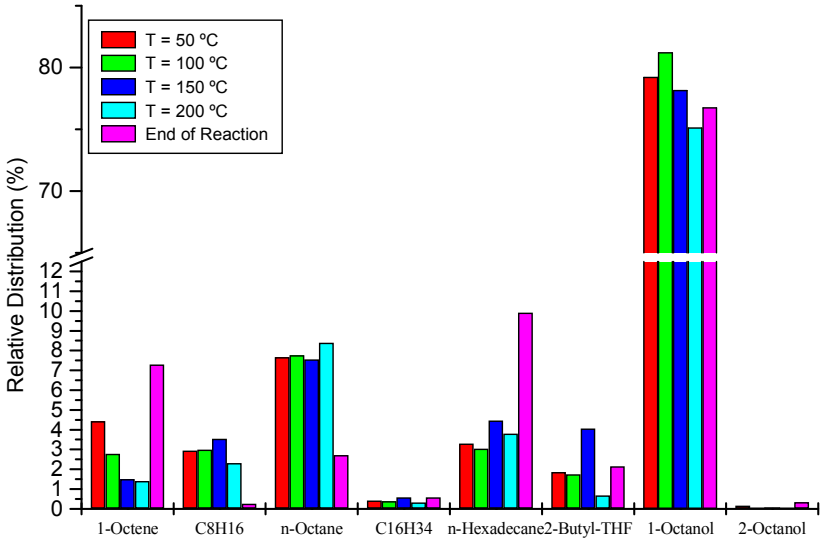

Figure 3.5 - Product distribution in the temperature dependence study on the thermal dealkylation of $B(octyl)_3$

The largest change in distribution on going from high temperature to room temperature is observed for *n*-octane and *n*-hexadecane. The average distribution of *n*-octane over the eight-hour period (**Table 3.3**) is 5.7% with a standard deviation of 1.1%, while the average distribution for hexadecane is 3.3% with a standard deviation of 0.5%. This invariance in the distribution of these species is reflected in the temperature-dependence study, where the distributions of *n*-octane and *n*-hexadecane in the 50-200 ºC range are 7.9 ± 0.4% and 3.7 ± 0.6%, respectively. The quantities of *n*-octane and *n*-hexadecane can be added to those of the octanol isomers (see **Section 3.1.5** for an explanation). While, the variation in these values on going to room temperature may appear significant on this basis, addition of the distributions of *n*-octane, *n*-hexadecane and the octanol isomers gives a distribution of 90 ± 2% on heating from 50-200 ºC and then cooling to room temperature. Thus, there is no significant change in the dealkylation process.

The distribution of octanol isomers indicates that there is no change in product distribution on heating the system from 50 to 200 ºC (**Figure 3.5**). Accordingly there is no liberation of 1-octene. This finding is in accordance with the results observed in the temperature dependence study on tri-*n*-decylborane (**Section 3.1.3**). The results in **Table 3.6** are in agreement with those of the time dependence study on tri-*n*-decylborane (**Section 3.1.1**) in that there are no other isomers of octanol further than 2-octanol, even when the

temperature is raised from 50 to 200 ºC. In contradiction to the amount of octanol isomers remaining constant, there is a decrease in the amount of 1-octene over the same temperature. Such a decrease can only be explained by vapourisation of unreacted 1-octene (boiling point = 122-123 ºC), as the results of the octanol isomers exclude the possibility of hydroboration. This is supported by the fact that the amount of unreacted 1-octene increased on cooling of the system to room temperature, while that of the octanol isomers did not change accordingly. Such an increase may be due to condensation of vapour phase 1-octene on cooling the reaction to room temperature.

The results of the temperature dependence studies on tri-*n*-decylborane and tri-*n*-octylborane have revealed that gradual heating of trialkylboranes has no marked influence on their distribution.

3.1.5. Formation of *n*-Alkanes during the Thermal Dealkylation of Trialkylboranes

In the case of the thermal dealkylation reactions of both tri-*n*-decylborane and tri-*n*-octylborane two unexpected products types were observed. The presence of *n*-decane and *n*-octane in the respective samples suggests the possibility of hydrogenation of an alkene or the reduction of an alkyl chain of an alkylborane having taken place during the thermal dealkylation reaction. The presence of *n*-hexadecane and *n*-eicosane indicates that dimerisation of the respective alkyl chains took place.

Most alkenes can be catalytically induced to add molecular hydrogen across their double bond at temperatures ranging from 0 to 275 ºC.[153] However this form of transition metal-catalysed hydrogenation/reduction of alkene double bonds bears no relevance to this discussion as no transition metals were used in any of the high temperature studies.

The most prominent explanation for borane-mediated hydrogenation in conjunction with alkylboranes is that of protonolysis.[154] In this indirect reduction of alkylboranes, an organic acid is used to cleave the boron-carbon bond of an alkylborane (equation *3.2*).

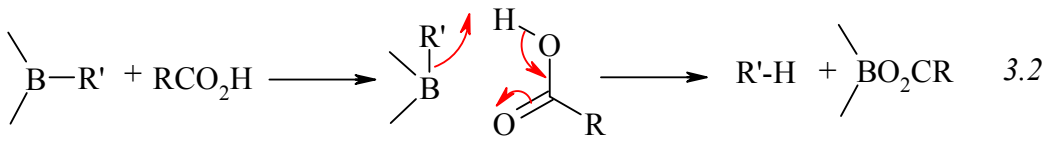

3.2

This, however, does not explain the formation of alkanes in time dependence studies, especially since there was no organic acid present.

It is also possible to indirectly reduce double bonds through the base hydrolysis of monoalkylboranes (equation *3.3*).[155] The reaction utilises dilute alkali solution as water alone cannot achieve this hydrolysis.

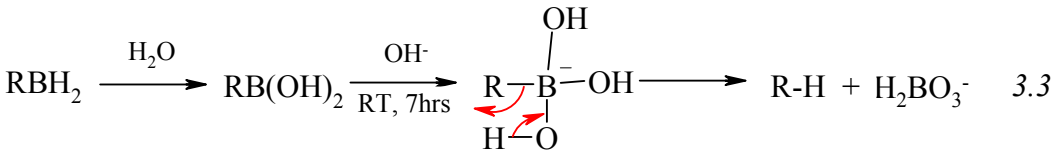

3.3

The combination of catecholborane in conjunction with Wilkinson's catalyst, $[RhCl(PPh)_3]^{3+}$, has also been used to reduce alkenes *via* the hydroboration reaction (equation *3.4*).[156] The reduction of the alkene is not the primary reaction as only 5% of the alkene affords the corresponding alkane.

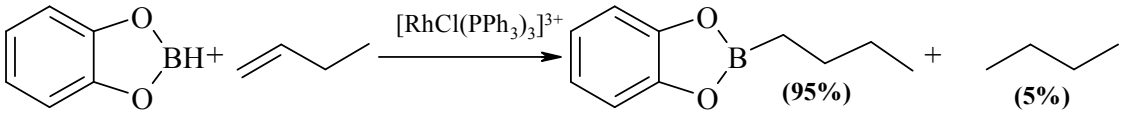

3.4

Borohydrides such as $NaBH_4$ are capable of reducing double bonds, often with the aid of metal catalysts. This indeed is the case in examples such as nickel boride[157] and the H_2PtCl_6-$NaBH_4$ or $RhCl_3$-$NaBH_4$ systems.[158]

There are, however, specialised examples in the literature in which metallic hydrides are capable of reducing double bonds without the aid of a transition metal catalyst. In such cases the double bond is polarised, as is the case with 1,1-diarylethenes[159]and double bonds that are conjugated with carbonyl groups.[160]

Non-transition metal-utilising examples of borane-mediated alkene reductions and hydrogenation can be found in the literature as early as 1961 (equation *3.5*).[161]

$$2\ B(C_4H_9)_3 + \underset{\textbf{(3 mole\%)}}{i\text{-}Bu_3B} \xrightarrow[H_2\ (17000\ kPa)]{3\ hrs,\ 225\ ^oC} \underset{\textbf{(100\%)}}{n\text{-butane}} \qquad 3.5$$

The results from this study indicated that any simple alkylborane is effective at hydrogenation of alkenes (equation *3.6*).

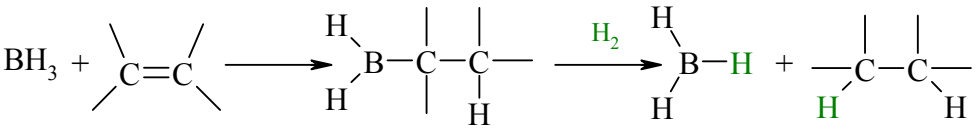

3.6

Lewis acids show an inhibitory effect on this reduction reaction. Lewis bases such as diglyme do not lower the required reaction temperature and the reaction is more dependent on temperature than hydrogen pressure.

Hydrogenolysis of trialkylboranes can also be used to reduce alkenes *via* the hydroboration reaction.[162] This method produces diborane as a product (equation *3.7*).

$$2\ B(C_4H_9)_3 + \underset{\textbf{(14000\ kPa)}}{6\ H_2} \xrightarrow[Pd\ Black]{12\ hrs,\ 200\ ^oC} 6\ n\text{-Butane} + B_2H_6 \qquad 3.7$$

The catalyst, palladium black, is not strictly necessary provided that the hydrogen to trialkylborane ratio is sufficiently high.

Tetrapropyldiborane and triethylborane catalyse the reduction of naphthalenes to tetralins (equation *3.8*). The borane acts as a pre-catalyst and is slowly converted to active polyborane catalyst.[163]

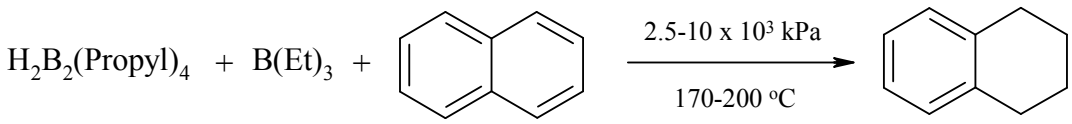

3.8

The most recent example of borane-mediated hydrogenation of alkenes involves the hydrogenation of sterically hindered alkenes with borane-methyl sulfide complex (BMS). BMS efficiently reduces sterically hindered alkenes like 2,3-diarylbicyclo[2.2.2]oct-2-ene to their corresponding hydrocarbons at room temperature and below in dichloromethane.[164] The process requires a mild one-electron oxidant (e.g., *Orange* $CRET^{+\cdot}$) or the anodic current (equation *3.9*).

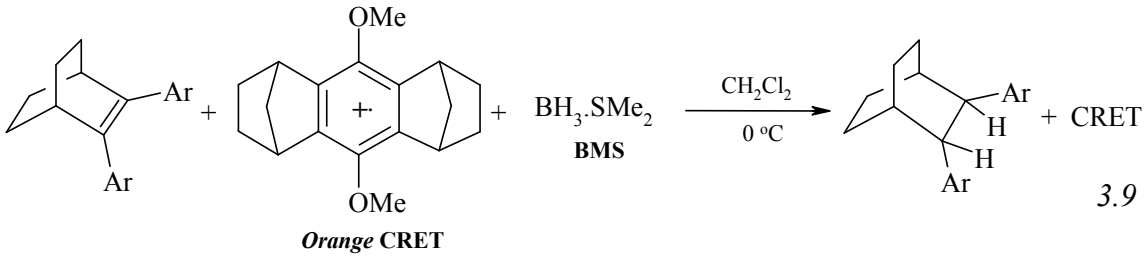

***Orange* CRET**

3.9

Alternatively, the reaction can be carried out without the oxidant or anodic current. It has been shown that a strong Brønsted acid such as HBF_4 can reduce alkenes.[164]

This direct protonation of the alkene affords a carbocationic intermediate that is efficiently reduced by borane (equation *3.10*).

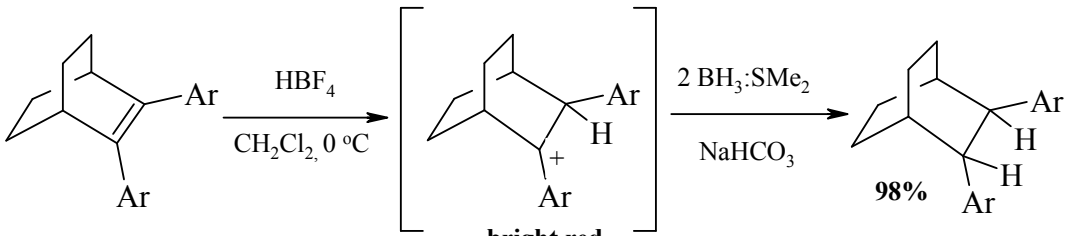

bright red

λ_{max} = 518 nm

3.10

The first step involves the transfer of a hydrogen atom to the radical to produce a carbocationic intermediate. BMS is capable of such rapid hydrogen atom transfer to

radicals. After this hydrogen atom transfer, the resultant boryl radical forms a complex with dimethyl sulfide (equation *3.11*).[165]

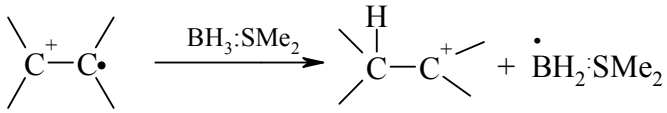

3.11

The second step involves a hydridic hydrogen transfer from another BMS to the carbocation intermediate to finally afford the hydrocarbon (equation *3.12*).

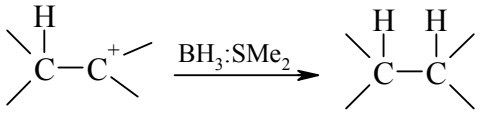

3.12

The formation of alkane, whether by reduction or hydrogenation, is therefore an explainable reaction. This type of product has been observed in decomposition studies of both tri-*n*-octylborane and tri-*n*-decylborane in the literature.[105b] The mechanism by which this process took place in the thermal dealkylation studies is however a point for consideration. The most likely explanation for the presence of alkanes during the thermal dealkylation is the base hydrolysis of monoalkylboranes (equation *3.3*). This is because the reactions were quenched with aqueous sodium hydroxide. All other reactions, leading to the reduction or hydrogenation of alkenes, which have been discussed, can be discounted since they typically require temperatures and hydrogen pressures (equations *3.5*, *3.7* and *3.8*) beyond the range of the dealkylation study that was undertaken.

There are two factors that favour the process of hydrogenation taking place. The first is that samples were quenched in an excess of sodium hydroxide. The second is that quenching was carried out at reaction temperatures of between 100-150 ^{o}C. The combination of these two factors makes a strong case for the formation of alkane from the hydrolysis route as shown in equation *3.13*. It is envisaged that under these conditions such a process would be accelerated, so that it would not require the seven hours stipulated in equation *3.3*. In this study quenched samples were left for four hours for hydrogen peroxide oxidation to take place.

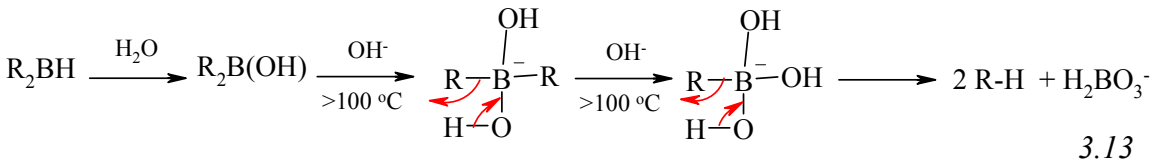

3.13

3.1.6. Dimerisation of Alkyl Chains during the Thermal Dealkylation of Trialkylboranes

The cause of the dimerisation or coupling of the alkene is more difficult to divine. It has been already mentioned (**Section 3.1.5**) that mass spectral analysis of alkylboranes leads to the formation of large amounts of alkane molecular ions with up to twice the number of carbons of a single alkyl group bonded to boron. This phenomenon is not observed for normal hydrocarbons. Certainly this may explain the presence of hexadecane in the case of octylborane and eicosane ($C_{20}H_{42}$) in the case of decylborane. The mechanism by which this process takes place is, however, still not clear.

The reactions of trialkylboranes with alkaline silver nitrate (equation *3.14*) were investigated by Brown *et al.*[166]. While this study by Brown is an example of borane-mediated dimerisation of alkyl chains, it does not explain the occurrence of the process in this thermal dealkylation study since no silver nitrate was used in the thermal dealkylation studies for which dimerisation was observed (**Table 3.1** and **Table 3.3**).

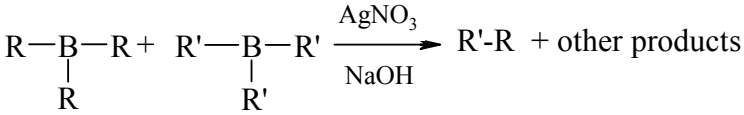

3.14

A patent by Johnson[167] offers another example of borane-mediated dimerisation of alkenes, yet the temperatures and the range of metal alkyls employed in that particular study make this an unsatisfactory explanation for alkene dimerisation in this thermal dealkylation study.

Table 3.7 displays a series of reagents that cause the simultaneous oxidation and dimerisation of the alkyl chains of alkylboranes.

Table 3.7 - Oxidation of tri-*n*-octylborane with different reagents at 0 °C[168]

Reagent	Product Distribution (%)	
	n-Hexadecane	1-Octanol
$AgNO_3/NaOH$	60-80	-
$Ce(NH_4)_2(SO_4)_3$	12	25
H_2O_2 (30 wt %)	max. 30	20-50
H_2O_2 (30 wt %)*	5	10
$H_2O_2/FeSO_4$ (6:10)	22	5
$H_2O_2/FeSO_4$ (6:0.1)	42	20
Nickel peroxide	10	-

* Reaction temperature = -50°C

From the reactions listed in **Table 3.7** only those employing hydrogen peroxide to achieve the oxidation and dimerisation of the alkyl chains are of relevance to this thermal displacement study.

The reaction of trialkylboranes with alkaline hydrogen peroxide affords the corresponding alcohols as the primary products in excellent yields. The reaction of neutral hydrogen peroxide, however, produces substantial quantities of dimeric hydrocarbons (equation *3.15*).[168]

$$\text{tri-}n\text{-hexylborane} \xrightarrow[\text{(ii) THF, RT}]{\text{(i) } H_2O_2,\ 0\ ^oC} n\text{-dodecane} + \text{1-hexanol} \qquad 3.15$$

Looking at **Table 3.8**, the reaction involving the H_2O_2/THF mixture to produce dimeric hydrocarbons is applicable over a range of tri-*n*-alkylboranes.[169]

Table 3.8 - Oxidation of trialkylboranes (BR_3) with neutral H_2O_2/THF solution[168]

Product	Product Distribution (%) for R Groups				
	C_4H_9	C_5H_{11}	C_6H_{13}	C_7H_{15}	C_8H_{17}
R-R	34	31.5	23	27	30
R-OH	35	35	40	40	20-50

This reaction is thought to involve a radical mechanism that affords alkyl radicals, which eventually react with each other to form the hydrocarbon dimers (**Scheme 3.2**).[168]

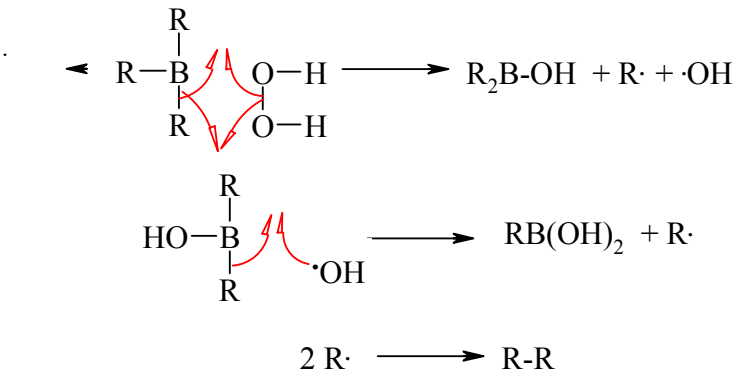

Scheme 3.2

When equimolar amounts of peroxide and trialkylborane are used, the primary products are the dimeric alkyl chain and the alcohol. If the amount of peroxide is higher, then the product distribution changes such that the oxidation of trihexylborane affords: *n*-dodecane, 5-methylundecane, 1-hexanol, 2-hexanol, *n*-hexane and 1-hexene.[169] This product distribution is not dissimilar to those obtained for the thermal dealkylation studies on tri-*n*-decylborane and tri-*n*-octylborane.

The finding that the oxidation of trialkylboranes also produces *n*-alkanes introduces some ambiguity in deciding which reaction is responsible for the formation of the reduced/hydrogenated alkyl chain derivatives in the dealkylation studies. Hence the formation of the *n*-decane and *n*-octane can be attributed to both the base hydrolysis of alkylboranes (equation *3.13*) and the oxidation/dimerisation of the alkyl chains (equation *3.15*).

The most important decision to make on the distribution of products from this dealkylation study is the importance of the contributions made by the various by-products to the mass balance. The data in **Table 3.6** and **Figure 3.5** indicate that the major components of the samples are those that arise from the primary reaction that is, the dealkylation of the trialkylborane to produce one molecule of terminal alkene and a molecule of dialkylborane. Furthermore, this mode of dealkylation is distinct from that seen in the

decomposition of trialkylboranes in that the first alkyl chain is liberated as a terminal alkene instead of a *cis* internal derivative. The data also indicate that the processes of decomposition, back-isomerisation, base hydrolysis and dimerisation contribute less than 6% to the total product distribution in the thermal dealkylation of tri-*n*-octylborane. These contribute less than 2% in the thermal dealkylation of tri-*n*-decylborane. These processes are, therefore, not seen as limiting factors in the future displacement reactions of trialkylboranes. In addition, it is evident that the thermal dealkylation is not an ideal route for displacement of alkenes from trialkylboranes.

3.1.7. Oxidation of trialkylboranes

The oxidation of organoboranes into the corresponding alcohols most used method in their quantitative and qualitative analysis. The reaction involves the attack of an oxygen nucleophile on the organoborane to afford an alcohol derivative and a boronic ester or acid. Organoboranes are quantitatively oxidised to alcohols by hydrogen peroxide and sodium hydroxide. This is by far the most commonly employed oxidation method for organoboranes (equation *3.16*).

$$R_3B + NaOH + 3\,H_2O_2 \rightarrow 3\,R-OH + B(OH)_3 \qquad 3.16$$

Oxidation proceeds well in water-miscible solvents such as diglyme and THF. However, oxidation is slow and gives lower yields in water-immiscible solvents such as diethyl ether and other hydrocarbon solvents. This problem is solved by the addition of ethanol as a co-solvent. The oxidation by alkaline hydrogen peroxide does not affect functional groups such as alkenes, alkynes, esters and nitriles. Aldehydes are slightly unstable under these oxidation conditions though they do not interfere with oxidation yields. It is not necessary to reflux the reaction mixture in order to achieve high yields of oxidation.[170] While this may hold true for short-chain organoboranes, longer-chain and both sterically hindered and branched organoboranes may need a heat input in order to accelerate oxidation. Typical yields for the oxidation of tri-*n*-hexylborane are shown in **Table 3.9**; where it is worth noting that the yields for oxidation decrease with increasing temperature. This is consistent with the erratic alcohol yields obtained in the dealkylation study undertaken.

Table 3.9 - Temperature Effects in the Oxidation of Tri-*n*-hexylborane[170]

Temperature (^{o}C)	1-Hexanol Yield (%)
0-5	97
25-35	96
50-55	94
75-80	89

The harsh nature of these oxidising agents is sometimes too harsh for some sensitive functional groups (e.g., aldehydes and allylic alcohols). Attempts at solving this problem have included the simultaneous addition of the hydroxide and the peroxide and the use of milder bases.[171,172,173] Sodium perborate (**Figure 3.6**) has been found to be an excellent oxidising agent for organoboranes.[174]

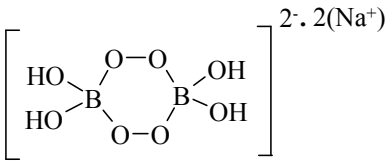

Figure 3.6 - Sodium perborate

Sodium perborate functions as a source of alkaline hydrogen peroxide in water or solvents with large aqueous content. The borate moiety helps to buffer and stabilise the compound against decomposition, and activate it towards nucleophilic oxidations through the associated $[B(OH)_3(OOH)]^-$ species. The reaction is temperature-dependent and, in extreme cases, can be enhanced by the addition of sodium hydroxide. In some cases, sodium perborate affords higher oxidation yields than those afforded by alkaline hydrogen peroxide oxidation.[174] Sodium perborate tolerates a variety of functional groups and has recently been shown to selectively oxidise the boron-carbon bond to a primary alcohol with ketones and aldehydes in close proximity on the alkyl chain.[175] The basis for distinctive chemistry of sodium perborate has been established by McKillop and Sanderson,[176] while the mechanism has been explored by Muzart.[177] More recently, a review has appeared furthering the information on the reaction of sodium perborate with various compounds.[178]

There are other oxidising agents reported in the literature. The oxidation of organoboranes by the molybdenum reagent MoO_5.py.HMPA (MoOPH) has been reported by Evans *et al.*[179] and further researched by Preston and Midland.[180]. Furthermore, a general, safe and scaleable method for the oxidation of boron-carbon bonds by Oxone® ($2KHSO_3.KHSO_4.K_2SO_4$) has also been reported.[181] Oxone® was found to have a higher onset of decomposition than 30% hydrogen peroxide, liberating less energy and thereby providing a better safety profile for the oxidation reaction. The fact that Oxone® is solid was an added advantage, allowing for the addition of precisely known amounts of oxidising agent. Yields of alkylboranes oxidation with Oxone® were found to be comparable to those of alkaline hydrogen peroxide oxidations.

The cheapness and mildness of oxidation by perborate, whose alkalinity obviates the need for addition of external base and solid form allows for the stoichiometric oxidation of organoboranes at room temperature in water, makes it the ideal candidate as a replacement for oxidation of trialkylboranes.

3.2. Thermal Dealkylation of Tri-*n*-octylborane after Removal of Solvent

The results of the temperature dependence study of tri-*n*-octylborane (**Section 3.1.4**) have shown that there was no significant increase in back-isomerisation taking place as a result of an increase in temperature. More importantly, the results have also shown that there are no significant levels of dealkylation (liberation) observed under the experimental conditions. Since the main purpose of the study is to ascertain if dealkylation is achievable through heating, the process was re-investigated with emphasis placed into determining the level of liberated olefin. The difference in this case was that the dealkylation process was carried out in the absence of any solvent.

The data presented in **Section 6.1** and **Section 6.2** of **Appendix A** show that the solvent forms by far the largest component in the system and is thought to hinder the dealkylation process by exerting an autogeneneous pressure that facilitates re-hydroboration. This is specifically in reference to the build up of pressure in the reactors, which would hinder the

liberation of olefin. Thus, in re-investigating temperature dependence in the thermal dealkylation of trialkylboranes, the solvent was removed from the reaction mixture after hydroboration. As stated above, the immediate objective of the study was to obtain the amount of liberated alkene, as opposed to general product distribution. Other than the removal of solvent after the hydroboration stage, the temperature dependence in the thermal dealkylation of tri-*n*-octylborane was undertaken similarly to **Section 3.1.4**. The results are presented in **Table 3.10** as a percentage increase in the amount of liberated alkene and illustrated graphically in **Figure 3.7**. The primary data used to calculate these results is shown in **Table 6.9** of **Appendix A**. The data were obtained by expressing the number of moles in the reaction mixture as a percentage of the total number of moles used in the hydroboration, as is shown in **Section 6.3** of **Appendix A**. Subtracting the amount of 1-octene in the solution before application of heat (25 ºC) from the amount of 1-octene in the sample (50-200 ºC) yielded the amount of 1-octene liberated through thermal dealkylation.

Table 3.10 - Temperature Dependence of the Liberation of 1-Octene from Thermal Dealkylation of $B(octyl)_3$

Temperature (^oC)	Liberated 1-Octene	
	mmol	%
25*	0.00	0.00
50	0.33	6.84
100	0.45	9.33
150	0.57	11.81
200	0.67	13.89

*After hydroboration

The trend shown in **Figure 3.7** shows that an increase in temperature corresponds to an increase in the amount of liberated 1-octene. The highest increase in 1-octene was observed at 200 ^oC with a value of 13.9%. The biggest increase in liberated 1-octene is in raising the temperature from 25 to 50 ^oC, after which the liberation of alkene increases linearly as the temperature in increased from 50 to 200 ^{o} C.

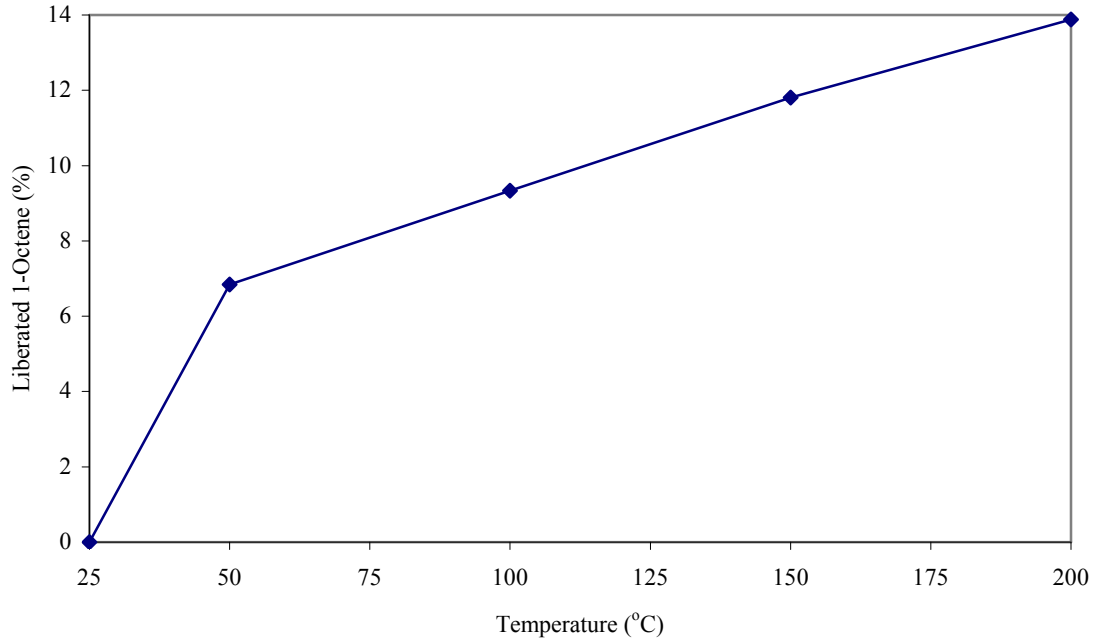

Figure 3.7 - Temperature dependence in liberation of 1-octene from the thermal dealkylation of $B(octyl)_3$

The clear trend observed in this study is in contrast to the lack of a clear trend in the case of the temperature dependence study in **Section 3.1.4**. This suggests that the Lewis base solvent (THF) does have an interfering role in the study of thermal dealkylation. The exact nature of this role remains a point for further investigation. There is the possibility that the solvent interacts with the dialkylboranes to form dialkylborane-solvent complexes. In a reaction that has no solvent dialkylboranes would exist as dimers. Dimers are known to react more slowly than their corresponding dialkylborane-solvent complexes.[78] This difference in hydroboration rates becomes important when considering that any liberated alkene is prone to re-hydroboration. In a reaction where there are dialkylborane dimers, such a process would be slow in comparison to a reaction where the dialkylborane exists as dialkylborane-solvent complex. Relatively slow re-hydroboration would then allow for the isolation of the liberated alkene. However, the pressure build-up caused by the THF in the reactor is more likely to be responsible for the lack of trend.

Having thus established that dealkylation does take place, it was decided to investigate the dealkylation process with the purpose of discovering what effect different Lewis bases have on the dealkylation itself and the product distribution with respect to the

trialkylborane. The choice of Lewis base was based on some of those proposed by Rutkowski as having an enhancing effect on the displacement reaction.[137] Studying the effect of these on the product distribution of the dealkylation reaction offers valuable insight into the fate of the trialkylborane – information which is scant in the literature. Accordingly, only catalytic amounts of Lewis base were used in the study and the selection of temperature and duration of the reactions was that of those felt to most mirror the conditions of the displacement reaction.

3.2.1. Effect of Lewis Base on Thermal Dealkylation of Tri-*n*-octylborane after Removal of Solvent

The dealkylation of tri-*n*-octylborane was investigated at 150 ºC (equation *3.17*) to monitor the effect of a selected series of Lewis bases on the dealkylation process in the absence of the other solvent.

$$B(n\text{-}C_8H_{17})_3 + \underset{\textbf{10 mol\%}}{\text{Lewis Base}} \xrightarrow[NaBO_3 \text{ oxidation}]{150\ ^\circ C,\ 8\ hrs} \text{Octanol isomers} + \text{Octenes} \qquad 3.17$$

The main objective of the study was to monitor the effect of these Lewis bases on the release of olefin from the trialkylborane with the expectation that carbonyl-type Lewis bases like DMSO, DMF and $(MeO)_3PO$ would enhance the liberation process through reductive elimination of the borane (equation *3.18*).

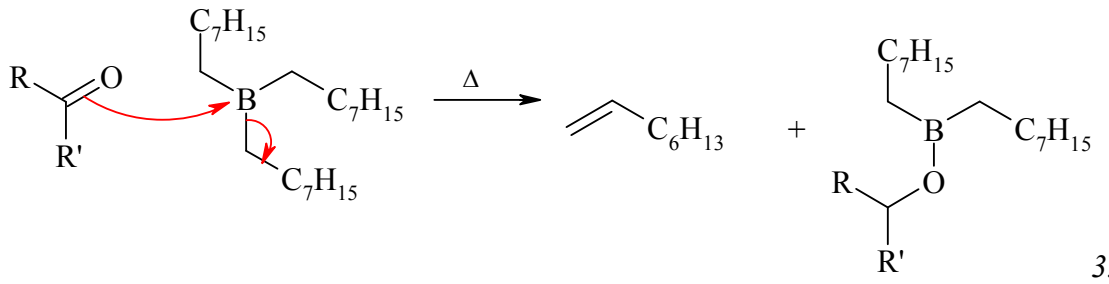

3.18

There are many examples in the literature where this approach is used to liberate olefins from their trialkylboranes[23,180] and it should be noted that this methodology is not suitable

for processes that would require the re-hydroboration of the trialkylborane. It was, however, thought interesting and important to investigate the effects of these compounds at low levels, especially as they are claimed to enhance the rate of the displacement reaction in the patent literature.[137] Phosphines and amines were also expected to enhance the dealkylation process by stabilising the dialkylborane formed after dealkylation of the first olefin molecule and inhibiting the dimerisation of the dialkylborane, thereby allowing further dealkylation.

The results of the study, presented in **Table 3.11, Figure 3.8** and **Figure 3.9**, show an interesting outcome from the use of catalytic amounts of Lewis base for the dealkylation process. The most interesting of these is that the use of DMF, DMSO, $(MeO)_3PO$ and HMPA results in the back-isomerisation of the octyl chain of B(*n*-octyl)$_3$ at 150 ºC, as is evident in the isomers of 3-octanol observed in **Table 3.11**. This occurrence of back-isomerisation is contrary to results presented in (**Table 3.3** and **Table 3.6**), where no isomerisation of the octyl chain was observed as an effect of temperature alone. It should be noted that the control study of the investigation (no Lewis base added) in **Table 3.11**, is in line with **Table 3.3** and **Table 3.6** and, accordingly, has an alcohol distribution of the typical hydroboration ratio. The back-isomerisation observed in **Table 3.11** can be explained in terms of the early investigations by Arase *et al.*[123,182] The earlier investigation into the effects of various solvents on the isomerisation of tri-2-pentylborane into tri-1-pentylborane shows that solvents such as anisole favour the forward isomerisation.[123] The later investigation shows that the effect of DMSO on heating of trihexylborane is to enhance back-isomerisation of the hexyl chain and that it it was only with the inclusion of anisole that this transformation was minimised.[182] Where the results observed in **Table 3.11** differ from those in the literature is in the recovery of alcohols. Whereas the results of Arase *et al.*[182] show that it is only with the use of equimolar amounts of DMSO that there is noticeable elimination of the alkyl group from the borane by the DMSO (67% hexanol balance), the results in **Table 3.11** show that such a significant diminishing of octanol balance is possible with a 10 mol%. Such a reduction in the octanol balance is also observed for DMF, HMPA and $(MeO)_3PO$, which also cause back-isomerisation of the alkyl chain. This elimination of the alkyl chain by these polar compounds, as indicated by the reduction in octanol balance, is in keeping with another investigation by Masuda *et al.*,[183] where polar compounds such as DMSO and DMF were found to eliminate an alkyl group from trialkylboranes. In the case of Arase *et al*.[182] such

a reduction can be justified by the elimination of some of the alkyl groups by the excess of DMSO. Such elimination is not conceivable in the case of the current study where only 10 mol% of Lewis base was used. In this instance, such a reduction in octanol balance can only be explained by thermal dealkylation of the trialkylboranes. Results from the same group[184] show that elimination of an alkyl group by polar compounds such as DMSO, DMF and benzaldehyde results in an inhibition of the isomerisation of the remaining alkyl chains or exchange (see **Section 1.6.1**) between trialkylboranes. Certainly, the data for the control experiment (**Table 3.11**) and, most especially, the Lewis base-catalysed reaction lends credence to this argument. It is interesting to note in the results of Arase *et al.*[184] that, in addition to curbing back-isomerisation of the alkyl chain, the addition of anisole (effectively as solvent) appears to curb elimination of the alkyl group by the elimination of the alkyl chain from trihexyl-, trioctyl- and tridodecylborane. There is no chemical means by which anisole could curb the elimination reaction, and the susceptibility of tributylborane to elimination when contrasted to the C_6-C_{12} olefins is in line with the increasing temperature requirements for dealkylating higher-chain trialkylboranes.[105-107]

The manner in which the polar Lewis bases add to the trialkylborane has bearing on the product distribution. Whereas the results of Masuda *et al.*[185] show that the there is no isomerisation of the alkyl chain after addition of the Lewis base, those of the current study are to the contrary. The study of Miyaura *et al.*[184] on the reactions of formaldehyde to trialkylboranes, shows that in the absence of air and free-radical initiators the addition of formaldehyde to a trialkylborane affords a borinate (R_2BOR) either directly or *via* dissociation of the trialkylborane, to the dialkylborane and olefin, and subsequent reaction with the formaldehyde. Such a scenario is possible for the addition of polar Lewis bases DMF, DMSO, HMPA and $(MeO)_3PO$ to trioctylborane. If the polar Lewis base adds directly (Equation *3.18*) to form borinates, then dealkylation of the borinate is possible and the boron-hydrogen bonds formed in this manner would enhance isomerisation. Isomerisation is also possible if the trialkylborane dissociates into a dialkylborane (whose boron-hydrogen bonds would catalyse isomerisation) and olefin prior to addition of the polar Lewis base. The lack of isomerisation observed by Masuda *et al.*[185] is explained by the diboron species (R_2B-O-BR_2), presented by Arase *et al.*,[182] formed during reaction with DMSO.

Another notable outcome from **Table 3.11** is that the other Lewis bases, while not causing back-isomerisation of the octyl chain, cause movement of the octanol to give a 2- to 1-octanol ratio uncharacteristic of the hydroboration reaction (as represented by the blank and control experiments). This suggests that isomerisation was taking place.

Table 3.11 - Effect of selected Lewis bases of the dealkylation of tri-*n*-octylborane 150 ºC

Lewis Base	Distribution of Octanol Isomers (%)[ϕ]			
	4-Octanol	3-Octanol	2-Octanol	1-Octanol
Blank[*]	0.0	0.0	6.1	92.9
Control[Ω]	0.0	0.0	4.0	83.9
DMF[‡]	0.0	0.1	5.4	65.9
DMSO[‡]	0.0	3.1	5.7	52.8
$(MeO)_3PO$	0.0	1.7	7.8	53.1
HMPA[‡]	0.0	1.8	6.0	54.4
Bu_3N	0.0	0.0	1.4	70.4
Bu_3P	0.0	0.0	2.5	78.1
$(MeO)_3P$	0.0	0.0	0.9	74.0
Tetramethylthiourea[‡]	0.0	0.0	1.1	69.5
Tetramethylurea[‡]	0.0	0.0	0.0	70.5

[ϕ] Octanol distribution corrected for octanol mass balance. Thus, the sum of the octanol isomers is the octanol mass balance

[*] Blank = Trialkylborane after hydroboration and removal of solvent

[Ω] Control = Trialkylborane without added Lewis base

[‡] DMF =  ; DMSO =  ; HMPA = 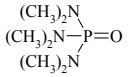 , Tetramethylurea = 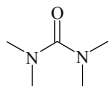 and Tetramethylthiourea = 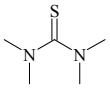

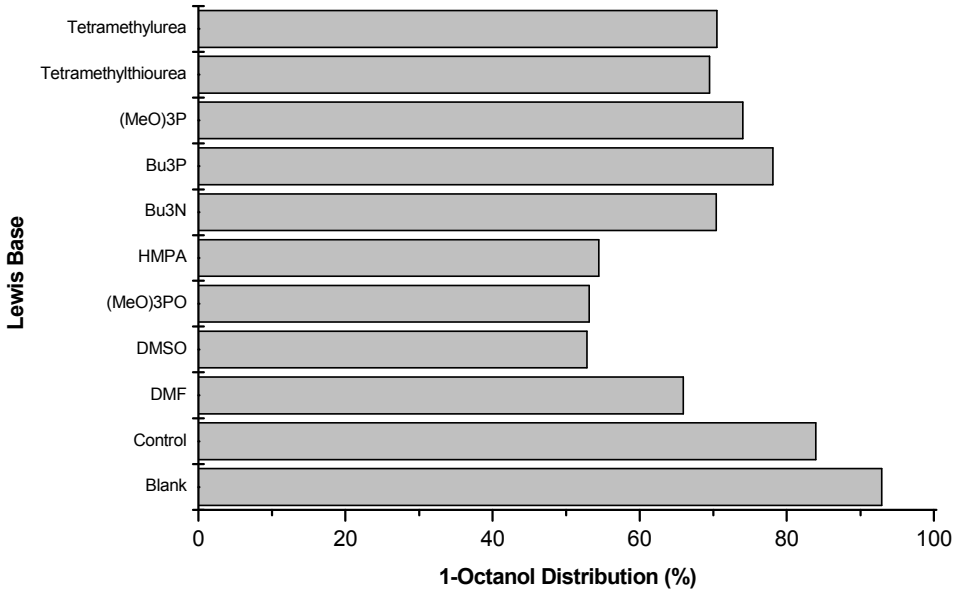

Figure 3.8 - Effect of selected Lewis bases on the alkyl chain distribution during the dealkylation of tri-*n*-octylborane 150 ºC

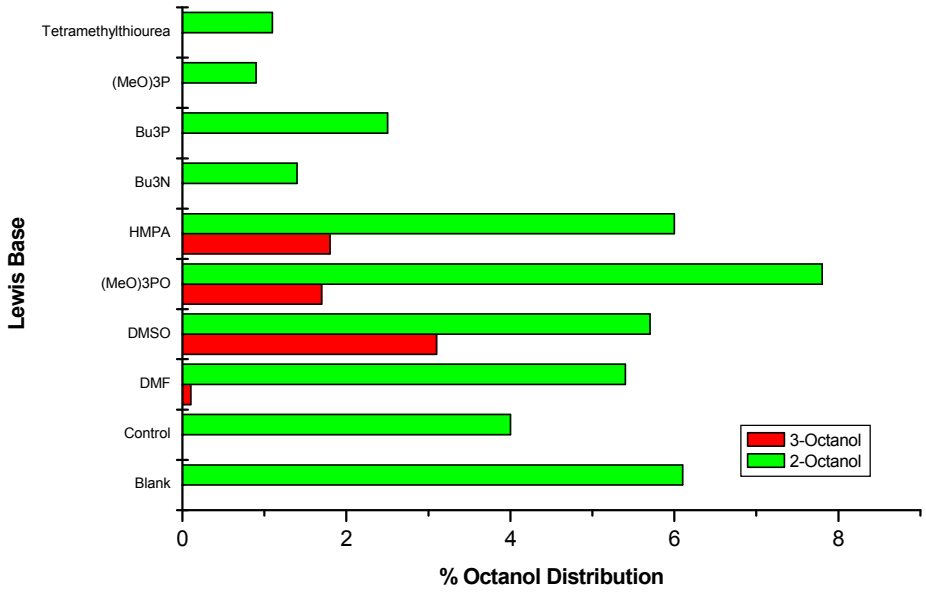

Figure 3.9 - Effect of selected Lewis bases on the alkyl chain distribution during the dealkylation of tri-*n*-octylborane 150 ºC

This effect, however, does not necessarily translate to the enhanced liberation of 1-octene through displacement of the olefin by the Lewis base (**Table 3.12** and **Figure 3.10**). This is the approach used by Arase *et al.*[123] to effect the displacement of olefins from trialkylboranes. In the current study, the amount of Lewis base added to the trialkylborane (10 mol%) is too minor to have a noticeable influence on the liberated alkene.

Table 3.12 and **Figure 3.10** also show that compounds that bind through the nitrogen atom (tributylamine and HMPA) inhibit the olefin liberation process, an effect that was observed by Logan.[185]

Table 3.12 - Effect of selected Lewis bases on the liberation of olefin during the dealkylation of tri-*n*-octylborane at 150 ºC

Lewis Base	Octene in sample (mmol)	Free octene in sample (As % of octene in trialkylborane)	Octene liberated through dealkylation (As % of octene in trialkylborane)
Blank*	1.9	8.0	0.0
Control	3.6	15.1	7.1
DMF	4.2	17.7	9.7
DMSO	10.6	44.9	36.9
$(MeO)_3PO$	5.5	23.3	15.3
HMPA	2.8	12.0	4.0
Bu_3N	1.5	6.3	0.0
Bu_3P	4.5	19.1	11.1
$(MeO)_3P$	17.6	74.7	66.7
Tetramethylthiourea	7.3	30.8	22.8
Tetramethylurea	13.1	55.8	47.8

* After hydroboration to generate the stock trioctylborane solution for the investigation. Liberated octene in this instance represents unreacted octene after hydroboration

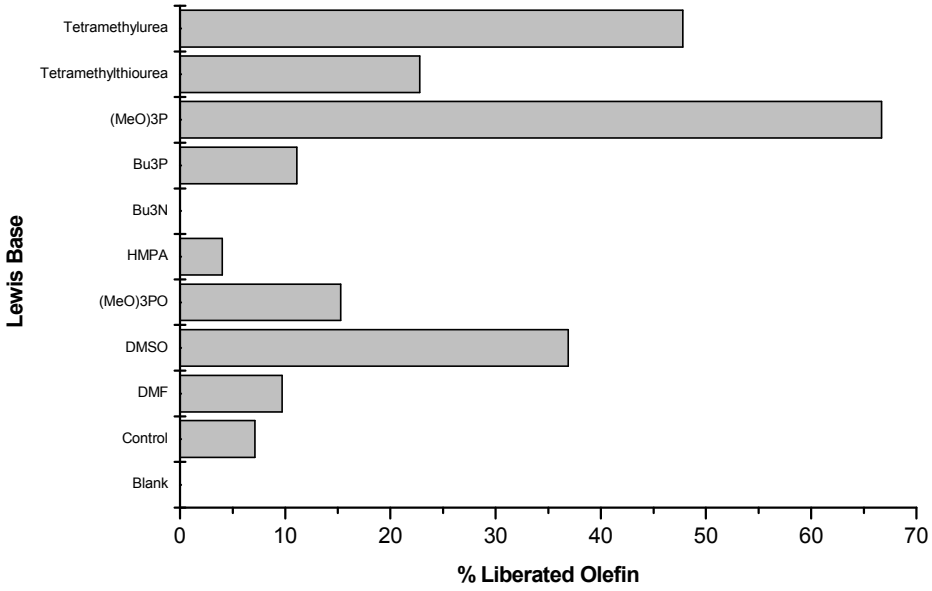

Figure 3.10 - Effect of selected Lewis bases on the liberation of olefin during the dealkylation of tri-*n*-octylborane 150 ºC

3.2.2. Effect of Lewis Base on Thermal Dealkylation of Tri-*4*-octylborane after Removal of Solvent

The dealkylation of B(*4*-octyl)$_3$ was also investigated at 150 ºC to monitor the effect of a selected series of Lewis bases on the dealkylation process in the absence of the other solvent.

$$B(4\text{-}C_8H_{17})_3 + \underset{\textbf{10 mol\%}}{\text{Lewis Base}} \xrightarrow[NaBO_3 \text{ oxidation}]{150\ ^\circ C,\ 8\ hrs} \text{Octanol isomers} + \text{Octenes} \qquad 3.19$$

Conventionally, this reaction is an isomerisation reaction, with temperature effecting the isomerisation of the octyl chain to afford the thermodynamically more stable tri-*n*-octylborane (see **Section 1.6.3**) as expected. The results due to the addition of catalytic amounts of Lewis base added to the reaction mixture are shown in **Table 3.13** and **Figure 3.11**. The results show that there is no beneficial effect from the addition of Lewis base to the trialkylborane on the extent of isomerisation of tri-4-octylborane to tri-*n*-octylborane,

with the distribution of octanols between 50 and 55% in the form of 4-octanol. **Figure 3.11** is constructed in assuming no effect for the addition of the Lewis base on the extent of isomerisation, such that all the data in **Table 3.13** would be the results of the small experiment. Thus, averaging these values for the different octanol isomers and investigating their standard deviations (black trend in **Figure 3.12**) shows that there is no appreciable difference between the "catalysed" and the control experiment. The lack of catalytic effect in the alkyl chain migration of tri-4-octylborane can be attributed to the lack of interaction between the Lewis base and the trialkylborane, which is due to the steric constraints around the boron atom.

Table 3.13 - Effect of selected Lewis bases on the alkyl chain distribution during dealkylation of tri-4-octylborane at 150 ºC

Lewis Base	Distribution of Octanol Isomers (%)			
	4-Octanol	3-Octanol	2-Octanol	1-Octanol
Blank	100	-	-	-
Control	53.2	24.9	12.6	9.7
DMF	55.3	21.0	11.4	11.2
DMSO	55.0	25.5	1.g3.0	6.5
$(MeO)_3PO$	54.4	25.1	12.3	8.1
HMPA	54.7	25.6	11.8	7.8
Bu_3N	53.7	25.4	14.4	6.5
Bu_3P	57.0	26.5	11.6	4.8
$(MeO)_3P$	52.9	25.5	13.0	8.5
Tetramethylthiourea	51.7	28.5	14.0	5.9
Tetramethylurea	51.3	27.5	13.4	7.8
Lit. Ref.*	1.4	1.8	4.5	92.2

*Isomerisation of tri-4-octylborane at 150 ºC in diglyme (bulk solvent) for 6 hours[186]

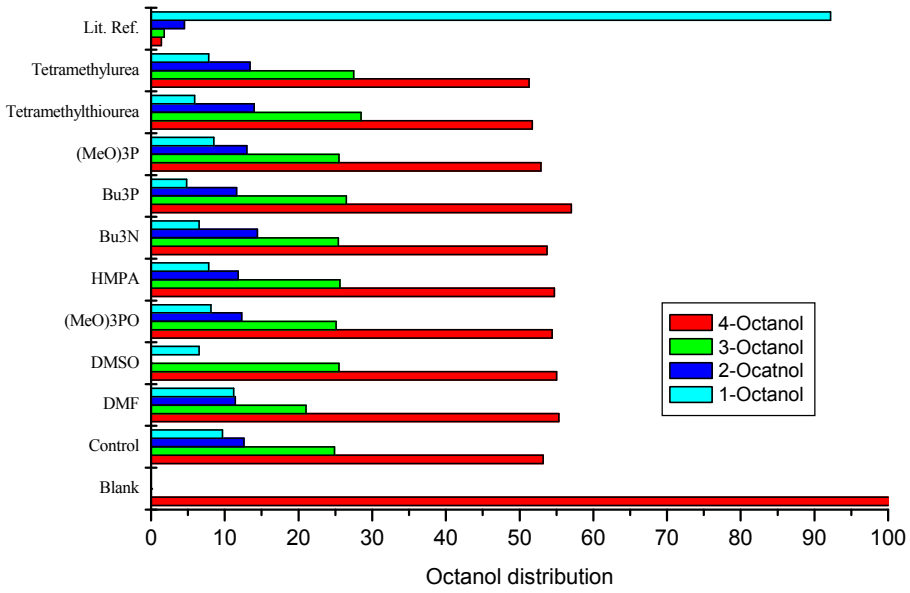

Figure 3.11 - Effect of selected Lewis bases on the alkyl chain distribution during the dealkylation of tri-4-octylborane 150 ºC

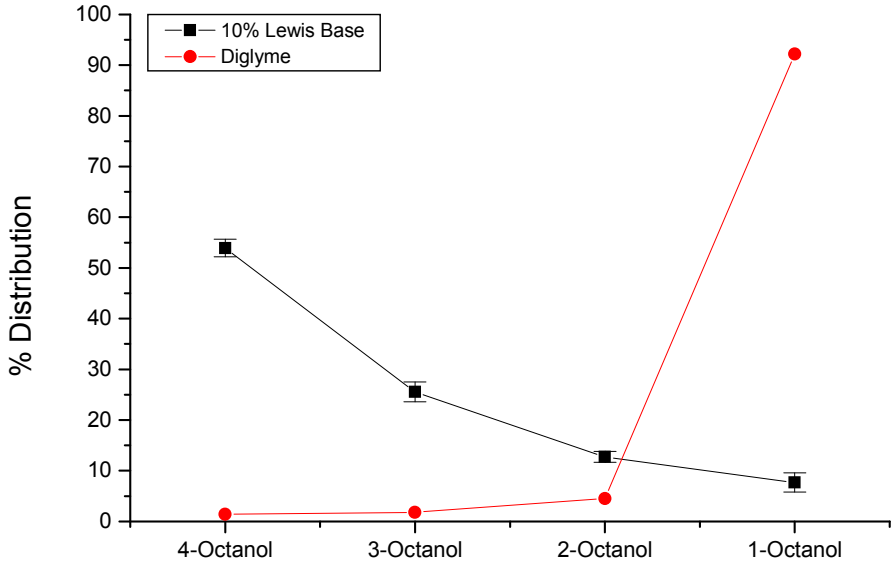

Figure 3.12 - Influence of solvent on the isomerisation of tri-4*i*-octylborane at 150 ºC

Another important observation from the results presented in **Table 3.13** is the relatively low level of isomerisation in the absence of solvent (table entry = Control) as compared to the isomerisation of tri-4-octylborane in diglyme at the same temperature

(table entry = Lit. Ref.*).[188] This suggests that diglyme does have an enhancing effect on the isomerisation reaction. That diglyme has been shown in the literature to have no marked effect on the isomerisation of (*t*-Bu)B(*i*-Bu)$_2$ to (*i*-Bu)$_3$B at 138 ºC[119] is not surprising in that *tert*-alkylboranes undergo isomerisation that involves complete dissociation.[119,120] Thus, the presence of excess boron-hydrogen bonds as proposed by Williams[121] would have no effect on the isomerisation reaction.

An investigation of the liberated olefin presents some supporting evidence for the lack of isomerising effect of Lewis bases in this instance (**Table 3.14** and **Figure 3.13**). The percentage of liberated olefin was calculated from the difference in the total number of moles of 4-octene of the samples from those of the blank experiment (i.e., the sample oxidised after the hydroboration process). Surprisingly, the levels of dealkylation are considerably lower than in the case of tri-*n*-octylborane, with no noticeable differences in the liberated olefin.

Table 3.14 - Effect of selected Lewis bases on the liberation of olefin during the dealkylation of tri-4-octylborane at 150 ºC

Lewis Base	Octene in sample (mmol)	Free octene in sample (As % of octene in trialkylborane)	Octene liberated through dealkylation (As % of octene in trialkylborane
Blank	1.9	0.26	0.00
Control	3.6	0.17	-0.09
DMF	4.2	0.26	0.00
DMSO	10.6	0.26	0.00
$(MeO)_3PO$	5.5	0.28	0.02
HMPA	2.8	0.24	-0.02
Bu_3N	1.5	0.25	-0.01
Bu_3P	4.5	0.21	-0.05
$(MeO)_3P$	17.6	0.31	0.05
Tetramethylthiourea	7.3	0.22	-0.04
Tetramethylurea	13.1	0.26	0.00

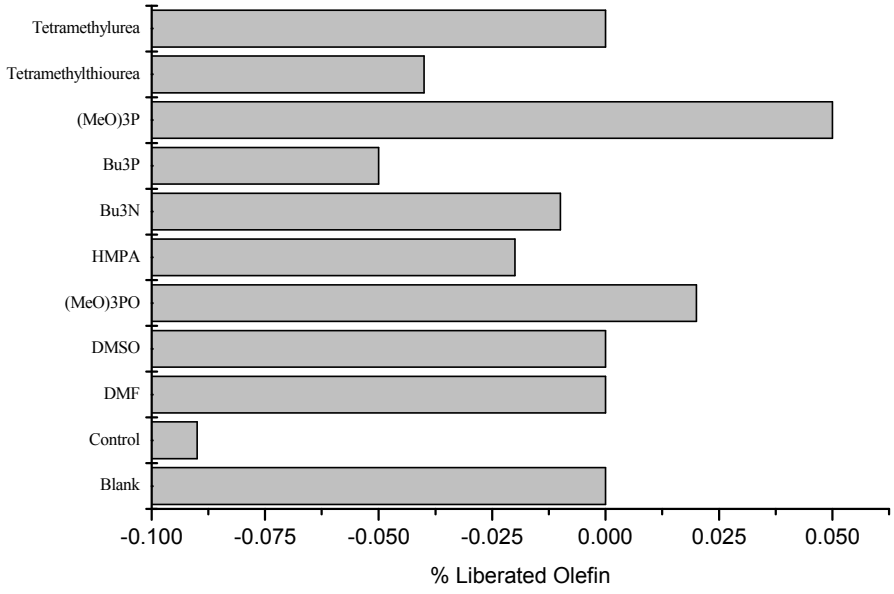

Figure 3.13 - Effect of selected Lewis bases on the liberation of octene during the dealkylation of tri-*n*-octylborane 150 ºC

The lack of observation of other isomers of octene suggests that there is no elimination/re-addition mechanism in operation. This is contrary to other dealkylation studies where extreme heating of trialkylboranes predominantly released the internal isomers of the olefins.[105-107] Interestingly, Rosenblum theorises that, in the liberation of butene during the pyrolysis of tri-*n*-butylborane,[106] the *trans*-2-butene observed is from 1-butene isomerised after its liberation from the trialkylborane. This makes sense in that *trans*-2-butene would be more stable than 1-butene at high temperature. If this is indeed the case, it would not be unreasonable to expect isomerisation of the liberated olefin into a more internal position under the high pyrolysis temperatures of Köster an co-workers.[105] This then begs the question of how isomerisation is taking place if there is no appreciable dealkylation (as part of an elimination/re-addition mechanism). An explanation that fits the isomers of octanol presented in **Table 3.11** is that, at 150 ºC, dealkylation generates a catalytic amount of boron-hydrogen bonds that allows isomerisation of the alkyl chain through a bridged mechanism, as opposed to the generally accepted successive de-hydroboration/re-hydroboration. Hennion and co-workers[119] have pointed out that a complete dissociation mechanism is likely not at play during the isomerisation of secondary alkylboranes. This is in much the same manner that isomerisation of *t*-tributylborane proceeds through a de-hydroboration mechanism while tri-*sec*-butylborane

derivatives isomerise through a partial dissociation mechanism.[120] The bridge hydrogen tautomerism mechanism (**Scheme 3.3**) championed by Williams[121] is in accordance with partial dissociation and is able to explain some observations that are not explained by the de-hydroboration/re-hydroboration mechanism.

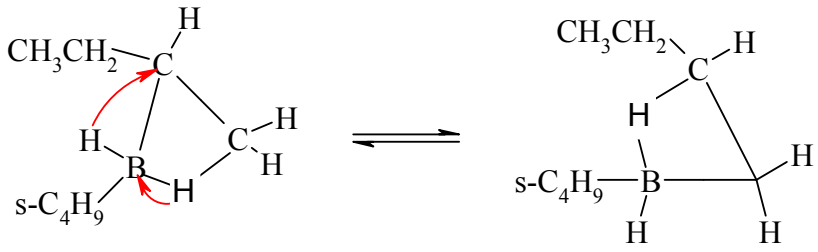

Scheme 3.3 - Bridge hydrogen tautomerism mechanism for partial dissociation of trialkylboranes[121]

Had there been successive de-hydroboration/re-hydroboration reactions other isomers of octene would have been expected in the reaction mixture. The lack of dealkylation of tri-4-octylborane might be viewed as surprising, especially since internal alkylboranes are expected to dealkylate more readily than *n*-alkylboranes.[105b] This statement should be qualified, however, by the reaction temperature at which Köster made this observation, which was a very high pyrolysis temperature. The temperature (150 ºC) at which the current dealkylation study was conducted is relatively low in comparison to the pyrolysis studies of Köster *et al* (> 200 ºC).[105] Under such conditions there would, presumably, not be enough energy for complete dissociation. The steric bulk of the tri-*i*-alkyl would also inhibit interaction with the catalysts; thereby eliminating any enhancement of the dealkylation process. The effect of the excess diglyme is explained by Williams who postulates that the catalytic effect of diglyme on the isomerisation reaction is brought about by persistent and remnant amount of diglyme-borane adduct, which provides borane for catalysis the isomerisation process.[121] Presumably, an isomerisation mechanism as envisaged in **Scheme 3.3** would not be as easy in a dimeric species. The diglyme would also be expected to enhance the dealkylation process.

3.3. Displacement Studies on Trialkylboranes

3.3.1. Displacement of Tri-*n*-butylborane with 1-octene

For the displacement reaction of alkenes to be feasible, fine-tuning of the standard displacement reaction is necessary. The most important factor to consider is the amount of time required to achieve quantitative displacement of an alkene from its trialkylborane. The literature generally describes the use of larger molecular weight alkenes to displace more volatile alkenes from their trialkylboranes, with the reaction being complete in 6-8 hours.[16] This is based on the assumption that the less volatile alkene will remain in the liquid phase to re-hydroborate the dialkyl- or monoalkylborane, while the more volatile displaced alkene can be recovered by distillation. Keeping both alkenes in solution can be achieved by applying pressure on the reaction system.

Kinetic evidence in the literature shows that boranes do not discriminate between straight chain alkenes of varying chain length.[80,81] This finding suggests that if both the displacing alkene and the displaced alkene were in solution, re-hydroboration would occur at the same rate for both alkenes. A contrary finding is that of Rutkowski,[134] which suggests that as the molecular weight difference between the trialkylborane and the displacing olefin is increased, then the rate of displacement increases.

The displacement reaction of tri-*n*-butylborane and 1-octene in large excess was investigated at 120 ºC in the absence of external solvent (**Scheme 3.4**) to investigate the influence of a selected series of Lewis bases on the displacement reaction as suggested by Rutkowski.[137] The results of the investigation are presented in **Table 3.15** and depicted graphically in **Figure 3.14**.

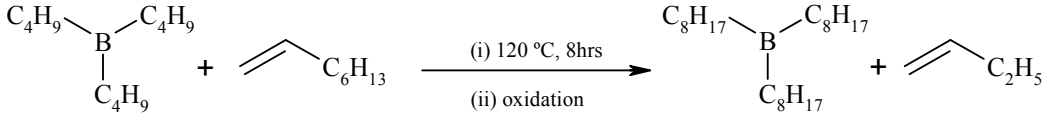

Scheme 3.4 - Experimental protocol for the investigation of the displacement reaction between tri-*n*-butylborane and 1-octene

The aim was of this investigation was not to re-investigate the influence of these Lewis bases investigated in **Section 3.2** on the rate of reaction, but the rather to look at the eventual outcome of the borane. In other words, it was deemed important to investigate the possibility of re-hydroboration after the liberation of the displaced alkene.

The results presented in **Table 3.15** show that the displacement reaction is slow, with less than 6% octanol being formed. It is worth noting that, in this study, only the formation of octanols, through hydroboration and subsequent oxidation, is taken as evidence of successful displacement. This contrasts with most literature investigations, where the formation of free (displaced/product) olefin is indicative of displacement. Monitoring only the concentration of displaced olefin gives a false picture as it does not give an indication of the fate of the alkylborane after the olefin release. It is of paramount importance for a successful catalytic cycle of hydroboration-isomerisation-displacement that the alkylborane does not undergo any reactions, other than hydroboration of the reactant olefin (displacing olefin), after release of the product olefin.

The data presented in **Table 3.15** and **Figure 3.14** show very little displacement having taken place. Primarily, this is due to the relatively low temperature (120 ºC) employed during the investigation. This was chosen in order that the bulk of the 1-octene (boiling point = 122-3 ºC) was in the liquid phase. The dealkylation study reported in **Section 3.2.1** has shown that results in the order of 9.3% and 11.8% (**Table 3.10**) can be expected for the dealkylation of tri-*n*-octylborane at 100 and 150 ºC, respectively. At 4.2% (**Table 3.15**), the value for the displacement of the control sample (*i.e.*, no Lewis base) appears low. It should be noted, though, that the value does not reflect displacement based on the amount of dealkylated butene, but rather displacement based on re-hydroboration by 1-octene. Save for tributylamine and tetramethylthiourea, the results for the oxygen-donor Lewis bases (DMF, DMSO, HMPA, trimethylurea and trimethyl phosphate) show negligible levels of displacement having taken place. Considering that displacement involves dissociation (dealkylation) of the trialkylborane into an olefin and dialkylborane (even monoalkylborane),[16,126] it becomes possible to rationalise the results observed for the oxygen-donor Lewis bases. It has already been discussed in **Section 3.2.1** how these Lewis bases do not interact with the trialkylborane *via* Lewis acid-base mechanism, but by

causing reductive elimination (equation *3.18*) of an alkyl group from the trialkylborane. This results in the formation of an alkoxyborane species, which is less likely to undergo re-hydroboration by 1-octene to afford the mixed trialkylborane.

Similarly low levels of displacement are observed for tributylphosphine and trimethylphosphite observed in the results presented in **Table 3.15**. Again the interaction of the Lewis base and the dialkylborane (formed through dealkylation) can be used to explain the observed results. Tributylphosphine and trimethylphosphite form very strong adducts to boranes. These adducts are extremely resistant to hydroboration even at elevated temperatures.[37] Thus, instead of a quick sequential hydroboration to afford a trialkylborane, the re-hydroboration in the case of these two Lewis bases is halted at some dialkyl or monoalkylborane-adduct stage, resulting in low displacement values.

The exceptions in **Table 3.15** are tributylamine and tetramethylthiourea. Tributylamine interacts, similarly to tribuylphosphine and trimethylphosphite, with the dialkylborane through a Lewis acid-base mechanism. At 120 ºC, dissociation of the amine-borane adduct can be expected as indicated by the hydroboration studies of Ashby[187] and Baker[188] and would result in re-hydroboration taking place. The difference is that the interaction is not as strong as that of the phosphines-donor compounds.

Table 3.15 - Effect of selected Lewis bases of the displacement reaction of tri-*n*-butylborane with 1-octene at 120 ºC

Lewis Base	% Distribution					Displacement*
	1-Butanol	4-Octanol	3-Octanol	2-Octanol	1-Octanol	(%)
Control	36.7	0.0	0.0	0.0	4.15	4.2
DMF	7.5	0.0	0.0	0.0	0.30	0.3
DMSO	15.4	0.0	0.0	0.0	0.44	0.4
$(MeO)_3PO$	10.3	0.0	0.0	0.0	0.00	0.0
HMPA	11.3	0.0	0.0	0.0	0.55	0.5
Bu_3N	50.3	0.0	0.0	0.0	3.53	3.5
Bu_3P	45.2	0.0	0.0	0.0	0.03	0.0
$(MeO)_3P$	64.3	0.0	0.0	0.3	0.09	0.4
Tetramethylthiourea	51.7	0.0	0.0	0.1	5.42	5.5
Tetramethylurea	56.8	0.0	0.0	0.0	0.07	0.1

* % Displacement = Sum of Octanol isomers

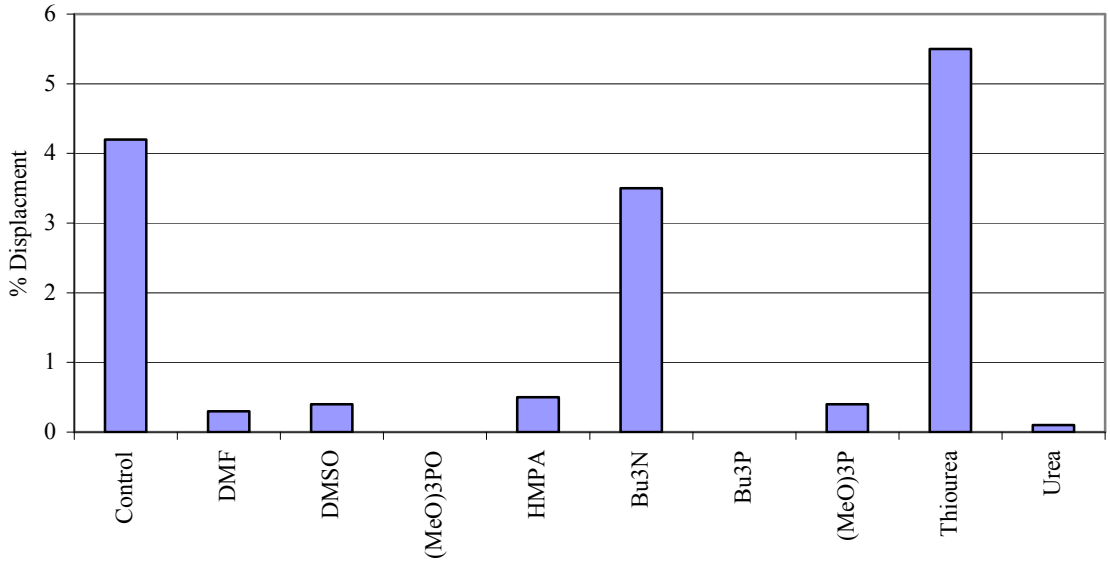

Figure 3.14 - Effect of selected Lewis bases on the yield of the displacement reaction of tri-*n*-butylborane and 1-octene at 120 ºC

In the case of tetramethylthiourea, conjugation means that a reductive elimination mechanism for interaction of tetramethylthiourea with the trialkylborane is not possible. This is further supported by the relatively low ionisation potential (8.02 eV) of tetramethylthiourea when compared to those of tetramethylurea (8.64 eV), DMF (9.12 eV), and DMSO (9.04 eV).[189] The ionisation potential can be used to gauge the probability of the π-electron in the carbonyl bond transferring completely to the boron atom to form a sigma bond as envisaged in equation *3.18*. This transfer is small in the case of tetramethylthiourea.

Contrary to the dealkylation study, the relative octanol distribution from the displacement study (**Table 3.15**) indicates that there is no back-isomerisation taking place during and after the displacement process. This is in the case of both the original and newly formed trialkylboranes. If anything, the product distribution of the octylborane favours the formation 1-octanol over 2-octanol. The major exceptions are tributylphosphine and trimethylphosphite. This may be explained by the very strong adducts they form with alkylboranes, which means that, instead of a quick sequential hydroboration to afford a trialkylborane, the re-hydroboration in the case of the two Lewis bases is halted at some dialkyl or monoalkylborane-adduct stage so that there are active boron-hydrogen bonds to

catalyse the isomerisation of 1-octanol to 2-octanol. This is essentially the reaction observed by Ashby[187] and Baker[189] in the high-temperature hydroboration with amine boranes. Surprisingly, though, no such observation can be made for tributylamine.

3.3.2. Displacement of Tri-*n*-butylborane with 4-octene

The displacement reaction of tri-*n*-butylborane and 4-octene in large excess was investigated at 120 ºC in the absence of external solvent (**Scheme 3.5**).

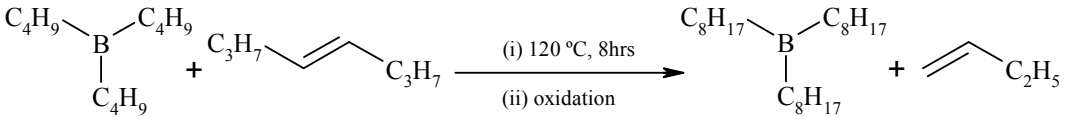

0.3 M **4.5 M**

Scheme 3.5 - Experimental protocol for the investigation of the displacement reaction between tri-*n*-butylborane and 4-octene

The results of the investigation are presented in **Table 3.16** and depicted graphically in **Figure 3.15** and **Figure 3.16**.

Table 3.16 - Effect of selected Lewis bases on the product distribution of the displacement reaction of tri-*n*-butylborane with 4-octene at 120 ºC

Lewis Base	% Distribution					Displacement*
	1-Butanol	4-Octanol	3-Octanol	2-Octanol	1-Octanol	(%)
Control	25.1	1.2	3.3	19.0	0.14	23.7
DMF	30.7	0.8	1.3	17.0	0.10	19.2
DMSO	31.3	1.6	1.2	17.3	0.10	20.2
$(MeO)_3PO$	23.5	0.9	1.6	16.8	0.08	19.3
HMPA	11.7	0.7	2.0	16.7	0.55	20.0
Bu_3N	14.2	1.0	1.6	19.6	0.00	22.2
Bu_3P	8.4	0.5	1.1	16.0	0.03	17.6
$(MeO)_3P$	15.7	0.9	1.5	13.9	0.09	16.3
Tetramethylthiourea	9.4	0.8	1.3	15.3	0.00	17.5
Tetramethylurea	8.1	0.8	1.5	15.8	0.07	18.2

* % Displacement = Sum of Octanol isomers

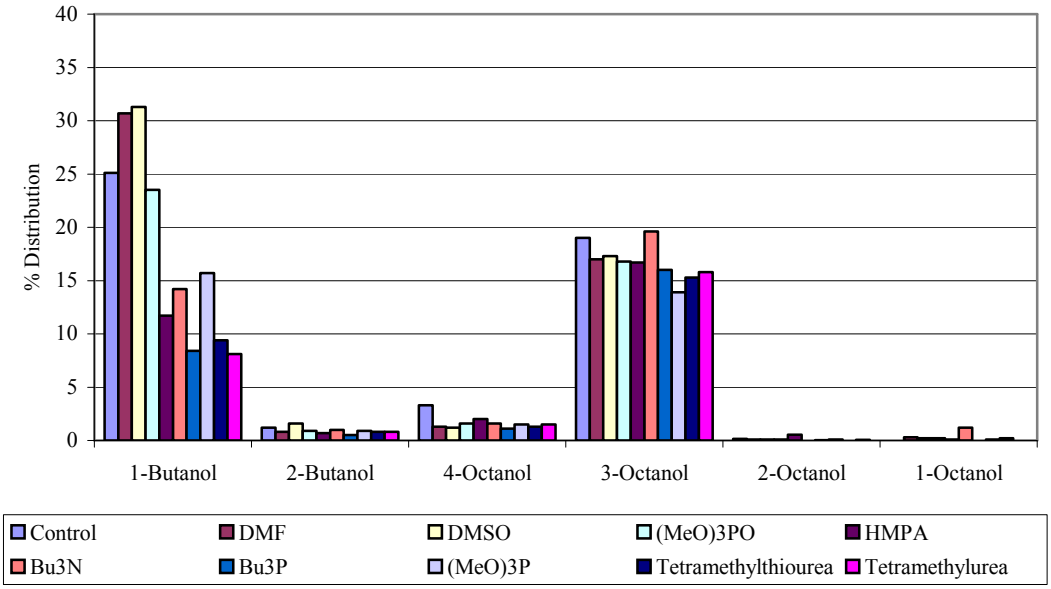

Figure 3.15 - Effect of selected Lewis bases on the product distribution of the displacement reaction of tri-*n*-butylborane with 4-octene at 120 ºC

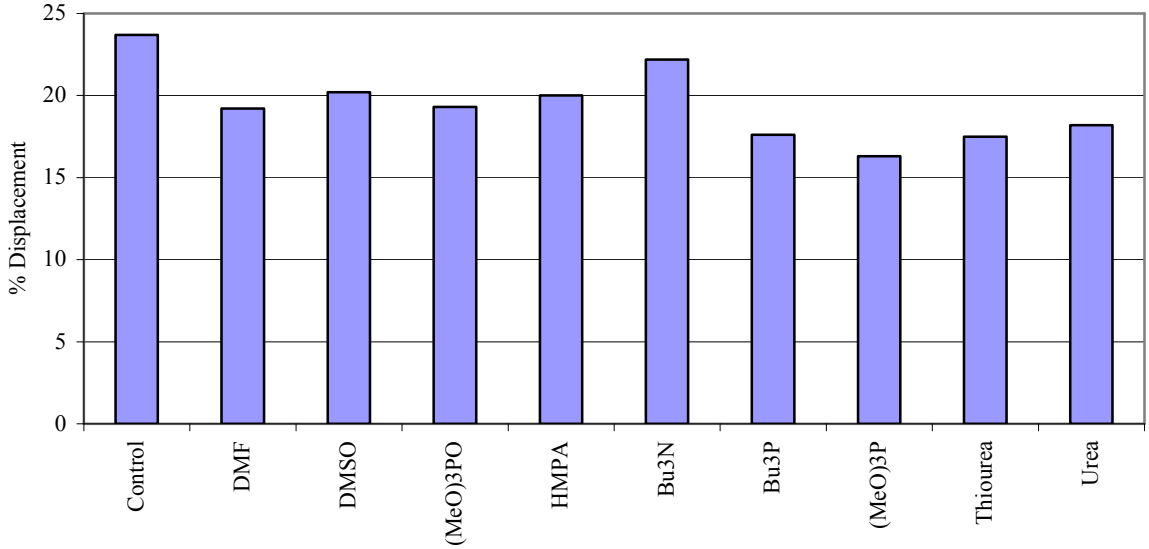

Figure 3.16 - Effect of selected Lewis bases on the displacement reaction of tri-*n*-butylborane with 4-octene at 120 ºC

In terms of the levels of displacement achieved (summation of the octanol isomers formed through re-hydroboration), the results presented in **Table 3.16** are in stark contrast with

those of the displacement study with 1-octene presented in **Section 3.3.1**. The results in **Table 3.16** show higher levels of displacement, ranging between 16% and 24%. Literature data presented in **Section 1.4.2** (**Table 1.4**)[80,81] show that hydroboration of internal olefins with dialkylboranes 9-BBN and diisoamylborane is markedly slower than hydroboration with a linear-α-olefin. Whereas this might appear contradictory to the data observed in **Table 3.16**, it should be noted that literature data is for investigation conducted at 25 ºC and 0 ºC for 9-BBN and diisoamylborane, respectively. Such differences in reactivity are not expected at high temperatures and extended time periods. Furthermore, upon dealkylation of the first butane molecule from tri-*n*-butylborane, re-hydroboration results in the formation of B(*n*-Bu)$_2$(4-octyl). Such a mixed trialkylborane is not as stable as a homo-trialkylborane and, as such, is expected to be more susceptible to the thermal transformations of alkylboranes. The result of this is that the mixed trialkylborane is more prone to dealkylation in order to relieve steric strain.[103] The increase in dealkylation propensity allows for increased re-hydroboration by 4-octene (*i.e.*, displacement). The mixed B(*n*-Bu)$_2$(*n*-octyl) is less likely to experience steric strain than B(*n*-Bu)$_2$(4-octyl)and is therefore less likely to undergo dealkylation, hence the lower observed levels of displacement. Though no dealkylation was observed for tri-4-octylborane in **Section 3.2.2** (**Table 3.14**), it should be noted that B(*n*-Bu)$_2$(4-octyl) would require less heat to dealkylate an alkyl chain. This has been shown in the literature by the increasing temperature requirements for pyrolysing trialkylboranes in the C_4 to C_{12} range.[105-107]

When viewed in terms of the distribution of octanol isomers, the results are also in contrast with those presented for the dealkylation study on tri-4-octylborane (**Section 3.2.2**). The enhanced levels of dealkylation result in the existence of boron-hydrogen bonds, which would catalyse the isomerisation of the 4-octyl chain. Thus, there is both a steric driver and the presence of boron-hydrogen bonds for the isomerisation of the 4-octyl chain. This is reflected in the high levels of 2-octanol in **Table 3.16**.

It is worth noting that the values of the Lewis base catalysed-displacement reaction are lower than those of the control experiment, suggesting that the interaction of these Lewis bases with the dialkylborane hinder re-hydroboration.

3.4. Conclusions

The dealkylation studies show that the greatest change in a trialkylborane system occurs within the first hour of the reaction when the system is heated from room temperature to the relevant high temperature. Liberation of the olefin at this stage at first appears not to be significant. However, this finding is influenced by the presence of solvent in the system, which interferes with the liquid-vapour equilibrium that must take place during dealkylation. Removal of the solvent from the system results in noticeable levels of displacement, which increase with temperature. This implies that, for commercial operation, continual removal of volatile solvent, and the olefin, is necessary. The results indicate that ca. 10% olefin liberation may be expected through heating alone. The combination of the studies of time and temperature dependence in the thermal dealkylation reaction indicate that rapid heating of a trialkylborane system is more effective in causing change in terms of positioning of the boron atom along the alkyl chain.

Analysis of the product spectrum of the decomposition products from the dealkylation study shows the formation of *n*-alkanes and dimeric derivatives of the alkyl chains of trialkylboranes. Although initially thought to be artefacts of the quenching and oxidation process, analysis of the gas eluted during the dealkylation reaction has shown that both these reactions can be results of the dealkylation process. This is a surprising finding given the relatively low temperature at which the dealkylation was investigated. This has implications for any isomerisation/displacement cycle, since extended periods of time during which the product trialkylborane is subjected to high temperatures in the absence of the displacing olefin would result in the decomposition of the trialkylborane.

Investigation of the placement of the boron atom along the alkyl chain during the dealkylation process yields interesting results. While tri-*n*-octylborane shows no thermal-induced back-isomerisation, the addition of 10 mol% of catalyst to the neat trialkylborane solution has revealed two effects. The first is the enhancement of the liberation of olefin by addition of catalyst. The second is the observation of back-isomerisation, catalysed by the addition of such catalysts as DMF, DMSO, HMPA and trimethyl phosphate. This serves as indication that an enhancement in dealkylation rate as reported by Rutkowski *et al.*[138] by the addition of Lewis base catalysts may be off-set by back-isomerisation of the alkyl

chain. This is acting against the objective of moving the boron atom away from an internal position in the carbon chain. This also requires that a judicious choice of Lewis catalyst be made, since the Lewis bases that catalyse back-isomerisation are among those that have a marked influence on the displacement rate as reported by Rutkowski *et al.*[137]

The study of the dealkylation of tri-4-octylborane shows that the Lewis bases are benign in alkyl chain migration. This may in part be due to the diminished interaction of the Lewis base and the boron atom because of steric crowding around the boron atom. That there was no significant dealkylation observed pointed to a mechanism other than the conventionally accepted complete dealkylation in operation. This mechanism involves the idea of partial dealkylation, which is a more satisfactory explanation for the isomerisation behaviour of trialkylboranes at the milder temperatures of the study.

3.5. Recommendations for future work

The results presented in this chapter have shown the importance of generation of the boron-hydrogen bond during the thermal transformation of trialkylboranes. **Section 3.2.2** showed that it is not necessary to completely dealkylate in order to achieve isomerisation (as explained by the bridge mechanism shown in **Scheme 3.3**); whereas **Section 3.3.2** has shown, in line with literature precedents, that isomerisation and displacement are enhanced by dealkylation. It is of great importance to observe the presence and/or absence of the boron-hydrogen bond during these processes. IR spectroscopy has the potential to elucidate the processes taking place during thermal transformations of alkylboranes. Bridging hydrogen atoms in alkylboranes have a characteristic shift at 1500 cm^{-1}, whereas the hydrogen atoms in monomeric boranes have a characteristic shift at 2500 cm^{-1}. This would allow for the identification of the species formed as a result of the exposure of trialkylboranes to heat as well as the rate of their formation. Furthermore, the IR shifts mentioned above are susceptible to change when the boron atom is coordinated to a Lewis base. This would allow for the investigation of the effect of the Lewis bases during dealkylation, isomerisation and displacement.

4. RESULTS AND DISCUSSION: ^{11}B NMR SPECTROSCOPY STUDIES

The importance of the hydroboration reaction in organic chemistry has been well established in the chemical literature.[1-3] Traditionally, gas chromatography has been the technique used for investigations into various aspects of organoborane chemistry. Several problems arise when considering both analysis of residual alkene or alcohol content by gas chromatography; not least being the tediousness of the sampling and quenching process. Furthermore, this method is particularly unsuitable for reactions whose reaction life-time is within that of the sampling and quenching time. also, the quality of the data from this type of analysis suffers from the limit placed on the number and size of sample aliquots that may be removed from the reaction medium. Thus, as has been discussed in **Chapter 1**, there is a need for the development of modern instrumental techniques for analysis of boron chemistry processes. This is particularly imperative in the field of kinetics.

The modern spectroscopic set-up is ideal for providing non-destructive, *in-situ* analysis under inert atmosphere conditions. To this end, infrared spectroscopy has been employed in the kinetic investigation of various organoboranes.[190] ^{11}B NMR spectroscopy has also been shown to be an invaluable qualitative tool for many studies, with several texts illustrating the wide variety of boron-containing compounds identifiable by this technique.[191] Further applications of ^{11}B NMR spectroscopy include its use in the determination of the effect of Lewis acid on apparent base strength[192] and, more recently, the study of dimer-monomer equilibria in organoboranes.[193]

Yet, despite all these applications, ^{11}B NMR spectroscopy has not been exploited in the direct investigation of kinetic and mechanistic aspects of the hydroboration reaction. This chapter illustrates the use of ^{11}B NMR spectroscopy towards this purpose. The reaction of nitriles with borane-dimethyl sulfide (BMS) has been investigated (**Section 4.1.2**). The conventionally adopted method for investigating the reactivity of nitriles toward reduction by borane-Lewis base adducts has been the determination of residual hydridic hydrogen at

the end of the reaction period.[194] This technique, while adequate for comparison of the relative reactivity of various boranes toward nitriles, cannot be used to determine precise kinetic and activation parameters.

In addition to illustrating the use of ^{11}B NMR spectroscopy for mechanistic investigations, the applicability of ^{11}B NMR spectroscopy to the determination of the thermodynamic parameters of the association of trialkylboranes to Lewis bases (**Section 4.1.3**) has been investigated. Computational chemistry has been used to account for the findings of both the kinetic and binding investigations.

4.1. Investigation of the Mechanism of the Reduction of Nitriles by $BH_3.SMe_2$ by ^{11}B NMR Spectroscopy

The reduction of nitriles by borohydrides has long been known,[195] with the reaction of diborane (B_2H_6) with acrylonitrile at room temperature shown to afford at least three products.[196] Studies on the room temperature reduction of *m*-nitrobenzonitrile[197] and benzonitrile[198,199] with diborane in ethereal solvents have shown the reaction to be rapid, reaching completion within two hours. Investigation of the rates and stoichiometry of the reduction of capronitrile and benzonitrile with diborane in tetrahydrofuran (THF) has shown that both compounds are readily reduced even at 0 ^{o}C.[200] The route by which nitrile reduction occurs has been elucidated during the reduction, by diborane, of methyl and ethyl cyanide, as well as that of acrylonitrile, where it has been shown that methyl and ethyl cyanide react reversibly with diborane at low temperature to form borane-nitrile adducts ($RC{\equiv}N.BH_3$).[201]

The stability of the ethyl cyanide adduct ($EtC{\equiv}N.BH_3$) towards decomposition was found to be lower than that of the methyl cyanide adduct ($MeC{\equiv}N.BH_3$). Acrylonitrile and benzonitrile have also been shown to form adducts with BH_3 that are less stable to decomposition through reduction than alkyl cyanides.[201] The decomposition of the alkyl cyanide-borane adducts ($R\text{-}C{\equiv}N.BH_3$) has been reported to eventually produce *NN'N''*-tri-*n*-alkylborazines at room temperature *via* two successive hydrogen shifts from the boron atom to the nitrile carbon atom (**Scheme 4.1**).[201,202] The decomposition of the

acrylonitrile-borane adduct (CH_2=CH-C≡N.BH_3) was found to take place vigorously above 0 ºC, such that borazine derivatives were not isolated.[201]

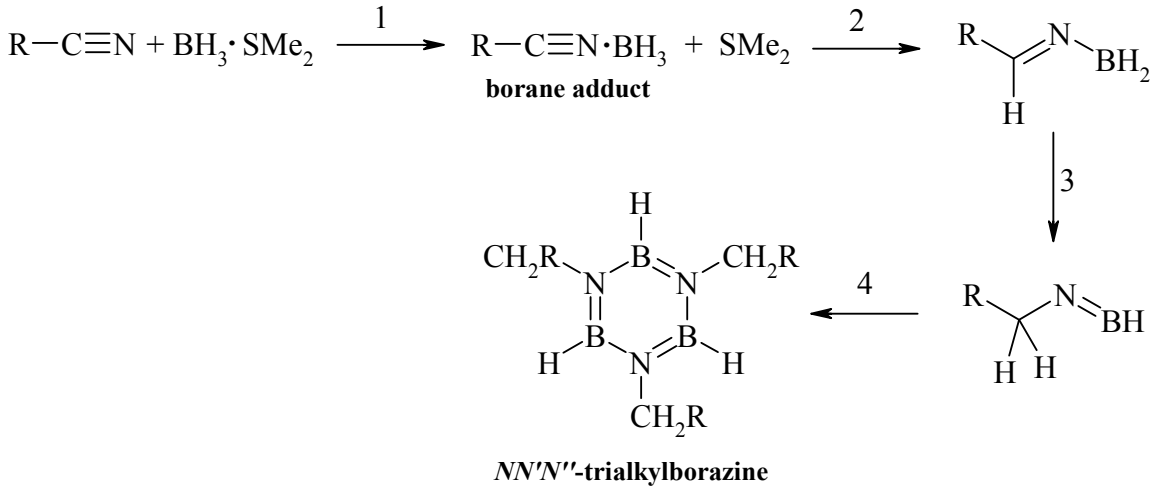

Scheme 4.1 - Formation of trialkylborazines *via* the reduction of nitriles by borane[210,203]

Jennings and Wade have shown that the borazines constitute only part of the total product mixture for the reduction of nitriles, with the reduction of ethyl cyanide affording 35-40% *NN'N''*-triethylborazine.[204] In addition, a further 25-37% of the product distribution has been attributed to bicyclic compounds.[205]

Complexes of borane with ethers (e.g., BH_3.THF and BH_3.OEt_2) effectively convert nitriles to their corresponding amines after hydrolysis.[197,198,206] The reduction is, however, more sluggish with the dimethyl sulfide complex.[207,208] While the greater stability of the borane-dimethyl sulfide complex (BH_3.SMe_2) towards dissociation was cited as a reason for the retardation in reactivity, its stability towards decomposition and better handling characteristics are the reason for the choice of this complex in hydroboration and reduction reactions.[208] An improved procedure for enhancing the reactivity of the borane–dimethyl sulfide complex towards nitriles has been published and its general applicability toward nitrile reduction established.[199,209,210] Tetrabutylammonium borohydrides have also been used for the reduction of nitriles,[211] while various strategies for the enhancement of the reactivity and selectivity of sodium borohydrides toward the reduction of nitrile compounds have also been developed.[212] No detailed kinetic investigation of the reduction of nitriles by boranes can, to date, be found in the literature. Thus, investigation of the reaction by boron ^{11}B NMR spectroscopy presents two novel opportunities, viz. the

use of ^{11}B NMR spectroscopy for kinetic studies and the investigation of the reduction itself. The report by Schlessinger and Burg[198] shows the time-scale of the room-temperature reduction of nitriles to be an ideal probe investigation. It was for these reasons that a kinetic ^{11}B NMR spectroscopy investigation of the reduction of selected nitriles by borane-dimethyl sulfide complex was conducted. The primary kinetic and spectroscopic data for the investigation may be found in **Section 7.1** and **Section 7.2** (**Appendix B**), respectively; whereas the computational data may be found in **Section 7.3**.

4.1.1. Reactivity of Benzonitrile, Propionitrile and Acrylonitrile towards Borane-Dimethyl Sulfide

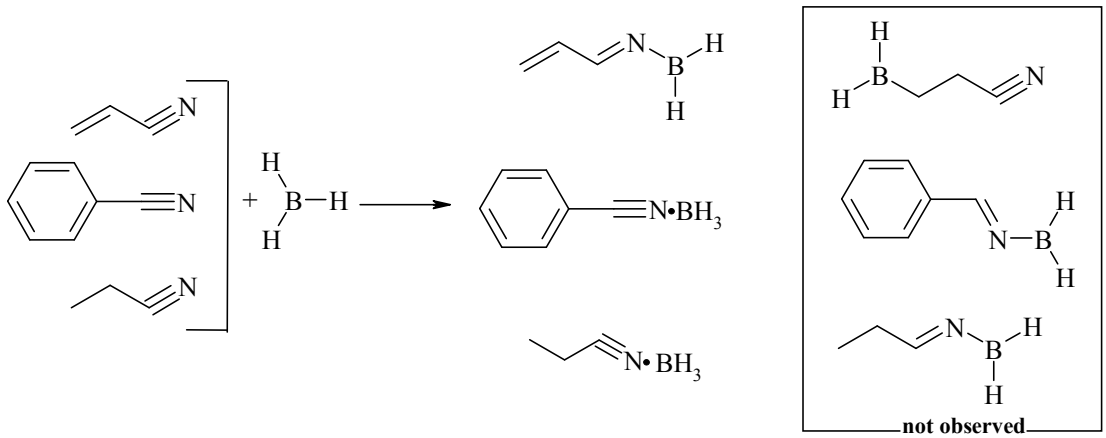

Scheme 4.2 - Summary of reactions of acrylonitrile, benzonitrile and propionitrile with borane-dimethyl sulfide complex in dichloromethane at 25 °C

No reduction was observed for the reaction involving borane dimethyl sulfide with propionitrile and benzonitrile. These compounds instead formed borane-nitrile adducts, $C_6H_5C{\equiv}N.BH_3$ ($\delta^{11}B$ = -25.8 ppm) and $CH_3CH_2C{\equiv}N.BH_3$ ($\delta^{11}B$ = -26.2 ppm), identifiable as quartets in the ^{11}B spectrum. Surprisingly, there are no NMR chemical shifts reported in the literature for these types of adducts. Both ^{1}H and ^{11}B NMR spectroscopy showed the equilibrium between the $Me_2S.BH_3$ and the $RC{\equiv}N.BH_3$ adducts to favour the former, with ^{1}H NMR investigation revealing $K = (7.45 \pm 0.20) \times 10^{-3}$ and $K = (1.16 \pm 0.02) \times 10^{-2}$ for $C_6H_5C{\equiv}N.BH_3$ and $EtC{\equiv}N.BH_3$, respectively. The small equilibrium constants for nitrile-borane adduct formation may be responsible for the lack of reactivity, reduction in this

case, of these two compounds. For reduction to occur, favourable interaction between the borane and nitrile molecules would first need to be established.

It was, however, possible to monitor the kinetics of the reaction up to the first reduction of acrylonitrile (steps 1 and 2 in **Scheme 4.1**) through ^{11}B NMR spectroscopy (**Figure 4.1**). The borane-nitrile adduct formed between acrylonitrile and BH_3 ($\delta^{11}B$ = -25.7 ppm, $J_{B\text{-}H}$ = 107 Hz) was completely depleted after 500 seconds and was generally present in such small concentrations that no meaningful kinetic data could be obtained for it. This is not surprising, as these adducts have been reported to be unstable at room temperature.[201] It can, therefore, be concluded that depletion of the borane-nitrile adduct is very fast processes. Kinetic investigation of the two hydride shifts prior to borazine formation (steps 3 and 4 in **Scheme 4.1**) was not possible owing to the polymerisation of the acrylonitrile. This polymerisation is expected under the reaction conditions of the study.[213,214] Analysis of the arrayed spectra shows that the reduction of acrylonitrile did not proceed to the borazine and carbozara stages. No peaks consistent with those reported for *NN'N''*-tri-*n*-alkylborazines[215] and carbozara derivatives[205] were identified in the ^{11}B NMR spectrum at the end of reaction. The relatively high field shift of the aldiminoborane indicates a shielded boron atom in a four-coordinate environment suggestive of a dimeric aldiminoborane species. This is supported by literature precedents that show that aldiminoboranes are, in general, dimeric rather than monomeric.[216-218]

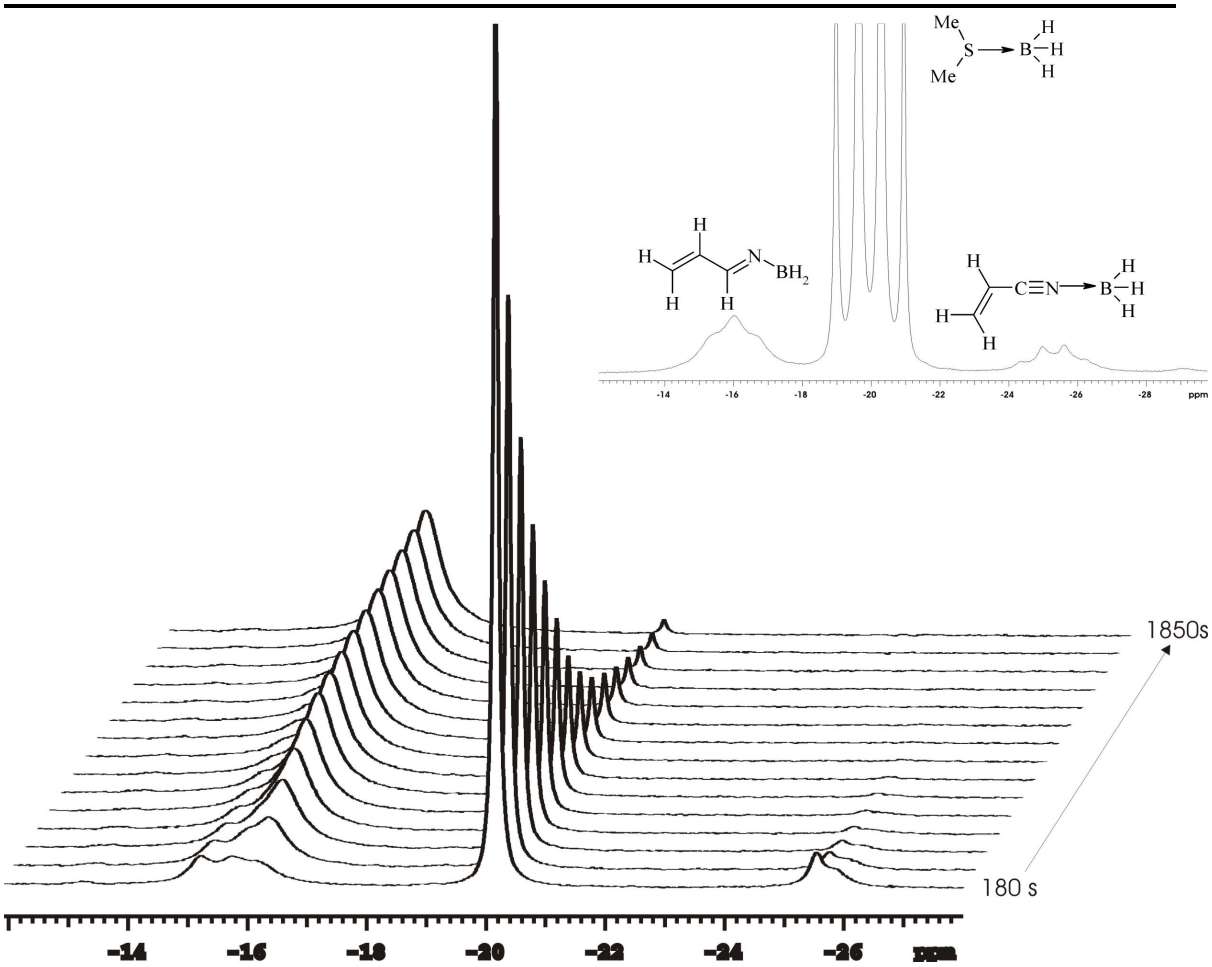

Figure 4.1 - Arrayed ^{11}B-{^{1}H} spectrum for reduction of acrylonitrile with borane dimethyl sulfide complex (0.16 M) in CH_2Cl_2 at 25 °C and ^{11}B spectrum (inset) showing species identified during reaction

4.1.2. Kinetic Measurements

Pseudo-first order rate constants, k_{obs}, for the reduction of acrylonitrile by the borane-dimethyl sulfide complex (0.16 M) at various concentrations (3-8 M) and temperatures (15-30 °C) were obtained from ^{11}B NMR arrayed experiments and subsequent integration of the borane and vinyliminoborane peaks. These resulted in the kinetic plot shown in **Fiigure 4.2**.

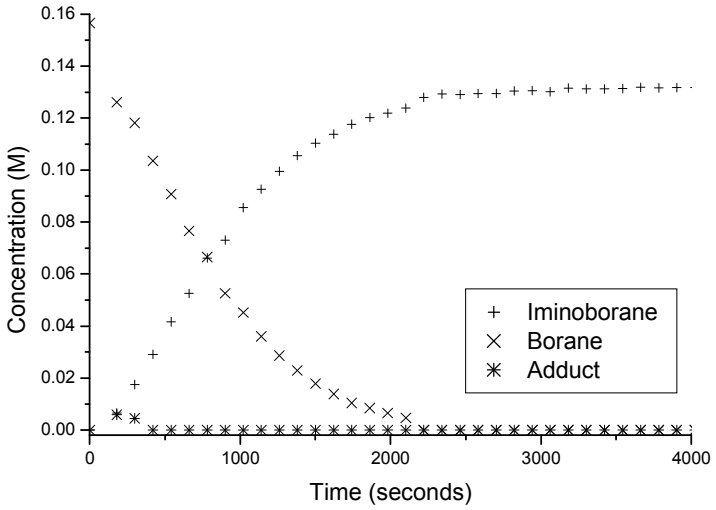

Figure 4.2 - Kinetic plot for reduction of acrylonitrile with borane dimethyl sulfide complex (0.16 M) in CH_2Cl_2 at 25 °C

A first-order exponential decay curve was then fitted over the data points for the depletion of the borane dimethyl sulfide complex in order to generate the pseudo-first order rate constants, k_{obs}. These were then plotted against the acrylonitrile concentration, resulting in a linear dependence of k_{obs} on the concentration of acrylonitrile with no meaningful y-intercept as shown in **Figure 4.3**.

The results imply that k_{obs} can be expressed by equation *4.1*.

$$k_{obs} = k_2'[\text{Acrylonitrile}] \qquad 4.1$$

On the basis of the observed ^{11}B NMR data and kinetics, the following pre-equilibrium mechanism that involves a dissociative step is proposed (**Scheme 4.3**). The dimethyl sulfide dissociated in the first step re-attaches to the boron atom of the aldiminoborane, as shown in the second step. This is borne out by the gradient HMQC spectrum for the product, which shows the correlation in the ^{11}B resonance of the BH_2 to the protons of dimethyl sulfide (**Figure 4.4**)

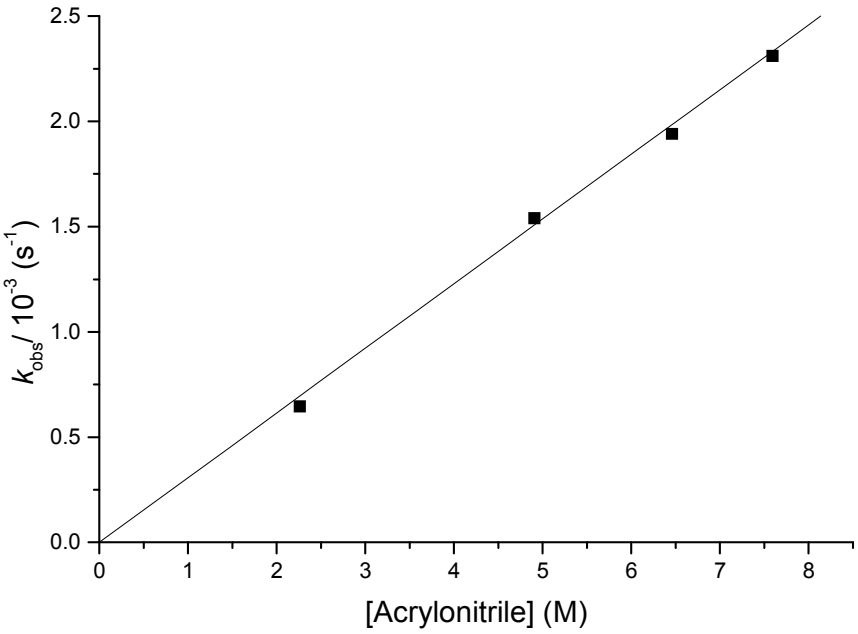

Figure 4.3 - Concentration dependence of k_{obs} on acrylonitrile concentration in the reduction of acrylonitrile with borane dimethyl sulfide complex (0.16 M) in CH_2Cl_2 at 25 °C

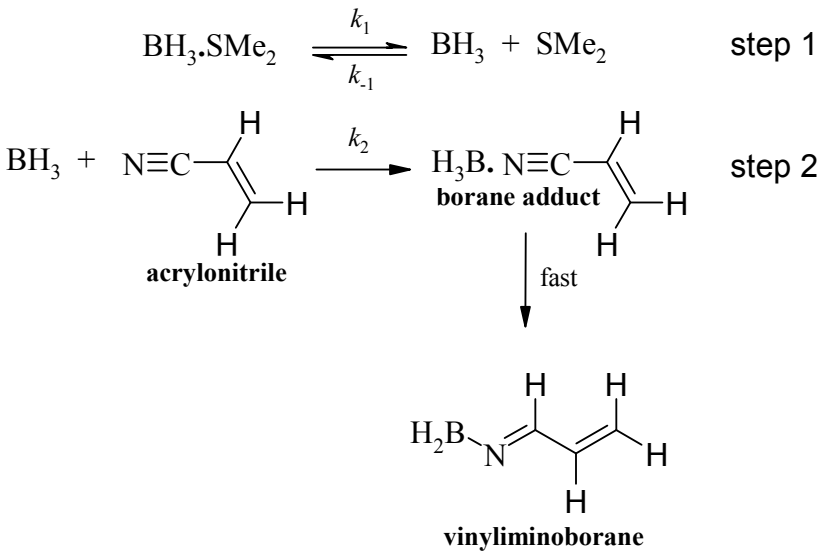

Scheme 4.3 - Proposed reaction pathway for the formation of vinyliminoborane from the reduction of acrylonitrile by borane dimethyl-sulfide complex

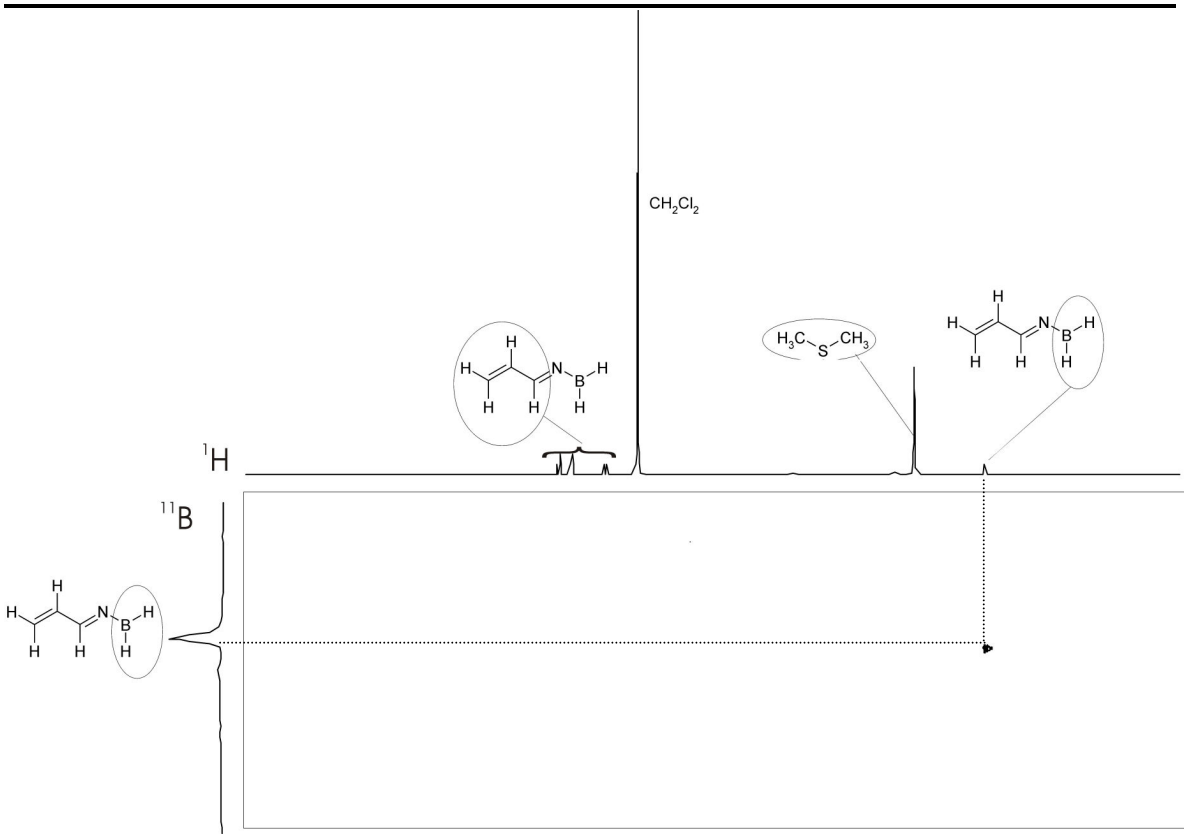

Figure 4.4 - Gradient HMQC depicting correlation of aldiminoborane product to dimethyl sulfide.

The rate law for this mechanism can be expressed as shown in equation *4.2* (the derivation of equation *4.2* is shown in details in **Section 7.1.1 of Appendix B**).

$$k_{obs} = \frac{k_1 k_2 [\text{Acrylonitrile}]}{k_{-1}[\text{SMe}_2] + k_2[\text{Acyrlonitrile}]} \qquad 4.2$$

In the presence of excess dimethyl sulfide, $k_{-1}[SMe_2]$ becomes greater than k_2[Acrylonitrile]. Hence, equation *4.2* reduces to equation *4.3* since $[SMe_2]$ is constant.

$$k_{obs} = \frac{k_1 k_2}{k_{-1}[\text{SMe}_2]}[\text{Acrylonitrile}]$$

$$= k_2'[\text{Acrylonitrile}] \qquad 4.3$$

The implication of equation *4.2* meant that it was important to determine whether the $BH_3.SMe_2$ complex obtained from Sigma-Aldrich had any excess SMe_2, which is of

importance for the determination of the dissociation rate constant, k_1. The commercial borane complex was, therefore, analysed by ^{1}H NMR spectroscopy. The integration of the peaks showed that free SMe_2 was present at an excess of 12.5%.

To test the mechanism further, equation *4.2* was expressed differently as shown in Equation *4.4*.

$$\frac{1}{k_{obs}} = \frac{k_{-1}}{k_1 k_2 [\text{Acrylonitrile}]}[SMe_2] + \frac{1}{k_1} \qquad 4.4$$

This equation was used to analyse the k_{obs} data obtained when the acrylonitrile concentration was held constant (4.911 M) while that of excess dimethyl sulfide was varied from 0.019 M to 0.193 M. Plotting $1/k_{obs}$ against $[SMe_2]$ resulted in the linear plot shown in **Figure 4.5**. The decrease in k_{obs} with increasing dimethyl sulfide concentration, even at very low added dimethyl sulfide levels, shows the k_1/k_{-1} equilibrium shown in the first step of **Figure 4.3** to be valid. Thus the first step in the reaction sequence must involve the dissociation of the Lewis base from BH_3 as proposed in the mechanism.

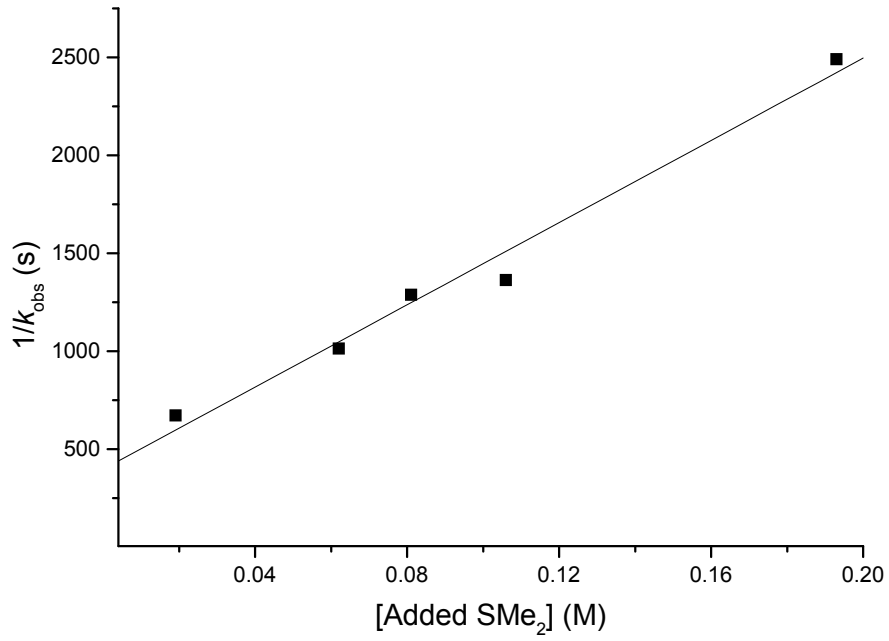

Figure 4.5 - Concentration dependence of k_{obs} on dimethyl sulfide concentration in the reduction of acrylonitrile with borane dimethyl sulfide complex (0.16 M) in CH_2Cl_2 at 25 °C

The rate constants obtained for acrylonitrile are summarised in **Table 4.1**.

Table 4.1 - Kinetic data for the reduction of acrylonitrile in CH_2Cl_2

Temp. (ºC)	k_{obs} / 10^{-3} (s^{-1})	$k_2'/10^{-4}$ ($M^{-1}.s^{-1}$) [a]	Thermodynamic Data
15.0	0.56 ± 0.01	0.94 ± 0.02	$\Delta H^{\neq}$ = 58 ± 3 kJ mol^{-1}
20.0	1.00 ± 0.03	2.32 ± 0.07	
25.0	1.16 ± 0.04	3.09 ± 0.08	
30.0	1.63 ± 0.07	4.86 ± 0.17	$\Delta S^{\neq}$ = -71 ± 10 J K^{-1} mol^{-1}
k_1 (25 ºC) [b]	(2.52 ± 0.57) × 10^{-3} s^{-1}		

[a] $k_2' = k_2k_1/k_{-1}[SMe_2]$

[b] From $[SMe_2]$ dependence study, [Acrylonitrile] = 4.911 M

The temperature dependence of the reduction of acrylonitrile was also investigated. Since Error! Reference source not found. showed the absence of a reverse reaction by passing through the origin, a single concentration (4.911 M) of acrylonitrile was used to investigate the temperature dependency of the reaction over a temperature range of 15-30 ºC. Because of the fairly low boiling point of the dichloromethane solvent (39.8-40.0 ºC), the maximum temperature of the investigation was limited to 30 ºC. The dichloromethane-dissolved borane dimethyl sulfide complex was chosen over the THF-dissolved complex because dichloromethane does not undergo exchange equilibria with dimethyl sulfide as THF does. The values of activation enthalpy, $\Delta H^{\neq}$, and activation entropy, $\Delta S^{\neq}$, were determined from the Eyring plot shown in **Figure 4.6**; which shows a linear correlation over the investigated temperature range. The values of the activation parameters, $\Delta H^{\neq}$ and $\Delta S^{\neq}$, are tabulated in **Table 4.1**.

The negative $\Delta S^{\neq}$ value indicates that the overall mechanism of the reduction of acrylonitrile by $BH_3.SMe_2$ in the presence of excess dimethyl sulfide is an associative process. However, it must be borne in mind that the $\Delta S^{\neq}$ value is calculated from a composite k_2' value (as defined in equation *4.3*). It has already been shown by the dimethyl sulfide dependence study that the rate-limiting step in the sequence of reaction steps that result in the reduction of the nitrile is the dissociation of the dimethyl sulfide, which can only be a dissociative process and, therefore, has a positive entropy contribution. Thus, for the nett entropy, calculated from the composite k_2' value, it can be concluded that the

entropy contribution due to the dissociative process is positive but smaller in magnitude when compared to the associative contributions of the adduct formation and reduction of the nitrile, which are negative. Substituting the value of k_1 at 25.0 ºC (**Table 4.1**), and [SMe_2] = 0.18 M, into the value of k_2' at 25.0 ºC (**Table 4.1**), yields a value for k_2/k_{-1} of 0.023.

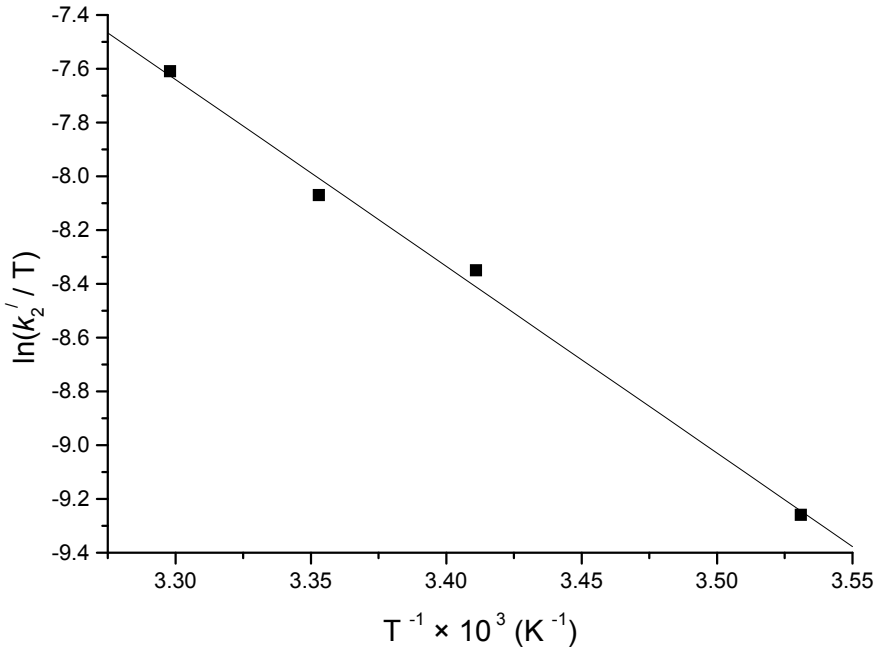

Figure 4.6 - Eyring plot illustrating the temperature dependence of k_2' for the depletion of borane dimethyl sulfide complex (0.16 M) in the first step of the reduction of acrylonitrile in CH_2Cl_2

4.1.3. Computational Study

Scheme 4.2 in **Section 4.1.1** summarises the reactivity of acrylonitrile, benzonitrile and propionitrile towards reduction by the borane-dimethyl sulfide complex. A computational study was undertaken in order to account for the different reactivities of these compounds. In addition, to the three nitriles investigated in **Section 4.1**, hydrogen cyanide was also modelled as there is data available in the literature on this compound.[219] The primary data for the investigation can be found in **Section 7.3** of **Appendix B**.

An energy profile (**Figure 4.7**) for the reaction of acrylonitrile, benzonitrile, propionitrile and hydrogen cyanide was generated at the B3LYP/6-31G* level of theory. In contrast to the MNDO (Modified Neglect of Diatomic Overlap computational theory) results of Ray and Chadha, [219] **Figuer 4.7** shows no transition state for the formation of a borane-nitrile adduct. The B3LYP calculations support the observation by Emeléus and Wade [201] that the stability of the borane-nitrile adducts affects their reactivities, with the adduct of acrylonitrile and BH_3 being about 6 – 8 kJ.mol^{-1} more stable than those of benzonitrile and propionitrile. A stable adduct is more likely to undergo step 2 of **Scheme 4.1**.

The concepts of absolute hardness, η , and absolute electronegativity, χ° ,[220] as defined by equation *4.5* can be invoked to explain the weakness of the BH_3 adducts of benzonitrile and propionitrile by accounting for the effect of the HOMO-LUMO gap.

$$\eta = \frac{(I - A)}{2} \quad \text{and} \quad \chi^\circ = \frac{(I + A)}{2} \qquad 4.5$$

Molecular orbital theory (Koopman's Theorem) shows that I = $-E_{LUMO}$ and A = $-E_{HOMO}$ in eV such that combining η and χ° to determine the transfer of electron density possible from a Lewis base to a Lewis acid, ΔN as defined in equation *4.6*, puts the stability of the nitrile-BH_3 adducts in perspective.

$$\Delta N = \frac{(\chi^\circ_A - \chi^\circ_B)}{2(\eta_A + \eta_B)} \qquad 4.6$$

The results in **Table 4.2** show the degree of electron transfer to BH_3 in the nitrile-BH_3 adduct, which is indicative of the degree of stability of the adduct between the nitrile and BH_3. The combination of a η value similar to the borane, a relatively high χ° value and a moderate degree of charge transfer explain the relative stability of the complex between BH_3 and acrylonitrile (**Figure 4.7**). Propionitrile, by contrast, even though it has a higher degree of electron transfer (ΔN) is in fact harder than BH_3, implying a much larger HOMO-LUMO gap and resistance to transferring charge (as confirmed by the lower absolute electronegativity value). Hydrogen cyanide is much harder than acrylonitrile but is also less electronegative. This manifests in a relatively smaller degree of charge transfer to BH_3 on complexation. This is evident in the calculated reaction energies (**Table 4.3**), which show a the higher $\Delta_{activation}E$ value and a $\Delta_{complexation}E$ value less exothermic than that of acrylonitrile. Though benzonitrile has a similar level of electron transfer to acrylonitrile, it is softer than BH_3; making charge transfer between the species less likely. Generally, the harder species will transfer charge to the softer species, though it is preferable that the species be of relatively similar hardness. **Table 4.3** shows that the change in energy of complex formation, $\Delta_{complexation}E$, is greatest for the formation of the acrylonitrile-BH_3 adduct at -75.1 kJ.mol^{-1}.

Table 4.2 - B3LYP/6-31G* calculated absolute hardness, absolute negativity and electron density transfer in adducts of selected nitriles with BH_3

Compound	η (eV)	χ^{o} (eV)	ΔN
BH_3	3.89	5.67	-
H–C≡N	5.17	4.61	0.059
H_2C=CH–C≡N	3.17	4.70	0.069
C_6H_5–C≡N	2.93	4.34	0.098
H_3C–CH_2–C≡N	4.83	3.93	0.100

In addition to the relative stability of the adducts, depicted in **Figure 4.7**, the activation energy requirements are critical for reduction to take place. As summarised in **Table 4.3**, the overall energy barriers ($\Delta_{activation}E$) for the reduction of propionitrile (42.7 kJ.mol^{-1}), hydrogen cyanide (40.7 kJ.mol^{-1}) and benzonitrile (42.3 kJ.mol^{-1}) are higher than the energy barrier (34.7 kJ.mol^{-1}) for the reduction of acrylonitrile. The B3LYP method gives a better account of the reaction with energy barriers calculated in the present work being

substantially lower and, thus, more reasonable than those calculated by Ray and Chadha's MNDO study.[219]

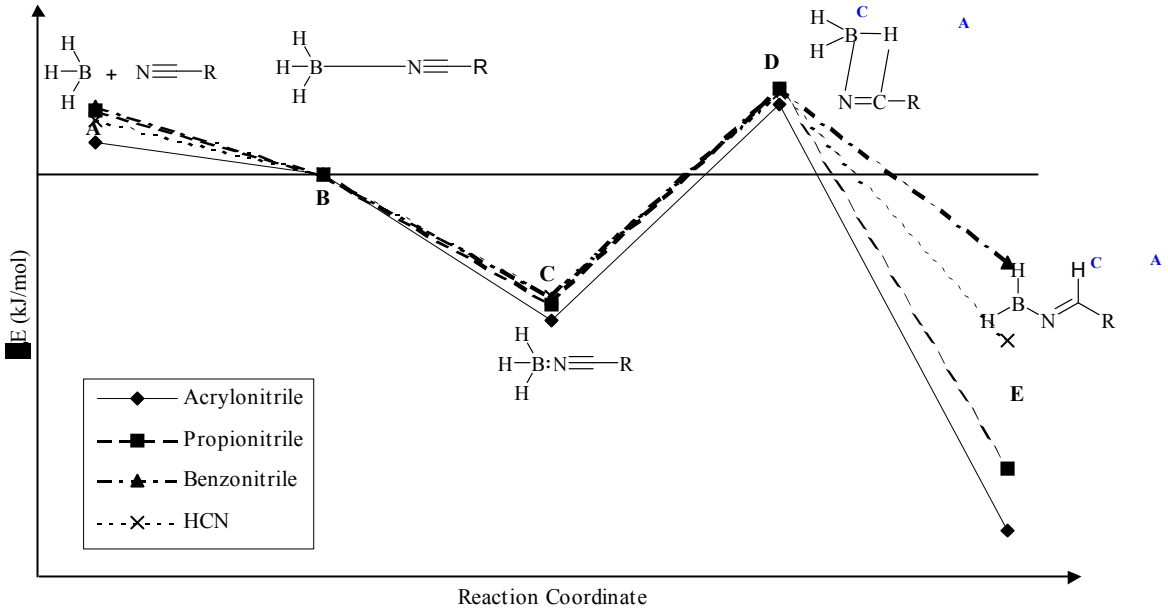

Figure 4.7 - B3LYP/6-31G* energy profile of stationary points for the reaction of BH_3 with acrylonitrile, propionitrile and benzonitrile

Table 4.3 - B3LYP/6-31G* calculated energies for the reaction of selected nitriles with BH_3

Adduct	$\Delta_{complexation}E$ (kJ.mol^{-1})	$\Delta_{activation}E$ (kJ.mol^{-1})
$H_2C{=}CH{-}C{\equiv}N$	-75.1	34.7
$H_3C{-}CH_2{-}C{\equiv}N$	-64.3	42.7
$C_6H_5{-}C{\equiv}N$	-61.4	42.3
$H{-}C{\equiv}N$	-60.8 (-66.9)*	40.7 (89.1)*

* Value in brackets refers to MNDO data of Ray and Chadha[219]

The B3LYP results for charge transfer (**Table 4.4**) agree with those of Ray and Chadha[219] in that there is a reversal of charge in the nitrile-BH_3 adduct for the atoms that make up the borane and the nitrogen and carbon atoms in the nitrile. These transfers of charge are of similar magnitude where 0.8 units of charge are transferred to the boron atom from the borane protons and the nitrogen and carbon atoms of the nitrile functionality.

Table 4.4 - B3LYP/6-31G* Changes in electrostatic charges of atoms in the stationary points C (nitrile-BH_3 adduct) on the reaction surface

Atom	H_2C=CH–C≡N	H_3C–CH_2–C≡N	C_6H_5–C≡N	H–C≡N
B	0.79	0.78	0.82	0.74 (0.21) *
H_A	-0.12	-0.11	-0.12	-0.11 (-0.08)
H_B	-0.12	-0.11	-0.12	-0.11 (-0.08)
H_C	-0.12	-0.11	-0.12	-0.11 (-0.08
N	-0.52	-0.56	-0.62	-0.53 (-0.10)
C	0.17	0.22	0.27	0.20 (-0.09)

* Values in brackets refers to MNDO data of Ray and Chadha[219]

Note: Original charge on the boron atom of the free borane is +0.30, thus if the boron atom gains 0.79 units of negative charge from acrylonitrile its final charge will be -0.49 in the borane-acrylonitrile adduct.

An interesting question arises when considering the preference of reduction at the nitrile as opposed to the alkene functionality of acrylonitrile, especially in relation to Brown and Kortnyk's [209] observation that, in solution, nitriles are less reactive than alkenes towards hydroboration/reduction. A look into the distribution of electrostatic charge in the acrylonitrile molecule (**Figure 4.8**) reveals that the nitrogen atom carries most of the electrostatic charge in the molecule and, as such, is the point most susceptible to electrophilic attack.

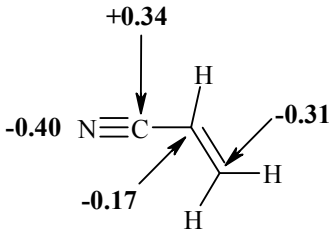

Figure 4.8 - B3LYP/6-31G* calculated electrostatic charge distribution in the acrylonitrile molecule

4.1.4. Conclusion

In summary, the results obtained in this study indicate that the overall reduction of acrylonitrile with $BH_3.SMe_2$ is associative. This was found to be evident frm the large and

negative activation entropy value of -71 ± 10 J K^{-1} mol^{-1}. In addition, the importance of the dissociation of the dimethyl sulfide from borane to the reduction process has also been illustrated as shown by the dependence of the observed rate of the reaction on the concentration of dimethyl sulfide (**Figure 4.4**). The gradient HSQC spectrum showed, though, that the dimethyl sulfide does re-attach to the boron atom after formation of the aldiminoborane. The lack of reaction with propionitrile and benzonitrile at 25 ºC can be attributed to the lack of stability of their adducts with BH_3 as demonstrated by the low equilibrium constants for the formation of their adducts with borane revealing K = (7.45 ± 0.20) × 10^{-3} and K = (1.16 ± 0.02) × 10^{-2} for $C_6H_5C{\equiv}N.BH_3$ and $EtC{\equiv}N.BH_3$) for derivation of K) and further illustrated by computational calculation of their energies which are found to be higher ($\Delta_{complexation}E$ = -64.3 and -61.4 kJ.mol^{-1}, respectively for propionitrile and benzonitrile) than the acrylonitrile-borane adduct ($\Delta_{complexation}E$ = -75.1 kJ.mol^{-1}), as illustrated in **Figure 4.7** and **Table 4.3**. Furthermore, the data in **Table 4.3** shows that these compounds have higher activation barriers ($\Delta_{activation}E$ = 42.7 and 42.3 kJ.mol^{-1}, respectively, for propionitrile and benzonitrile) for reduction by BH_3 when compared to acrylonitrile ($\Delta_{activation}E$ = 34.7 kJ.mol^{-1}).

4.2. Application of ^{11}B NMR Spectroscopy to the Investigation of Hydroboration with Amine-Boranes

4.2.1. Effect of methyl iodide on hydroboration with amine-boranes

Whereas Pelter *et al.*[37] claim respective yields of 93 % and 88 % for the hydroboration of 1-octene with trimethylamine-borane and triphenylphosphine-borane, respectively, in refluxing THF over six hours, a ^{11}B NMR spectroscopy investigation of hydroboration of 1-octene with trimethylamine-borane in *n*-decane at 100 ºC over ten hours shows no similar improvement in reaction yield. The data in **Figure 4.9** show that the inclusion of methyl iodide increases the rate of the reaction in *n*-decane only marginally. This implies that the effect observed by Pelter *et al.*[37] is a combination of the methyl iodide and the ethereal solvent.

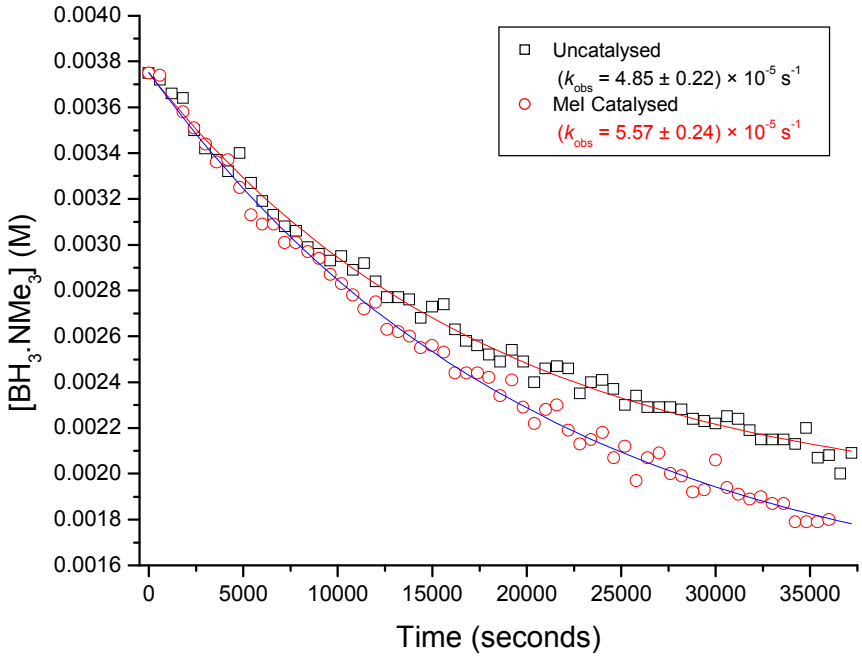

Figure 4.9 - ^{11}B NMR spectroscopic investigation of the effect of MeI on hydroboration of 1-octene (2.3 M) with BH_3.NMe_3 (0.1 M) in *n*-decane at 100 °C

The lack of marked catalytic activity of methyl iodide is not a major concern in terms of a boron-mediated catalytic cycle since the hydroboration step is not the most crucial (rate-determining step) in the cycle. Furthermore, catalysis of the hydroboration reaction would only be required for the reactor start-up period, after which all further re-hydroboration would take with dialkyl- and monoalkylboranes during the displacement reaction. The reaction of methyl iodide with the amine to form an amine salt ($(Me)_4N^+I^-$), would result in a loss of borane through formation of an unrecoverable amine salt. This would require constant dosing of fresh borane reagent into the reactor, which might not be economically viable.

4.3. Investigation of the Association of Lewis Bases to Tributylborane by ^{11}B NMR Spectroscopy

A study into the binding of the selected Lewis bases to trialkylborane was undertaken in order to test whether there was any correlation between the reported catalytic effects[137] of certain Lewis acids with their ability to bind to the boron atom. This was, chiefly, to test the hypothesis that the interaction of the Lewis base and empty *p*-orbital on the boron atom of the trialkylborane would have a labilising effect on the boron carbon bonds of the trialkylborane. It has been noted earlier (**Section 1.6.4**) that the displacement reaction is controlled by the dissociation of the carbon boron bond to release an olefin.[11,115,120] Thus, any compound with the ability to interact strongly with the boron atom of a trialkylborane would be expected to enhance the rate and/or extent of the displacement reaction. Rablen's high-level computational study[221] of the bond dissociation energies (BDEs) of a series of borane-Lewis base complexes (**Table 4.5**) certainly supports this hypothesis.

Table 4.5 - CBS-4 calculated bond dissociation energies (298 K) for selected Lewis base-borane complex

Complex	Bond Dissociation Energy (kJ/mol)	
	$BH_3.L \rightarrow {}^{\bullet}BH_2.L + {}^{\bullet}H$	$BH_3.L \rightarrow BH_3 + L$
$H_3B\text{-}BH_3$	100.3	38.8
$(CH_3)_2O.BH_3$	103.9	18.0
$(CH_3)_2S.BH_3$	95.5	24.1
$(CH_3)_2CO.BH_3$	65.5	15.9
$(CH_3)_3N.BH_3$	102.6	38.1
$(CH_3)_3P.BH_3$	92.8	40.0
$(CH_3)_2SO.BH_3$	100.5	19.6
$THF.BH_3$	103.5	19.7
$Pyridine.BH_3$	68.8	33.0

4.3.1. NMR Spectroscopy of Alkylboranes

^{11}B NMR Spectroscopy has been extensively discussed in a book by Nöth and Wrackmeyer.[191b] Chemical shifts for trialkylboranes are found in a very narrow range, 83-93 ppm (see **Table 4.6**).[222] It has been stated that, all other things remaining equal, the ^{11}B resonance occurs at higher field (i.e., upfield) the greater the electron density on the boron atom.[223] The chemical shifts of tervalent (BX_3) boron atoms are a function of σ- and π-bonding and anisotropic effects.

$$\delta^{11}\mathrm{B} = \delta_{\sigma} + \delta_{\pi} + \delta_{n}$$

The contribution of the σ-bonding effects is a function of the absolute electronegativity of the atom bonded to boron (X), while the σ-polarising ability of X is important for π-bonding. The influence of anisotropic effects is not always predictable. Elements with easily polarised electrons in their *d*-orbitals (e.g., iodine) cause a high-field shift in δ^{11}B. Elements with open *s*-shell electrons (e.g., silicon) cause a low-field shift in δ^{11}B.[224] Overall, the π-electron density on the boron atom controls δ^{11}B. Consequently, groups bonded to boron that remove electron density from the boron atom will cause a low-field shift. Once the electron density is removed from boron deshielding takes place.

It has been reported that the electron density at the boron atom does not increase significantly with the increase of alkyl chain length in trialkylboranes.[225,226] This is in direct agreement with the general rule that the chemical shifts of boron atoms are controlled largely by π–electron density on the boron atom.

Table 4.6 - ^{11}B NMR Chemical Shifts for Trialkylboranes in Diethyl Ether[222]

Compound	δ^{11}B (ppm)
$(CH_3)_3B$	86.2
$(C_2H_5)_3B$	86.6
$(n\text{-}C_3H_7)_3B$	86.6
$(n\text{-}C_4H_9)_3B$	86.5

Since boranes contain hydrogen atoms, it becomes useful to exploit the very sensitive ^{1}H NMR technique in order to analyse alkylboranes. ^{1}H shifts of alkylboranes appear only a few ppm from zero. Terminal hydrogens in diborane derivatives resonate in the 0-4 ppm region of the ^{1}H NMR spectrum. These signals exhibit quartets of equal intensity and span 360 - 570 Hz. The peaks themselves have widths of about 20 ± 10 Hz. The bridging hydrogen atoms resonate in the –1 ppm to –5 ppm region of the ^{1}H NMR spectrum. They occur as broad signals with line widths of 100-300 Hz. Boron-hydrogen coupling constants for both types of diborane protons may be larger than the actual widths of the peaks.

The problem with the ^{1}H signals of terminal and bridging hydrogen atoms is that they are often overlapped or masked by the signals of the alkyl groups bonded to the boron atom, as well as those of the solvent. Onak and co-workers have managed to exploit the fact that lowering temperature can differentiate between bulk solvent protons and those solvent molecules coordinated to the borane.[227] The results of Onak and co-workers[227] also have shown that lowering the temperature could also be used to show previously undetectable boron-hydrogen coupling, as is shown in **Table 4.7**.

A ^{1}H NMR study by Stone and Coyle has shown the donating ability of various Lewis bases by investigating the change in the chemical shifts of the methyl protons of trimethylborane adducts (**Table 4.8**).[228] In the present instance the approach of lowering the measurement temperature to discriminate between peaks would be untenable, owing to the complex nature of the reaction mixture and overlapping of the alkylborane peaks.

Table 4.7 - Chemical Shift Data for Diborane-Ether Solutions[225]

System	Temp (°C)	^{11}B NMR Data			^{1}H NMR Data		
		Peak	δ (ppm)	J [^{11}B-$^{1}H_t$] (Hz)	Peak	δ (ppm)	J [^{11}B-$^{1}H_t$] (Hz)
B_2H_6:5Et_2O	30	singlet (broad)	-17	-	-	-	-
	-36	no change	-17	135	1:1:1:1 weak quartet	4.05	133
B_2H_6:5Me_2O	30	1:6:15:20:15:6:1 septet	-15.9	60	broad peak (400 Hz)	2.4	-
	-60	-	-	-	1:1:1:1 quartet	2.47	104
B_2H_6:5THF	30	1:3:31 quartet	1.9	97	1:1:1:1 quartet	2.5	95 ± 5

Table 4.8 - Chemical Shifts of B-Methyl Protons in $B(Me)_3$:Lewis Base Adducts[228]

Compound	δ ^{1}H (ppm)
$B(Me)_3$	4.57

$Et_3N.B(Me)_3$	4.67
$Et_2O.B(Me)_3$	4.57
$Et_2S.B(Me)_3$	4.57

4.3.2. Theory of Binding Constant Methodology

The bulk of the literature on the strength of borane-Lewis base adducts is derived from gas-phase dissociation or calorimetric data.[229,230] Calorimetry can be correlated with NMR chemical shift data to determine the relative acidity of boron Lewis acids toward Lewis bases.[231] NMR spectroscopy may be used by itself to study the donating ability of various Lewis bases by investigating the change in chemical shifts, but it is not uniformly successful in predicting the stabilities of adducts.[232] Thus, while it is possible to obtain a qualitative measure of the dative bond between a boron atom and the donor atom through NMR spectroscopy, it is not always possible to quantify the strength of this bond.[233-238] Höpfl gives an indication on how crystallographic and computational data can be used to define the tetrahedral character of the boron atom in amine-boranes and, thus, quantify the strength of the Lewis acid-base dative bond.[239] Where crystallographic data is not available, measuring the binding constants of boranes with Lewis bases to organoboranes in solution provides a means of quantifying the interaction between organoboranes and Lewis bases. The previous discussion (**Section 4.3.1**) has shown that ^{11}B NMR spectroscopy has long been established as an analytical technique able to provide fast access to reliable quantitative and qualitative information on various species.

The application of NMR spectroscopy to the determination of binding parameters is discussed in great detail by Connors.[240] The following discussion is, thus, a review of the more salient points, which have applicability to the results presented in this work *i.e.*, binding at the fast exchange limit. This approach is different from the classically defined one of Cowley and Mills, where thermodynamic parameters for binding of boranes are determined at the slow exchange limit (i.e., at very low temperature).[241]

For an NMR-observable nucleus, a substrate (S) that associates with a ligand (L) to form an equilibrium complex (SL), the observed first-order rate constant (k) for the binding may be defined as follows:

$$k = k_{SL} + k_S \qquad 4.7$$

where k_{SL} and k_S are the pseudo first-order (i.e., [L] >>> [S]) rate constant for binding and the first-order rate constant for dissociation, respectively. Relating the rate constants to lifetime (τ) yields equation *4.8*.

$$\frac{1}{\tau} = \frac{1}{\tau_{SL}} + \frac{1}{\tau_S} \quad \text{or} \quad \tau = \frac{\tau_S \tau_{SL}}{\tau_S + \tau_{SL}} \qquad 4.8$$

If the fractional occupancy of the substrate and the complex are the same and τ_S and τ_{SL} are also the same, then the frequency of the rotating frame of reference, ν_0, the mean of Larmor processional frequencies for the substrate (ν_S) and the complex (ν_{SL}), is defined by equation *4.9*.

$$\nu_0 = \frac{1}{2}(\nu_S + \nu_{SL}) \qquad 4.9$$

The nuclei in the substrate precess at a frequency of (ν_0-ν_S) and those in the complex precess at a frequency of (ν_0-ν_{SL}). The nuclei, therefore, precess in opposing directions. At the fast exchange limit where lifetimes are short (i.e., less than 10^{-2} s for ^{1}H NMR), precessional motions at the substrate and the complex are indistinguishable. Consequently, only one absorption band is seen at ν_0. It becomes necessary to define ν_0 in terms of fractional occupancy of the two states, as they may not be equal. Thus, the definition of ν_0 becomes equation *4.10*.

$$\nu_0 = f_S \nu_S + f_{SL} \nu_{SL} \qquad 4.10$$

The term ν_0 expressed in equation *4.10*, where f_S and f_{SL} respectively represent the fractional occupancy of the substrate and the complex, may be related to NMR shift by equation *4.11*.

4.11

$$\delta = f_S\delta_S + f_{SL}\delta_{SL}$$

Since $(f_S + f_{SL}) = 1$, then:

$$\delta = f_{SL}(\delta_{SL} - \delta_S) + \delta_S \qquad 4.12$$

Thus, the chemical shift change due to association of the substrate with the ligand, Δ_{BIND}, is defined by equation *4.13*:

$$\Delta_{BIND} = \delta_{SL} - \delta_S \qquad 4.13$$

The binding constant, K_{BIND}, may be extracted from the following binding isotherm (equation *4.14*):

$$\Delta = \frac{\Delta_{BIND} K_{BIND}[L]}{1 + K_{BIND}[L]} \qquad 4.14$$

This isotherm defines the binding curve (a direct plot of Δ *vs.* [L]) that defines one half of a rectangular hyperbola when [L] approaches very large values. It is worth noting that, generally, the ligand concentration is always much larger than that of the substrate. This is so that it becomes possible to determine the asymptotic limit of the binding curve.

A reciprocal plot of observed shift change (Δ) *vs.* free ligand concentration [L] gives a linear plot, the Benesi-Hilderbrand plot,[242] described by equation *4.15*:

$$\frac{1}{\Delta} = \frac{1}{\Delta_{BIND} K_{BIND}} \cdot \frac{1}{[L]} + \frac{1}{\Delta_{BIND}} \qquad 4.15$$

The advantage of using this double reciprocal plot is that the x- and y-variables remain separated on the axes. The notation $\Delta^{11}B$ and $\Delta\delta_{11B}$ was used in this study to denote Δ (total chemical shift change) and Δ_{BIND} (chemical shift change contribution of binding), respectively. Drago comes out in favour of NMR spectroscopy as a means of determining

the binding constant (K_{BIND}) and binding enthalpy (ΔH_{BIND}) data for adduct formation. Its advantage over IR and UV spectroscopy is that solvation effects (essentially solvation of the adduct by a polar solvent) do not affect enthalpy values.[243] Drago and Rose have, however, also pointed out cases where the Benesi-Hilderbrand approach has led to misleading results.[244] This may be due to the fact that most of these cases are under conditions where the concentration of the ligand (or Lewis base) is equivalent to the concentration of the substrate (*i.e.*, [L] ≈ [S]) leading to erroneous estimations of the adduct chemical shift. Koening certainly emphasises the point that the approach works best when [L] > > [S] or *vice versa*. That said, some success can be had with the ^{11}B NMR method. The NMR method has been shown to successfully determine binding constants and related thermodynamic parameters.[240,245]

When the pressure is constant then the change in the Gibbs free energy may be related to the binding constant by equation *4.16*:

$$\Delta G_{BIND} = -RT\ln K_{BIND} \qquad 4.16$$

where ΔG_{BIND} represents the Gibbs free energy of binding, R represents the gas constant and T represents temperature in Kelvin. The Gibbs free energy may also be expressed in terms of the binding enthalpy (ΔH_{BIND}) and entropy (ΔS_{BIND}) as shown in equation *4.17*.

$$\Delta G_{BIND} = \Delta H_{BIND} - T\Delta S_{BIND} \qquad 4.17$$

The binding constant (K_{BIND}) may be obtained by equating the two Gibbs equations, equations *4.*16 and *4.*17, which affords equation *4.18*.

$$\ln K_{BIND} = \frac{-\Delta H_{BIND}}{R} \cdot \frac{1}{T} + \frac{\Delta S_{BIND}}{R} \qquad 4.18$$

If ΔH and ΔS are temperature independent, then a straight line (the van't Hoff plot) is obtained for a plot of $\ln K_{BIND}$ against 1/T.

4.3.3. Binding of Lewis Bases to Tributylborane

The obvious advantage of ^{11}B NMR spectroscopy as an investigative technique for the determination of thermodynamic parameters for trialkylborane-Lewis base association, at room temperature and above, becomes clear when considering the ^{1}H and ^{13}C spectra of tributylborane. The primary spectroscopic data for the investigation may be found in **Section 8.1** (**Appendix C**).

Figure 4.10 and **Figure 4.11** respectively show the ^{13}C and ^{1}H NMR spectra of tributylborane, which show the crowding of peaks within a narrow range. This is particularly evident in the ^{1}H spectrum.

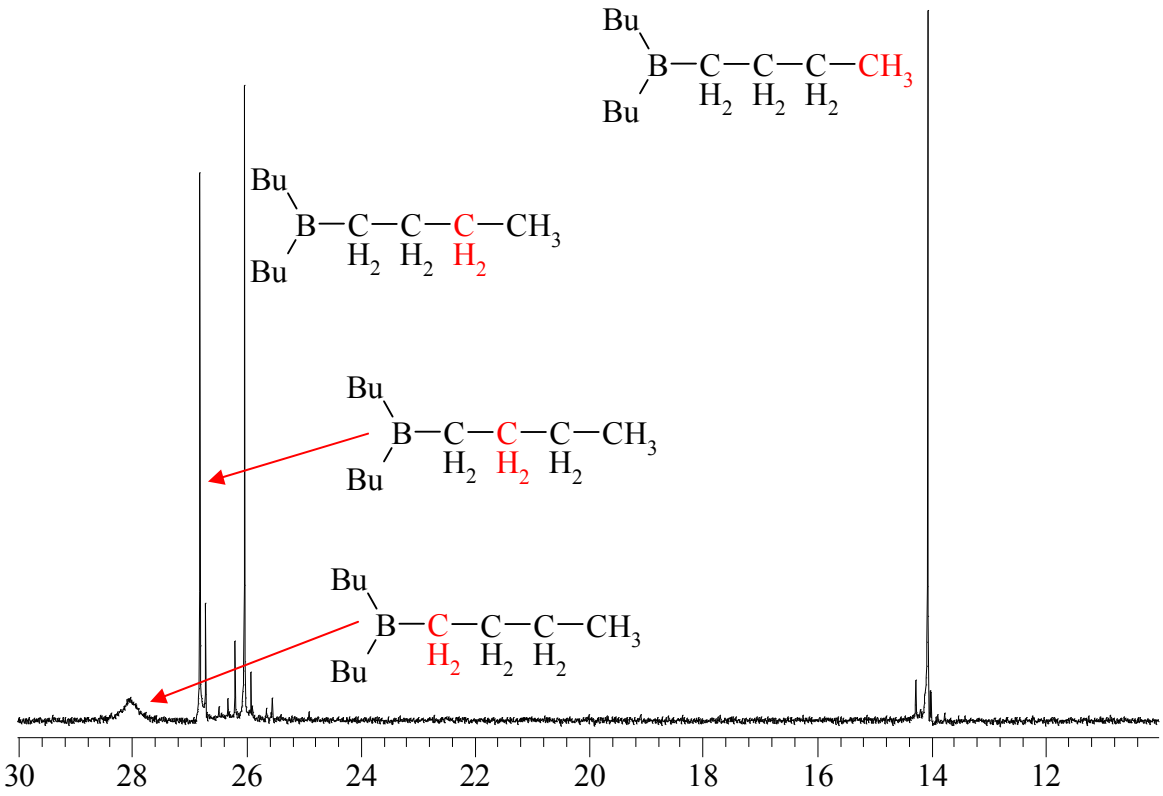

Figure 4.10 – ^{13}C NMR spectrum of tributylborane

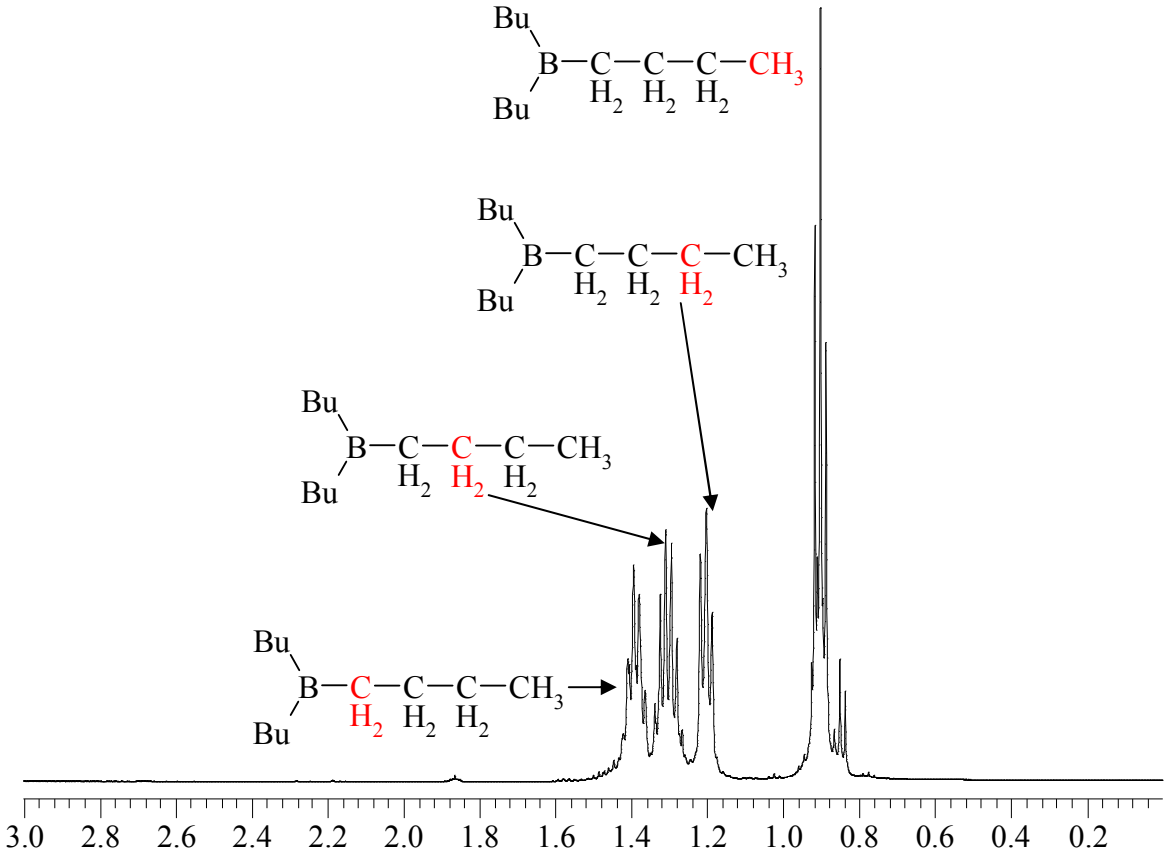

Figure 4.11 - ^{1}H NMR spectrum of tributylborane

The data in **Table 4.9** show the invariance of the ^{1}H and ^{13}C chemical shifts when an adduct is formed. The data from the ^{11}B NMR spectra shows that even the addition of fractional amounts of Lewis base results in an observable change in the chemical shift in the spectrum (**Figure 4.12**).

Whereas ^{1}H and ^{13}C NMR spectroscopy are usable for very low temperatures,[241] it therefore appears as if ^{11}B NMR spectroscopy is the only viable option for the determination of association parameters of trialkylboranes.

The first step in the investigation was to try and establish a scale of relative basicities of the Lewis bases to tributylborane, with the view of comparing these with the thermodynamic parameters.

Table 4.9 - ^{1}H and ^{13}C Chemical shifts for tributylborane-Lewis base adducts$^{\Phi}$

Lewis Base	$\delta^{13}C$ (ppm)	$\delta^{1}H$ (ppm)
Control	28.04	1.20
DMF	27.78	1.11
DMSO	27.84	1.13
HMPA	27.69	1.05
$(MeO)_3PO$	27.79	1.10
$(MeO)_3P$	Signal overlap	0.96
Bu_3P	Signal overlap	1.07
Pr_3N	Signal overlap	Signal overlap
Bu_3N	27.88	1.14

$^{\Phi}$ Shifts are reported for the carbon and hydrogen atoms adjacent to the boron atom

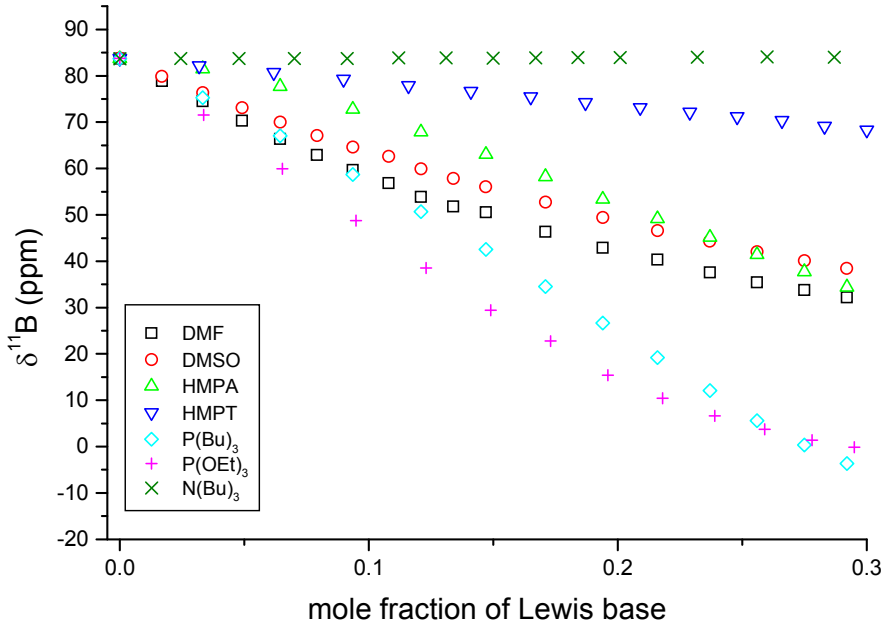

Figure 4.12 - Change in ^{11}B chemical shift of tributylborane with addition of Lewis base

A typical ^{11}B NMR spectrum of the tributylborane solution used in the binding studies is shown in **Figure 4.13**. A possible source of concern is the exchange of side chains between the trialkylborane and the alkoxyborane species (~53 ppm and ~33 ppm). The literature shows that the exchange of trialkylborane with alkoxyboranes is controlled by The B-O π-bond to give the following order:[246,247]

$R_2BOR' > RB(OR')_2 > B(OR')_3$

Furthermore, exchange is slowed down where the boron atom has an intramolecular dative bond, such that it is four-coordinate.[248,249] The exchange reactions of alkoxyalkylboranes take a few days to reach equilibrium at temperatures between 160 and 200 ºC.[250]

For these reasons, it is not necessary to account for any exchange taking place between the alkoxyborane and the trialkylboranes in the binding constant study. In addition to this, the concentration of Lewis base is much larger than that of the borane such that, statistically, the trialkylborane has more chance of interacting with the Lewis base than with the alkoxyboranes. As such, the concentration of the trialkylborane becomes irrelevant, which also simplifies the mathematics.

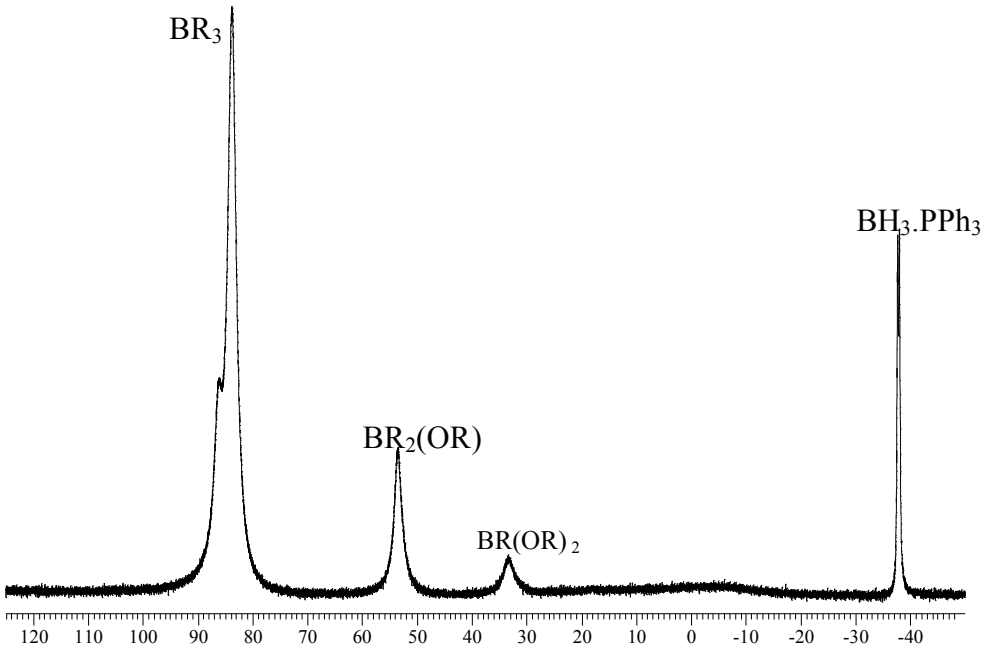

Figure 4.13 - Typical ^{11}B NMR spectrum of tributylborane solution used for binding studies

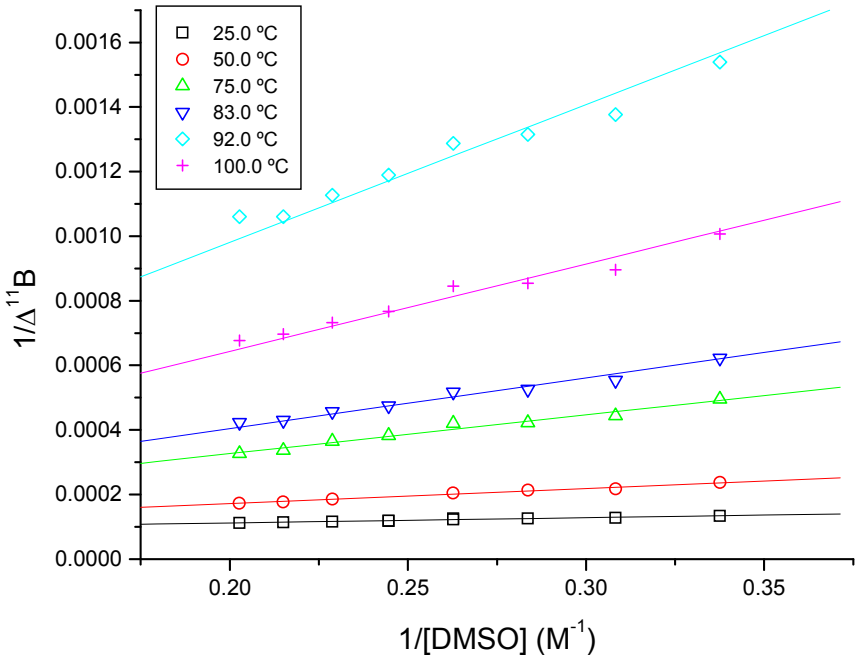

Figure 4.14 - Benesi-Hilderbrand plot for the binding of DMSO to tributylborane in toluene [20% (v/v) C_7D_8] at different temperatures

Table 4.10 - Summary of Benesi-Hilderbrand plot data for the binding of DMSO to tributylborane in toluene [20% (v/v) C_7D_8]

T (K)	1/T (K^{-1})	K_{BIND}	$\ln K_{BIND}$
298.15	0.00335	$(4.90 \pm 0.38) \times 10^{-1}$	-0.71
323.15	0.00309	$(1.67 \pm 0.86) \times 10^{-1}$	-1.79
348.15	0.00287	$(7.22 \pm 0.50) \times 10^{-2}$	-2.63
356.15	0.00281	$(5.72 \pm 0.17) \times 10^{-2}$	-2.86
365.15	0.00274	$(2.94 \pm 0.12) \times 10^{-2}$	-3.53
373.15	0.00268	$(3.76 \pm 0.13) \times 10^{-2}$	-3.28

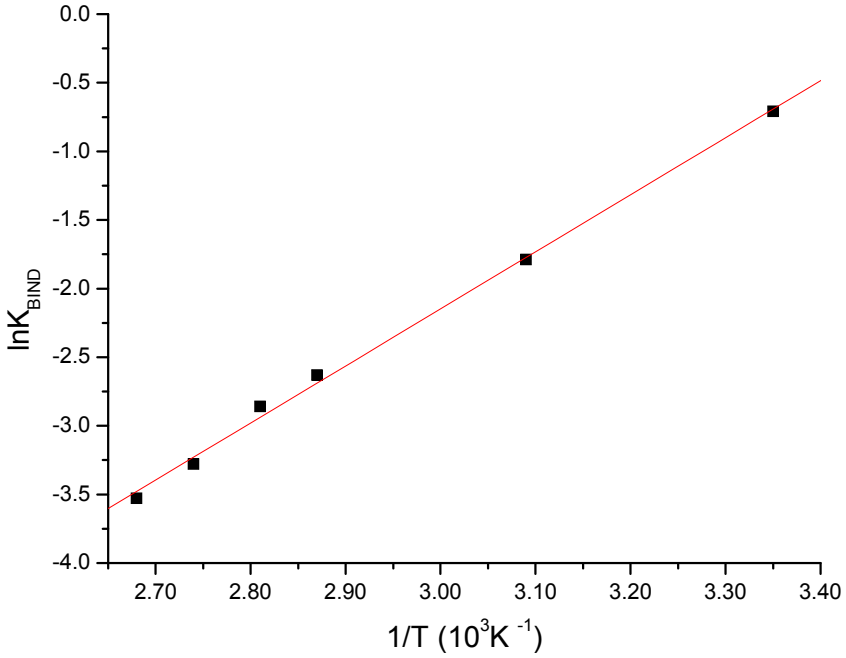

Figure 4.15 - van't Hoff plot for the binding of DMSO to tributylborane in toluene [20% (v/v) C_7D_8]

Figure 4.14 shows a Benesi-Hilderbrand plot for the association of DMSO to tributylborane at different temperatures, while **Figure 4.15** depicts the temperature dependence (van't Hoff plot) of the binding of DMSO to tributylborane, the data for which is shown in **Table 4.10**. The two figures are representative of the trends observed for the binding of the other investigated Lewis bases to tributylborane, the data for which can be found in **Section 8.1** of **Appendix C**. The enthalpies and entropies of binding of the selected Lewis bases to tributylborane originating from the plots are summarised in **Table 4.11**. The table also shows the chemical shift of the borane-Lewis adduct at infinite dilution, obtained from the y-intercept of the Benesi-Hilderbrand plot. This value represents the chemical shift of the Lewis base-trialkylborane complex when all the trialkylborane molecules are associated to the Lewis base.

The rows in **Table 4.11** are grouped according to donor atom in the Lewis base; thus the oxygen atom donors (DMF, DMSO, HMPA and trimethyl phosphate) are grouped together, whereas the phosphorous atom donors (HMPT, tributylphosphate and trimethylphosphite) and nitrogen atom donors (tributylamine and tripropylamine are grouped separately.

Table 4.11 - Summary of thermodynamic parameters and spectroscopic data obtained for the binding of selected Lewis bases to tributylborane in toluene [20% (v/v) C_7D_8]

Lewis Base	ΔS_{BIND} (J/K.mol)[#]	ΔH_{BIND} (kJ/mol)[#]	ΔG_{BIND} (kJ/mol)[#,*]	$\Delta\delta^{11}B_{\infty}$ (ppm)[#,*]	K_{BIND}^{298}
DMSO[‡]	-40 ± 3	-35 ± 1	-23 ± 2	86	5.00×10^{-1}
DMF[‡]	-122 ± 3	-35 ± 1	1 ± 0.1	77	9.76×10^{3}
HMPA[‡]	-107 ± 5	-63 ± 2	-31 ± 2	80	2.67×10^{5}
$(MeO)_3PO$	-182 ± 19	-48 ± 6	6 ± 1	39	5.81×10^{-4}
Bu_3P	-205 ± 12	-75 ± 4	-14 ± 1	97	3.27×10^{2}
$(MeO)_3P$	-173 ± 6	-58 ± 2	-6 ± 0.3	94	1.26×10^{1}
HMPT[‡]	-172 ± 17	-59 ± 6	-8 ± 1	89	2.23×10^{1}
Bu_3N	103 ± 15	47 ± 5	16 ± 3	22	6.90×10^{-1}
Pr_3N	22 ± 4	7 ± 1	0.4 ± 0.1	8	1.42×10^{-3}

[#] $\Delta\delta^{11}B_{\infty}$ calculated according to equation *4.15*. ΔG_{BIND} calculated according to equation *4.*17. ΔS_{BIND} and ΔH_{BIND} calculated according to equation *4.18*.

* ΔG_{BIND} and $\Delta\delta^{11}B_{\infty}$ calculated at 25.0 ºC

[‡] DMF =  ; DMSO =  ; HMPA = 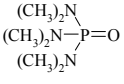 and HMPT = 

The enthalpy data in **Table 4.11** show that binding of the selected Lewis bases to tributylborane is an exothermic (favourable) process in all cases, with the exception of the amines. Amines are classified as being hard Lewis bases, whereas tributylborane and the other Lewis bases in **Table 4.11** are soft. Of these, the phosphorous donors (tributylphosphine, trimethylphosphite and HMPT) show the most exothermic association with tributylborane. HMPA, though having amine functionality, also shows very favourable association to tributylborane. The enthalpy data in **Table 4.11** show the association of a trialkylborane to an amine to be an energy requiring process.

The entropy values in **Table 4.11** follow a similar trend to the enthalpy values. Association of the Lewis base to the acid restricts the translational freedom of the interacting species, which results in a negative value for the entropy. Thus, for species where meaningful association takes place between the trialkylborane and the Lewis base, negative entropy values are observed. Consequently, the oxygen and phosphorous donors reflect large negative entropy values, whereas the nitrogen donors have positive entropy values.

Another factor to consider is the spontaneity of the process, which is reflected in the ΔG_{BIND} value at 25.0 C. Thus, even though an interaction may be exothermic, it might not be necessarily spontaneous; which is the case with DMF and trimethyl phosphate. In such instances the importance of the $T\Delta S$ term (equation *4.17*) overrides the enthalpy of the interaction. The data in **Table 4.11** reveal that the phosphorous donors, HMPA and DMSO have spontaneous interaction with tributylborane, which might be expected given the high $\Delta\delta^{11}B_{\infty}$ values.

It would be convenient to correlate favourable association (in terms of enthalpy and entropy) to large shift changes at infinite dilution ($\Delta\delta^{11}B_{\infty}$). The shift of the Lewis base-trialkylborane adduct at infinite dilution indicates the chemical environment of the boron atom. As has been stated in **Section 4.3.1**, it is the amount of electron density on the empty *p*-orbital of the boron atom that is the primary determinant of the chemical shift of a boron species. However, this effect is most noticeable when the π-donation occurs from an atom bonded directly to the boron atom. Interaction with the *p*-orbital of the boron atom may not be as predictable if taking place through a dative bond, as in the case of adduct formation of a trialkylborane-Lewis base adduct. It may, hence, be difficult to evaluate the extent of electron transfer by a Lewis base to the boron atom during adduct formation and how this will affect the shift of the adduct, as reflected by the adduct chemical shift at infinite dilution. The IR study of Lewis acid-base adducts by Drago[243] suggests that no correlation can be made between enthalpy and chemical shift of such an adduct. Examining the data from the current investigation of tributylborane-Lewis base adducts, however, suggests that some generalities may be made. **Figure 4.16** shows that Lewis bases that are involved in favourable interaction (large negative enthalpies) are clustered together, whereas those with a poor interaction (positive enthalpies) are clustered at the opposite end of the graph. Trimethyl phosphate, which has intermediate interaction, if the chemical shift at infinite dilution is to be used as a measure thereof, is in the middle of this trend. **Figure 4.17**, the plot of the Gibbs free energy of binding against the chemical shift of the adduct infinite dilution at 25.0 ºC shows a similar clustering pattern.

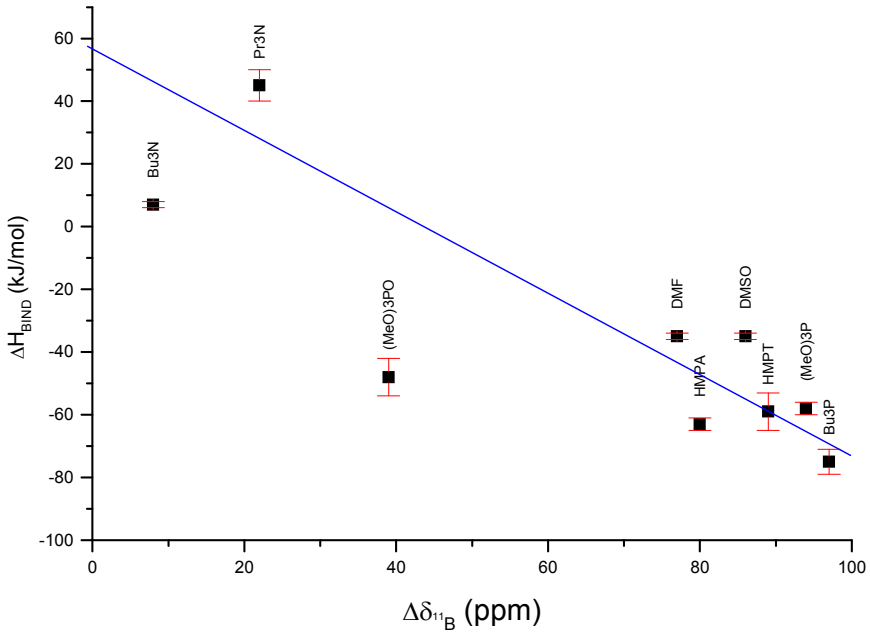

Figure 4.16 - Relationship of binding enthalpy to room temperature adduct chemical shift

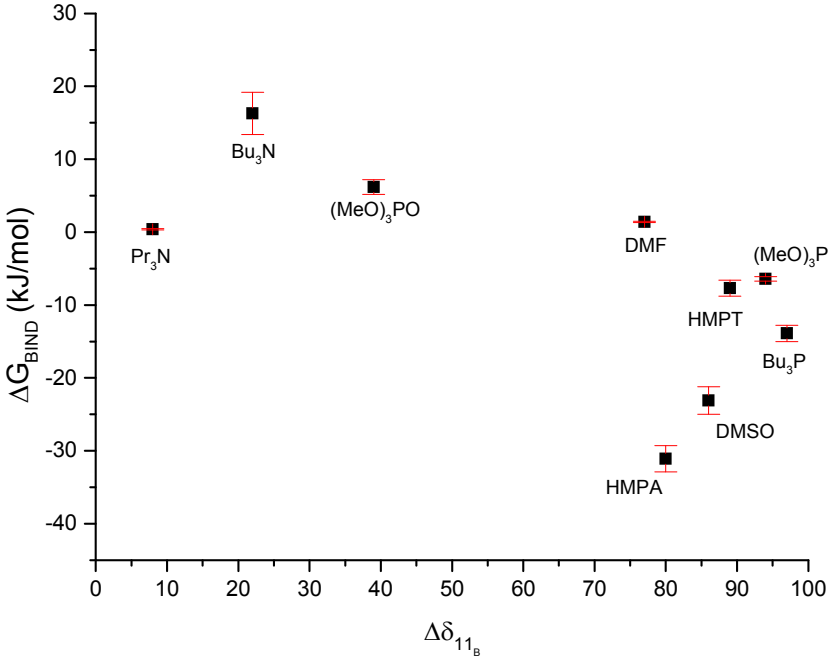

Figure 4.17 - Relationship of Gibbs free energy to the adduct chemical shift at infinite dilution at 25.0 °C

However, plotting the Gibbs free energy of binding against the $\log K_{BIND}$ at 25.0 ºC reveals a linear relationship (**Figure 4.18**), which illustrates the data tabulated in **Table 4.11** in a much more useful manner, bearing in mind that Lewis bases can only be ordered according to strength against the same acid. That is, **Figure 4.18** illustrates the connection between the spontaneity of the interaction between the Lewis base and tributylborane and the strength of the interaction, K_{BIND}, at 25.0 ºC. The weak binders (Bu_3N, trimethyl phosphate and Pr_3N) can be found along the top of the trend, whereas the strong binders are found at the bottom of the linear trend. That DMF and DMSO do not form part of this trend means that the spontaneity of their interaction with tributylborane does not indicate a strong interaction. DMF might not initially have an interaction with tributylborane, but when this interaction does take place it results in the formation of a strong dative bond between the two. DMSO, on the other hand, has a high initial attraction to tributylborane, but a weak bond is formed between the two. This is reflected in the relatively small entropy value in **Table 4.11** which points to minor restriction in the translational motion of the adduct.

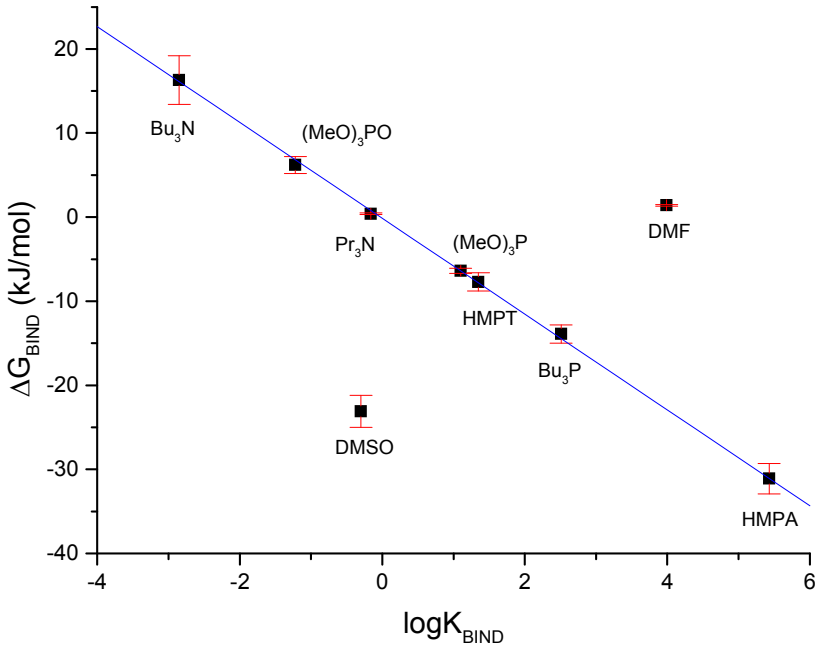

Figure 4.18 - Relationship of Gibbs free energy to the binding constant, K_{BIND}, at 25.0 ºC

A plot of ΔH_{BIND} against $\log K_{BIND}$ at room temperature (**Figure 4.19**) also reveals some interesting trends. The data in **Figure 4.19** can be grouped according to the donor atom of

the Lewis base. Thus, the phosphorous atom donors can be grouped along a linear trend, whereas the oxygen donors can be grouped along a Gaussian curve.

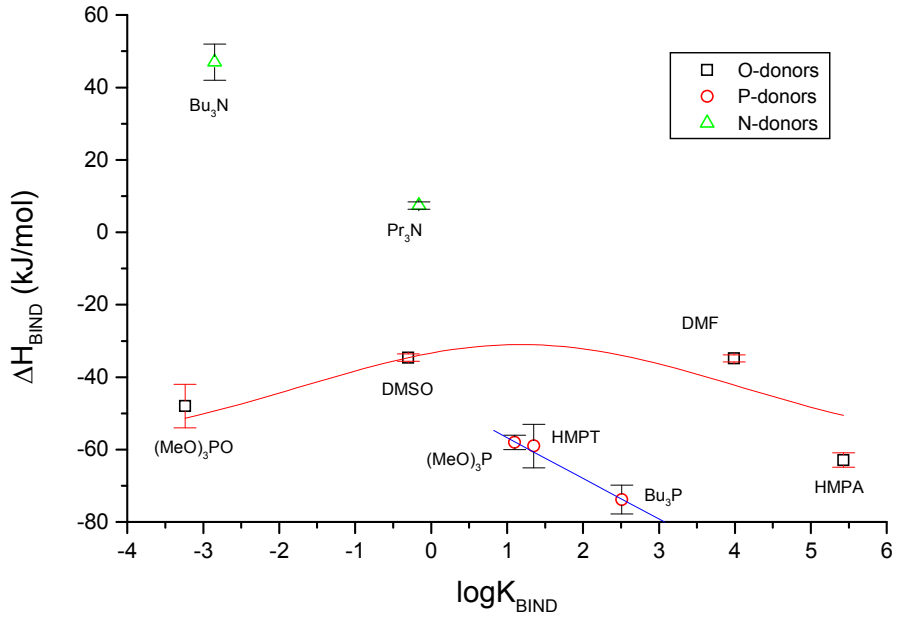

Figure 4.19 - Relationship of binding enthalpy to the binding constant, K_{BIND}, at 25.0 °C

4.3.4. Summary

The results of the investigation of the thermodynamics of the interaction of Lewis bases to tributylborane have revealed some interesting revelations. The most striking is that the chemical shift of the adduct at infinite dilution is not a reliable measure of the interaction between the two species. At best, the parameter can be used to cluster groups of Lewis bases into strong or weak binders according to enthalpy or Gibbs free energy values. More value maybe extracted from the data by correlating the binding constant to the Gibbs free energy and the enthalpy. The former defines a linear trend that orders the Lewis bases spontaneity of the interaction with the strength of the dative bond formed. Only DMF and DMSO were found not to fit this trend.

In order to further understand the effects of electrostatic charge transfer and distribution between the Lewis base and the alkylborane moiety, computational calculations at the

Density Functional level of theory (DFT) were carried out. This was to help put the results into context with chemical theory. The findings are discussed in **Section 4.4**.

4.4. Computational Rationalisation of Binding of Lewis Bases to Trialkylboranes

Reichardt points out that the interaction of Lewis acids and bases is a hybrid of electrostatic and covalent forces and not a hybrid of electrostatic and charge transfer forces.[242,251] The system of E and C parameters introduced by Drago and co-workers[252] takes this into account such that the enthalpy of adduct formation can be described by equation *4.19*.

$$-\Delta H = (E_A \times E_B) + (C_A \times C_B) \qquad 4.19$$

The E terms represent the electrostatic interactions of the acid (A) and the base (B), while the C term represents the covalent interactions. The E-to-C ratio therefore represents the contribution of these two terms to adduct formation.

Gutmann calls the term $-\Delta H$ for the formation of the adduct formed between donors and $SbCl_5$ the donor number (ΔN)[253] and has shown that it can be correlated to thermodynamic (e.g., the linear relationship of $-\Delta H_{BIND}$ *vs.* $\log K_{BIND}$), kinetic, electrochemical (half-wave and reduction potentials) as well as spectroscopic data.[254]

4.4.1. Theory of Absolute Hardness and Absolute Electronegativity

Trialkylboranes are defined as soft acids in terms of hard-soft acid-base (HSAB) theory and accordingly prefer to associate with soft bases.[255] This definition is somewhat imprecise as it fails to supply a measurable quantity that defines the degree of "softness" or "hardness" of a molecule. Pearson has introduced the parameter η to define absolute

hardness of a molecule, which complements HSAB theory.[256] Generally, the larger the η value is, the harder the molecule. The η value is defined by equation *4.20*, where, according to Koopman's theorem, $I = E_{LUMO}$ and $A = -E_{HOMO}$.

$$\eta = \frac{(I - A)}{2} \qquad 4.20$$

Equation *4.20* follows from the observation that the slope of the plot of the total electronic energy of a species (E) against the number of electrons in that species (N), **Figure 4.20**, defines the electronic chemical potential, μ, which measures the polarizability of electrons in that molecule.[257]

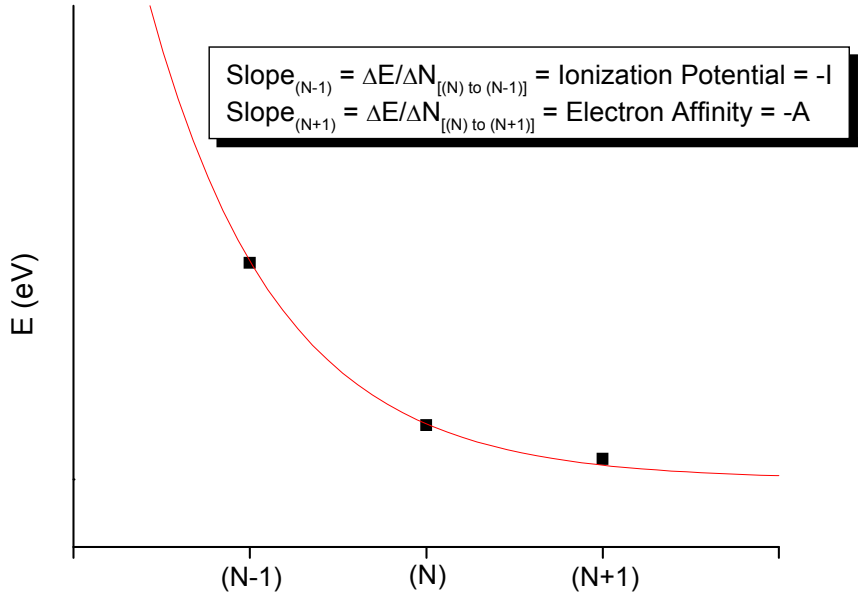

Figure 4.20 - Graph showing relationship between electronic energy (E) and number of electrons (N)

Since the instantaneous slope, $-(\partial E/\partial N)$, of **Figure 4.20** is not known, mean slopes can be used as shown in **Figure 4.20** to find the approximate slope or μ:

$$-\mu = -\left(\frac{\partial E}{\partial N}\right) \cong \frac{(I + A)}{2} = \chi_M \qquad 4.21$$

It is evident from the above equation that the chemical potential is related to absolute electronegativity, χ_M.[257,258] Much as bringing a Lewis acid (A) and a Lewis base (B) to form an adduct (AB) with a coordinate bond results in an equalisation of chemical potentials such that $\mu_A = \mu_B = \mu_{AB}$ at equilibrium, the same procedure results in equalisation of absolute electronegativity.[259] It should be noted that absolute electronegativity (χ^o) refers to the whole chemical species (ion, molecule or radical), not just an individual atom. In general, large values of χ^o are associated with electron acceptors (acids) while smaller values are associated with electron donors (bases).

The change in slope of **Figure 4.20** with N (or the change in the chemical potential with N) is used to define absolute hardness, η, as shown in equation *4.22*.

$$\eta = \frac{1}{2}\left(\frac{\partial^2 E}{\partial N^2}\right) = \frac{1}{2}\left(\frac{\partial \mu}{\partial N}\right) = \frac{(I - A)}{2} \qquad 4.22$$

Molecular orbital (MO) theory teaches that $I = -E_{LUMO}$ and $A = -E_{HOMO}$ in eV. Thus, hardness is the resistance of the chemical potential to electrical transfer (ΔN). To appreciate the effect of absolute electronegativity and absolute hardness, equation *4.23* may be used for the association of an acid (A) and a base (B). The μ°_A and μ°_B parameters in equation *4.23* respectively define the standard electronic chemical potential of the acid (A) and base (B).

$$\mu_A = \mu^\circ_A + 2\eta_A \Delta N \text{ and } \mu_B = \mu^\circ_B - 2\eta_B \Delta N \qquad 4.23$$

The addition of the $(2\eta_A \Delta N)$ term in the case of the acid indicates an increase in electrical potential by gaining electron density from the base, while the subtraction of the $(2\eta_A \Delta N)$ term in the case of the base indicates a loss of electric potential in donating electron density to the acid. As mentioned earlier there is a balancing of absolute electronegativity on formation of the adduct such that $\mu_A = \mu_B = \mu_{AB}$. Accordingly, equating μ_A and μ_B yields equation *4.24*.

$$\Delta N = \frac{(\mu_A^\circ - \mu_B^\circ)}{2(\eta_A + \eta_B)} = \frac{(\chi_A^\circ - \chi_B^\circ)}{2(\eta_A + \eta_B)} \qquad 4.24$$

The upshot of this is that the absolute electronegativity difference facilitates electron transfer while the sum of the hardness term, by definition, accounts for resistance to electron transfer. Thus, soft acids generally have small η_A and η_B values meaning a larger ΔN value implying facile electron transfer. It should be noted that this transfer might occur in either one direction or both directions during the formation of a covalent bond.

Pearson[260] gives a detailed review on the subject of absolute hardness and absolute electronegativity, while Chattaraj and Maiti[261] provides a summary of the relationship between the shell structure of compounds and their stability in terms of absolute hardness and absolute electronegativity.

4.4.2. Effect of Absolute Electronegativity and Absolute Hardness on the Association of Lewis Bases to Trialkylboranes

The theory of absolute hardness detailed in **Section 4.4.1** is the ideal tool with which to interrogate the interaction of the Lewis bases investigated by ^{11}B NMR spectroscopy in **Section 4.3.3**. In addition to these, other Lewis bases were also used in the computational investigation. The energy value for the LUMO and HOMO orbitals were determined at the B3LYP/6-31G* level of theory from HF/6-31G*-optimised structures. The suitability of density functional theory for the determination of the parameters for the determination of absolute hardness and absolute electronegativity has been demonstrated by Pearson.[261] The details of the computational regime used in the current investigation are described in **Section 2.7** and the primary data may be found in **Section 9** of **Appendix C**.

Table 4.12 lists the electron transfer between a series of Lewis bases and boranes (*i.e.*, LB→BR_3, where R = H, Me or Bu). The data shows that the degree of electron transfer (ΔN) from the Lewis base decreases drastically (*ca.* 50%) as hydrogen is replaced by a

methyl group in the borane moiety. The trialkylboranes are similarly influenced, with only a minor decrease in the electron transfer when the methyl substituents are replaced by butyl substituents. This is to be expected since the HOMO and LUMO energy levels of the two trialkylboranes are similar (**Table 4.12**). More importantly, the absolute electronegativity values for trimethylborane and tributylborane (χ^o = 4.07 eV and 3.49 eV, respectively) are similar. Since the absolute electronegativity can be equated with the chemical potential of a species (equation *4.21*), it follows then that the two trialkylboranes will have a similar response to the equalisation of chemical potential that occurs during bond formation during adduct formation.

The decrease in ΔN on going from trimethylborane to tributylborane across the series of selected Lewis bases is an effect of the increasing steric hindrance about the boron atom as the hydrogen atoms are replaced by methyl substituents, and the methyl substituents are replaced by butyl substituents in the borane structure. This hinders the approach of the Lewis base towards the boron atom. The second factor influencing the ΔN value is the increasing inductive effect from the alkyl substituents about the boron atom. This renders the boron atom less electrophilic and is, therefore, less likely to interact with an incoming Lewis base.

Table 4.12 - B3LYP/6-31G*-calculated η and χ^o data for selected boranes and Lewis bases

Compound	I (eV)	A (eV)	χ^o (eV)	η (eV)	$\Delta N_{(LB\rightarrow BH_3)}$	$\Delta N_{(LB\rightarrow BMe_3)}$	$\Delta N_{(LB\rightarrow BBu_3)}$	$\Delta\delta^{11}B_\infty$ (ppm) [#,*]	K_{BIND}^{298}
BH_3	1.78	9.56	5.67	3.89	-	-	-	-	-
BMe_3	0.16	7.99	4.07	3.92	-	-	-	-	-
BBu_3	0.29	7.26	3.49	3.78	-	-	-	-	-
HMPA	-1.82	5.78	1.98	3.80	0.240	0.136	0.123	80	2.67×10^5
DMSO	-1.16	6.05	2.45	3.61	0.215	0.108	0.094	86	5.00×10^{-1}
Tetramethylurea	-1.69	6.72	2.52	4.21	0.195	0.096	0.082	-	-
Me_3PO	-1.70	6.87	2.59	4.29	0.189	0.091	0.077	-	-
DMF	-1.01	6.57	2.78	3.79	0.188	0.084	0.068	77	9.76×10^3
$(MeO)_3PO$	-1.57	7.73	3.08	4.65	0.152	0.058	0.043	39	5.81×10^{-4}
Tetramethylthiourea	0.18	5.58	2.88	2.70	0.212	0.090	0.072	-	-
Pr_3N	-2.45	5.50	1.53	3.98	0.264	0.162	0.151	8	1.42×10^{-3}
Bu_3N	-2.34	5.56	1.61	3.95	0.259	0.157	0.146	22	6.90×10^{-1}
HMPT	-1.45	5.25	1.90	3.35	0.260	0.150	0.137	89	2.23×10^1
Bu_3P	-1.58	5.86	2.14	3.72	0.232	0.127	0.113	97	3.27×10^2
$(MeO)_3P$	-1.04	6.31	2.64	3.68	0.201	0.095	0.080	94	1.26×10^1

Note: $I = -E_{LUMO}$, $A = -E_{HOMO}$, $\chi^\circ = \frac{|I + A|}{2}$, $\eta = \frac{|I - A|}{2}$, $\Delta N = \frac{(\chi_A^\circ - \chi_B^\circ)}{2(\eta_A + \eta_B)}$

The rows in **Table 4.12** have been divided according to donor atom, *i.e.* nitrogen, oxygen and phosphorous and ordered according to decreasing values of ΔN within each donor atom group. Tetramethylthiourea is included with the oxygen atom donors because sulfur lies in the same group as oxygen in the period table. No trends on this basis are immediately apparent. It is apparent from scrutinising the HOMO energies (A values) that compounds that contain oxygen atoms (irrespective of whether oxygen is the donor atom or not) have lower energy HOMOs. The compounds have higher χ^o values and report lower levels of electron transfer. Thus, even in the phosphorous donor series trimethylphosphite is found to have the lower-lying HOMO (A = 6.31 eV). The opposite is true of compounds that contain nitrogen atoms, with the nitrogen donor compounds having the higher-lying HOMOs (A = 5.56 eV and 5.50 eV for tributylamine and tripropylamine, respectively). The effect of the nitrogen is also reflected in HMPA (A = 5.78 eV), HMPT (A = 5.25 eV) and tetramethylthiourea (A = 5.58 eV). The effects of the nitrogen and oxygen atoms are not so obvious on the LUMO energies, which are of similar magnitude in the oxygen and phosphorous donor atoms. The notable exceptions are the high-lying LUMOs of the nitrogen donors, tributylamine (I = -2.34 eV) and tripropylamine (I = 2.45 eV); as well as the high-energy LUMO of tetramethylthiourea (I = 0.18 eV). The effect of the nitrogen atoms on the HOMO energy level is reflected most strongly in the absolute electronegativity (χ^o values), where HMPA, tributylamine, tripropylamine and HMPT have lower absolute electronegativity values ($\chi^o < 2$ eV).

Unexpectedly, the interaction of amines with the selected trialkylborane is the most favourable (higher ΔN values) across the borane series. Only HMPA and HMPT have similarly high ΔN values (0.123 and 0.137, respectively). This again is the effect of the nitrogen atom these compounds contain, which is reflected in the low χ^o values for these compounds which, in turn, are a result of their higher-energy HOMO orbitals. **Figure 4.22** shows an inverse relationship between ΔN and absolute electronegativity, unlike the HOMO level which show a direct correlation to ΔN (**Figure 4.21**).

Figure 4.21 shows that the compounds with higher lying HOMOs result in a higher degree of electron transfer to the borane moiety and that there is a substantial decrease in transfer of electron density on going from BH_3 to a trialkylborane.

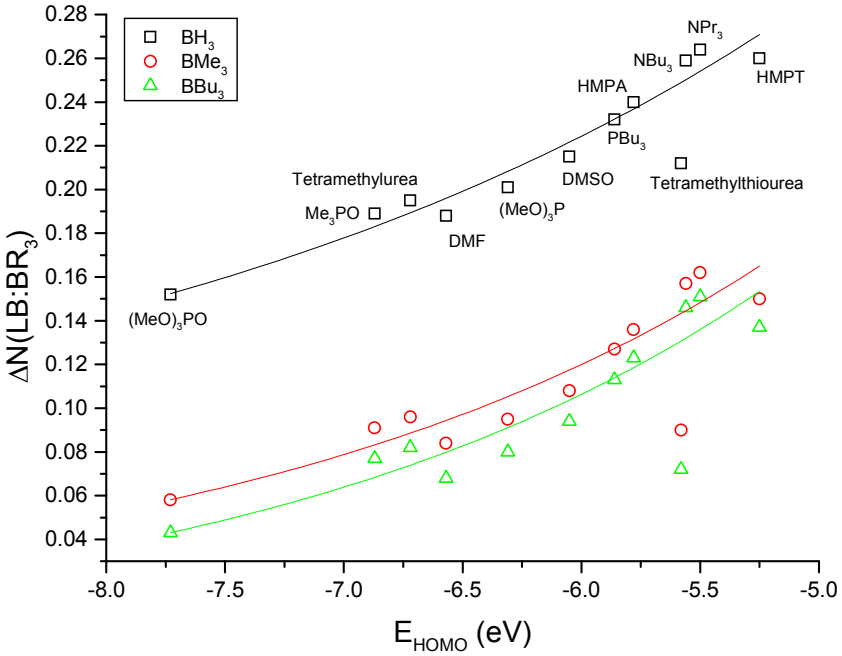

Figure 4.21 - Effect of HOMO energy level of the Lewis base on transfer of electron density the bases from to boranes

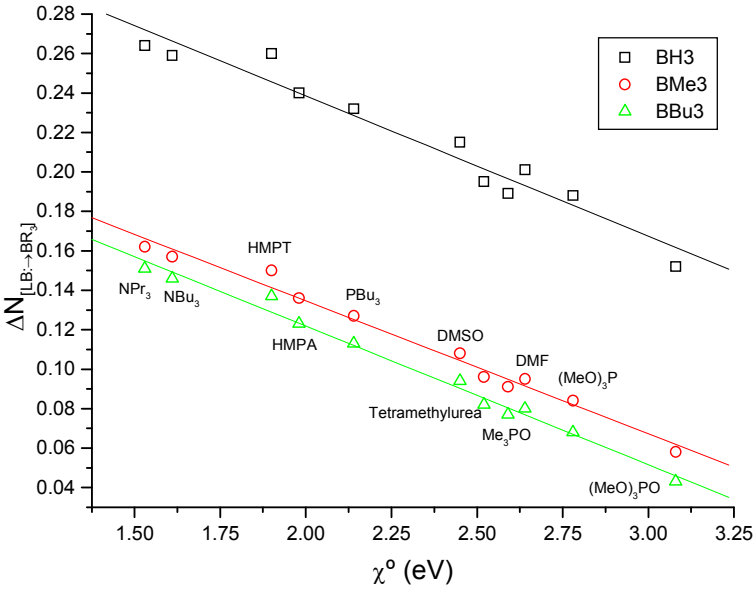

Figure 4.22 - Effect of absolute electronegativity of the Lewis base on transfer of electron density from bases to boranes

These trends mean that the Lewis bases are becoming more basic down a donor group as listed in **Table 4.12**. The exception from this is better electron transfer down a group, which is what can be observed for all three boranes.

In analysing the χ^o values in **Table 4.12** it becomes evident that as absolute electronegativity decreases, the ΔN values increase in all the boranes within the same donor atom group. Analysis of the absolute hardness values (η) in **Table 4.12** reveals an interesting trend within the oxygen donor atoms. This is the same trend as that described for χ^o, with tetramethylurea and trimethylphosphate being the exception, when compared to electron transfer. The data in **Table 4.12** also show that the magnitude of the η values is related to the energy of the HOMO orbital; with only tetramethylurea and trimethylphosphate being the exception. Based on these η values, it would be expected that the ΔN values would decrease in the order $\Delta N_{(LB\rightarrow BMe_3)} > \Delta N_{(LB\rightarrow BH_3)} > \Delta N_{(LB\rightarrow BBu_3)}$. The also show that the order is: $\Delta N_{(LB\rightarrow BH_3)} > \Delta N_{(LB\rightarrow BMe_3)} > \Delta N_{(LB\rightarrow BBu_3)}$. The reversal in the order between BMe_3 and BH_3 can be attributed to the steric hindrance as the Lewis base approaches BMe_3, which subsequently causes less favourable interaction between these two species. However, the data in **Table 4.12** show that the ΔN values are also influenced by the χ^o values of the boranes which decrease in the expected order of: $\Delta N_{(LB\rightarrow BMe_3)} > \Delta N_{(LB\rightarrow BH_3)} > \Delta N_{(LB\rightarrow BBu_3)}$.

While sufficient for explaining the differences in absolute hardness within compounds of similar donor atom, polarisability of the electrons as defined by the dielectric constant cannot explain differences between compounds with different donor atoms. It is the energy levels of the HOMO and LUMO orbitals of the interacting species that have to be considered. The amines have A values similar to the other species and, by this reasoning, would be expected to have similar η values, yet they display resistance to electron transfer (high η values). Scrutinising the I values shows them, however, to have very high lying LUMO orbitals when compared to the other Lewis bases. This results in a higher resistance to electron transfer (high η values). The η values of the amines and trimethylphosphate are higher than those of tributylborane in**Table4.12**, which indicates that these Lewis bases are harder than tributylborane. This is evident in the very low $\Delta\delta^{11}B_\infty$ values observed in the

spectroscopic study of the interaction of these compounds with tributylborane (**Table 4.11** in **Section 4.3.3**).

Comparison of the ΔN data against the ^{11}B NMR spectroscopic data ($\Delta\delta^{11}B_{\infty}$ values in **Table 4.11** in **Section 4.3.3**) reflects the grouping of the selected series of Lewis bases according to their donor atoms (**Figure 4.23**). The figure shows that a large ΔN value does not necessarily equate with a large $\Delta\delta^{11}B_{\infty}$ values. This is most evident with the amine donors, which have very high ΔN values but low $\Delta\delta^{11}B_{\infty}$ values.

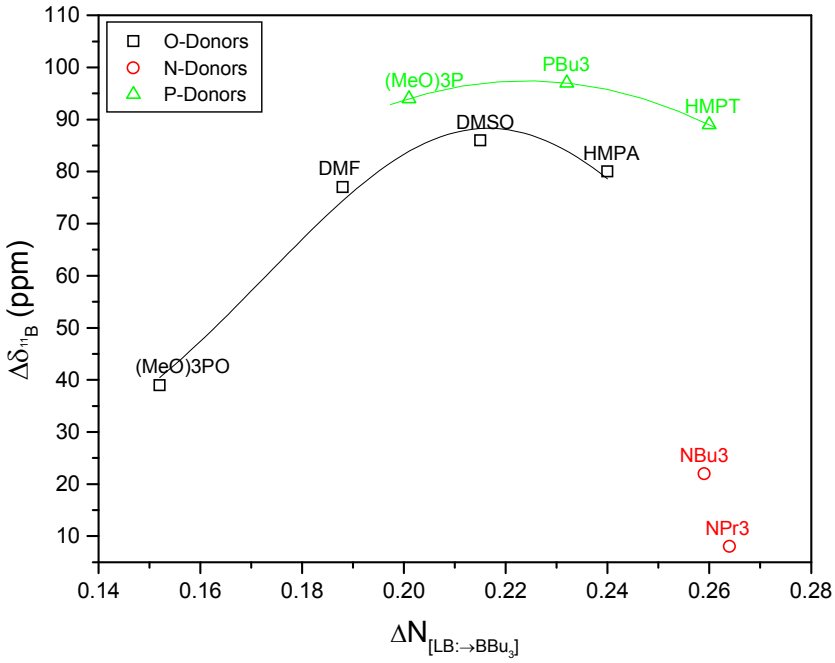

Figure 4.23 - Relationship between B3LYP/6-31G*-calculated ΔN parameter and experimentally-observed chemical environment of tributylborane, as reflected in the change of ^{11}B chemical sift, during interaction with selected series of Lewis bases at 25.0 ºC

Trimethylphosphate, $(MeO)_3PO$ presents an interesting case in **Table 4.11** in having negative enthalpy and entropy values, but a low $\Delta\delta^{11}B_{\infty}$ value (**Table 4.11** in **Section 4.3.3**). The amine Lewis bases report positive enthalpies and entropy values, such that a low $\Delta\delta^{11}B_{\infty}$ value is expected. The data in **Table 4.12** show that trimethylphosphate has a high absolute electronegativity value (3.08 eV), which accounts for the favourable enthalpy and entropy values. The high absolute hardness value (4.65 eV), *i.e.* resistance to

complex formation, accounts for the low $\Delta\delta^{11}B_{\infty}$ value. A similar argument may be made for the amine Lewis bases, which, though having large ΔN values, have low $\Delta\delta^{11}B_{\infty}$ values. Tributylamine and tripropylamine have low absolute electronegativity values (1.61 and 1.53, respectively) which accounts for the low enthalpy and entropy values. They also have relatively high absolute hardness values (3.95 and 3.98, respectively) accounting for the low $\Delta\delta^{11}B_{\infty}$ values.

The absolute hardness and electronegativity parameters serve as a powerful tool with which to evaluate the interactions of Lewis bases and acids. This type of analysis is based on the orbital energy levels of the interacting species and does not take structural changes when adduct formation take place. It was decided to investigate the influence of adduct formation on the conformation of the trialkylborane. **Section 4.4.3** therefore discusses the results of an investigation of the changes of the computationally generated structures of trialkylborane-Lewis base adducts.

4.4.3. Effect of Adduct Formation on Trialkylborane Structure

The strength of the interaction between a Lewis base and a Lewis acid can be evaluated according to the structure of the borane-Lewis base complex. The premise is that, as an adduct is formed and more electron density is transferred to the boron atom, the geometry about the boron atom becomes less trigonal planar to being more tetrahedral. Thus, measuring the bond angles about the boron atom in the borane-Lewis base adduct gives an indication of the strength of the interaction between the two species in the adduct. Ōki's tetrahedral character ($\%THC_{\bar{O}ki}$) parameter is originally defined for the investigation of the interaction of amines and boron compounds.[262] As such, it cannot be ignored in the current investigation as a means of evaluating the dative bond strength between Lewis bases and trialkylboranes. The tetrahedral character parameter measures the deviation of the angles around the boron atom in an adduct from the ideal angle of 109.5º in a tetrahedral environment. Though originally applied to crystallographic data, the method is applicable to theoretical structural data, as shown in the study of the dative bond in $Me_3N.BMe_3$.[263] Höpfl has redefined this parameter ($\%THC_{DA}$), proposing the use of all

six bonds about the boron atom to define the tetrahedral character of the boron atom brought on by a donor atom (equation *4.25*).[264]

$$\%THC_{DA} = 100 \times \left[1 - \frac{\sum_{n=1-6} \left| 109.5 - \theta_n \right|^{\circ}}{3(120 - 109.5)^{\circ} + 3(109.5 - 90)^{\circ}} \right] = 100 \times \left[1 - \frac{\sum_{n=1-6} \left| 109.5 - \theta_n \right|^{\circ}}{90^{\circ}} \right] \qquad 4.25$$

The data in **Table 4.13** was obtained by measuring the angle defined by the donor atom of the Lewis base, the boron atom and the carbon atom of the trialkylborane, as well as the carbon-boron-carbon angle in the trialkylborane, from HF-optimised Lewis base trimethylborane structures. These angles are represented as the symbol θ_n in equation *4.25*. The primary angle and bond distance data may be found in **Section 9** of **Appendix C**.

Table 4.13 details the results of the calculation of the tetrahedral character of the complexes formed between the various Lewis bases and trimethylborane. The distances between the donor and acceptor atoms ($L_{D\rightarrow A}$), *i.e.* dative bond lengths, are also reported in **Table 4.13**. The dative bond length is not a parameter required for the determination of tetrahedral character. It is measured in the current investigation in order to investigate whether there is a relationship between the amount of electron transfer between the borane and the Lewis base and, perhaps more importantly, to investigate whether the size of the Lewis base affects the degree of association.

The results indicate that, with the exception of DMSO, the compounds that do not bond through oxygen atoms (*i.e.*, HMPT, the phosphines, amines and phosphites) have more favourable interaction with THC_{DA} values ≥99.0%. This is reflected in **Figure 4.24**, which shows the phosphine and amine donors to have high tetrahedral character. This is not necessarily related to the ΔN value.

Table 4.13 - HF/6-31G*-calculated tetrahedral character and donor atom to boron atom distance ($L_{D\rightarrow A}$) data

Lewis Base	THC_{DA} (%)	$L_{D\rightarrow A}$ (Å)
DMSO	98.9	1.584
Me_3PO	96.4	1.818
Urea	96.0	1.833
HMPA	95.8	1.861
$(MeO)_3PO$	93.5	1.936
DMF	93.5	1.834
Bu_3N	99.8	1.758
Me_3N	99.7	1.733
Me_3P	99.7	1.581
Bu_3P	99.6	1.581
HMPT	99.4	1.620
$(MeO)_3P$	99.0	1.601
Tetramethylthiourea	93.5	1.958

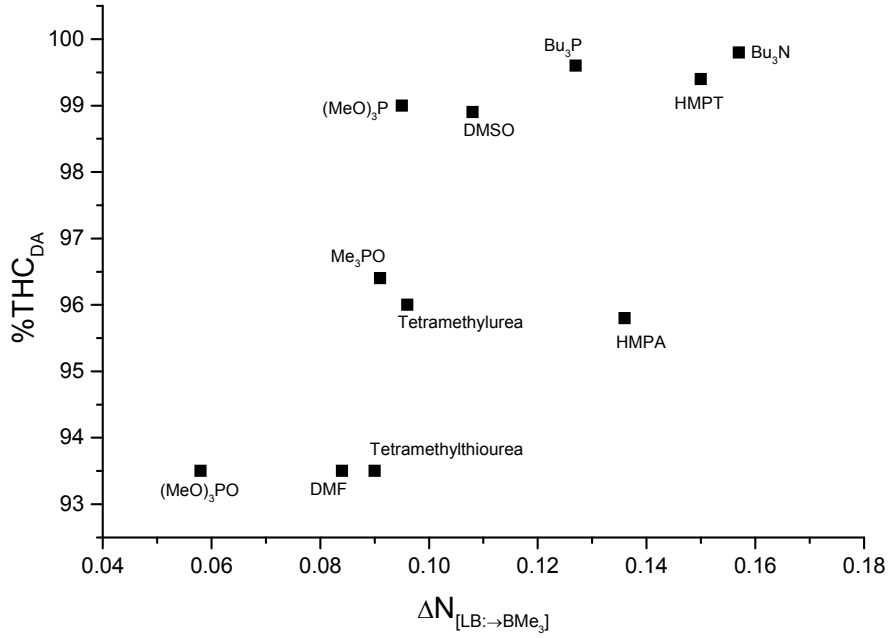

Figure 4.24 - Relationship between B3LYP/6-31G*-calculated ΔN parameter and tetrahedral character about the boron atom in trimethylborane from B3LYP/6-31G*-calculated structures of the Lewis base complex structures.

Plotting $L_{D\rightarrow A}$ against ΔN generally groups the Lewis bases according to donor atom type (**Figure 4.25**), with DMSO being an exception. **Figure 4.25** shows, however, that the length of the dative bond length is linked to the degree of electron transfer.

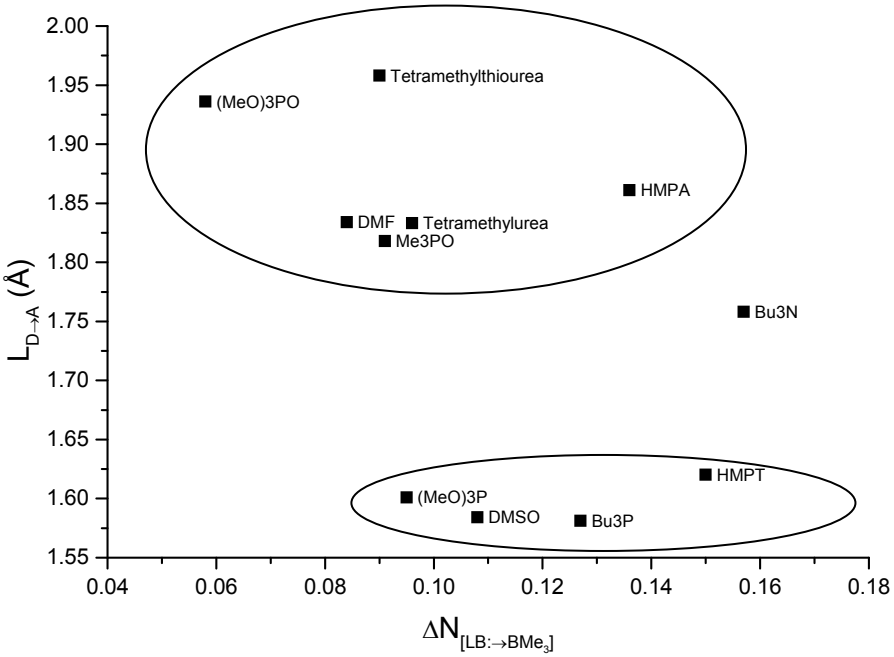

Figure 4.25 - Influence of electron transfer on adduct dative bond length

4.5. Conclusions

The applicability of ^{11}B NMR spectroscopy to physical organic chemistry has been demonstrated in this chapter. The investigation of the reduction of nitriles by borane has shown that valuable mechanistic information may be obtained by the use of ^{11}B NMR spectroscopy. The application of the technique as such provides a new route to valuable data. The synergy of the technique with computational chemistry methods has also been shown.

The investigation of the thermodynamics of the association of Lewis bases to tributylborane shows that ^{11}B NMR spectroscopy lends itself to this type of investigation. Though the application of the technique for this purpose is not as novel as its use in

kinetics, there are very few examples in the literature where its use for the determination of association behaviour of trialkylboranes may be found. Given the direct information about the environment state of the boron nucleus, the technique would be of major importance to those investigating the behaviour of trialkylboranes with various Lewis bases and catalysts.

The symbiosis of the concepts chemical hardness and tetrahedral character has also been shown. Of these two, the concepts of chemical hardness is the more robust as it shows more direct correlation to the experimentally observed findings.

5. References

1. C. A. Houston and Associates, http://ceh.sric.sri.com/Enframe/Report.html?report-681.5030&show-Abstract.html (Accessed 12/02/2004).
2. Nexant, Ltd, http://www.chemsystems.com/newsletters/perp/Jan04_N02-4.cfm (Accessed 10/05/2005).
3. K. Weissermel and H. –J. Arpe, *Industrial Organic Chemistry*, 3rd Edn, Wiley-VCH, Weinheim, **1997**, pp. 74-75.
4. C. A. Houston and Associates, www.colin-houston.com/Press_Releases/591PR.MLB.pdf (Accessed 11/05/2005).

(a) Sasol, Ltd, http://www.sasol.com/sasol_internet/frontend/common/printarticles.jsp?article_id=9200001 (Accessed 14/06/2005); (b) H. Mahomed, A. Bollmann, J. T. Dixon, V. Gokul, L. Griesel, C. Grove, F. M. Hess, H. Maumela and L. Pepler, *Appl. Catal, A*, **2003**, *255*, 355; (c) J. T. Dixon, M. J. Green, F. M.Hess and D. H. Morgan, *J. Oganomet. Chem.,* **2004**, 689, 3641; (d) M. J. Overett, K. Blann, A. Bollmann, J. T. Dixon, F. M. Hess, E. Killian, H. Maumela, D. H Morgan, A. Neveling and S. Otto, *J. Chem. Soc., Chem. Commun*, **2005**, 622; (e) A. Bollmann, K. Blann, J. T. Dixon, F. M. Hess, E. Killian, H. Maumela, D. S. McGuinness, D. H.; Morgan, A. Neveling, S. Otto, M. J. Overett, A. M. Z. Slawin, P. Wasserscheid and S. Kuhlmann, *J. Am. Chem. Soc.*, **2004**, 126, 14712.

5. (e) M. J. Overett, K. Blann, A. Bollmann, J.T. Dixon, D. Haasbroek, E. Killian, H. Maumela, D. S. cGuinness and D. H. Morgan, *J. Am. Chem. Soc.*, **2005**, 127, 10723.
6. http://business.iafrica.com/news/222745.htm (Accessed 11/05/2005).
7. http://www.busrep.co.za/index.php?fArticleId=3068358 (Accessed 17/01/2006)
8. U. Wahner, http://academic.sun.ac.za/unesco/PolymerED2000/Conf2000/WahnerC.pdf (Accessed 11/05/2005).
9. A. de Klerk & H. Struass, *SNDBIP Bulletin 7* (18 October 2002).
10. H. C. Brown and B. C. Subba Rao, *J. Am. Chem. Soc.*, **1956**, 78, 5694.
11. H. C. Brown and B. C. Subba Rao, *J. Org. Chem.*, **1957**, 28, 1136.
12. H. C. Brown, H. I. Schlesinger and A. B. Burg, *J. Am. Chem. Soc.*, **1959**, 81, 673.
13. H. C. Brown and B. C. Subba Rao, *J. Org. Chem.*, **1957**, 22, 1135.

14. H. C. Brown in *Comprehensive Organometallic Chemistry*, Vol. 7, Ed. G. Wilkinson *et. al.*, Permagon Press, Oxford, pp. 111-142.
15. T. C. Hurd*, J. Amer. Chem. Soc.*, **1948**, 70, 2053.
16. H. C. Brown, *Hydroboration*, Benjamin, Inc., New York, **1962**.
17. J. R. Elliott, W. L. Roth, G. F. Roedel and E. M. Boldebuck, *J. Am. Chem. Soc.*, **1952**,74, 5211.
18. B. Rice, J. A. Livasy and G. W. Schaeffer, *J. Am. Chem. Soc.*, **1955**, 77, 2750.
19. H. C. Brown and B. C. Subba Rao, *J. Am. Chem. Soc.*, **1959**, 81, 6428.
20. H. C. Brown, *Organic Synthesis via Boranes*, Wiley-Interscience, New York, **1975**.
21. H. C. Brown and G. Zweifel, *J. Am. Chem. Soc.*, **1960**, 82, 4708.
22. H. C. Brown and R. L. Sharp, *J. Am. Chem. Soc.*, **1966**, 88, 5851.
23. H. C. Brown and G. J. Klender, *Inorg. Chem.*, **1962**, 1, 204.
24. D. J. Pasto in *Boron Hydride Chemistry*, Ed. E. L. Muetterties, Academic Press, Inc., New York, **1974**, pp. 197-220.
25. J. V. B. Kanth and H. C. Brown, *Tetrahedron Lett.*, **2000**, 41, 9361.
26. H. C. Brown and U. S. Racherla, *Tetrahedron Lett.*, **1985**, 26, 2187.
27. R. M. Adams, L. M. Braun, R. A. Braun, H. R. Crissman and M. Opperman, *J. Org. Chem.*, **1971**, 36, 2388.
28. A. B. Burg and R. I. Wagner, *J. Am. Chem. Soc.*, **1954**, 76, 3307.
29. T. D. Coyle, H. D. Kaesz and F. G. A. Stone, *J. Am. Chem. Soc.*, **1959**, 81, 2989.
30. C. F. Lane, *J. Org. Chem.*, **1974**, 39, 1437.
31. L. M. Braun, R. A. Braun, H. R. Crissman, M. Opperman and R. M. Adams, *J. Org. Chem.*, **1971**, 36, 2388.
32. H. C. Brown and A. K. Mandal, *J. Org. Chem.*, **1992**, 57, 4970.
33. H. C. Brown, J. V. B. Kanth and M. Zaidlewicz, *J. Org. Chem.*, **2000**, 65, 6697.
34. H. C. Brown, M. Zaidlewicz, P. V. Dalvi and G. K. Biswas, *J. Org. Chem.*, **2001**, 66, 4795.
35. D. Crich and S. Neelamkavil, *Org. Lett.*, **2002**, 4, 4175.
36. H. C. Brown, *Boranes in Organic Synthesis*, Cornell University Press, Ithaca, **1972**.
37. A. Pelter, R. Rosser and S. Mills, *J. Chem. Soc., Chem. Commun.*, **1981**, 1014.
38. C. F. Lane, *Aldrichim. Acta*, **1973**, 6, 51.
39. H. C. Brown, J. V. B. Kanth and M. Zaidlewicz, *J. Org. Chem.*, **1998**, 63, 5154.
40. H. C. Brown, J. V. B. Kanth and M. Zaidlewicz, *Tetrahedron*, 55, **1999**, 5991.

41. H. C. Brown, J. V. B. Kanth, P. V. Dalvi and M. Zaidlewicz, *J. Org. Chem.*, **1999**, 64, 6263.
42. H. C. Brown, J. V. B. Kanth, P. V. Dalvi and M. Zaidlewicz, *J. Org. Chem.*, **2000**, 65, 4655.
43. J. V. B. Kanth, *Aldrichimica Acta*, **2002**, 35, 57.
44. H. C. Brown and A. K. Mandal, *J. Org. Chem.*, **1980**, 45, 916.
45. H. C. Brown and J. J. Chandrasekharan, *J. Am. Chem. Soc.*, **1984**, 106, 1863.
46. A. M. Salunkhe and E. R. Burkhardt, *Tetrahedron Lett.*, **1997**, 38, 1519.
47. J. A. Soderquist, J. R. Medina and H. Huertas, *Tetrahedron Lett.*, **1998**, 39, 6119.
48. J. A. Soderquist, J. R. Medina and H. Huertas, *Tetrahedron Lett.*, **1998**, 39, 6123.
49. H. C. Brown, *Hydroboration*, Benjamin, Inc., New York, **1962**, pp. 93-101.
50. M. Periasamy and M. Thirumelaikumar, *J. Organomet. Chem.*, **2000**, 609**,** 137.
51. B. Rice, L. A. Livasy and G. W. Schaeffer, *J. Am. Chem. Soc.*, **1950**, 77, 2750.
52. J. A. Marshall and W. S. Johnson, *J. Org. Chem.*, **1963**, 28, 595.
53. V. Hach, *Synthesis*, **1974**, 340.
54. N. Satyanarayana and Periasamy, *Tetrahedron Lett.*, **1984**, 25, 2501.
55. H. S. Lee, K. Isagawa and Y. Otsuji, *Chem. Lett.*, **1984**. 363.
56. H. S. Lee, K. Isagawa, H. Toyoda and Y. Otsuji, *Chem. Lett.*, **1984**, 673.
57. C. Narayana and M. Periasamy, *J. Organomet. Chem.*, **1987**, 323, 145.
58. A. S. B. Prasad, J. V. B. Kanth and M. Periasamy, *Tetrahedron*, **1992**, 48, 4623.
59. R. Shundo, Y. Matsubara, I. Nishiguchi and T. Hirashima, *Bull. Chem. Soc. Jpn.*, **1992**, 65, 530.
60. S. K. Singh, P. S. Martin and G. C. Joshi, *Tetrahedron Lett.*, **1992**, 33, 2419.
61. N. Suzuki, Y. Kaneko, T. Tsunaka, T. Nomoto, Y. Ayaguchi and Y. Izawa, *Tetrahedron*, **1985**, 41, 2387.
62. S. Basakaran, V. Gupta, N. Chidambaran and S. Chndrasekaran, *J. Chem. Soc., Chem. Commun.*, **1989**, 903.
63. K. S. Ravikumar, S. Baskaran and S. Chndrasekaran, *Tetrahedron Lett.*, **1193**, 34, 171.
64. S. Naarasimham, S. Swarnalakshmi and B. Balakuma, *Indian J. Chem., Sect. B*, **1998**, 37, 189.
65. D. A. Albanese, D. Landini, A. Maia and M. Penso, *Synlett*, **2000**, 997.
66. V. V. Volkov and K. G. Myakishev, *Inorg. Chim. Acta*, **1999**, 289, 51.

67. H. C. Brown, *Boranes in Organic S ynthesis*, Cornell University Press, Ithaca, **1972**.
68. M. Zaidlewicz in *Comprehensive Organometallic Chemistry*, **Vol 7,** Ed. G. Wilkinson *et. al.*, Permagon Press, Oxford, pp. 161-197.
69. H. C. Brown and P. V. Ramachandran, *J. Organomet. Chem.*, **1995**, 500, 1.
70. M. Srebnik and P. V. Ramachandran, *Aldrichim. Acta*, **1987**, 20, 9.
71. A. Pelter, K. Smith and H. C. Brown, *Borane Reagents*, Academic Press, London, **1988**.
72. D. J. Pasto, B. Lepeska and T. –C. Cheng, *J. Am. Chem. Soc.,* **1972**, 94, 6083.
73. T. P. F. Brown, A. Tsukamoto and D. B. Bingley, *J. Am. Chem. Soc.,* **1960**, 83, 4703.
74. M. Srebnik, T. E. Cole and H. C. Brown, *J. Org. Chem.*, **1990**, 55, 5051.
75. D. J. Pasto, B. Lepeska and B. Balalsubramaniyan, *J. Am. Chem. Soc.*, **1972**, 94, 6090.
76. A. T. Whatley and R. N. Pease, *J. Am. Chem. Soc.*, **1954**, 76, 835.
77. T. P. Fehlner, *J. Am. Chem. Soc.*, **1971**, 93, 6366.
78. H. C. Brown and K. K. Wang, *J. Am. Chem. Soc.*, **1982**, 104, 7148.
79. C. K. Ingold and F. R. Shaw, *J. Chem. Soc.*, **1927**, 2818.
80. H. C. Brown, R. Liotta and C. G. Scouten, *J. Am. Chem. Soc.*, **1976**, 98, 5297.
81. H. C. Brown and A. W. Moerikofer, *J. Am. Chem. Soc.*, **1963**, 85, 2063.
82. R. B. Turner and W. R. Meador, *J. Am. Chem. Soc.*, **1957**, 79, 4133.
83. K. R. Sundberg, G. D. Graham and W. N. Lipscomb, *J. Am. Chem. Soc.*, **1979**, 101, 2683.
84. H. C. Brown and G. Zweifel, *J. Am. Chem. Soc.*, **1959**, 81, 247.
85. H. C. Brown and A. W. Moerikofer, *J. Am. Chem. Soc.*, **1961**, 83, 3417.
86. A. Streitwieser, Jr., L. Verbit and R. Bittman, *J. Org. Chem.*, **1967**, 32, 1530.
87. D. J. Pasto and F. M. Klein, *J. Org. Chem.*, **1968**, 33, 1468.
88. P. R. Jones, *J. Org. Chem.*, **1972**, 37, 1886.
89. T. Clark and P. von Ragué Schleyer, *J. Organomet. Chem.*, **1978**, 156, 191
90. M. J. S. Dewar and M. L. McKee, *Inorg. Chem.*, **1978**, 17, 1075.
91. J. Klein, E. Dunkelblum, and M. A. Wolff, *J. Organomet. Chem.*, **1967**, 7, 377
92. S. Nagase, N. K. Ray and K. Morokuma, *J. Am. Chem. Soc.*, **1980**,102, 4536.
93. G. D. Graham, S. C. Freilich and W. N. Lipscomb, *J. Am. Chem. Soc.*, **1981**, 103, 2546.

94. X. Wang, Y. Li, Y. –D. Wu, M. N. Paddon-Row, N. G. Rondan and K. N. Houk, *J. Org. Chem.*, **1990**, 55, 2601.

95. T. Clark, D. Wilhelm and P. von Ragué Schleyer, *J. Chem. Soc., Chem. Commun.*, **1983**, 606.

96. G. Tonachini, *Gazz. Chim. Ital.*, **1988**, 118, 149.

97. A. B. Burg, *J. Am. Chem. Soc.*, **1940**, 62, 2228.

98. T. D. Parsons and D. M. Ritter, *J. Am. Chem. Soc.*, **1954**, 83, 1710.

99. P. A. McKusker, G. F. Henion and E. C. Ashby, *J. Am. Chem. Soc.*, **1957**, 79, 5192.

100. B. Bartocho, W.A. Graham and F. G. A. Stone, *J. Inorg. Nucl. Chem.*, **1957**, 6, 5192.

101. R. Köster, *Angew. Chem.*, **1961**, 73, 66.

102. G. F. Hennion, P. A. McKusker and A. J. Rutkowski, *J. Am. Chem. Soc.*, **1958**, 80, 617.

103. G. F. Hennion, P. A. McKusker and J. V. Marra, *J. Am. Chem. Soc.*, **1958**, 80, 3481.

104. P. A. McCusker, J. V. Marra and G. F. Hennion, *J. Am. Chem. Soc.*, **1961**, 83, 1924.

105. (a) R. Köster, W. Larbig and G. W. Rottermund, *Ann. Chem.*, **1965**, 682, 21; (b) R. Koster, *Angew. Chem. Int. Ed.*, **1964**, 3, 174; (c) R. Köster, G. Benedikt, W. Larbig, K. Reinert and G. Rotermund, *Angew. Chem.*, **1963**, 75, 1079; (d) R. Köster and G. Rotermund, *Angew. Chem.*, **1962**, 74, 269; (e) R. Köster and G. Rotermund, *Angew. Chem.*, **1960**, 72, 563.

106. L. Rosenblum, *J. Am. Chem. Soc.*, **1955**, 77, 5016.

107. P. F. Winternitz and A. A. Carotti, *J. Am. Chem. Soc.*, **1960**, 82, 2430.

108. H. C. Brown, K. J. Murray, H. Muller and G. Zweifel, *J. Am. Chem. Soc.*, **1966**, 88, 1443.

109. G. W. Kabalka and R. F. Daley, *J. Am. Chem. Soc.*, **1973**, 95, 4428.

110. M. F. Lappert, in *The Chemistry of Boron and Its Compounds*, Ed. E. L. Muetterties, Wiley, New York, **1967**, Chapter 8.

111. E. Mincione and F. Feliziani, *J. Chem. Soc., Chem. Comm.*, **1973**, 24, 942.

112. L. D. Field and S. P. Gallager, *Tetrahedron Lett.*, **1985**, 26, 6125.

113. G. F. Henion, P. A. McCusker, E. C. Ashby and A. J. Rutkowski, *J. Am. Chem. Soc.*, **1957**, 79, 5190.

114. H. C. Brown and B. C. Subba Rao, *J. Am. Chem. Soc.*, **1959**, 81, 6434.

115. H. C. Brown and M. V. Bhatt, *J. Am. Chem. Soc.*, **1966**, 88, 1440.

116. H. C. Brown and G. Zweifel, *J. Am. Chem. Soc.*, **1960**, 82, 1504.
117. K. Smith, *Chem. Soc. Rev.*, **1974**, 4, 443.
118. H. C. Brown and G. Zweifel, *J. Org. Chem.*, **1957**, 22, 1137.
119. F. M. Rossi, P. A. McCusker and G. F. Hennion, *J. Org. Chem.*, **1967**, 32, 450.
120. A. T. Cocks and K. W. Eggers, *J. Chem. Soc. A*, **1971**, 3606.
121. R. E. Williams, *Inorg. Chem.*, **1962**, 1, 971.
122. H. A. Skinner, *Adv. Organomet. Chem.*, **1964**, 2, 49; J. E. Bennett and H. A. Skinner, *J. Chem. Soc.*, **1961**, 2472.
123. A. Arase, K. Kihara, Y. Masuda, M. Itoh and A. Suzuki*, Kogyo Kagaku Zasshi*, **1970**, 73, 1155. (*Chem. Ab.*, **1970**, 73, 520707)
124. S. A. Leone and A. A. Hinckley, *Am. Chem. Soc. Abstracts of Papers*, **1960**, p. 60.
125. F. L. Ramp, E. J. DeWitt and L. E. Trapasso, *J. Org. Chem.*, **1962**, 27, 4368.
126. H. C. Brown and G. Zweifel, *J. Am. Chem. Soc.*, **1967**, 89, 561.
127. S. B. Wood and B. Rickborn, *J. Org. Chem.*, **1983**, 48, 555.
128. L. D. Field and S. P. Galagher, *Tetrahedron Lett*., **1985**, 26, 6125.
129. F. Lhermitte and P. Knochel, *Angew. Chem. Int. Ed.*, **1988**, 37, 2460.
130. H. Laaziri, L. O. Bromm, F. Lhermitte, R. M. Gschwind and P. Knochel, *J. Am. Chem. Soc.*, **1999**, 121, 6940.
131. H. Laaziri, L. O. Bromm, K. Harms and P. Knochel, *J. Am. Chem. Soc.*, **2000**, 122, 10218.
132. **US 3,173,967**, H. C. Brown (3/1965).
133. **US 3,065,281**, L. W. Hall, Jr. and C. L. Thomas (11/1962)
134. A. J. Rutkowsi, *Am. Chem. Soc., Div. Petrol. Chem. (Preprints)*, **1963**, 8, B13.
135. K. L. Lindsay, J. D. Byrd, G. N. Grammmer and R. W. Johnson, *Am. Chem. Soc., Div. Petrol. Chem. (Preprints)*, **1963**, 8, B25.
136. **US 3,101,376**, S. J. Stanley and A. J. Rutkowski (8/1963)
137. **US 3,131,225**, A. J. Rutkowski, E. J. Inchalik and A. Schrieshein (4/1964).
138. B. M. Mikhailov, M. E. Kuimova and E. A. Shagova, *Dokl. Akad. Nauk. SSR*, 179, **1968**, 1344; B. M. Mikhailov and M. E. Kuimova, *Zh. Obshch. Khim.*, **1971**, 41, 1714.
139. H. C. Brown, M. V. Bhatt and T. Munekata, *J. Am. Chem. Soc.*, **1967**, 89, 567.
140. T. Taniguchi, *Bull. Chem. Soc., Jpn.*, **1979**, 52, 2943.

141. M. Rousseau, *A Study of the Displacement Reaction in the Borane Induced Isomerisation of Alkenes* (MSc Thesis), Potchefstroom University of Christian Education, **2002**.
142. G. B. Kistiakowsky, H. Romeyn, Jr., J. R. Ruhoff, H. A. Smith and W. E. Vaughan, *J. Am. Chem. Soc.*, **1935**, 57, 65.
143. G. B. Kistiakowsky, J. R. Ruhoff, H. A. Smith and W. E. Vaughan, *J. Am. Chem. Soc.*, **1935**, 57, 867.
144. G. B. Kistiakowsky, H. Romeyn, Jr., J. R. Ruhoff, H. A. Smith and W. E. Vaughan, *J. Am. Chem. Soc.*, **1936**, 58, 141.
145. J. D. Odom, in Comprehensive Organometallic Chemistry, Permagon Press, Ed. E. W. Abel, Oxford, **Vol. 1**, pp. 253-269.
146. D.F. Shriver, *The Manipulation of Air-Sensitive Compounds*, McGraw-Hill, Inc., New York, **1969**.
147. G. W. Kramer, A. B. Levy and M. M. Midland in *Organic Synthesis via Boranes*, Ed. H. C. Brown, John Wiley and Sons, Inc., New York, **1975**, pp. 191-261.
148. Wavefunction: Irvine, CA 92612; *http://www.wavefun.com/*
149. HF Theory: C. J. Roothaan, *Rev. Mod. Phys.*, **1951**, 23, 69.
150. 6-31G* basis set: W. J. Hehre, R. Ditchfield and A. J. Pople, *J. Chem. Soc.*, **1972**, 56, 2257; P. C. Hariharan and J. A. Pople, *Theor. Chim. Acta*, **1973**, 28, 213; J. D. Dill and J. A. Pople, *J. Chem. Phys.*, **1975**, 62, 2921.
151. B3LYP method: P. J. Stevens, J. F. Devlin, C. F. Chabalowski and M. J. Frisch, *J. Phys. Chem.*, **1994**, 98, 11623.
152. A. R. Gatti and T. Wartik, *Inorg. Chem.*, **1966**, 5, 2075.
153. J. March, *Advanced Organic Chemistry*, **4th Ed.**, John Wiley and Sons, Inc., New York, pp. 771-776.
154. H. C. Brown and K. J. Murray, *Tetrahedron*, **1986**, 42, 5497.
155. A. J. Weinheimer and W. E. Marsico, *J. Am. Chem. Soc.*, **1962**, 27, 1926.
156. S. A. Westcott, H. P. Blom, T. B. Marder and T. R. Baker, *J. Am. Chem. Soc.*, **1992**, 114, 8863.
157. B. Ganem and J. O. Osby, *Chem. Rev.*, **1986**, 86, 763.
158. C. A. Brown and H. C. Brown, *J. Org. Chem.*, **1966**, 31, 3989.
159. I. Granoth, Y. Segall, H. Leader and R. Alkabets. *J. Org. Chem.*, **1976**, 41, 3682.
160. H. C. Brown and H. M. Hess, *J. Org. Chem.*, **1969**, 34, 2206.

161. (a) E. J. De Witt, F. L. Ramp and L. E. Trapasso, *J. Am. Chem. Soc.*, **1961**, 83, 4672; (b) F. L. Ramp, E. J. De Witt and L. E. Trapasso, *J. Org. Chem.*, **1962**, 27, 4368.
162. R. Klein, A. Bliss, L. Schoen and H. G. Nadeau, *J. Am. Chem. Soc.*, **1961**, 83, 4131.
163. M. Yalpani, T. Lunow and R. Köster, *Chem. Ber.*, **1989**, 122, 687.
164. R. Rathore, U. Weigand and J. K. Kochi, *J. Org. Chem.*, **1996**, 61, 5246.
165. J. A. Baban, B. P. Roberts, *J. Chem. Soc., Perkin Trans. 2*, **1987**, 497.
166. (a) H. C. Brown, N. C. Hébert, C. H. Snyder, *J. Am. Chem. Soc.*, **1961**, 83, 1001; (b) H. C. Brown, N. C. Hébert, C. H. Snyder, *J. Am. Chem. Soc.*, **1961**, 83, 1002; (c) H. C. Brown, N. C. Hébert, C. H. Snyder, *J. Am. Chem. Soc.*, **1961**, 83, 1003.
167. **US 3,009,972**, W. K. Johnson (9/1959).
168. G. Schlegel and H. J. Schaefer, *Chem. Ber.*, **1984**, 117, 1400.
169. D. B. Bingley and D. W. Payling, *Chem. Commun.*, **1968**, 938.
170. H. C. Brown and C. Snyder, *Tetrahedron,* **1986**, 42, 5525.
171. H. C. Brown and G. Zweifel, *J. Am. Chem. Soc.*, **1959**, 81, 1512.
172. H. C. Brown, G. W. Kabalka and M. W. Rathke, *J. Am. Chem. Soc.*, **1967**, 89, 4528.
173. H. C. Brown, E. Knights and R. A. Coleman, *J. Am. Chem. Soc.*, **1969**, 91, 2144.
174. G. W. Kabalka, T. M. Shoup and N. M. Goudgaon, *J. Org. Chem.*, **1989**, 54, 5930.
175. G. W. Kabalka, S. Yu and S. Li, *Tetrahedron Lett.*, **1997**, 38, 5455.
176. A. McKillop and W. R. Sanderson, *Tetrahedron*, **1995**, 51, 6145.
177. J. Muzart, *Synthesis*, **1995**, 1325.
178. A. McKillop and W. R. Sanderson, *J. Chem. Soc., Perkin Trans 1*, **2000**, 471.
179. D. A. Evans, E. Vogel and J. N. Nelson, *J. Am. Chem. Soc.*, **1979**, 101, 6120.
180. M. M. Midland and S. B. Preston, *J. Org. Chem.*, **1980**, 45, 4514.
181. D. H. Brown Rippin, W. Cai and S. J. Brenek, *Tetrahedron Lett.*, **2000**, 41, 5817.
182. Y. Masuda, M. Hishi and A. Arase, *Bull. Chem. Soc. Jpn.*, **1979**, 52, 271.
183. Y. Masuda, M. Itoh, and A. Arase*, Nippon Kagaku Kiashi*, **1972**, 72, 395. (*Chem.. Ab.*, **1972**, 76, 113285)
184. N. Miyaura, M. Itoh, A. Suzuki, H. C. Brown, M. M. Midland and P. Jacob, *J. Am. Chem. Soc.*, **1972**, 94, 6549.
185. T. J. Logan, *J. Org. Chem.*, **1961**, 26, 3657.
186. W. Janse van Rensburg, *Contrathemodynamic Isomerisaiton of Internal Olefins by Exploring the Migratory Aptitude of Various Substrates. The Significance of*

Concurring Molecular Modelling (PhD Thesis), University of the Orange Free State, **2001**.

187. E. C. Ashby, *J. Am. Chem. Soc.*, **1959**, 81, 4791.
188. C. S. L. Baker, *J. Organomet. Chem.*, **1969**, 19, 287.
189. (a) Tetramethylthiourea: B. K. Seal, B. Banerjee and D. C. Mukherjee, *Indian J. Chem, Sect. A*, **1986**, 25, 799; (b) Tetramethylurea: L. Treschanke and P. Rademacher, *J. Mol. Struct.*, **1985**, 131, 61; (c) DMF: D. M. Lubamn and M. N. Kronick, *Anal. Chem.*, **1983**, 55, 867; (d) DMSO: T. Vondrak and Z. Bastl, *J. Mol. Struct.*, **1987**, 160, 117.
190. (a) H. C. Brown and J. Chandrasekharan, *J. Org. Chem.*, **1988**, 53, 4811; (b) H. C. Brown and J. Chandrasekharan, *J. Org. Chem.*, **1988**, 53, 4811; (c) H. C. Brown and J. Chandrasekharan, *Gazz. Chim. Ital.,* **1987**, 117, 517; (d) H. C. Brown and J. Chandrasekharan *J. Org. Chem.*, **1985**, 50, 518; (e) H. C. Brown and J. Chandrasekharan and D. J. Nelson, *J. Am. Chem. Soc.*, **1984**, 106, 3768 (f) H. C. Brown and L. T. Murray, *Inorg. Chem*., **1984**, 23, 2746; (g) H. C. Brown and N. Ravindran, *J. Am. Chem. Soc.*, **1984**, *106*, 1863; (h) H. C. Brown and J. Chandrasekharan, *Orgamometallics*, **1983**, 2, 1261; (j) K. K. Wang and H. C. Brown, *J. Org. Chem.*, **1980**, 45, 5303.
191. (a) S. Heřmánek, *Inorg. Chim. Acta*, **1999**, 20, 289; (b) H. Nöth and B Wrackmeyer, *Nuclear Magnetic Resonance Spectroscopy of Boron Compounds*, Spronger-Verlag, Berlin Heidelberg, New York, **1978**; (c) G. R. Eaton and W. N. Lipscomb, *NMR Studies of Boron Hydrides and Related Compounds*, Benjamin, Inc., New York, **1969**.
192. D.E. Young, G. E. McAchran and S.G. Shore, *J. Am. Chem. Soc*., **1965**, 87, 4390.
193. C. D. Entwistle, T. B. Marder, P. S. Smith, J. A. K. Howard, M. A. Fox and S. A. Mason, *J. Organometal. Chem*., **2003**, 680, 165.
194. For a recent example see: H. C. Brown, J. V. B. Kanth and M. Zaidlewicz*, J. Org. Chem.*, **1998**, 63, 5154.
195. For a review of early developments see: H. I. Schlessinger and A. B. Burg, *Chem. Rev.*, **1942**, 31, 1.
196. F.G. A. Stone and J. Emeléus, *J. Chem. Soc.*, **1950**, 2755.
197. H. C. Brown and B. C. Subba Rao, *J. Org. Chem.*, **1957**, 22, 1135.
198. H. C. Brown and B. C. Subba Rao, *J. Am. Chem. Soc.*, **1960**, 82, 681.
199. H. C. Brown and W. Kortnyk, *J. Am. Chem. Soc.*, **1960**, 82, 3866.

200. H. C. Brown, P. Heim and M. M. Yoon, *J. Am. Chem. Soc.*, **1970**, 92, 1637.
201. J. Emeléus and K. Wade, *J. Chem. Soc.*, **1960**, 2614.
202. A. B. Burg, *Record of Chemical Progress*, Kresge-Hooker Sci. Lab., **1954**, 15, 159. (*Chem. Ab.*, **1955**, 49, 35313)
203. A. B. Burg, *Record of Chemical Progress*, Kresge-Hooker Sci. Lab., **1954**, 15, 159. (*Chem. Ab.*, **1955**, 49, 35313)
204. J. R. Jennings and K. Wade, *J. Chem. Soc. A*, **1968**, 1946.
205. R. Coult, M. A. Fox, B. Rand, K. Wade and A. V. K. Westwood, *J. Chem. Soc., Dalton Trans.*, **1997**, 3411.
206. J. S. Fowler, R. R. MacGregor, A. N. Ansari, H. L. Atkins and A. P. Wolf, *J. Med. Chem.*, **1974**, 17, 246.
207. L. M. Braun, R. A. Braun, H. R. Crissman, M. Opperman and R. M. Adams, *J. Org. Chem.*, **1971**, 36, 2388.
208. C. F. Lane, *Adrichimica Acta*, **1976**, 8, 20.
209. H. C. Brown and W. Kortnyk, *J. Am. Chem. Soc.*, **1960**, 82, 3866.
210. H. C. Brown, Y. M. Choi and S Narasimhan, *J. Org. Chem.*, **1981**, 47, 3153.
211. T. Wakamatsu, H. Inaki, A. Ogawa, M. Watanabe and Y. Ban, *Heterocycles*, 1980, **4**, 1437.
212. M. Periasamy and M. Thirumalaikumar, *J. Organomet. Chem.*, **2000**, 69, 137.
213. D. R. Schultz, *J. Polymer Science*, **1963,** 1B, 613.
214. Y. Ogata and Y. Minoura, *Kogyo Kagaku Zasshi*, **1963**, 66, (a) 1707; (b) 1710 and (c) 1714.
215. H. C. Brown, J. V. B. Kanth and M. Zaidlewicz, *J. Org. Chem.*, **1998**, 63, 5154.
216. M. F. Hawthorne, *Tetrahedron*, **1962**, 17, 117.
217. J. E. Lloyd and K. Wade, *J. Chem. Soc.*, **1961**, 649.
218. J. R. Jennings, R. Snaith, M. M. Mahmoud, S. C. Wallwork, S. J. Bryan, J. Halfpenny, E. A. Petch and K. Wade, *J. Organomet. Chem.*, **1983**, 249, C1.
219. R. Chadha and Naba K. Ray, *J. Indian. Chem. Soc.*, **1982**, 204.
220. R. G. Pearson, Chemical Hardness: Applications From Molecules To Solids, Wiley-VCH, Weinheim, **1997**.
221. P. R. Rablen, *J. Am. Chem. Soc.*, **1997**, 115, 8350.
222. R. J. Thompson and J. C. Davis, Jr., *Inorg. Chem.*, **1965**, 4, 1019.
223. G.R. Eaton and W. N. Lipscomb, *NMR Studies of Boron Hydrides and Related Compounds*, Benjamin, Inc., New York, **1969**.

224. J. D. Kennedy, W. Mcfarlane and B. Wrackmeyer, *Inorg. Chem.*, **1976**, 15, 1299.
225. J. Kroner, D. Nöle and H. Nöth, *Z. Naturforsch*, **1973**, 28B, 416.
226. J. Kroner and B. Wrackmeyer, *J. Chem. Soc., Faraday Trans. II*, **1976**, 72, 2283.
227. A. Fratiello, T. P. Onak and R. E. Schuster, *J. Am. Chem. Soc.*, **1968**, 90, 1194.
228. T. D. Coyle and F. G. A. Stone, *J. Am. Chem. Soc.*, **1961**, 83, 4138.
229. W. A. G. Graham and F. G. A. Stone, *J. Inorg. Nucl. Chem.*, **1956**, 3, 164.
230. F. G. A. Stone, *Chem. Rev.*, **1958**, 58, 101.
231. N. Farfan and R. Contreras, *J. Chem. Soc., Perkin Trans. 2*, **1987**, 6, 771.
232. T. D. Coyle and F. G. A. Stone, *J. Amer. Chem. Soc.*, **1961**, 83, 4138.
233. R. W. Rudolph and C. W. Schultz, *J. Am. Chem. Soc.,* **1971**, 93, 682.
234. H. Nöth, W. Tinhof and B. Wrackmeyer, *Chem. Ber.*, **1974**, 107, 518.
235. H. Nöth and U. Schuchardt, *Chem. Ber.*, **1974**, 107, 3104.
236. B. Wrackmeyer, *Ann. Rep. NMR. Spectrosc.*, **1988**, 20, 61.
237. R. Kawecki, E. Bednarek and J. Jerzy, *J. Chem. Soc., Perkin Trans 2*, **2001**, 8, 1400.
238. G. Vargas, N. Farfan, R. Santillan, A. Gutierrez, E. Gomez and V. Barba, *Inorg. Chim. Acta*, **2005**, 358, 2996.
239. H. Höpfl, *J. Organomet. Chem.*, **1999**, 581, 129.
240. K. A. Connors, *Binding Constants: The Measurement of Molecular Complex Stability*, Wiley-Interscience, New York, **1987**, Chapter 5.
241. A. H. Cowley and J. L. Mills, *J. Am. Chem. Soc.*, **1969**, 91, 2911.
242. H. Benesi and J. H. Hilderbrand, *J. Am. Chem. Soc.*, **1949**, 71, 2703.
243. R. S. Drago, *Structure and Bonding*, **1973**, 15, 73.
244. R. S. Drago and N. S. Rose, *J. Am. Chem. Soc.*, **1959**, 81, 6141.
245. For a recent example on the application of the technique see: R. Boshra, A. Sundararaman, L. N. Zakharov, C. D. Incarvito, A. L.Rheingold and F. Jäkle, *Chem. Eur. J.*, **2005**, 11, 2810.
246. T. Onak, *Organoborane Chemistry*, Academic Press, New York, **1975**.
247. B. M. Mikhailov and L. S. Vasil'ev, *Zh. Obshch. Khim.*, **1965**, 35, 925.
248. R. L. Letsinger and J. R. Nazy, J. Org. Chem., **1958**, 23, 914.
249. R. A. Braun, D. C. Brown and R. M. Adams, *J. Am. Chem. Soc.*, **1971**, 93, 2823.
250. D. J. Pasto, V. Balasubramaniyan and P. W. Wojtkowsta, *Inorg. Chem.*, **1969**, 8, 594 (primary source: P. L. Pennaritz, PhD Dissertation, University of Notre Dame, **1963**).

251. C. Reichardt, *Solvent Effects in Organic Chemistry*, Vol. 3, Chemie, Weinheim, **1979**, p. 15.

252. (a) R. S. Drago and B. B. Wayland, *J. Am. Chem. Soc.*, **1965**, 87, 3571; (b) R. S. Drago, *J. Chem. Ed.*, **1974**, 51, 300; (c) R. S. Drago, L. B. Parr and C. S. Chamberlain, *J. Am. Chem. Soc.*, **1977**, 99, 3203.

253. (a) V. Gutmann, *Coord. Chem. Rev.*, **1967**, 2, 239; (b) V. Gutmann and A. Scherhaufer, *Monatsh. Chem.*, **1968**, 99, 335; (c) V. Gutmann, *Chimia*, **1969,** 23, 285; V. Gutmann, *Electrochim. Acta*, **1976**, 21, 661; V. Gutmann, *Coord. Chem. Rev.*, 18, **1976**, 225.

254. (a) V. Gutmann, *Pure Appl. Chem.*, **1971**, 27, 73; (b)V. Gutmann, *Fortschr. Chem. Forsch*, **1972**, 27, 59; (c) V. Gutmann, *Structre and Bonding*, **1973**, 15, 141.

255. R. G. Pearson, *J. Am. Chem. Soc.*, **1983**, 85, 3533.

256. R. G. Pearson, *J. Chem. Ed.*, **1987**, 64, 561.

257. (a) R. G. Parr, R. A. Donnelly, M. Levy and W. E. Palke, *J. Chem. Phys*., **1978**, 68, 3801 (b) R. G. Parr and L. J. Bartolotti, *J. Am. Chem. Soc.*, **1982**, 104, 3801.

258. R. S. Mulliken, *J. Chem. Phys.*, **1934**, 2, 782.

259. W. T. Sanderson, *Science*, **1955**, 121, 207.

260. R. G. Pearson, *Chemical Hardness*, Wiley-VCH, Weinheim, **1997**.

261. P. K.Chattaraj and B. Maiti, *J. Chem. Ed.*, **2001**, 78, 811.

262. S. Toyota and M. Ōki, *Bull. Chem. Soc. Jpn.*, **1992**, 65, 1832.

263. J. M. Schulman and R. L. Disch, *J. Mol. Struc.*, **1995**, 338, 109.

264. H. Höpfl, *J. Organomet. Chem.*, **1999**, 581, 129.

6. Appendix A: Dealkylation Studies

6.1. Thermal Dealkylation: Time Dependence Studies

6.1.1. Tri-*n*-decylborane

Data used to generate **Table 3.1** in **Section 3.1.1**

Table 6.1 - Primary data for the time dependence study on $B(decyl)_3$ at 150 ^oC

Component	Product distribution (Mass Percentage)							
	0	1	2	3	4	6	7	8
THF	78.06	76.61	75.24	80.96	74.70	78.52	74.31	75.02
1-Butanol	7.71	8.33	8.93	7.87	8.69	7.85	9.21	8.21
Dihydro-2(3H)-furanone	0.03	0.11	0.09	0.14	0.09	0.06	0.09	0.02
n-Octane	4.63	4.16	4.22	3.47	3.81	4.09	3.36	3.76
1-Decene	0.05	0.04	0.02	0.02	0.02	0.02	0.02	0.01
n-Decane	0.44	0.70	0.35	0.28	0.18	0.19	0.28	0.17
5-Decanol	0.00	0.00	0.00	0.00	0.30	0.00	0.00	0.00
4-Decanol	0.00	0.44	0.60	0.21	0.35	0.57	0.76	0.69
3-Decanol	0.00	0.23	0.31	0.08	0.34	0.30	0.40	0.35
2-Decanol	0.55	0.61	0.76	0.23	0.74	0.65	0.91	0.76
1-Decanol	8.22	8.42	9.19	6.22	10.43	7.54	10.38	10.73
n-Eicosane	0.12	0.07	0.08	0.06	0.06	0.05	0.08	0.05
Unknown	0.19	0.30	0.21	0.46	0.29	0.16	0.20	0.23

Table 6.2 - Relative mass percentage ratios for the time dependence study on B(decyl)$_3$ at 150 ^{o}C

Component	Relative Mass Percentage Ratio							
	0	1	2	3	4	6	7	8
1-Decene	0.01	0.01	0.00	0.01	0.01	0.00	0.01	0.00
n-Decane	0.10	0.17	0.08	0.08	0.05	0.05	0.08	0.05
5-Decanol	0.00	0.00	0.00	0.00	0.08	0.00	0.00	0.00
4-Decanol	0.00	0.11	0.14	0.06	0.09	0.14	0.23	0.18
3-Decanol	0.00	0.06	0.07	0.02	0.09	0.07	0.12	0.09
2-Decanol	0.12	0.15	0.18	0.07	0.19	0.16	0.27	0.20
1-Decanol	1.78	2.02	2.18	1.79	2.74	1.84	3.09	2.85
n-Eicosane	0.03	0.02	0.02	0.02	0.02	0.01	0.02	0.01
Sum	2.03	2.53	2.68	2.05	3.26	2.28	3.82	3.39

An explanation of how the results shown in **Chapter 3** (**Tables 3.1**, **3.3**, **3.5** and **3.6**) were obtained from the relative mass percentage ratios is provided below:

i. Mass percentages of components in **Tables 6.1**, **6.3**, **6.5** and **6.7** were all divided by the mass percentage of the internal standard (*n*-octane) to give the corresponding relative mass percentage ratios in **Tables 6.2**, **6.4**, **6.6** and **6.8**, respectively.

ii. The relative mass percentage ratios were added to give a sum, which is denoted in red in **Tables 6.2**, **6.4**, **6.6** and **6.8**.

iii. Each relative mass percentage ratio was divided by the corresponding calculated sum and multiplied by a hundred in order to express it as a percentage of the sum, to give the data shown in **Tables 3.1**, **3.2**, **3.5** and **3.6**.

The expression used in the calculation is given by equation *6.1*.

$$\%\,\text{component} = \frac{\dfrac{\text{component mass}\,\%}{\text{internal standard mass}\,\%}}{\dfrac{\sum \text{component mass}\,\%}{\text{internal standard mass}\,\%}} \times 100 \qquad 6.1$$

6.1.2. Tri-*n*-octylborane

Data used to generate **Table 3.3** in **Section 3.1.2**

Table 6.3 - Primary data for time dependence study on B(octyl)$_3$ at 100 ^{o}C

Component	Product Distribution (Mass Percentage)								
	0	1	2	3	4	5	6	7	8
THF	69.72	68.91	66.03	63.95	71.04	67.39	69.44	64.72	70.26
1-Butanol	8.03	7.14	8.17	8.71	6.71	7.23	6.79	7.85	6.58
1-Octene	0.02	0.94	0.64	0.00	1.27	0.32	1.90	0.90	1.33
n-Octane	0.89	0.67	0.81	0.90	1.03	0.75	0.94	0.94	0.73
C_8H_{16}	0.63	0.14	0.16	0.15	0.14	0.15	0.16	0.17	0.15
C_8H_{14}	0.39	0.28	0.34	0.36	0.38	0.41	0.46	0.53	0.47
Octanal	0.52	0.06	0.09	0.14	0.12	0.08	0.10	0.09	0.08
2-Octanol	1.15	0.71	0.67	0.60	0.41	0.60	0.43	0.55	0.45
n-Decane	7.03	6.80	7.56	8.20	6.65	7.33	6.74	7.92	6.51
1-Octanol	10.69	13.26	14.03	14.98	10.81	14.32	11.67	14.77	11.95
2-Butyl-THF	0.12	0.16	0.23	0.33	0.22	0.20	0.19	0.20	0.16
$C_{16}H_{34}$	0.05	0.06	0.08	0.11	0.08	0.08	0.08	0.10	0.06
$C_{16}H_{32}$	0.05	0.09	0.13	0.19	0.13	0.14	0.13	0.15	0.12
n-Hexadecane	0.31	0.41	0.54	0.69	0.55	0.58	0.57	0.68	0.48
Dioctyl ether	0.08	0.11	0.19	0.28	0.18	0.14	0.15	0.14	0.11
Unknown	0.20	0.29	0.32	0.39	0.28	0.26	0.24	0.26	0.23

Table 6.4 - Relative mass percentage ratios for the time dependence study on B(octyl)$_3$ at 100 ^{o}C

Component	Relative Mass Percentage Ratio								
	0	1	2	3	4	5	6	7	8
1-Octene	0.00	0.14	0.08	0.00	0.19	0.04	0.28	0.11	0.20
n-Octane	0.03	0.02	0.02	0.02	0.02	0.02	0.02	0.02	0.02
C_8H_{16}	0.07	0.10	0.11	0.11	0.15	0.10	0.14	0.12	0.11
2-Octanol	0.12	0.10	0.09	0.07	0.06	0.08	0.06	0.07	0.07
1-Octanol	1.93	1.95	1.86	1.83	1.63	1.95	1.73	1.86	1.84
2-Butyl-THF	0.02	0.02	0.03	0.04	0.03	0.03	0.03	0.03	0.02
$C_{16}H_{34}$	0.01	0.01	0.01	0.01	0.01	0.01	0.01	0.01	0.01
n-Hexadecane	0.06	0.06	0.07	0.08	0.08	0.08	0.08	0.09	0.07
Sum	2.23	2.40	2.27	2.17	2.18	2.32	2.37	2.31	2.35

6.2. Thermal Dealkylation: Temperature Dependence Studies

6.2.1. Tri-*n*-decylborane

The data from the thermal dealkylation study on tri-*n*-decylborane were manipulated as outlined in equation *8.1*.

Data used to generate **Table 3.5** in **Section 3.1.3**

Table 6.5 - Primary data for temperature dependence study on $B(decyl)_3$

Component	Product Distribution (Mass Percentage) at Temperature				
	50 °C	100 °C	150 °C	200 °C	End of Reaction
THF	50.64	48.87	37.90	54.84	41.22
1-Butanol	7.50	7.65	11.37	6.43	6.36
Dihydro-2(3H)-furanone	0.05	0.04	0.05	0.03	0.04
n-Octane	7.77	7.78	7.66	7.08	7.85
1-Decene	4.11	3.87	3.67	2.60	0.68
n-Decane	2.33	2.07	2.50	1.98	4.80
5-Decanol	0.04	0.02	0.03	0.02	0.02
4-Decanol	0.00	0.02	0.00	0.00	0.00
3-Decanol	1.41	1.13	0.57	0.11	0.44
2-Decanol	0.09	0.09	0.10	0.10	0.06
1-Decanol	23.78	25.99	31.55	23.78	15.01
n-Eicosane	0.71	0.34	1.02	0.43	2.42
Unknown	1.57	2.13	3.58	2.60	3.54

Table 6.6 - Relative mass percentage ratios for the temperature dependence study on B(decyl)$_3$

Component	Product Distribution (Mass Percentage) at Temperature				
	50 °C	100 °C	150 °C	200 °C	End of Reaction
1-Decene	0.53	0.50	0.48	0.37	0.09
n-Decane	0.30	0.27	0.33	0.28	0.61
5-Decanol	0.00	0.00	0.00	0.00	0.00
4-Decanol	0.00	0.00	0.00	0.00	0.00
3-Decanol	0.18	0.15	0.07	0.02	0.01
2-Decanol	0.01	0.01	0.01	0.01	0.01
1-Decanol	3.06	3.34	4.12	3.36	1.91
n-Eicosane	071	0.34	1.02	0.43	2.42
Sum	4.18	4.31	5.15	4.10	2.98

6.2.2. Tri-*n*-octylborane

Data used to generate **Table 3.6** in **Section 3.1.4**

Table 6.7 - Primary data for temperature dependence study on B(octyl)$_3$

Component	Product Distribution (Mass Percentage) at Temperature				
	50 °C	100 °C	150 °C	200 °C	End of Reaction
THF	64.39	61.83	37.78	72.07	31.17
1-Butanol	6.05	6.49	6.88	0.72	15.49
1-Octene	0.86	0.59	0.44	2.37	3.27
n-Octane	1.49	1.65	2.21	1.60	1.22
C_8H_{16}	0.57	0.63	1.04	0.44	0.11
C_8H_{14}	0.01	0.01	0.02	0.01	0.06
Octanal	0.14	0.14	0.09	0.00	0.36
2-Octanol	0.03	0.01	0.03	0.01	0.15
n-Decane	8.65	8.96	22.96	7.34	5.49
1-Octanol	15.42	17.22	22.86	14.35	34.40
2-Butyl-THF	0.36	0.37	1.19	0.13	0.96
$C_{16}H_{34}$	0.08	0.08	0.17	0.06	0.26
$C_{16}H_{32}$	0.24	0.27	0.66	0.02	1.04
n-Hexadecane	0.64	0.64	1.30	0.13	4.44
Dioctyl ether	0.05	0.05	0.07	0.00	0.08

Unknown	0.42	0.42	1.00	0.62	1.67

Table 6.8 - Relative mass percentage ratios for the temperature dependence study on B(octyl)$_3$

Component	Product Distribution (Mass Percentage) at Temperature				
	50 ^{o}C	100 ^{o}C	150 ^{o}C	200 ^{o}C	End of Reaction
1-Octene	0.10	0.07	0.02	0.32	0.60
n-Octane	0.17	0.18	0.10	0.22	0.22
C_8H_{16}	0.07	0.07	0.05	0.06	0.02
2-Octanol	0.00	0.00	0.00	0.00	0.03
1-Octanol	1.78	1.92	1.00	1.95	6.27
2-Butyl-THF	0.04	0.04	0.05	0.02	0.17
$C_{16}H_{34}$	0.01	0.01	0.01	0.01	0.05
n-Hexadecane	0.07	0.07	0.06	0.02	0.81
Sum	2.25	2.36	1.27	2.60	8.16

6.3. THERMAL DEALKYLATION OF TRI-*N*-OCTYLBORANE AFTER REMOVAL OF SOLVENT

The data from the thermal dealkylation study on tri-*n*-octylborane were obtained from peak area ratios, obtained by dividing the 1-octene peak areas by those of the corresponding *n*-decane (internal standard) peaks. Multiplication of these peak area ratios by the response factor (R_f = 3.47, see **Section 2.5**) of 1-octene afforded the corresponding number of moles. These numbers of moles are listed in **Table 6.9** in red. The numbers of moles were converted into percentages of the total number of moles used in the hydroboration. A worked example for the increase in 1-octene at 50 ^{o}C is shown below:

$$\%\ \text{increase} = \frac{\text{moles of 1 - octene at temperature - moles of 1 - octene after hydroboration}}{\text{moles of 1 - octene before hydroboration - moles of 1 - octene after hydroboration}} \times 100 \qquad 6.2$$

Thus for the sample at 50 ^{o}C

$$\%\ \text{increase}\,(50\ ^{o}\text{C}) = \frac{0.82\ \text{mmol} - 0.48\ \text{mmol}}{5.38\ \text{mmol} - 0.48\ \text{mmol}} \times 100 = 6.94\ \%$$

Table 6.9 Primary data for temperature dependence study on B(octyl)$_3$ after removal of solvent

Temperature (^{o}C)	Component	Retention Time (min.)	Peak Height (V)	Peak Area (mV.sec)	Peak Area Ratio
Before Hydroboration	1-Octene	9.31	261.95	1286.82	1.5515
	n-Decane	14.55	113.51	851.33	(5.38 mmol)
After Hydroboration	1-Octene	9.50	45.97	103.94	0.1374
	n-Decane	14.59	145.88	756.24	(0.48 mmol)
50	1-Octene	9.51	76.48	207.76	0.2354
	n-Decane	14.60	154.41	882.52	(0.82 mmol)
100	1-Octene	9.51	78.61	207.68	0.2676
	n-Decane	14.55	111.38	776.11	(0.93 mmol)
150	1-Octene	9.51	81.71	223.28	0.3027
	n-Decane	14.56	128.32	737.62	(1.05 mmol)
200	1-Octene	9.50	64.23	244.35	0.3313
	n-Decane	14.56	118.10	737.62	(1.15 mmol)

6.3.1. Effect of Lewis Base on Thermal Dealkylation of Tri-*n*-octylborane after Removal of Solvent

Data for the investigation of the effect of the Lewis base on the dealkylation of tri-*n*-ocytlborane and tri-4-octylborane were obtained by the GC analysis (Perkin-Elmer Elite Wax column) of duplicate injection of oxidised samples and determination of their octanol content by the calibration in **Section 2.5** by using equation *6.3*.

$$\text{Octanol Isomer Concentration (M)} = \frac{\text{Area of Octanol Isomer}}{\text{Area of } n-\text{decane}} \div \text{Slope of Octanol Calibration Curve (Figure 2.2)} \qquad 6.3$$

Thus, for the 1-octanol concentration of the control sample (replicate 1) in was determined as follows:

$$\text{Octanol Isomer Concentration (M)} = \frac{13.8 \text{ mV.sec}}{684 \text{ mV.sec}} \div 6.39687 \text{ M}^{-1} = 0.00315 \text{ M}$$

The distribution of the octanol isomers was obtained as follows (equation *6.4*):

6.4

$$\%\,\text{Distribution of Octanol Isomer} = \frac{\text{Concentration of Octanol Isomer}}{\sum(\text{Concentration of Octanol Isomers})} \times 100$$

Thus, for the 1-octanol concentration of the control sample (replicate 1) in **Table 6.10** was determined as follows:

$$\% \text{ Distribution of Octanol Isomer} = \frac{0.00315 \text{ M}}{(0.0173 + 0.00809 + 0.00409 + 0.00315)} \times 100 = 9.7\%$$

Table 6.10 contains the data used to generate **Table 3.11** in **Section 3.2.1**.

Table 6.10 - Primary octanol distribution (Elite Wax Column) data for the study of Lewis base effect on the dealkylation and isomerisation of B(*n*-octyl)$_3$ at 150 ^{o}C

Sample	Component	Retention Time (min.)	Peak Area (mV.sec)	Peak Height (mV)	Area Ratio	[Octnol] (M)	% Distribution.
Control Replicate 1	*n*-Decane	3.1113	684	44.8	-		
	4-Octanol	4.7175	75.6	11.8	0.111	1.73E-02	53.0
	3-Octanol	6.6160	35.4	4.36	0.052	8.09E-03	24.8
	2-Octanol	6.7688	17.9	2.81	0.026	4.09E-03	12.5
	1-Octanol	8.0647	13.8	2.2	0.020	3.15E-03	9.7
Control Replicate 2)	*n*-Decane	3.1258	685	46	-		
	4-Octanol	4.7402	77.6	11.8	0.113	1.77E-02	53.9
	3-Octanol	6.6355	34.7	4.37	0.051	7.92E-03	24.1
	2-Octanol	6.7945	18	2.87	0.026	4.11E-03	12.5
	1-Octanol	8.088	13.8	2.19	0.020	3.15E-03	9.6
DMF Replicate 1	*n*-Decane	3.2372	964	49.1	-		
	4-Octanol	4.7797	111	15.7	0.115	1.80E-02	55.4
	3-Octanol	6.6683	44.2	5.16	0.046	7.17E-03	22.0
	2-Octanol	6.8262	22.7	3.49	0.024	3.68E-03	11.3
	1-Octanol	8.1378	22.6	3.26	0.023	3.66E-03	11.3

Sample	Component	Retention Time (min.)	Peak Area (mV.sec)	Peak Height (mV)	Area Ratio	Conc. (M)	% Distribution.
DMF Replicate 2	*n*-Decane	3.3460	896	51.9	-		
	4-Octanol	4.9375	109	16.1	0.122	1.90E-02	55.3
	3-Octanol	6.8453	43.7	5.26	0.049	7.62E-03	22.2
	2-Octanol	7.0012	22.5	3.48	0.025	3.93E-03	11.4
	1-Octanol	8.2832	22	3.33	0.025	3.84E-03	11.2
DMSO Replicate 1)	*n*-Decane	3.7160	563	42.5	-		
	4-Octanol	4.8303	59.3	9.81	0.105	1.65E-02	54.7
	3-Octanol	6.7412	27.7	3.68	0.049	7.69E-03	25.5
	2-Octanol	6.9035	14	2.32	0.025	3.89E-03	12.9
	1-Octanol	8.1787	7.49	1.4	0.013	2.08E-03	6.9
DMSO Replicate 2	*n*-Decane	3.1987	652	45.3	-		
	4-Octanol	4.8135	67.9	10.3	0.104	1.63E-02	55.3
	3-Octanol	6.7285	31.3	4.04	0.048	7.50E-03	25.5
	2-Octanol	6.8885	16.1	2.51	0.025	3.86E-03	13.1
	1-Octanol	8.5185	7.58	1.44	0.012	1.82E-03	6.2
$(MeO)_3PO$ Replicate 1	*n*-Decane	3.3162	501	39.7	-		
	4-Octanol	4.9767	60.5	9.26	0.121	1.89E-02	54.2
	3-Octanol	6.8895	28.7	4.08	0.057	8.96E-03	25.7
	2-Octanol	7.0452	13.9	2.46	0.028	4.34E-03	12.4
	1-Octanol	8.3022	8.57	1.76	0.017	2.67E-03	7.7

Sample	Component	Retention Time (min.)	Peak Area (mV.sec)	Peak Height (mV)	Area Ratio	Conc. (M)	% Distribution.
$(MeO)_3PO$ Replicate 2	*n*-Decane	3.0087	385	34.9	-		
	4-Octanol	4.7077	39.6	6.41	0.103	1.61E-02	54.6
	3-Octanol	6.62225	17.8	2.37	0.046	7.23E-03	24.5
	2-Octanol	6.789	8.88	1.37	0.023	3.61E-03	12.2
	1-Octanol	8.0521	6.24	1.1	0.016	2.53E-03	8.6
HMPA Replicate 1	*n*-Decane	3.0988	593	43.3	-		
	4-Octanol	4.7190	69.6	10.3	0.117	1.83E-02	54.9
	3-Octanol	6.6308	31.5	3.84	0.053	8.30E-03	24.9
	2-Octanol	6.7883	15	2.32	0.025	3.95E-03	11.8
	1-Octanol	8.0747	10.6	1.47	0.018	2.79E-03	8.4
HMPA Replicate 2	*n*-Decane	3.0182	376	34.1	-		
	4-Octanol	4.7168	38.4	6.16	0.102	1.60E-02	54.5
	3-Octanol	6.6493	18.6	2.11	0.049	7.73E-03	26.4
	2-Octanol	6.8157	8.32	1.31	0.022	3.46E-03	11.8
	1-Octanol	8.0897	5.12	0.899	0.014	2.13E-03	7.3
NBu_3 Replicate 1	*n*-Decane	3.1405	533	42.8	-		
	4-Octanol	4.7750	51.8	7.75	0.097	1.52E-02	53.8
	3-Octanol	6.7043	24.5	3.41	0.046	7.19E-03	25.4
	2-Octanol	6.8635	14.2	2.06	0.027	4.16E-03	14.7
	1-Octanol	8.1192	5.78	1.02	0.011	1.70E-03	6.0

Sample	Component	Retention Time (min.)	Peak Area (mV.sec)	Peak Height (mV)	Area Ratio	Conc. (M)	% Distribution.
NBu_3 Replicate 2	*n*-Decane	3.0832	460	39.9	-		
	4-Octanol	4.7440	44.8	6.86	0.097	1.52E-02	53.5
	3-Octanol	6.6803	21.3	3.1	0.046	7.24E-03	25.4
	2-Octanol	6.8383	11.7	1.85	0.025	3.98E-03	14.0
	1-Octanol	8.1023	5.93	1.01	0.013	2.02E-03	7.1
PBu_3 Replicate 1	*n*-Decane	3.1663	622	41.8	-		
	4-Octanol	4.8125	63.8	9.68	0.103	1.60E-02	57.6
	3-Octanol	6.7267	28.4	3.4	0.046	7.14E-03	25.6
	2-Octanol	6.8900	13	2.13	0.021	3.27E-03	11.7
	1-Octanol	8.1592	5.56	1.12	0.009	1.40E-03	5.0
PBu_3 Replicate 2	*n*-Decane	3.1122	371	33.7	-		
	4-Octanol	4.8190	39.3	6.3	0.106	1.66E-02	56.4
	3-Octanol	6.7550	19.1	2.01	0.051	8.05E-03	27.4
	2-Octanol	6.9178	8.04	1.28	0.022	3.39E-03	11.5
	1-Octanol	8.8163	3.22	0.715	0.009	1.36E-03	4.6
$(MeO)_3P$ Replicate 1	*n*-Decane	3.0617	390	34.5	-		
	4-Octanol	4.7655	37	4.85	0.095	1.48E-02	52.9
	3-Octanol	6.6965	17.9	2.14	0.046	7.17E-03	25.6
	2-Octanol	6.8616	9.08	1.36	0.023	3.64E-03	13.0
	1-Octanol	8.1297	5.96	0.917	0.015	2.39E-03	8.5

Sample	Component	Retention Time (min.)	Peak Area (mV.sec)	Peak Height (mV)	Area Ratio	Conc. (M)	% Distribution.
$(MeO)_3P$ Replicate 2	*n*-Decane	3.1403	389	33.6	-		
	4-Octanol	4.8792	36.3	4.68	0.093	1.46E-02	52.9
	3-Octanol	6.8195	17.5	2.11	0.045	7.03E-03	25.5
	2-Octanol	6.9842	8.96	1.33	0.023	3.60E-03	13.1
	1-Octanol	8.2563	5.87	0.886	0.015	2.36E-03	8.6
Tetramethylthiourea Replicate 1	*n*-Decane	3.225	728	45.2	-		
	4-Octanol	4.8997	68	10.4	0.093	1.46E-02	51.4
	3-Octanol	6.8232	36.7	4.34	0.050	7.88E-03	27.7
	2-Octanol	6.9763	18.4	2.84	0.025	3.95E-03	13.9
	1-Octanol	8.2527	9.16	1.1	0.013	1.97E-03	6.9
Tetramethylthiourea Replicate 2	*n*-Decane	3.3758	700	43.3	-		
	4-Octanol	4.9585	70.7	10.3	0.101	1.58E-02	51.9
	3-Octanol	6.9092	39.7	4.86	0.057	8.87E-03	29.2
	2-Octanol	7.0607	19.2	3.18	0.027	4.29E-03	14.1
	1-Octanol	8.3042	6.56	1.24	0.009	1.47E-03	4.8
Tetramethylurea Replicate 1	*n*-Decane	3.2553	688	42.3	-		
	4-Octanol	4.8632	63.1	9.43	0.092	1.43E-02	52.5
	3-Octanol	6.7845	31.3	3.82	0.045	7.11E-03	26.0
	2-Octanol	6.9410	15.7	2.42	0.023	3.57E-03	13.1
	1-Octanol	8.2242	10.1	1.36	0.015	2.29E-03	8.4

Sample	Component	Retention Time (min.)	Peak Area (mV.sec)	Peak Height (mV)	Area Ratio	Conc. (M)	% Distribution.
Tetramethylurea Replicate 2	*n*-Decane	3.2798	541	41	-		
	4-Octanol	4.8930	54.8	9.02	0.101	1.58E-02	50.1
	3-Octanol	6.8145	31.7	4.22	0.059	9.16E-03	29.0
	2-Octanol	6.9725	15.1	2.73	0.028	4.36E-03	13.8
	1-Octanol	8.2530	7.82	1.65	0.014	2.26E-03	7.1
Blank Replicate 1	*n*-Decane	3.0097	586	40.3	-		
	4-Octanol	4.6762	72.9	11.6	0.135	2.11E-02	54.6
	3-Octanol	6.5898	34.2	4.42	0.063	9.88E-03	25.6
	2-Octanol	6.7410	16.1	2.43	0.030	4.65E-03	12.1
	1-Octanol	8.0877	10.4	1.92	0.019	3.01E-03	7.8
Blank Replicate 2	*n*-Decane	3.1715	930	51.3	-		
	4-Octanol	4.4730	129	17.9	0.238	3.73E-02	56.3
	3-Octanol	6.6193	59.9	6.36	0.111	1.73E-02	26.1
	2-Octanol	6.7740	23.8	3.61	0.044	6.88E-03	10.4
	1-Octanol	8.1068	16.4	2.75	0.030	4.74E-03	7.2

Table 6.11 contains the data used to generate **Table 3.12** in **Section 3.2.1**

Table 6.11 - Primary octene data (PONA Column) for the study of Lewis base effect on the dealkylation of B(*n*-octyl)$_3$ at 150 ^{o}C

Sample	Component	Ret. Time (min.)	Peak Area (mV.sec)	Peak Height (mV)	Area Ratio	mmole of Octene
Pre-Blank-1	1-Octene	7.7870	651	208	1.661	478.6
Replicate 1	*n*-Decane	11.4738	392	124	-	
Pre-Blank-1	1-Octene	7.7905	638	207	1.623	467.8
Replicate 2	*n*-Decane	11.4767	393	126	-	
Blank-1	1-Octene	7.7500	1.57	0.947	0.004	1.1
Replicate 1	*n*-Decane	11.4678	430	115	-	
Blank-1	1-Octene	7.7548	1.49	0.883	0.004	1.2
Replicate 2	*n*-Decane	11.4732	353	115	-	
Blank-2	1-Octene	7.7472	1.94	1.1	0.018	5.3
Replicate 1	*n*-Decane	11.4298	106	52.5	-	
Blank-2	1-Octene	7.7475	2.55	1.36	0.018	5.1
Raplicate 2	*n*-Decane	11.4342	143	63.3	-	
Blank-3	1-Octene	7.7503	0.984	0.514	0.010	2.8
Replicate 1	*n*-Decane	11.4315	100	50.7	-	
Blank-3	1-Octene	7.7517	0.794	0.45	0.008	2.3
Replicate 2	*n*-Decane	11.4325	98.3	49.5	-	
Control-1	1-Octene	7.7517	4.11	2.19	0.012	3.5
Replicate 1	*n*-Decane	11.4668	341	116	-	

Control-1 Replicate 2	1-Octene	7.7472	4.75	2.36	0.012	3.3
	n-Decane	11.4712	410	127	-	
Control-2 Replicate 1	1-Octene	7.7484	1.49	0.986	0.008	2.4
	n-Decane	11.4440	180	77.5	-	
Control-2 Replicate 2	1-Octene	7.7433	1.67	1.02	0.009	2.6
	n-Decane	11.4398	183	78.8	-	
Control-3 Replicate 1	1-Octene	7.7482	1.97	1.18	0.015	4.2
	n-Decane	11.4348	134	63.2	-	
Control-3 Replicate 2	1-Octene	7.7470	2.07	1.27	0.014	4.1
	n-Decane	11.4368	145	67.1	-	
DMF Replicate 1	1-Octene	7.7505	35.7	15.2	0.133	38.2
	n-Decane	11.4643	269	98.2	-	
DMF Replicate 2	1-Octene	7.7470	35.6	153.1	0.132	38.0
	n-Decane	11.4602	270	103	-	
DMF1(Repeat)	1-Octene	7.7482	1.97	1.18	0.015	4.2
	n-Decane	11.4348	134	63.2	-	
DMF2 (Repeat)	1-Octene	7.7470	2.07	1.27	0.014	4.1
	n-Decane	11.4368	145	67.1	-	
DMSO Replicate 1	1-Octene	7.7492	12.1	4.89	0.036	10.4
	n-Decane	11.4677	335	115	-	
DMSO Replicate 2	1-Octene	7.7492	12.1	4.91	0.037	10.8
	n-Decane	11.4677	324	112	-	
DMSO (Repeat) Replicate 1	1-Octene	7.7460	14.4	5.89	0.035	10.2
	n-Decane	11.4777	408	125	-	

DMSO (Repeat)	1-Octene	7.7427	13.2	5.26	0.035	10.1
Replicate 2	*n*-Decane	11.4688	375	119	-	
$(MeO)_3PO$	1-Octene	7.7520	6.23	2.58	0.019	5.6
Replicate 1	*n*-Decane	7.9468	322	112	-	
$(MeO)_3PO$	1-Octene	7.7492	5.74	2.38	0.019	5.4
Replicate 2	*n*-Decane	11.4630	307	108	-	
HMPA	1-Octene	7.7518	3.11	1.56	0.009	2.7
Replicate 1	*n*-Decane	11.4635	328	112	-	
HMPA	1-Octene	7.7545	3.03	1.41	0.010	2.9
Replicate 2	*n*-Decane	11.4560	298	96.6	-	
HMPA (Repeat)	1-Octene	7.4430	3.69	1.71	0.010	2.9
Replicate 1	*n*-Decane	11.4647	367	119	-	
HMPA (Repeat)	1-Octene	7.7462	3.67	1.72	0.010	2.9
Replicate 2	*n*-Decane	11.4678	363	117	-	
NBu_3	1-Octene	7.7542	1.43	0.725	0.005	1.5
Replicate	*n*-Decane	11.4585	278	101	-	
NBu_3	1-Octene	7.7533	1.44	0.726	0.005	1.5
Replicate 2	*n*-Decane	11.4588	276	101	-	
NBu_3 (Repeat)	1-Octene	7.7467	1.92	0.929	0.005	1.6
Replicate 1	*n*-Decane	11.4650	352	117	-	
NBu_3 (Repeat)	1-Octene	7.7497	1.83	0.891	0.005	1.5
Replicate 2	*n*-Decane	11.4683	349	117	-	
PBu_3	1-Octene	7.7502	4.72	2.14	0.015	4.4
Replicate 1	*n*-Decane	11.4625	306	108	-	

PBu_3 Replicate 2	1-Octene *n*-Decane	7.7522 11.4653	4.83 306	2.18 108	0.016 -	4.5
$(MeO)_3P$ Replicate 1	1-Octene *n*-Decane	7.7470 11.4668	20.2 331	8.4 114	0.061 -	17.6
$(MeO)_3P$ Replicate 2	1-Octene *n*-Decane	7.7498 11.4658	19.5 319	8.17 111	0.061 -	17.6
$(MeO)_3P$ (Repeat) Replicate 1	1-Octene *n*-Decane	7.7382 11.4677	23.9 368	10.6 116	0.065 -	18.7
$(MeO)_3P$ (Repeat) Replicate 2	1-Octene *n*-Decane	7.7402 11.4657	22.5 373	9.6 119	0.060 -	17.4
Tetramethylthiourea Replicate 1	1-Octene *n*-Decane	7.7477 11.4603	7.26 286	2.74 102	0.025 -	7.3
Tetramethylthiourea Replicate 2	1-Octene *n*-Decane	7.7470 11.4600	7.27 290	2.76 104	0.025 -	7.2
TetramethylthioureaR Replicate 1	1-Octene *n*-Decane	7.7412 11.4647	8.83 360	3.31 118	0.025 -	7.1
TetramethylthioureaR Replicate 2	1-Octene *n*-Decane	7.7432 11.4663	8.72 361	3.28 116	0.024 -	7.0
TetramethylureaR Replicate 1	1-Octene *n*-Decane	7.7437 11.4543	11.2 257	4.64 96.3	0.044 -	12.6
TetramethylureaR Replicate 2	1-Octene *n*-Decane	7.7458 11.4563	11 255	4.55 96	0.043 -	12.4
Tetramethylurea Replicate 1	1-Octene *n*-Decane	7.7520 11.4570	10.3 228	4.26 89.3	0.045 -	13.0

Tetramethylurea Replicate 2	1-Octene *n*-Decane	7.7495 11.4505	9.3 202	4.06 83.3	0.046 -	13.3

Sample	mmole of Octene		Average mmole of Octene	% Lib	% of Orig.
Pre-Blank	478.6	467.8	467.8	473.2	
Blank1	1.1	1.2	1.1		
Blank2	5.3	5.1	5.2	-	-
Blank3	2.8	2.3	2.6		
Average Blank			2.8	0.0	10.5
Control 1	3.5	3.3	3.4		
Control 2	4.3	4.0	4.1	-	-
Control 3	3.2	3.2	3.2		
Average Control			3.8	35.8	14.2
DMFR	4.2	4.1	4.2	51.2	15.9
DMSO	10.4	10.8	10.6	283.3	40.2
DMSOR	10.2	10.1	10.2	267.8	38.6
$(MeO)_3PO$	5.6	5.4	5.5	98.5	20.8
HMPA	2.7	2.9	2.8	2.5	10.8
HMPAR	2.9	2.9	2.9	5.2	11.0
Bu_3N	1.5	1.5	1.5	-45.9	5.7
Bu_3NR	1.6	1.5	1.5	-44.2	5.9
Bu_3P	4.4	4.5	4.5	62.8	17.1
$(MeO)_3P$	17.6	17.6	17.6	537.4	66.9

$(MeO)_3PR$	18.7	17.4	18.1	553.6	68.6
Thiourea	7.3	7.2	7.3	163.3	27.6
ThioureaR	7.1	7.0	7.0	154.0	26.6
Urea	13.0	13.3	13.1	375.9	49.9
UreaR	12.6	12.4	12.5	352.5	47.5

Table 6.12 - Effect of Lewis base on dealkylation of B(*n*-octyl)$_3$ at 150 ^{o}C – Octene mass balance

Lewis Base	Sum of Octanol Concentrations		
	mmol Octene	% of original	% Lib
Blank	0.054	-	
Control	0.081	0.7	49.5
DMF	0.035	-0.5	-36.2
DMSO	0.078	0.6	44.8
$(MeO)_3P$	0.076	0.5	40.5
$(MeO)_3PO$	0.085	0.8	57.0
HMPA	0.072	0.4	33.1
Bu_3N	0.074	0.5	35.9
Bu_3P	0.065	0.3	20.0
Thiourea	0.095	1.0	75.5
Urea	0.067	0.3	23.6

6.3.2. Effect of Lewis Base on Thermal Dealkylation of Tri-4-octylborane after Removal of Solvent

Data for the investigation of the effect of the Lewis base on the dealkylation of tri-4-octylborane (**Section 3.2.2**) were obtained by the GC analysis (Perkin-Elmer Elite Wax column) of duplicate injection of oxidised samples. The alcohol content and relative distribution was obtained as explained by equations *6.3* and *6.4* in **Section 6.3.1**. **Table 6.13** contains the data used to generate **Table 3.13** in **Section 3.2.2**.

Table 6.13 - Primary data for the study of Lewis base effect on the dealkylation and isomerisation of $B(4\text{-octyl})_3$ at 150 ^{o}C

Sample	Component	Retention Time (min.)	Peak Area (mV.sec)	Peak Height (mV)	Area Ratio	Conc (M)	% Distribution.
Control Replicate 1	*n*-Decane	3.1113	684	44.8	-		
	4-Octanol	4.7175	75.6	11.8	0.111	1.73E-02	53.0
	3-Octanol	6.6160	35.4	4.36	0.052	8.09E-03	24.8
	2-Octanol	6.7688	17.9	2.81	0.026	4.09E-03	12.5
	1-Octanol	8.0647	13.8	2.2	0.020	3.15E-03	9.7
Control Replicate 2)	*n*-Decane	3.1258	685	46	-		
	4-Octanol	4.7402	77.6	11.8	0.113	1.77E-02	53.9
	3-Octanol	6.6355	34.7	4.37	0.051	7.92E-03	24.1
	2-Octanol	6.7945	18	2.87	0.026	4.11E-03	12.5
	1-Octanol	8.088	13.8	2.19	0.020	3.15E-03	9.6

Sample	Component	Retention Time (min.)	Peak Area (mV.sec)	Peak Height (mV)	Area Ratio	Conc (M)	% Distribution.
DMF Replicate 1	*n*-Decane	3.2372	964	49.1	-		
	4-Octanol	4.7797	111	15.7	0.115	1.80E-02	55.4
	3-Octanol	6.6683	44.2	5.16	0.046	7.17E-03	22.0
	2-Octanol	6.8262	22.7	3.49	0.024	3.68E-03	11.3
	1-Octanol	8.1378	22.6	3.26	0.023	3.66E-03	11.3
DMF Replicate 2	*n*-Decane	3.3460	896	51.9	-		
	4-Octanol	4.9375	109	16.1	0.122	1.90E-02	55.3
	3-Octanol	6.8453	43.7	5.26	0.049	7.62E-03	22.2
	2-Octanol	7.0012	22.5	3.48	0.025	3.93E-03	11.4
	1-Octanol	8.2832	22	3.33	0.025	3.84E-03	11.2
DMSO Replicate 1)	*n*-Decane	3.7160	563	42.5	-		
	4-Octanol	4.8303	59.3	9.81	0.105	1.65E-02	54.7
	3-Octanol	6.7412	27.7	3.68	0.049	7.69E-03	25.5
	2-Octanol	6.9035	14	2.32	0.025	3.89E-03	12.9
	1-Octanol	8.1787	7.49	1.4	0.013	2.08E-03	6.9
DMSO Replicate 2	*n*-Decane	3.1987	652	45.3	-		
	4-Octanol	4.8135	67.9	10.3	0.104	1.63E-02	55.3
	3-Octanol	6.7285	31.3	4.04	0.048	7.50E-03	25.5
	2-Octanol	6.8885	16.1	2.51	0.025	3.86E-03	13.1
	1-Octanol	8.5185	7.58	1.44	0.012	1.82E-03	6.2

Sample	Component	Retention Time (min.)	Peak Area (mV.sec)	Peak Height (mV)	Area Ratio	Conc (M)	% Distribution.
$(MeO)_3PO$ Replicate 1	*n*-Decane	3.3162	501	39.7	-		
	4-Octanol	4.9767	60.5	9.26	0.121	1.89E-02	54.2
	3-Octanol	6.8895	28.7	4.08	0.057	8.96E-03	25.7
	2-Octanol	7.0452	13.9	2.46	0.028	4.34E-03	12.4
	1-Octanol	8.3022	8.57	1.76	0.017	2.67E-03	7.7
$(MeO)_3PO$ Replicate 2	*n*-Decane	3.0087	385	34.9	-		
	4-Octanol	4.7077	39.6	6.41	0.103	1.61E-02	54.6
	3-Octanol	6.62225	17.8	2.37	0.046	7.23E-03	24.5
	2-Octanol	6.789	8.88	1.37	0.023	3.61E-03	12.2
	1-Octanol	8.0521	6.24	1.1	0.016	2.53E-03	8.6
HMPA Replicate 1	*n*-Decane	3.0988	593	43.3	-		
	4-Octanol	4.7190	69.6	10.3	0.117	1.83E-02	54.9
	3-Octanol	6.6308	31.5	3.84	0.053	8.30E-03	24.9
	2-Octanol	6.7883	15	2.32	0.025	3.95E-03	11.8
	1-Octanol	8.0747	10.6	1.47	0.018	2.79E-03	8.4
HMPA Replicate 2	*n*-Decane	3.0182	376	34.1	-		
	4-Octanol	4.7168	38.4	6.16	0.102	1.60E-02	54.5
	3-Octanol	6.6493	18.6	2.11	0.049	7.73E-03	26.4
	2-Octanol	6.8157	8.32	1.31	0.022	3.46E-03	11.8
	1-Octanol	8.0897	5.12	0.899	0.014	2.13E-03	7.3

Sample	Component	Retention Time (min.)	Peak Area (mV.sec)	Peak Height (mV)	Area Ratio	Conc (M)	% Distribution.
NBu_3 Replicate 1	*n*-Decane	3.1405	533	42.8	-		
	4-Octanol	4.7750	51.8	7.75	0.097	1.52E-02	53.8
	3-Octanol	6.7043	24.5	3.41	0.046	7.19E-03	25.4
	2-Octanol	6.8635	14.2	2.06	0.027	4.16E-03	14.7
	1-Octanol	8.1192	5.78	1.02	0.011	1.70E-03	6.0
NBu_3 Replicate 2	*n*-Decane	3.0832	460	39.9	-		
	4-Octanol	4.7440	44.8	6.86	0.097	1.52E-02	53.5
	3-Octanol	6.6803	21.3	3.1	0.046	7.24E-03	25.4
	2-Octanol	6.8383	11.7	1.85	0.025	3.98E-03	14.0
	1-Octanol	8.1023	5.93	1.01	0.013	2.02E-03	7.1
PBu_3 Replicate 1	*n*-Decane	3.1663	622	41.8	-		
	4-Octanol	4.8125	63.8	9.68	0.103	1.60E-02	57.6
	3-Octanol	6.7267	28.4	3.4	0.046	7.14E-03	25.6
	2-Octanol	6.8900	13	2.13	0.021	3.27E-03	11.7
	1-Octanol	8.1592	5.56	1.12	0.009	1.40E-03	5.0
PBu_3 Replicate 2	*n*-Decane	3.1122	371	33.7	-		
	4-Octanol	4.8190	39.3	6.3	0.106	1.66E-02	56.4
	3-Octanol	6.7550	19.1	2.01	0.051	8.05E-03	27.4
	2-Octanol	6.9178	8.04	1.28	0.022	3.39E-03	11.5
	1-Octanol	8.8163	3.22	0.715	0.009	1.36E-03	4.6

Sample	Component	Retention Time (min.)	Peak Area (mV.sec)	Peak Height (mV)	Area Ratio	Conc (M)	% Distribution.
$(MeO)_3P$ Replicate 1	*n*-Decane	3.0617	390	34.5	-		
	4-Octanol	4.7655	37	4.85	0.095	1.48E-02	52.9
	3-Octanol	6.6965	17.9	2.14	0.046	7.17E-03	25.6
	2-Octanol	6.8616	9.08	1.36	0.023	3.64E-03	13.0
	1-Octanol	8.1297	5.96	0.917	0.015	2.39E-03	8.5
$(MeO)_3P$ Replicate 2	*n*-Decane	3.1403	389	33.6	-		
	4-Octanol	4.8792	36.3	4.68	0.093	1.46E-02	52.9
	3-Octanol	6.8195	17.5	2.11	0.045	7.03E-03	25.5
	2-Octanol	6.9842	8.96	1.33	0.023	3.60E-03	13.1
	1-Octanol	8.2563	5.87	0.886	0.015	2.36E-03	8.6
Tetramethylthiourea Replicate 1	*n*-Decane	3.225	728	45.2	-		
	4-Octanol	4.8997	68	10.4	0.093	1.46E-02	51.4
	3-Octanol	6.8232	36.7	4.34	0.050	7.88E-03	27.7
	2-Octanol	6.9763	18.4	2.84	0.025	3.95E-03	13.9
	1-Octanol	8.2527	9.16	1.1	0.013	1.97E-03	6.9
Tetramethylthiourea Replicate 2	*n*-Decane	3.3758	700	43.3	-		
	4-Octanol	4.9585	70.7	10.3	0.101	1.58E-02	51.9
	3-Octanol	6.9092	39.7	4.86	0.057	8.87E-03	29.2
	2-Octanol	7.0607	19.2	3.18	0.027	4.29E-03	14.1
	1-Octanol	8.3042	6.56	1.24	0.009	1.47E-03	4.8

Sample	Component	Retention Time (min.)	Peak Area (mV.sec)	Peak Height (mV)	Area Ratio	Conc (M)	% Distribution.
Tetramethylurea Replicate 1	*n*-Decane	3.2553	688	42.3	-		
	4-Octanol	4.8632	63.1	9.43	0.092	1.43E-02	52.5
	3-Octanol	6.7845	31.3	3.82	0.045	7.11E-03	26.0
	2-Octanol	6.9410	15.7	2.42	0.023	3.57E-03	13.1
	1-Octanol	8.2242	10.1	1.36	0.015	2.29E-03	8.4
Tetramethylurea Replicate 2	*n*-Decane	3.2798	541	41	-		
	4-Octanol	4.8930	54.8	9.02	0.101	1.58E-02	50.1
	3-Octanol	6.8145	31.7	4.22	0.059	9.16E-03	29.0
	2-Octanol	6.9725	15.1	2.73	0.028	4.36E-03	13.8
	1-Octanol	8.2530	7.82	1.65	0.014	2.26E-03	7.1
Blank Replicate 1	*n*-Decane	3.0097	586	40.3	-		
	4-Octanol	4.6762	72.9	11.6	0.135	2.11E-02	54.6
	3-Octanol	6.5898	34.2	4.42	0.063	9.88E-03	25.6
	2-Octanol	6.7410	16.1	2.43	0.030	4.65E-03	12.1
	1-Octanol	8.0877	10.4	1.92	0.019	3.01E-03	7.8
Blank Replicate 2	*n*-Decane	3.1715	930	51.3	-		
	4-Octanol	4.4730	129	17.9	0.238	3.73E-02	56.3
	3-Octanol	6.6193	59.9	6.36	0.111	1.73E-02	26.1
	2-Octanol	6.7740	23.8	3.61	0.044	6.88E-03	10.4
	1-Octanol	8.1068	16.4	2.75	0.030	4.74E-03	7.2

Table 6.14 - Effect of Lewis base on dealkylation of B(*i*-octyl)$_3$ at 150 ^{o}C – Octanol mass balance

Lewis Base	Sum of Octanol Concentrations			
	Replicate 1	Replicate 2	Average	% Decrease in Octanol Mass Balance
Blank	3.86×10^{-2}	6.62×10^{-2}	5.24×10^{-2}	0.00 × +00
Control	3.26×10^{-2}	3.29×10^{-2}	3.27×10^{-2}	37.5
DMF	3.25×10^{-2}	3.44×10^{-2}	3.35×10^{-2}	36.1
DMSO	3.01×10^{-2}	2.95×10^{-2}	2.98×10^{-2}	43.1
$(MeO)_3PO$	3.48×10^{-2}	2.94×10^{-2}	3.21×10^{-2}	38.7
HMPA	3.34×10^{-2}	$2.93 \times 10^{-2}2$	3.13×10^{-2}	40.2
Bu_3N	2.82×10^{-2}	2.85×10^{-2}	2.83×10^{-2}	45.9
Bu_3P	2.78×10^{-2}	2.94×10^{-2}	2.86×10^{-2}	45.4
$(MeO)_3P$	2.80×10^{-2}	2.76×10^{-2}	2.78×10^{-2}	46.9
Thiourea	2.84×10^{-2}	3.04×10^{-2}	2.94×10^{-2}	43.9
Urea	2.73×10^{-2}	3.16×10^{-2}	2.95×10^{-2}	43.8

Table 6.15 - Effect of Lewis base on dealkylation of B(*i*-octyl)$_3$ at 150 ^{o}C – Octanol mass balance

Lewis Base	mmol Octene	% of original	% Lib
Blank	0.054	-	
Control	0.081	0.7	49.5
DMF	0.035	-0.5	-36.2
DMSO	0.078	0.6	44.8
$(MeO)_3P$	0.076	0.5	40.5
$(MeO)_3PO$	0.085	0.8	57.0
HMPA	0.072	0.4	33.1
Bu_3N	0.074	0.5	35.9
Bu_3P	0.065	0.3	20.0
Thiourea	0.095	1.0	75.5
Urea	0.067	0.3	23.6

6.4. DISPLACEMENT STUDIES ON TRIALKYLBORANES

Data for the investigation of the effect of the Lewis base on the dealkylation of tri-*n*-octylborane and tri-4-octylborane (**Section 3.3**) were obtained by the GC analysis (Perkin-Elmer Elite Wax column) of duplicate injection of oxidised samples. The alcohol content and relative distribution was obtained as explained by equations *6.3* and *6.4* in **Section 6.3.1**. **Table 6.16** contains the data used to generate **3.15** in **Section 3.3**.

Table 6.16 - Primary data for effect of selected Lewis bases of the displacement reaction of tri-*n*-butylborane with 1-octene at 120 °C

Sample	Component	Retention Time (min.)	Peak Area (mV.sec)	Peak Height (mV)	Area Ratio	Conc (M)	% Distribution.
Control Repliacte 1	*n*-Decane	2.8508	160	32.6	-		
	1-Butanol	3.9370	36.7	8.59	0.284	0.15	61.2
	2-Octanol				0.000	0.00	0.0
	1-Octanol	8.0342	13.7	2.26	0.106	0.02	6.9
Control Replicate 2	*n*-Decane	2.8308	18	35.3	-		
	1-Butanol	3.9330	41	9.81	0.323	0.17	69.5
	2-Octanol				0.000	0.00	0.0
	1-Octanol	8.0097	15.3	2.44	0.120	0.02	7.9
NBu_3 Replicate 1	*n*-Decane	2.8425	205	37.3	-		
	1-Butanol	3.9565	67.8	13.1	0.551	0.28	118.6
	2-Octanol	6.6413	0.127	0.872	0.001	0.00	0.1
	1-Octanol	8.7030	16.7	1.63	0.136	0.02	8.9

	n-Decane	2.7808	155	30.6	-		
NBu_3	1-Butanol	3.9357	46	9.84	0.374	0.19	80.5
Replicate 2	2-Octanol				0.000	0.00	0.0
	1-Octanol	8.0950	9.85	1.31	0.080	0.01	5.2
	n-Decane	2.7642	170	40.2	-		
PBu_3	1-Butanol	3.9653	57.9	11	0.508	0.26	109.3
Replicate 1	2-Octanol				0.000	0.00	0.0
	1-Octanol	8.0950	11.4	1.68	0.100	0.02	6.5
	n-Decane	2.8392	174	32.1	-		
PBu_3	1-Butanol	3.9203	38.9	8.26	0.341	0.18	73.4
Replicate 2	2-Octanol	6.5842	0.144	0.733	0.001	0.00	0.1
	1-Octanol	8.0245	14.8	1.92	0.130	0.02	8.5
	n-Decane	2.7292	130	33.7	-		
$(EtO)_3P$	1-Butanol	3.9730	61.6	10.7	0.501	0.26	107.7
Replicate 1	2-Octanol	6.8228	0.983	0.841	0.008	0.00	0.5
	1-Octanol	8.0027	17.9	2.25	0.146	0.02	9.5
	n-Decane	2.7542	118	29.5	-		
$(EtO)_3P$	1-Butanol	3.9045	38.7	9.32	0.328	0.17	70.6
Replicate 2	2-Octanol	6.8368	0.743	1.01	0.006	0.00	0.4
	1-Octanol	7.9980	14	2.46	0.119	0.02	7.7

Sample	Component	Retention Time (min.)	Peak Area (mV.sec)	Peak Height (mV)	Area Ratio	Conc (M)	% Distribution.
	n-Decane	2.7685	140	30.5	-		
Tetramethylthiourea	1-Butanol	3.9345	51.2	9.66	0.430	0.22	92.6
Replicate 1	2-Octanol	6.8580	0.571	0.87	0.005	0.00	0.3
	1-Octanol	8.0223	15.6	1.84	0.131	0.02	8.6
	n-Decane	2.7992	159	34.2			
Tetramethylthiourea	1-Butanol	3.9300	44.3	10.4	0.375	0.19	80.8
Replicate 2	2-Octanol				0.000	0.00	0.0
	1-Octanol	8.0385	17.7	1.91	0.150	0.02	9.8
	n-Decane	2.7842	158	32.6	-		
Tetranethylurea	1-Butanol	3.9267	42.8	9.87	0.354	0.18	76.1
Replicate 1	2-Octanol	6.6053	0.103	0.934	0.001	0.00	0.1
	1-Octanol	8.0227	12.4	1.72	0.102	0.02	6.7
	n-Decane	2.6892	111		-		
Tetranethylurea	1-Butanol	3.9295	48.5	8.57	0.398	0.20	85.5
Replicate 2	2-Octanol				0.000	0.00	0.0
	1-Octanol	7.9850	8.66	1.54	0.071	0.01	4.6
	n-Decane	2.7792	129	19.5	-		
Control	1-Butanol	3.8995	56.1	7.46	0.435	0.22	89.9
Replicate 1	2-Octanol				0.000	0.00	0.0
	1-Octanol				0.000	0.00	0.0

Sample	Component	Retention Time (min.)	Peak Area (mV.sec)	Peak Height (mV)	Area Ratio	Conc (M)	% Distribution.
Control Replicate 2	*n*-Decane	2.7787	127	19	-		
	1-Butanol	3.8973	53.5	6.08	0.421	0.22	87.1
	2-Octanol				0.000	0.00	0.0
	1-Octanol				0.000	0.00	0.0
DMF Replicate 1	*n*-Decane	2.7720	123	18.3	-		
	1-Butanol	3.6755	59.5	7.05	0.484	0.25	100.0
	2-Octanol				0.000	0.00	0.0
	1-Octanol				0.000	0.00	0.0
DMF Replicate 2	*n*-Decane	2.7720	123	18.1	-		
	1-Butanol	3.9132	57.5	6.36	0.467	0.24	96.6
	2-Octanol				0.000	0.00	0.0
	1-Octanol				0.000	0.00	0.0
DMSO Replicate 1	*n*-Decane	2.7657	114	17	-		
	1-Butanol	3.9213	54.6	5.66	0.479	0.25	99.0
	2-Octanol				0.000	0.00	0.0
	1-Octanol				0.000	0.00	0.0
DMSO Replicate 2	*n*-Decane	2.7670	114	16.9	-		
	1-Butanol	3.9330	54	5.17	0.474	0.24	97.9
	2-Octanol				0.000	0.00	0.0
	1-Octanol				0.000	0.00	0.0

Sample	Component	Retention Time (min.)	Peak Area (mV.sec)	Peak Height (mV)	Area Ratio	Conc (M)	% Distribution.
	n-Decane	2.7758	123	18.1	-		
$(MeO)_3PO$	1-Butanol	3.9437	59.4	5.81	0.483	0.25	99.8
Replicate 1	2-Octanol				0.000	0.00	0.0
	1-Octanol				0.000	0.00	0.0
	n-Decane	2.7785	118	18.2	-		
$(MeO)_3PO$	1-Butanol	3.9522	58.4	5.35	0.495	0.25	102.3
Replicate 2	2-Octanol				0.000	0.00	0.0
	1-Octanol				0.000	0.00	0.0
	n-Decane	2.7740	119	17.7	-		
HMPA	1-Butanol	3.9518	64.4	5.96	0.541	0.28	111.9
Replicate 1	2-Octanol				0.000	0.00	0.0
	1-Octanol				0.000	0.00	0.0
	n-Decane	2.7685	118	17.5	-		
HMPA	1-Butanol	3.9550	65.1	5.95	0.552	0.28	114.0
Replicate 2	2-Octanol				0.000	0.00	0.0
	1-Octanol				0.000	0.00	0.0

Table 6.17 - Primary data for effect of selected Lewis bases of the displacement reaction of tri-*n*-butylborane with 4-octene at 120 °C

Sample	Component	Retention Time (min.)	Peak Area (mV.sec)	Peak Height (mV)	Area Ratio	Conc (M)	% Distribution.
Control Repliacte 1	*n*-Decane	2.8778	220	29.8	-		
	1-Butanol	3.8648	63	8.07	0.176	0.09	27.3
	2-Butanol	3.6065	3.93	1.21	0.011	0.01	1.7
	4-Octanol	4.7943	3.35	1.84	0.009	0.00	0.4
	3-Octanol	6.1770	10.1	0.71	0.028	0.00	1.3
	2-Octanol	6.6642	56.7	4.36	0.159	0.02	7.5
	1-Octanol	8.0032	0.558	0.219	0.002	0.00	0.1
Control Replicate	*n*-Decane	2.8577	216	29.6	-		
	1-Butanol	3.8427	50.1	7.5	0.148	0.08	22.9
	2-Butanol	3.5909	5.89	1.21	0.017	0.01	2.7
	4-Octanol	4.8417	3.8	0.551	0.011	0.00	2.6
	3-Octanol	6.1362	9.02	0.692	0.027	0.00	1.3
	2-Octanol	6.6595	54.1	3.06	0.160	0.02	7.5
	1-Octanol	8.0263	0.238	0.208	0.001	0.00	0.0
DMF Replicate 1	*n*-Decane	2.8507	205	28.3	-		
	1-Butanol	3.8530	61.6	5.7	0.188	0.10	31.0
	2-Butanol	3.5983	5.71	1.17	0.017	0.01	2.9
	4-Octanol	4.8640	2.86	0.511	0.009	0.00	0.4
	3-Octanol	6.4642	3.43	0.562	0.010	0.00	0.5
	2-Octanol	6.7110	48.8	2.33	0.149	0.02	7.4
	1-Octanol	8.0417	0.275	0.212	0.001	0.00	0.0

Sample	Component	Retention Time (min.)	Peak Area (mV.sec)	Peak Height (mV)	Area Ratio	Conc (M)	% Distribution.
DMF Replicate 2	*n*-Decane	2.8622	206	28.6	-		
	1-Butanol	3.8626	62.8	5.08	0.185	0.10	30.5
	2-Butanol	3.6065	5.73	1.12	0.017	0.01	2.8
	4-Octanol	4.8672	1.27	0.488	0.004	0.00	0.2
	3-Octanol	6.4668	3.56	0.536	0.010	0.00	0.5
	2-Octanol	6.7622	44.7	2.08	0.132	0.02	6.6
	1-Octanol	8.0725	0.277	0.204	0.001	0.00	0.0
DMSO Replicate 1	*n*-Decane	2.8680	212	29.3	-		
	1-Butanol	3.8803	68.7	4.99	0.203	0.10	33.4
	2-Butanol	3.6055	6.13	1.1	0.018	0.01	3.0
	4-Octanol	4.8733	3.05	0.436	0.009	0.00	0.4
	3-Octanol	6.4676	3.4	0.4927	0.010	0.00	0.5
	2-Octanol	6.6657	49.5	3.44	0.146	0.02	7.3
	1-Octanol	8.0482	0.278	0.143	0.001	0.00	0.0
DMSO Replicate 2	*n*-Decane	2.8522	207	29.2	-		
	1-Butanol	3.8673	60.2	4.51	0.178	0.09	29.2
	2-Butanol	3.5822	5.76	1.19	0.017	0.01	2.8
	4-Octanol	4.8582	5.65	0.481	0.017	0.00	0.8
	3-Octanol	6.4693	3.49	0.52	0.010	0.00	0.5
	2-Octanol	6.6708	47.2	3.22	0.139	0.02	7.0
	1-Octanol	8.0533	0.272	0.163	0.001	0.00	0.0

Sample	Component	Retention Time (min.)	Peak Area (mV.sec)	Peak Height (mV)	Area Ratio	Conc (M)	% Distribution.
$(MeO)_3P$ Replicate 1	*n*-Decane	2.8565	213	29.2	-		
	1-Butanol	3.9612	31.9	2.79	0.094	0.05	15.5
	2-Butanol	3.5975	4.86	1.16	0.014	0.01	2.4
	4-Octanol	4.8572	2.48	0.546	0.007	0.00	0.4
	3-Octanol	6.4805	4.18	0.476	0.012	0.00	0.6
	2-Octanol	6.8383	39.7	1.75	0.117	0.02	5.9
	1-Octanol	8.1220	0.245	0.187	0.001	0.00	0.0
$(MeO)_3P$ Replicate 2	*n*-Decane	2.8677	217	29.1	-		
	1-Butanol	3.9913	32.9	2.62	0.097	0.05	16.0
	2-Butanol	3.6043	5.18	1.05	0.015	0.01	2.5
	4-Octanol	4.8693	2.49	0.496	0.007	0.00	0.4
	3-Octanol	6.4797	4.15	0.444	0.012	0.00	0.6
	2-Octanol	6.8548	40	1.71	0.118	0.02	5.9
	1-Octanol				0.000	0.00	0.0
$(MeO)_3PO$ Replicate 1	*n*-Decane	2.8467	196	27.4	-		
	1-Butanol	3.8427	38.6	2.84	0.114	0.06	18.8
	2-Butanol	3.6027	5.27	1.08	0.016	0.01	2.6
	4-Octanol	4.7918	2.33	0.491	0.007	0.00	0.3
	3-Octanol	6.4553	4.1	0.467	0.012	0.00	0.6
	2-Octanol	6.8303	44	1.66	0.130	0.02	6.5
	1-Octanol	8.0197	0.232	0.179	0.001	0.00	0.0

Sample	Component	Retention Time (min.)	Peak Area (mV.sec)	Peak Height (mV)	Area Ratio	Conc (M)	% Distribution.
$(MeO)_3PO$ Replicate 2	*n*-Decane	2.8518	194	27.4	-		
	1-Butanol	3.9480	27.8	1.13	0.082	0.04	13.5
	2-Butanol	3.6068	5.13	2.17	0.015	0.01	2.5
	4-Octanol	4.7860	2.24	0.529	0.007	0.00	0.3
	3-Octanol	6.4585	4.05	0.469	0.012	0.00	0.6
	2-Octanol	6.8770	43.3	1.59	0.128	0.02	6.4
	1-Octanol	8.1198	0.185	0.186	0.001	0.00	0.0
HMPA Replicate 1	*n*-Decane	2.8890	239	31.7	-		
	1-Butanol	4.0537	25.6	1.8	0.075	0.04	12.4
	2-Butanol	3.6278	6.77	1.4	0.020	0.01	3.3
	4-Octanol	4.8028	2.47	0.65	0.007	0.00	0.4
	3-Octanol	6.4702	6.41	0.566	0.019	0.00	0.9
	2-Octanol	6.9873	52.9	0.457	0.156	0.02	7.8
	1-Octanol	8.1627	1.74	0.228	0.005	0.00	0.3
HMPA Replicate 2	*n*-Decane	2.8805	238	31.3	-		
	1-Butanol	4.0790	22.5	1.66	0.066	0.03	10.9
	2-Butanol	3.6165	6.53	1.36	0.019	0.01	3.2
	4-Octanol	4.7988	2.28	0.675	0.007	0.00	0.3
	3-Octanol	6.4695	6.5	0.554	0.019	0.00	1.0
	2-Octanol	7.0882	53.4	1.67	0.157	0.02	7.9
	1-Octanol				0.000	0.00	0.0

Sample	Component	Retention Time (min.)	Peak Area (mV.sec)	Peak Height (mV)	Area Ratio	Conc (M)	% Distribution.
Control Replicate 1	*n*-Decane	2.8073	182	25.7	-		
	1-Butanol	3.5695	4.35	0.856	0.013	0.01	2.1
	2-Butanol	3.8362	37.2	3.36	0.110	0.06	18.1
	4-Octanol	4.8435	2.7	0.381	0.008	0.00	0.4
	3-Octanol	6.5793	3.83	0.523	0.011	0.00	0.6
	2-Octanol	6.8993	37.9	1.52	0.112	0.02	5.6
	1-Octanol				0.000	0.00	0.0
Control Replicate 2	*n*-Decane	2.8102	180	25.9	-		
	1-Butanol	3.8455	37.4	2.9	0.110	0.06	17.1
	2-Butanol	3.5707	4.12	0.933	0.012	0.01	1.9
	4-Octanol	4.8400	2.38	0.443	0.007	0.00	0.3
	3-Octanol	6.4792	2.34	0.399	0.007	0.00	0.3
	2-Octanol	7.0440	37	1.27	0.109	0.02	5.1
	1-Octanol				0.000	0.00	0.0
NBu_3 Replicate 1	*n*-Decane	2.8055	174	25.1	-		
	1-Butanol	3.8738	35.2	2.97	0.104	0.05	16.1
	2-Butanol	3.5675	3.88	0.911	0.011	0.01	1.8
	4-Octanol	4.8397	2.39	0.408	0.007	0.00	0.3
	3-Octanol	6.5793	3.87	0.665	0.011	0.00	0.5
	2-Octanol	7.0653	45.4	1.1	0.134	0.02	6.3
	1-Octanol				0.000	0.00	0.0

Sample	Component	Retention Time (min.)	Peak Area (mV.sec)	Peak Height (mV)	Area Ratio	Conc (M)	% Distribution.
NBu_3 Replicate 2	*n*-Decane	2.8023	172	25.1		-	
	1-Butanol	3.8920	26.8	2.72	0.079	0.04	12.3
	2-Butanol	3.5658	3.77	0.914	0.011	0.01	1.7
	4-Octanol	4.8403	2.24	0.415	0.007	0.00	0.3
	3-Octanol	6.4788	3.49	0.396	0.010	0.00	0.5
	2-Octanol	7.0592	45.4	1.15	0.134	0.02	6.3
	1-Octanol				0.000	0.00	0.0
PBu_3 Replicate 1	*n*-Decane	2.8043	172	25.6		-	
	1-Butanol	3.9067	17.8	2.18	0.052	0.03	8.1
	2-Butanol	3.5548	3.84	1.03	0.011	0.01	1.8
	4-Octanol	4.8377	1.16	0.456	0.003	0.00	0.2
	3-Octanol	6.4682	2.69	0.447	0.008	0.00	0.4
	2-Octanol	6.6673	36.8	2.49	0.109	0.02	5.1
	1-Octanol	8.0525	0.202	0.152	0.001	0.00	0.0
PBu_3 Replicate 2	*n*-Decane	2.8048	175	25.5		-	
	1-Butanol	3.9117	19	2.14	0.056	0.03	8.7
	2-Butanol	3.5557	4.05	0.905	0.012	0.01	1.9
	4-Octanol	4.8408	1.04	3.93	0.003	0.00	0.1
	3-Octanol	6.4793	2.63	0.412	0.008	0.00	0.4
	2-Octanol	6.6715	37.2	2.38	0.110	0.02	5.2
	1-Octanol				0.000	0.00	0.0

Sample	Component	Retention Time (min.)	Peak Area (mV.sec)	Peak Height (mV)	Area Ratio	Conc (M)	% Distribution.
Tetramethylthiourea Replicate 1	*n*-Decane	2.8012	176	2.51	-		
	1-Butanol	4.0187	22.9	1.44	0.068	0.03	10.5
	2-Butanol	3.5767	3.38	0.839	0.010	0.01	1.5
	4-Octanol	4.7742	1.96	0.44	0.006	0.00	0.3
	3-Octanol	6.4808	3.09	0.345	0.009	0.00	0.4
	2-Octanol	7.0798	36.5	1.11	0.108	0.02	5.1
	1-Octanol				0.000	0.00	0.0
Tetramethylthiourea Replicate 2	*n*-Decane	2.8128	177	25.2	-		
	1-Butanol	4.0527	18	1.4	0.053	0.03	8.2
	2-Butanol	3.5850	2.93	0.848	0.009	0.00	1.3
	4-Octanol	4.7767	1.89	0.455	0.006	0.00	0.3
	3-Octanol	6.4815	3.24	0.346	0.010	0.00	0.4
	2-Octanol	7.1427	35.8	1.1	0.106	0.02	5.0
	1-Octanol				0.000	0.00	0.0
Tetramethylurea Replicate 1	*n*-Decane	2.8082	171	24.9	-		
	1-Butanol	4.0027	17.9	1.66	0.053	0.03	8.2
	2-Butanol	3.5737	3.78	0.857	0.011	0.01	1.7
	4-Octanol	4.8500	1.95	0.415	0.006	0.00	0.3
	3-Octanol	6.5120	3.5	0.374	0.010	0.00	0.5
	2-Octanol	6.8332	37.8	1.41	0.111	0.02	5.2
	1-Octanol	8.8092	0.153	0.141	0.000	0.00	0.0

Sample	Component	Retention Time (min.)	Peak Area (mV.sec)	Peak Height (mV)	Area Ratio	Conc (M)	% Distribution.
Tetramethylurea Replicate 2	*n*-Decane	2.8080	172	24.9	Mass Balance		15.9
	1-Butanol	4.0128	17.6	1.62	0.052	0.03	8.1
	2-Butanol	3.5707	3.73	0.87	0.011	0.01	1.7
	4-Octanol	4.8423	1.94	0.42	0.006	0.00	0.3
	3-Octanol	6.5088	3.34	0.371	0.010	0.00	0.5
	2-Octanol	6.8533	34.5	1.13	0.102	0.02	4.8
	1-Octanol				0.000	0.00	0.0
					Mass Balance		15.3

7. Appendix B: Kinetic Studies

7.1. Kinetic Data

7.1.1. Acrylonitrile Concentration Dependence

Data for the construction of Error! Reference source not found. in **Section 4.1.2.**

Table 7.1 - Concentration dependence of k_{obs} on acrylonitrile concentration in the reduction of acrylonitrile with borane dimethyl sulfide complex (0.16 M) in CH_2Cl_2 at 25.0 °C

[Acrylonitrile] (M)	t_1 (seconds)	k_{obs} / 10^{-3} (s^{-1})
2.26	1799.97593 ± 42.72779	0.56 ± 0.01
3.49	997.91443 ± 30.86821	1.00 ± 0.03
4.91	861.78794 ± 27.24503	1.16 ± 0.04
6.64	612.62788 ± 25.26924	1.63 ± 0.07
7.60	605.93231 ± 34.04728	1.65 ± 0.09

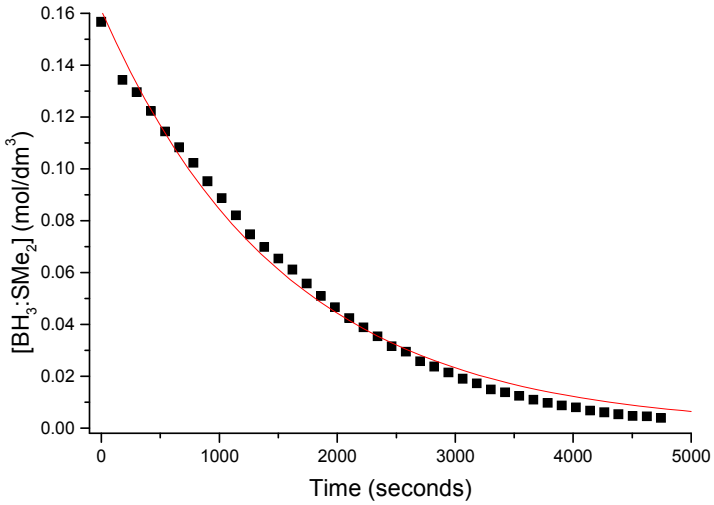

Figure 7.1 - Reduction of acrylonitrile (2.26 M) with borane dimethyl sulfide complex (0.16 M) in CH_2Cl_2 at 25.0 °C

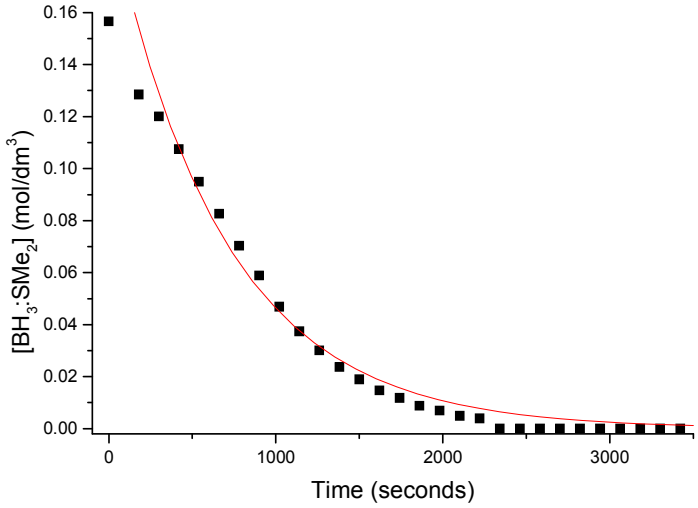

Figure 7.2 - Reduction of acrylonitrile (3.49 M) with borane dimethyl sulfide complex (0.16 M) in CH_2Cl_2 at 25.0 °C

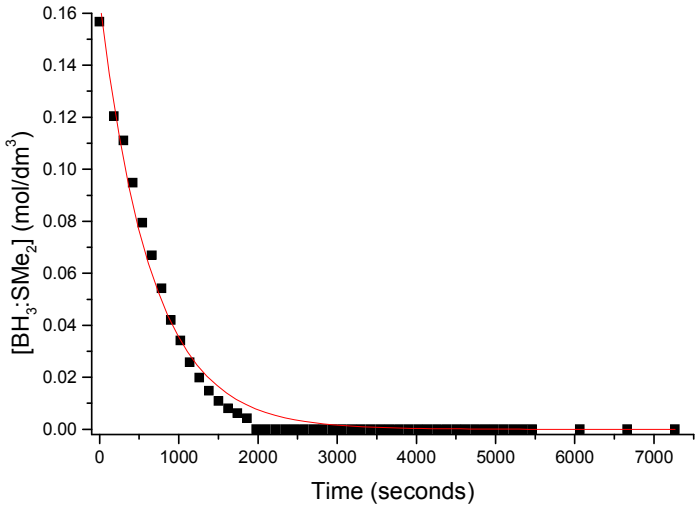

Figure 7.3 - Reduction of acrylonitrile (4.91 M) with borane dimethyl sulfide complex (0.16 M) in CH_2Cl_2 at 25.0 °C

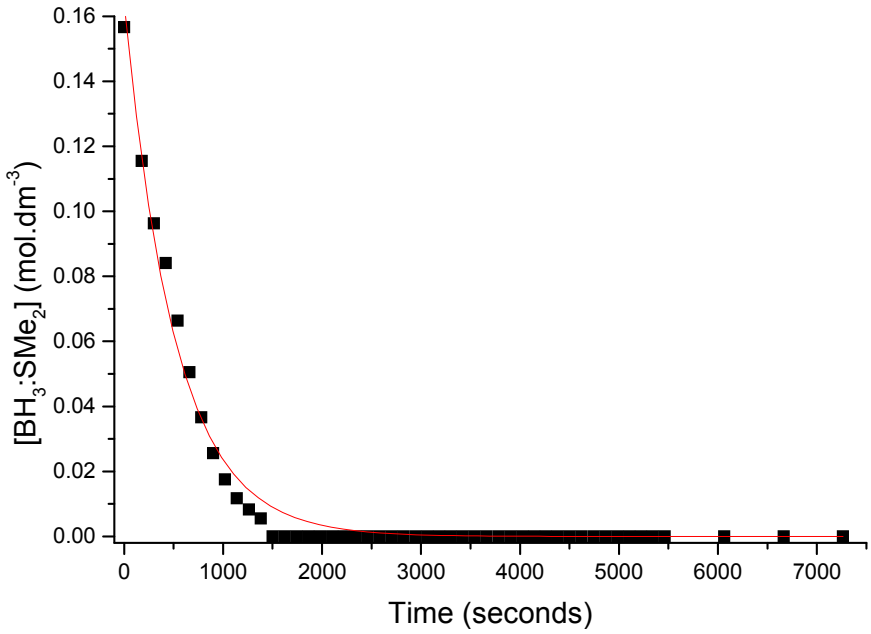

Figure 7.4 - Reduction of acrylonitrile (6.46 M) with borane dimethyl sulfide complex (0.16 M) in CH_2Cl_2 at 25.0 °C

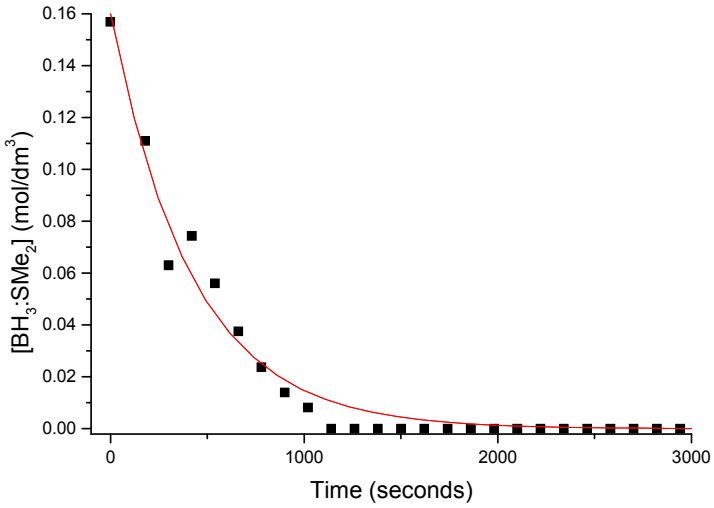

Figure 7.5 - Reduction of acrylonitrile (7.60 M) with borane dimethyl sulfide complex (0.16 M) in CH_2Cl_2 at 25.0 °C

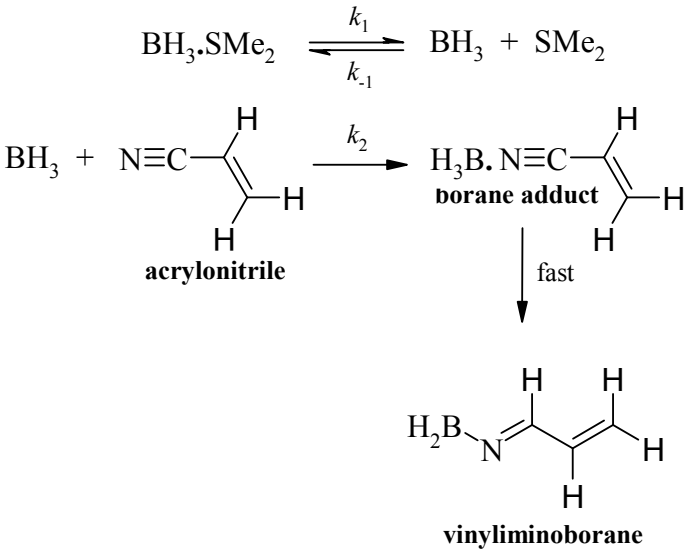

Scheme 7.1

Scheme 7.1, the formation of the vinyliminoborane (CH_2=CH-CH=N-BH_2) is directly proportional to the depletion of the borane dimethyl sulfide complex (BH_3.SMe_2), as defined by equation *7.1*:

$$\frac{d[CH_2=CH-CH=N-BH_2]}{dt} = -\frac{d[BH_3.SMe_2]}{dt} = k_3[CH_2=CH-C\equiv N.BH_3] \qquad 7.1$$

The formation of the borane-nitrile adduct (CH_2=CH-C≡N.BH_3) is a process at steady state defined by equation *7.2*:

$$\frac{d[CH_2=CH-C\equiv N.BH_3]}{dt} = k_2[BH_3][CH_2=CH-C\equiv N] - k_3[CH_2=CH-C\equiv N.BH_3] = 0 \qquad 7.2$$

The formation of free borane (BH_3) is an equilibrium process at steady state, shown by equation *7.3*:

$$\frac{d[BH_3]}{dt} = k_1[BH_3.SMe_2] - k_{-1}[BH_3][SMe_2] = 0 \qquad 7.3$$

Which affords a mass balance for BH_3, as shown by equation *7.4*:

$$\frac{k_1[BH_3.SMe_2]}{k_{-1}[SMe_2]} = [BH_3] \qquad 7.4$$

Combining equation *7.1* with equation *7.2* affords equation *7.5*.

$$-\frac{d[BH_3.SMe_2]}{dt} = k_2[BH_3][CH_2 = CH - C \equiv N] \qquad 7.5$$

Substitution of equation *7.5* into equation *7.4* results in an expression defining the rate of the reaction, equation *7.6*.

$$-\frac{d[BH_3.SMe_2]}{dt} = \frac{k_2k_1}{k_{-1}[SMe_2]}[BH_3.SMe_2][CH_2 = CH - C \equiv N] \qquad 7.6$$

At pseudo-first order conditions, however, $[CH_2{=}CH\text{-}C{\equiv}N] >>> [BH_3.SMe_2\}$, such that equation *7.6* reduces to equation *7.7*:

$$k_{obs} = \frac{k_2k_1}{k_{-1}[SMe_2]}[CH_2 = CH - C \equiv N] \qquad 7.7$$

7.1.2. Dimethyl Sulfide Concentration Dependence

Data for the construction of Error! Reference source not found. in **Section 4.1.2.**

Table 7.2 - Concentration dependence of k_{obs} on dimethyl sulfide concentration in the reduction of acrylonitrile with borane dimethyl sulfide complex (0.15 M) in CH_2Cl_2 at 25.0 °C

[Added SMe_2] (mol/dm^3)	t_1 (seconds)	k_{obs} / 10^{-3} (s^{-1})
0.000	670.92301 ± 16.1427	1.49 ± 0.04
0.043	699.95487 ± 10.25344	1.05 ± 0.02
0.043	1487.49713 ± 24.22028	
0.062	1287.08484 ± 10.86812	0.78 ± 0.01
0.087	1935.96918 ± 48.22251	0.52 ± 0.01
0.174	2490.27542 ± 32.87445	0.40 ± 0.01

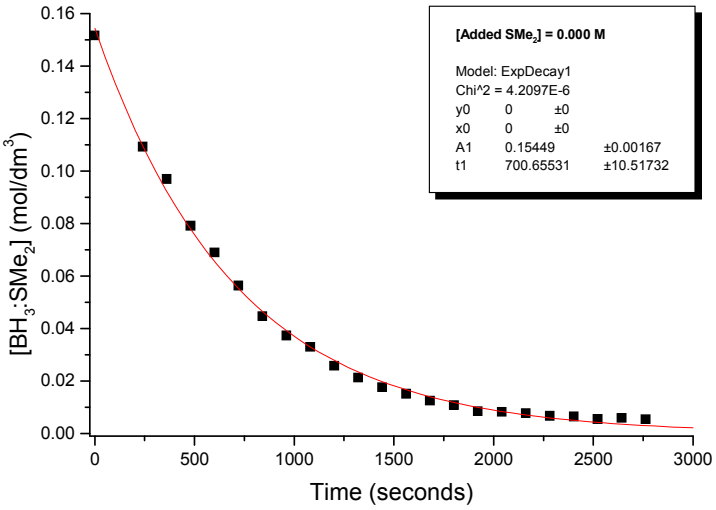

Figure 7.6 – Profile for reduction of acrylonitrile (4.91 M) with borane dimethyl sulfide complex (0.15 M) with dimethyl sulfide (0.043 M) in CH_2Cl_2 at 25.0 ^oC

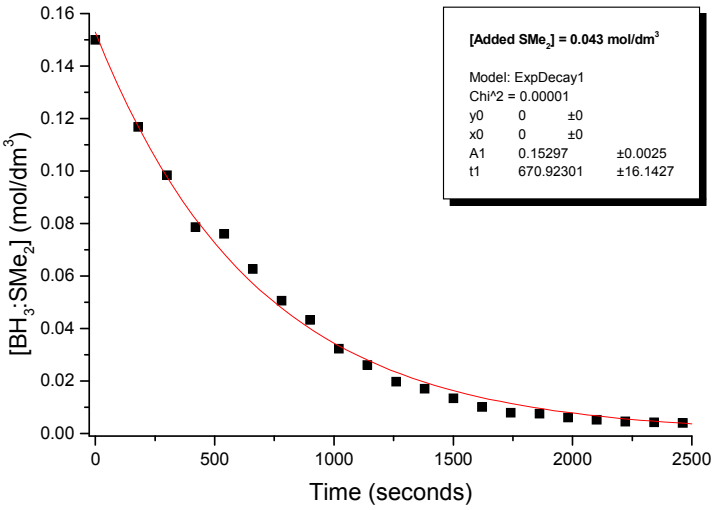

Figure 7.7 – Profile for the reduction of acrylonitrile (4.91 M) with borane dimethyl sulfide complex (0.15 M) with added dimethyl sulfide (0.043 M) in CH_2Cl_2 at 25.0 ^oC

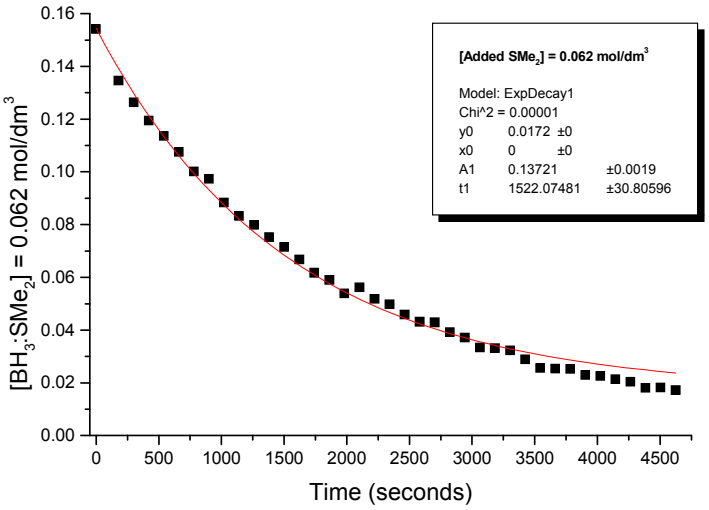

Figure 7.8 – Profile for the reduction of acrylonitrile (4.91 M) with borane dimethyl sulfide complex (0.15 M) with added dimethyl sulfide (0.062 M) in CH_2Cl_2 at 25.0 ^oC

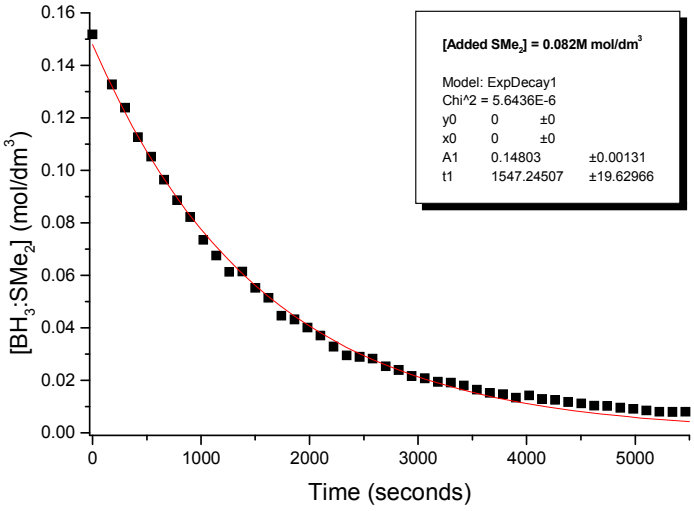

Figure 7.9 – Profile for the reduction of acrylonitrile (4.91 M) with borane dimethyl sulfide complex (0.15 M) with added dimethyl sulfide (0.087 M) in CH_2Cl_2 at 25.0 ^oC

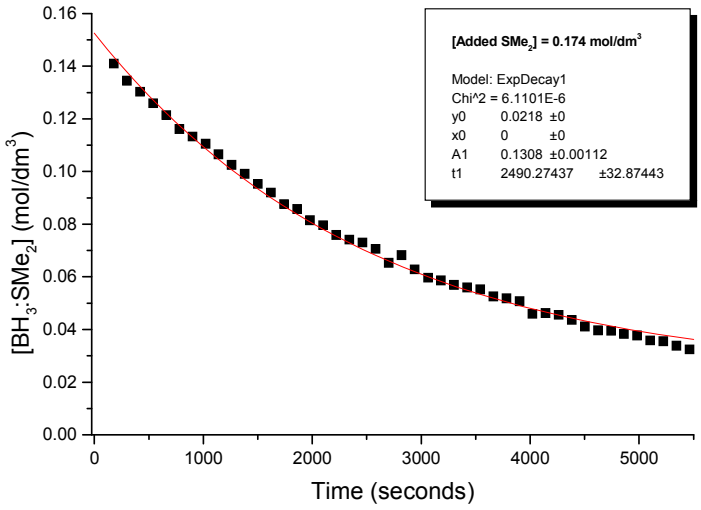

Figure 7.10 – Profile for the reduction of acrylonitrile (4.91 M) with borane dimethyl sulfide complex (0.15 M) with added dimethyl sulfide (0.174 M) in CH_2Cl_2 at 25.0 ^oC

7.1.3. Temperature Dependence

Data for the construction of **Table 4.1** in **Section 4.1.2.**

Table 7.3 - Temperature dependence of k_2 in the reduction of acrylonitrile (4.911 M) with borane dimethyl sulfide complex (0.1604 M) in CH_2Cl_2. Depletion of BH_3:SMe_2

Temp.(°C)	T^{-1} / 10^{-3} (K^{-1})	t_1 (seconds)	k_{obs} / 10^{-3} (s^{-1})	ln(k_2/T)
10.0	3.53	2150.19656 ± 38.44601	0.47 ± 0.01	-9.26
15.0	3.47	2125.83483 ± 35.61221	0.47 ± 0.01	-9.25
20.0	3.41	863.87082 ± 26.71432	1.16 ± 0.04	-8.35
25.0	3.35	648.23817 ± 17.29030	1.54 ± 0.04	-8.07
30.0	3.30	412.67170 ± 14.78003	2.42 ± 0.09	-7.61
	$\Delta H^{\neq}$ (kJ.mol^{-1})		58 ± 3	
	$\Delta S^{\neq}$ (J.K^{-1}.mol^{-1})		-71 ± 10	

The value of k_2 was obtained through the following equation: $k_2 = k_{obs}$/[Acrylonitrile]

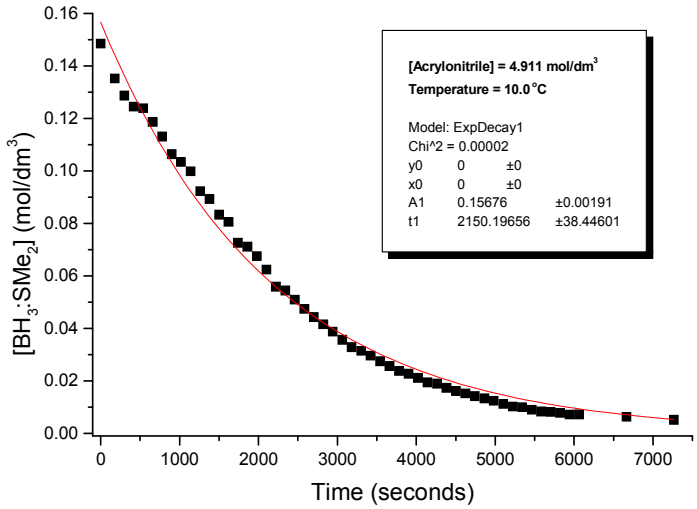

Figure 7.11 – Profile for the reduction of acrylonitrile (4.91 M) with borane dimethyl sulfide complex (0.16 M) in CH_2Cl_2 at 10.0 °C

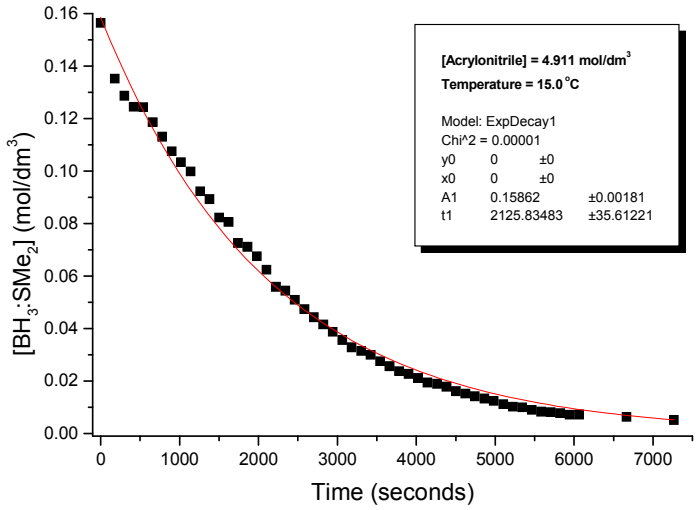

Figure 7.12 - Profile for the reduction of acrylonitrile (4.91 M) with borane dimethyl sulfide complex (0.16 M) in CH_2Cl_2 at 15.0 °C

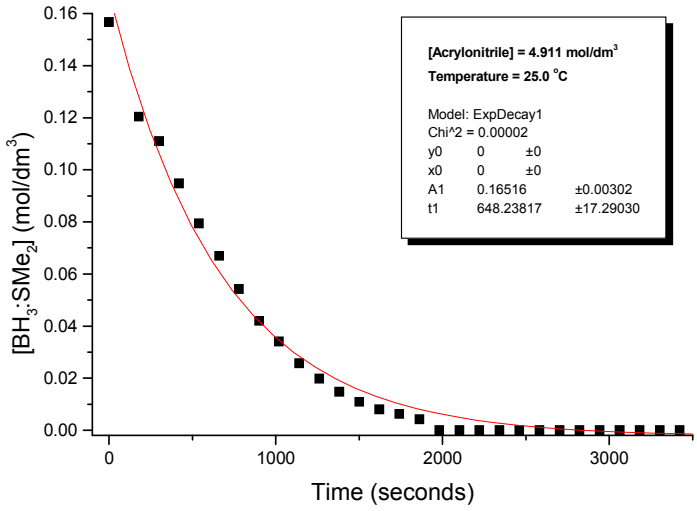

Figure 7.13 - Profile for the reduction of acrylonitrile (4.91 M) with borane dimethyl sulfide complex (0.16 M) in CH_2Cl_2 at 25.0 °C

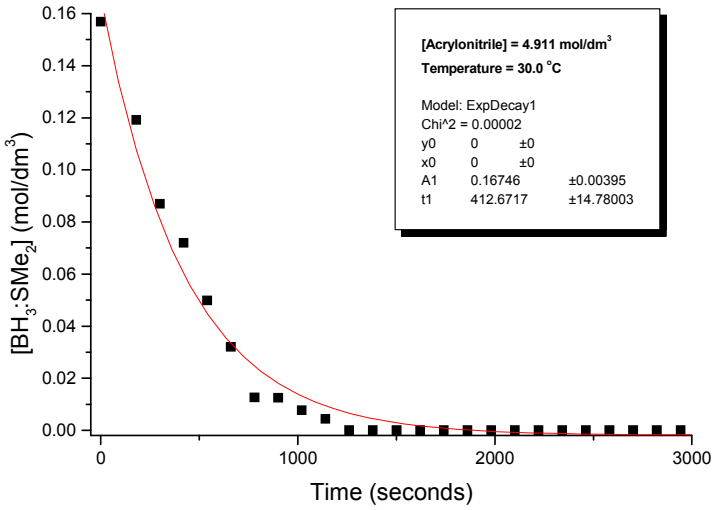

Figure 7.14 - Profile for the reduction of acrylonitrile (4.91 M) with borane dimethyl sulfide complex (0.16 M) in CH_2Cl_2 at 30.0 °C

7.2. Spectroscopic Data

The results for the integration of the ^1H signals in **Figure 7.15** were used to calculate the amount of excess dimethyl sulfide in the commerscial dichloromethane solution of borane dimethyl sulfide.

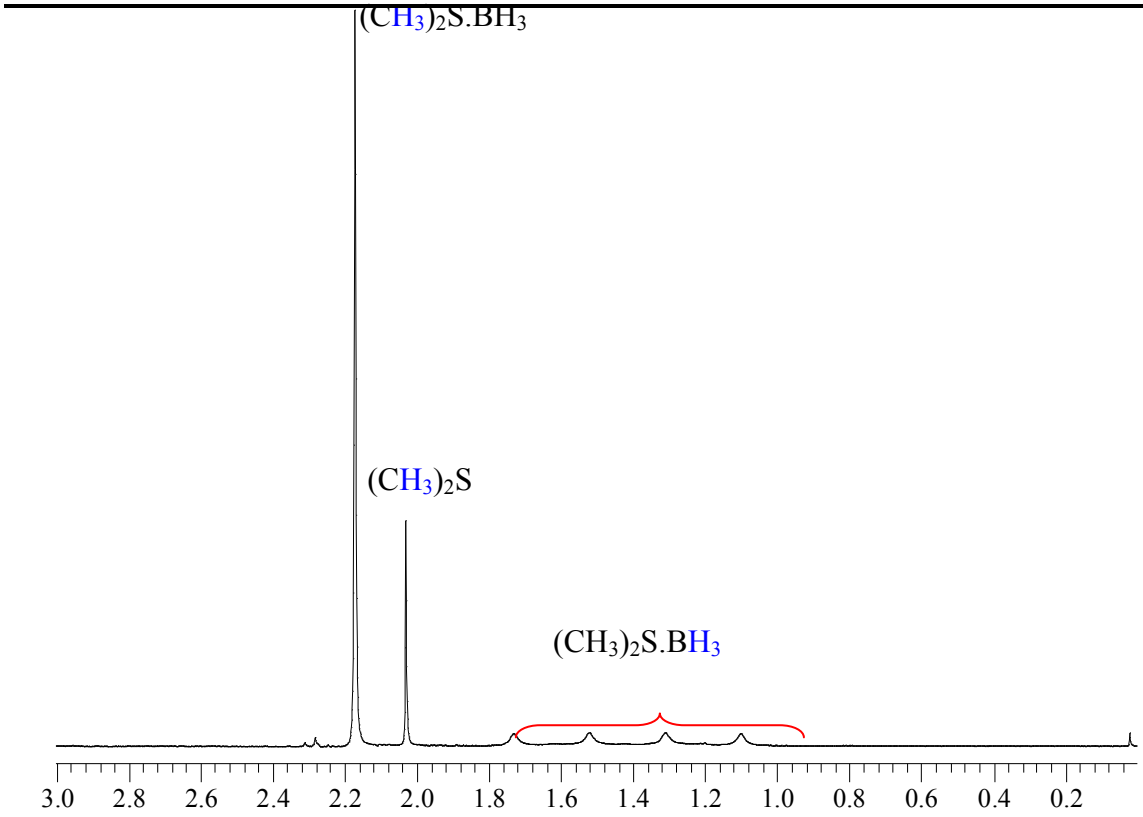

Figure 7.15 - Borane region of the ^{1}H NMR spectrum of $Me_2S.BH_3$ after addition of benzonitrile

Using benzonitrile as an example, the equilibrium constant was calculated from the equation below.

$$K = \frac{[Me_2S][C_6H_5C \equiv N.BH_3]}{[Me_2S.BH_3][C_6H_5C \equiv N]} = \frac{[Me_2S]^2}{[Me_2S.BH_3][C_6H_5C \equiv N]}$$

At the start of the investigation [$Me_2S.BH_3$] = (a) and [$C_6H_5C{\equiv}N$] = (b). As nitrile is titrated into the borane solution and its concentration defined as (x), then [$Me_2S.BH_3$] = (a-x) and [$C_6H_5C{\equiv}N$] = (b-x), such that K can be defined as follows.

$$K = \frac{(x)^2}{(a - x)(b - x)}$$

Table 7.4 - ^{1}H NMR integral and concentration data from the titration of propionitrile into a 0.295 M solution of $Me_2S.BH_3$ in CH_2Cl_2 at 25 ºC

[PrCN] (M)	Integral Area		Mole Fraction		Corrected Mole Fraction	
	$Me_2S.BH_3$	Me_2S	$Me_2S.BH_3$	Me_2S	$Me_2S.BH_3$	Me_2S
0.000	0.4415	0.0534	0.892	0.108	1.000	0.000
0.070	0.4380	0.0746	0.854	0.146	0.958	0.042
0.139	0.3949	0.0736	0.843	0.157	0.945	0.055
0.207	0.3806	0.0799	0.826	0.174	0.926	0.074
0.275	0.3854	0.0905	0.810	0.190	0.908	0.092
0.342	0.3596	0.0895	0.801	0.199	0.898	0.102
0.408	0.3611	0.0941	0.793	0.207	0.889	0.111
0.474	0.3826	0.1039	0.786	0.214	0.882	0.118
0.539	0.3803	0.1077	0.779	0.221	0.874	0.126
0.604	0.3548	0.1052	0.771	0.229	0.865	0.135
0.667	0.3466	0.1095	0.760	0.240	0.852	0.148
0.793	0.3402	0.1154	0.747	0.253	0.837	0.163
0.917	0.3550	0.1268	0.737	0.263	0.826	0.174
1.038	0.3287	0.1274	0.721	0.279	0.808	0.192
1.274	0.2957	0.1223	0.707	0.293	0.793	0.207

[PrCN] (M)	Moles (mmol)		Concentration (M)		$[Me_2S.BH_3][EtC\equiv N]$	$10^3 \times [Me_2S]^2$
	$Me_2S.BH_3$	Me_2S	$Me_2S.BH_3$	Me_2S		
0.000	0.295	0.000	0.295	0.000	0.000	0.000
0.070	0.281	0.012	0.281	0.012	0.016	0.153
0.139	0.276	0.016	0.276	0.016	0.034	0.260
0.207	0.269	0.021	0.269	0.021	0.050	0.457
0.275	0.263	0.027	0.263	0.027	0.065	0.712
0.342	0.258	0.029	0.258	0.029	0.081	0.870
0.408	0.255	0.032	0.255	0.032	0.096	1.01
0.474	0.251	0.034	0.251	0.034	0.111	1.14
0.539	0.248	0.036	0.248	0.036	0.125	1.29
0.604	0.244	0.038	0.244	0.038	0.138	1.46
0.667	0.239	0.042	0.239	0.042	0.150	1.73
0.793	0.233	0.045	0.233	0.045	0.174	2.06
0.917	0.228	0.048	0.228	0.048	0.198	2.30
1.038	0.221	0.053	0.221	0.053	0.218	2.76
1.274	0.213	0.056	0.213	0.056	0.259	3.08

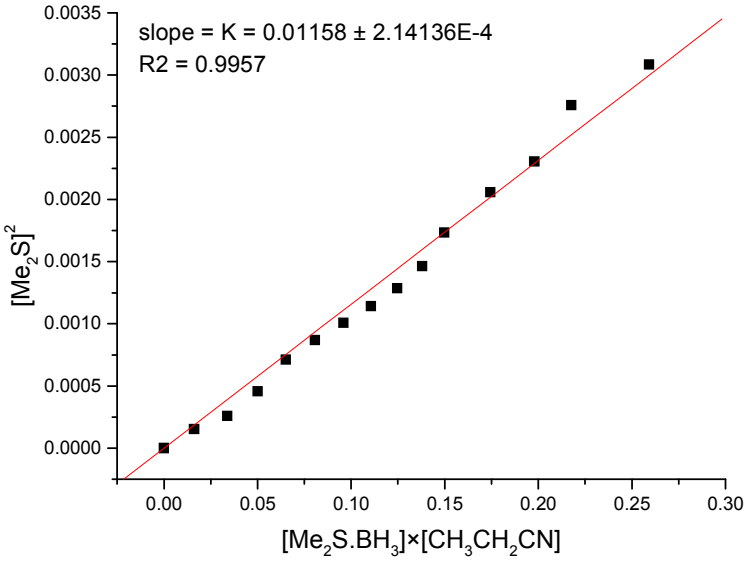

Figure 7.16 - Graph for determination of K from the titration of propionitrile into a 0.295 M solution of $Me_2S.BH_3$ in CH_2Cl_2 at 25 ºC

Table 7.5 - ^{1}H NMR integral and concentration data from the titration of benzonitrile into a 0.295 M solution of $Me_2S.BH_3$ in CH_2Cl_2 at 25 ºC

[PrCN] (M)	Integral Area		Mole Fraction		Corrected Mole Fraction	
	$Me_2S.BH_3$	Me_2S	$Me_2S.BH_3$	Me_2S	$Me_2S.BH_3$	Me_2S
0.000	0.4195	0.0545	0.885	0.115	1.000	0.0000
0.039	0.4166	0.0584	0.877	0.123	0.991	0.0090
0.078	0.4131	0.0587	0.876	0.124	0.989	0.0107
0.117	0.4072	0.0577	0.876	0.124	0.990	0.0103
0.155	0.4117	0.0613	0.870	0.130	0.983	0.0165
0.231	0.3959	0.0777	0.836	0.164	0.945	0.0555
0.304	0.3797	0.0797	0.827	0.173	0.934	0.0661
0.377	0.3782	0.0844	0.818	0.182	0.924	0.0762
0.448	0.3703	0.0880	0.808	0.192	0.913	0.0870
0.518	0.3665	0.0908	0.801	0.199	0.906	0.0944
0.586	0.3598	0.0935	0.794	0.206	0.897	0.1031
0.720	0.3502	0.1084	0.764	0.236	0.863	0.1372
0.848	0.2863	0.0919	0.757	0.243	0.855	0.1446
0.972	0.3007	0.0997	0.751	0.249	0.849	0.1514
1.092	0.2948	0.1044	0.738	0.262	0.834	0.1656
1.207	0.2904	0.1016	0.741	0.259	0.837	0.1629

[PrCN] (M)	Moles (mmol)		Concentration (M)		$[Me_2S.BH_3][EtC\equiv N]$	$10^4 \times [Me_2S]^2$
	$Me_2S.BH_3$	Me_2S	$Me_2S.BH_3$	Me_2S		
0.000	0.295	0.000	0.295	0.000	0.000	0.000
0.039	0.291	0.003	0.291	0.003	0.011	0.070
0.078	0.289	0.003	0.289	0.003	0.022	0.097
0.117	0.288	0.003	0.288	0.003	0.033	0.090
0.155	0.285	0.005	0.285	0.005	0.043	0.228
0.231	0.271	0.016	0.271	0.016	0.058	2.52
0.304	0.265	0.019	0.265	0.019	0.076	3.52
0.377	0.260	0.021	0.260	0.021	0.092	4.59
0.448	0.254	0.024	0.254	0.024	0.108	5.87
0.518	0.250	0.026	0.250	0.026	0.123	6.78
0.586	0.245	0.028	0.245	0.028	0.137	7.94
0.720	0.231	0.037	0.231	0.037	0.158	13.5
0.848	0.225	0.038	0.225	0.038	0.183	14.5
0.972	0.220	0.039	0.220	0.039	0.205	15.4
1.092	0.212	0.042	0.212	0.042	0.223	17.7
1.207	0.209	0.041	0.209	0.041	0.244	16.6

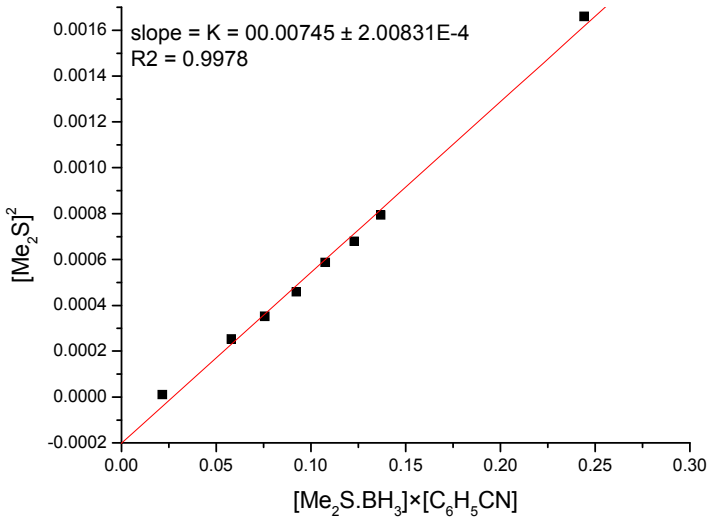

Figure 7.17 - Graph for determination of K from the titration of benzonitrile into a 0.295 M solution of $Me_2S.BH_3$ in CH_2Cl_2 at 25 ºC

7.3. Computational Data

Data used for the generation of **Table 4.2** in **Section 4.1.3** are detailed in **Table 7.6**.

Table 7.6 - B3LYP/6-31G* calculated energies (au) for HOMO and LUMO orbitals for BH_3, acrylonitrile, propionitrile, benzonitrile and HCN by borane.

Compound	I (eV)	A (eV)	η (eV)	χ^o (eV)	ΔN
BH_3	-1.78	-9.56	3.89	5.67	-
$H_2C{=}CH{-}C{\equiv}N$	-1.53	-7.87	3.17	4.70	0.059
$C_6H_5{-}C{\equiv}N$	-1.41	-7.26	2.93	4.34	0.069
$H_3C{-}CH_2{-}C{\equiv}N$	0.90	-8.75	4.83	3.93	0.098
$H{-}C{\equiv}N$	0.56	-9.77	5.17	4.61	0.100

Data used for the generation of **Figure 4.7** in **Section 4.1.3** are detailed in **Table 7.7** to **Table 7.8**.

Table 7.7 - B3LYP/6-31G* calculated energies (au) for stationary point in the reduction of acrylonitrile, propionitrile, benzonitrile and HCN by borane.

Compound	Acrylonitrile	Propionitrile	Benzonitrile	HCN
BH_3 + Nitrile	-197.443780	-198.678848	-351.104324	-120.035503
Pre-complex	-197.449616	-198.690938	-351.116919	-120.045766
Complex	-197.477330	-198.715438	-351.140290	-120.068911
Transition state	-197.436403	-198.674673	-351.100819	-120.030272
Product	-197.516707	-198.746440	-351.133537	-120.076990

Table 7.8 - B3LYP/6-31G* calculated relative energies (au) for stationary point in the reduction of acrylonitrile, propionitrile, benzonitrile and HCN by borane

Compound	ΔE (hartrees)			
	Acrylonitrile	Propionitrile	Benzonitrile	HCN
BH_3 + Nitrile	0.000	0.000	0.000	0.000
Pre-complex	-0.006	-0.012	-0.013	-0.010
Complex	-0.034	-0.037	-0.036	-0.033
Transition state	0.007	0.004	0.004	0.005
Product	-0.073	-0.068	-0.029	-0.041

Data used for the generation of **Table 4.4** and **Figure 4.8** in **Section 4.1.3** are detailed in **Table 7.9** to **Table 7.12**.

Table 7.9 - B3LYP/6-31G* calculated electrostatic charges for stationary point in the reduction of acrylonitrile by borane

Atom	Reactants	Pre-complex	Complex	Transition State	Product
B	0.305	0.090	-0.487	-0.235	0.032
H_A	-0.102	-0.069	0.015	0.032	0.097
H_B	-0.102	-0.067	0.019	0.003	-0.041
H_C	-0.102	-0.067	0.019	-0.009	-0.041
N	-0.401	-0.275	0.120	-0.274	-0.174
C_1	0.341	0.274	0.170	-0.361	0.083
C_2	-0.166	-0.111	-0.100	-0.196	-0.340
H	0.170	0.166	0.170	0.182	0.138
C_3	-0.311	-0.325	-0.320	0.443	-0.443
H_A	0.174	0.182	0.170	0.203	0.193
H_B	0.193	0.202	0.210	0.211	0.193

Table 7.10 - B3LYP/6-31G* calculated electrostatic charges for stationary point in the reduction of propionitrile by borane

Atom	Reactants	Pre-complex	Complex	Transition State	Product
B	0.305	0.102	-0.470	-0.221	-0.052
H_A	-0.102	-0.071	0.008	0.047	0.072
H_B	-0.103	-0.075	0.003	-0.014	-0.032
H_C	-0.103	-0.073	0.004	-0.007	-0.032
N	-0.406	-0.255	0.153	-0.267	-0.049
C_1	0.280	0.159	0.059	0.328	-0.034
C_2	-0.097	0.034	0.033	-0.092	0.095
H_A	0.115	0.093	0.104	0.113	0.050
H_B	0.115	0.093	0.104	0.113	0.050
C_3	-0.445	-0.417	-0.430	-0.413	-0.483
H_A	0.133	0.119	0.127	0.147	0.118
H_B	0.153	0.145	0.153	0.132	0.148
H_C	0.153	0.145	0.153	0.135	0.148

Table 7.11 - B3LYP/6-31G* calculated electrostatic charges for stationary point in the reduction of benzonitrile by borane

Atom	Reactants	Pre-complex	Complex	Transition State	Product
B	0.305	0.091	-0.514	-0.216	0.561
H_A	-0.102	-0.072	0.013	0.027	0.039
H_B	-0.103	-0.073	0.013	-0.006	-0.200
H_C	-0.103	-0.075	0.013	-0.007	-0.178
N	-0.372	-0.203	0.244	-0.250	-0.584
C_7	0.206	0.076	-0.067	0.270	0.241
C_1	0.130	0.250	0.279	0.141	0.156
C_6	-0.168	-0.214	-0.222	-0.183	-0.241
H	0.149	0.162	0.169	0.151	0.136
C_5	-0.102	-0.082	-0.079	-0.083	-0.060
H	0.119	0.125	0.128	0.122	0.112
C_4	-0.090	-0.101	-0.101	-0.102	-0.091
H	0.119	0.123	0.127	0.123	0.116
C_3	-0.102	-0.079	-0.078	-0.069	-0.100
H	0.123	0.124	0.129	0.129	0.115
C_2	-0.168	-0.218	-0.223	-0.223	-0.189
H	0.149	0.163	0.169	0.169	0.169

Table 7.12 - B3LYP/6-31G* calculated electrostatic charges for stationary point in the reduction of HCN by borane

Atom	Reactants	Pre-complex	Complex	Transition State	Product
B	0.305	0.115	-0.431	-0.174	0.578
H_A	-0.102	-0.076	0.007	0.043	0.028
H_B	-0.103	-0.076	0.007	-0.008	-0.166
H_C	-0.103	-0.076	0.007	-0.008	-0.186
N	-0.281	-0.139	0.249	-0.199	-0.562
C_1	0.046	-0.024	-0.154	0.140	0.257
H_1	0.235	0.275	0.315	0.207	0.051

8. Appendix C: Binding Studies

8.1. Spectroscopic Studies

The following section lists the data for the binding constant studies (**Section 4.3**), namely the change in resonance shift ($\delta^{11}B$) of the tributylborane peaks relative to the internal standard, $BH_3.PPh_3$. Change in shift ($\Delta^{11}B$) is defined by the following equation:

$$\Delta^{11}B = \Delta^{11}B_{max} - (\delta^{11}B_{[BBu_3]} - \delta^{11}B_{[BH_3.PPh_3]})$$

where $\Delta^{11}B_{max} = (\delta^{11}B_{[BBu_3]} - \delta^{11}B_{[BH_3.PPh_3]})$ when [Lewis Base] = 0 M. The inverse shift change ($1/\Delta^{11}B$) is defined in terms of shift change in Hz as shown below:

$$1/\Delta^{11}B_{Hz} = 1 \div (\Delta^{11}B_{ppm} \times 160.413 \text{ Hz})$$

where 160.413 Hz is the frequency of the ^{11}B channel in the spectrometer used for this investigation. The terms 'mixed chain' and 'linear chain' refer to B(*s*-butyl)(*n*-butyl)$_2$ and B(*n*-butyl)$_3$, respectively.

For the sake of simplicity only the complete data set (data for Benesi-Hilderbrand and van't Hoff plots) for the binding of DMF to tributylborane is shown in this section. For the other Lewis bases, only the variable temperature Benesi-Hilderbrand (slope and intercept) data (**Table 8.5** to **Table 8.13**) for determining the thermodynamic parameters (van't Hoff plot) will be shown. The corresponding spectroscopic data for construction of the Benesi-Hilderbrand plots is archived in the compact disc supplied with the text. The slope and intercept data from the van't Hoff plots are shown in summarised form in (**Table 8.14**).

Table 8.1 - ^{11}B NMR spectroscopic data for binding of DMF to tributylborane at 25.0 ºC

n_{DMF} (mmol)	[DMF]	1/[DMF]	δ_{BBu_3} (ppm)	$\delta_{BH_3.PPh_3}$ (ppm)	$\delta_{BH_3.PPh_3}$ (ppm)	Av. $\delta_{BH_3.PPh_3}$ (ppm)	$\Delta\delta_{11B}$ (Hz)	$1/\Delta^{11}B$
0	0		84.292	-39.600	-39.888	-39.744	0.000	-
0.1300	3.222	0.3104	24.907	-39.512	-39.839	-39.676	59.454	1.049E-04
0.2600	3.482	0.2872	24.283	-39.522	-39.839	-39.681	60.073	1.038E-04
0.3899	3.742	0.2672	23.258	-39.532	-39.829	-39.681	61.098	1.020E-04
0.3899	3.742	0.2672	22.322	-39.541	-39.865	-39.703	62.011	1.005E-04
0.5199	4.002	0.2499	21.834	-39.556	-39.834	-39.695	62.507	9.973E-05
0.6499	4.262	0.2346	20.673	-39.556	-39.849	-39.703	63.661	9.792E-05
0.7799	4.522	0.2212	20.624	-39.561	-39.844	-39.703	63.710	9.785E-05

Table 8.2- ^{11}B NMR spectroscopic data for binding of DMF to tributylborane at 50.0 °C

n_{DMF} (mmol)	[DMF]	1/[DMF]	δ_{BBu_3} (ppm)	$\delta_{BH_3.PPh_3}$ (ppm)	$\delta_{BH_3.PPh_3}$ (ppm)	Av. $\delta_{BH_3.PPh_3}$ (ppm)	$\Delta\delta_{11B}$ (Hz)	$1/\Delta^{11}B$
0	0		84.248	-39.551	-39.858	-39.705	0.000	-
0.1300	3.222	0.3104	45.346	-39.473	-39.795	-39.634	38.973	1.600E-04
0.2600	3.482	0.2872	44.380	-39.473	-39.790	-39.632	39.942	1.561E-04
0.3899	3.742	0.2672	42.780	-39.473	-39.805	-39.639	41.534	1.501E-04
0.3899	3.742	0.2672	41.205	-39.483	-39.810	-39.647	43.102	1.446E-04
0.5199	4.002	0.2499	40.405	-39.483	-39.805	-39.644	43.904	1.420E-04
0.6499	4.262	0.2346	39.642	-39.492	-39.824	-39.658	44.653	1.396E-04
0.7799	4.522	0.2212	38.375	-39.488	-39.819	-39.654	45.925	1.357E-04

Table 8.3 - ^{11}B NMR spectroscopic data for binding of DMF to tributylborane at 75.0 °C

n_{DMF} (mmol)	[DMF]	1/[DMF]	δ_{BBu_3} (ppm)	$\delta_{BH_3.PPh_3}$ (ppm)	$\delta_{BH_3.PPh_3}$ (ppm)	Av. $\delta_{BH_3.PPh_3}$ (ppm)	$\Delta\delta_{11B}$ (Hz)	$1/\Delta^{11}B$
0	0		84.195	-39.502	-39.810	-39.656	0.000	-
0.1300	3.222	0.3104	64.156	-39.336	-39.658	-39.497	20.198	3.086E-04
0.2600	3.482	0.2872	63.244	-39.424	-39.751	-39.588	21.020	2.966E-04
0.3899	3.742	0.2672	61.995	-39.429	-39.751	-39.590	22.266	2.800E-04
0.3899	3.742	0.2672	60.917	-39.351	-39.673	-39.512	23.422	2.662E-04
0.5199	4.002	0.2499	59.927	-39.429	-39.756	-39.593	24.332	2.562E-04
0.6499	4.262	0.2346	59.205	-39.439	-39.761	-39.600	25.046	2.489E-04
0.7799	4.522	0.2212	58.917	-39.366	-39.683	-39.525	25.410	2.453E-04

Table 8.4 - ^{11}B NMR spectroscopic data for binding of DMF to tributylborane at 100.0 ºC

n_{DMF} (mmol)	[DMF]	1/[DMF]	δ_{BBu_3} (ppm)	$\delta_{BH_3.PPh_3}$ (ppm)	$\delta_{BH_3.PPh_3}$ (ppm)	Av. $\delta_{BH_3.PPh_3}$ (ppm)	$\Delta\delta_{11_B}$ (Hz)	$1/\Delta^{11}B$
0	0		84.136	-39.458	-39.761	-39.610	0.000	
0.1300	3.222	0.3104	74.102	-39.228	-39.610	-39.419	10.225	6.097E-04
0.2600	3.482	0.2872	73.644	-39.371	-39.692	-39.532	10.571	5.897E-04
0.3899	3.742	0.2672	72.970	-39.292	-39.614	-39.453	11.323	5.506E-04
0.3899	3.742	0.2672	72.209	-39.302	-39.614	-39.458	12.079	5.161E-04
0.5199	4.002	0.2499	71.775	-39.302	-39.619	-39.461	12.511	4.983E-04
0.6499	4.262	0.2346	71.263	-39.302	-39.624	-39.463	13.020	4.788E-04
0.7799	4.522	0.2212	71.009	-39.307	-39.629	-39.468	13.269	4.698E-04

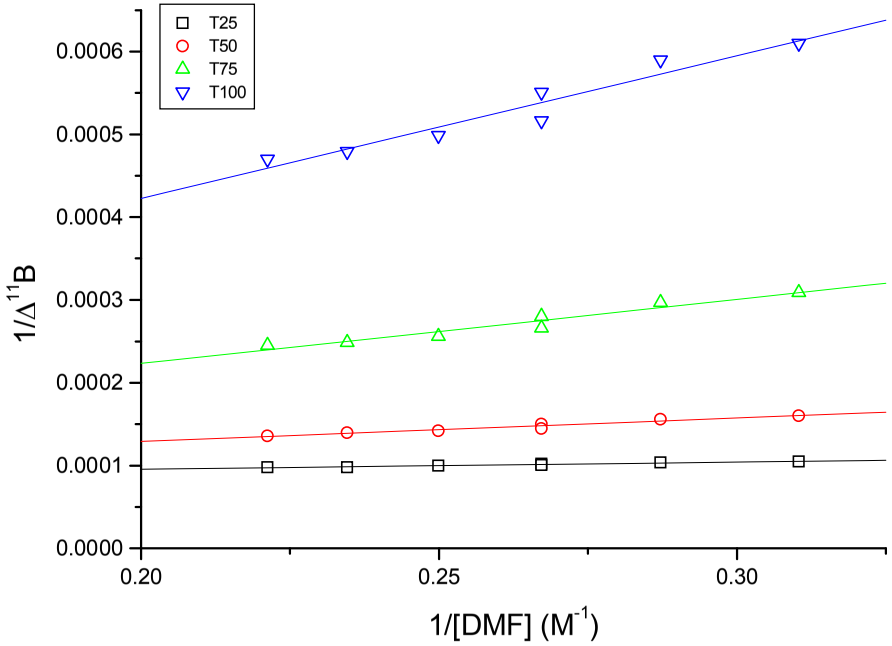

Figure 8.1 - Benesi-Hilderbrand plot for the determination of the binding constants (K_{BIND}) of DMF to tributylborane in toluene

Table 8.5 - Summary of thermodynamic data for the binding of DMF to tributylborane

T (K)	1/T	Slope	Std Dev	Intercept	Std Dev	K_{BIND}	Error	lnK	$\Delta\delta_{^{11}B}$ (ppm)	Error
298.15	3.35E-03	1.07E-04	3.41E-06	7.28E-05	8.43453E	9335.586	2.98E+02	9.14	85.65803	2.731
323.15	3.09E-03	2.84E-04	7.81E-06	7.24E-05	1.93E-06	3523.484	9.70E+01	8.17	86.14762	2.371
348.15	2.87E-03	7.60E-04	2.28E-05	7.21E-05	5.62E-06	1315.208	3.94E+01	7.18	86.44795	2.589
373.15	2.68E-03	1.74E-03	5.45E-05	7.28E-05	1.35E-05	574.713	1.80E+01	6.35	85.65885	2.681

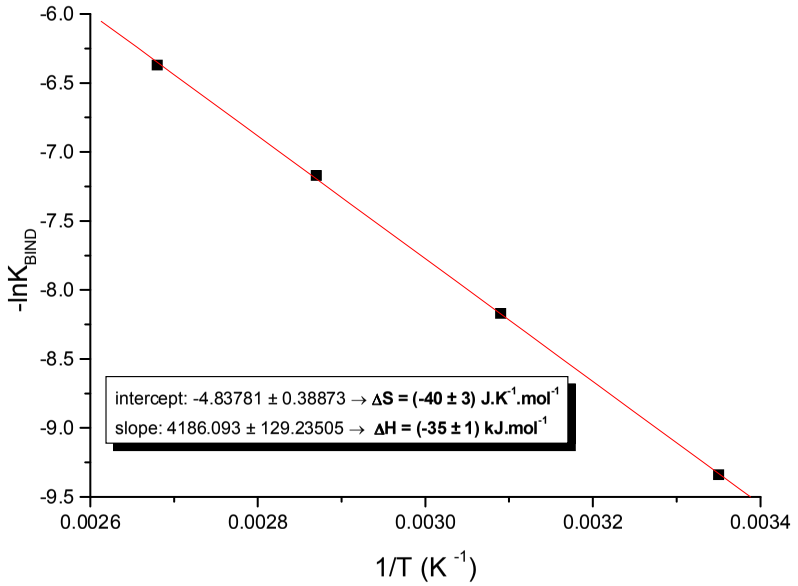

Figure 8.2 - van't Hoff plot for the determination of thermodynamic parameters (ΔH_{BIND} and ΔS_{BIND}) for the binding of DMF to tributylborane in toluene

Table 8.6 - Summary of thermodynamic data for the binding of DMSO to tributylborane

T (K)	1/T	Slope	Std Dev	Intercept	Std. Dev.	K_{BIND}	Error	lnK	$\Delta\delta_{^{11}B}$ (ppm)	Error
298.15	3.35E-03	1.62E-04	1.25E-05	7.94E-05	3.27E-06	4.90E-01	3.77E-02	-0.71	78.517	6.039
323.15	3.09E-03	4.68E-04	2.40E-05	7.80E-05	6.40E-06	1.67E-01	8.55E-03	-1.79	79.871	4.095
348.15	2.87E-03	1.20E-03	8.25E-05	8.67E-05	2.18E-05	7.22E-02	4.97E-03	-2.63	71.904	4.943
356.15	2.81E-03	1.57E-03	4.56E-05	8.99E-05	1.13E-05	5.72E-02	1.66E-03	-2.86	69.362	2.014
365.15	2.74E-03	4.27E-03	1.68E-04	1.26E-04	4.19E-05	2.94E-02	1.16E-03	-3.53	49.574	1.953
373.15	2.68E-03	2.71E-03	9.11E-05	1.02E-04	2.27E-05	3.76E-02	1.26E-03	-3.28	61.155	2.055

Table 8.7 - Summary of thermodynamic data for the binding of HMPA to tributylborane

T (K)	1/T	Slope	Std Dev	Intercept	Std Dev	K_{BIND}	Error	lnK	$\Delta\delta_{^{11}B}$ (ppm)	Error
298.15	3.35E-03	3.49E-06	7.01E-07	7.90E-05	5.44E-07	2.87E+05	5.77E+04	12.57	78.87968	15.86036
323.15	3.09E-03	3.00E-05	1.99E-06	7.85E-05	2.32E-06	3.34E+04	2.21E+03	10.41	79.42115	5.266753
348.15	2.87E-03	1.43E-04	8.48E-06	7.85E-05	2.32E-06	6.98E+03	4.14E+02	8.85	79.42115	4.703632
373.15	2.68E-03	5.65E-04	3.64E-05	7.68E-05	9.99E-06	1.77E+03	1.14E+02	7.48	81.12199	5.223391

Table 8.8 - Summary of thermodynamic data for the binding of HMPT to tributylborane

T (K)	1/T	Slope	Std Dev	Intercept	Std. Dev.	K_{BIND}	Error	lnK	$\Delta\delta_{^{11}B}$ (ppm)	Error
298.15	3.35E-03	-4.83E-07	4.13E-07	7.13E-05	1.30E-07	-	1.26E+02		87.384	-74.699
310.65	3.22E-03	6.25E-06	2.79E-06	7.12E-05	8.81E-07	1.14E+01	5.08E+00	2.43	87.513	39.028
323.15	3.09E-03	2.61E-05	7.35E-06	6.94E-05	2.32E-06	2.66E+00	7.49E-01	0.98	89.840	25.315
348.15	2.87E-03	1.02E-04	1.03E-05	6.92E-05	3.34E-06	6.77E-01	6.81E-02	-0.39	90.106	9.058
373.15	2.68E-03	1.11E-04	8.65E-06	6.96E-05	2.81E-06	6.28E-01	4.90E-02	-0.46	89.533	6.985
373.15	2.68E-03	3.61E-04	2.52E-05	7.87E-05	8.19E-06	2.18E-01	1.52E-02	-1.52	79.179	5.523

Table 8.9 - Summary of thermodynamic data for the binding of $(MeO)_3P$ to tributylborane

T (K)	1/T	Slope	Std Dev	Intercept	Std. Dev.	K_{BIND}	Error	lnK	$\Delta\delta_{^{11}B}$ (ppm)	Error
298.15	3.35E-03	4.68E-06	2.75E-08	6.41E-05	7.11E-09	1.37E+01	8.06E-02	2.62	97.237	0.572
323.15	3.09E-03	3.57E-05	2.79E-06	6.52E-05	7.22E-07	1.83E+00	1.43E-01	0.60	95.660	7.495
348.15	2.87E-03	1.58E-04	8.72E-06	6.72E-05	2.25E-06	4.25E-01	2.35E-02	-0.86	92.823	5.125
373.15	2.68E-03	5.32E-04	1.72E-05	6.79E-05	4.47E-06	1.27E-01	4.13E-03	-2.06	91.865	2.977

Table 8.10 - Summary of thermodynamic data for the binding of $(MeO)_3PO$ to tributylborane

T (K)	1/T	Slope	Std Dev	Intercept	Std. Dev.	K_{BIND}	Error	lnK	$\Delta\delta_{11}{}_B$ (ppm)	Error
298.15	3.35E-03	1.04E-03	1.85E-04	6.18E-05	5.84E-05	5.94E-02	1.06E-02	-2.82	100.864	17.939
310.65	3.22E-03	1.58E-03	1.61E-04	7.37E-05	4.61E-05	4.66E-02	4.75E-03	-3.07	84.580	8.614
323.15	3.09E-03	3.11E-03	2.27E-04	5.51E-05	6.52E-05	1.77E-02	1.30E-03	-4.03	113.193	8.278
348.15	2.87E-03	1.19E-02	4.60E-04	5.03E-05	1.32E-04	4.24E-03	1.64E-04	-5.46	123.814	4.797

Table 8.11 - Summary of thermodynamic data for the binding of Pr_3N to tributylborane

T (K)	1/T	Slope	Std Dev	Intercept	Std. Dev.	K_{BIND}	Error	lnK	$\Delta\delta_{11}{}_B$ (ppm)	Error
298.15	3.35E-03	2.05E-03	7.90E-05	1.02E-05	2.07E-05	4.97E-03	1.91E-04	-5.30	612.092	2.36E+01
298.15	3.35E-03	1.60E-03	7.67E-05	2.53E-06	1.92E-05	1.58E-03	7.60E-05	-6.45	2459.291	1.18E+02
310.65	3.22E-03	1.77E-03	5.79E-05	1.08E-05	1.45E-05	6.09E-03	1.99E-04	-5.10	578.779	1.89E+01
323.15	3.09E-03	2.26E-03	1.05E-04	3.49E-05	2.68E-05	1.55E-02	7.18E-04	-4.17	178.398	8.28E+00
348.15	2.87E-03	3.57E-03	2.88E-04	2.88E-04	7.82E-05	8.08E-02	6.52E-03	-2.52	21.618	1.75E+00
373.15	2.68E-03					#DIV/0!	#DIV/0!	#DIV/0!	#DIV/0!	#DIV/0!

Table 8.12 - Summary of thermodynamic data for the binding of Bu_3N to tributylborane

T (K)	1/T	Slope	Std Dev	Intercept	Std. Dev.	K_{BIND}	Error	lnK	$\Delta\delta_{11}{}_B$ (ppm)	Error
298.15	3.35E-03	9.85E-04	5.37E-05	6.87E-04	1.47E-05	6.98E-01	3.80E-02	-0.36	9.072	0.494
310.65	3.22E-03	9.51E-04	1.15E-04	7.22E-04	3.18E-05	7.60E-01	9.20E-02	-0.28	8.629	1.045
323.15	3.09E-03	1.03E-03	9.94E-04	9.03E-04	2.64E-04	8.77E-01	8.46E-01	-0.13	6.902	6.662

Table 8.13 - Summary of thermodynamic data for the binding of Bu_3P to tributylborane

T (K)	1/T	Slope	Std Dev	Intercept	Std. Dev.	K_{BIND}	Error	lnK	$\Delta\delta_{11B}$ (ppm)	Error
298.15	3.35E-03	-1.81E-07	7.24E-07	6.41E-05	2.11E-07	~	~	~	~	
310.65	3.22E-03	7.12E-07	1.33E-07	6.42E-05	3.69E-08	9.02E+01	1.69E+01	4.50	97.104	18.160
323.15	3.09E-03	3.07E-06	4.12E-07	6.44E-05	1.16E-07	2.10E+01	2.81E+00	3.04	96.819	12.995
335.65	2.98E-03	1.03E-05	1.02E-06	6.45E-05	2.72E-07	6.24E+00	6.15E-01	1.83	96.673	9.536
348.15	2.87E-03	2.39E-05	2.62E-06	6.45E-05	7.47E-07	2.70E+00	2.97E-01	0.99	96.700	10.623
360.65	2.77E-03	4.88E-05	4.53E-06	6.47E-05	1.29E-06	1.32E+00	1.23E-01	0.28	96.383	8.947
373.15	2.68E-03	9.76E-05	7.65E-06	6.50E-05	2.18E-06	6.66E-01	5.22E-02	-0.41	95.878	7.514

Table 8.14 - Data from van't Hoff plots for the binding of selected Lewis bases to tributylborane

Lewis Base	Intercept	Std. Dev.	Slope	Std. Dev.	ΔS_{BIND} (J/K.mol)	ΔH_{BIND} (kJ/mol)
DMF	-4.83781	0.38873	4186.093	129.2351	-40 ± 3	-35 ± 1
DMSO	-14.6201	0.3216	4157.382	109.6704	-122 ± 3	-35 ± 1
HMPA	-12.8518	0.64004	7566.083	212.7857	-107 ± 5	-63 ± 2
HMPT	-20.6593	2.06057	7094.207	693.2831	-172 ± 17	-59 ± 6
MeO3P	-20.831	0.74079	6974.487	246.2824	-173 ± 6	-58 ± 2
MeO3PO	-21.8549	2.33744	5749.353	744.9976	-182 ± 19	-48 ± -6
NPr3	12.39754	1.8069	-5657.23	600.7193	103 ± 15	47 ± 5
NBu3	2.59179	0.50079	-884.615	155.4405	22 ± 4	7 ± 1
PBu3	-23.9398	0.2691	8874.252	95.18259	-205 ± 12	-75 ± 4

9. Appendix D: Computational Studies

Primary data for the generation of χ^o, η and ΔN data in **Table 4.12** in **Section 4.42** are detailed **Table 9.1**. Bond length and angle data for the generation of tetrahedral character values in **Table 4.13** of **Section 4.4.3** are described in **Table 9.1**. **Figure 9.1** indicates the allocation of atom labels in the Lewis base-BMe_3 adducts for the description of bond angles.

Table 9.1 - B3LYP/6-31G*-calculated energy levels for free molecules

Lewis Base	Total energy (au)	E_{HOMO} (eV)		E_{LUMO} (eV)	
		Database	Calculated	Database	Calculated
DMF	-248.511	-	-6.57	-	1.01
DMSO	-553.108	-6.05	-4.24	1.16	-0.45
HMPA	n.d.*	-5.78	-	1.82	-
HMPT	n.d.*	-5.25	-	1.45	-
Me_3PO	-536.351	-6.87	-6.95	1.70	1.74
$(MeO)_3P$	-686.776	-6.31	-6.38	1.04	1.21
$(MeO)_3PO$	-762.035	-7.73	-7.49	1.57	1.31
NMe_3	-174.472	-	2.35	-	-5.56
NBu_3	n.d.*	-5.56	-	2.34	-
PMe_3	-461.096	-	1.87	-	-5.88
PBu_3	n.d.8	-5.86	-	1.58	-
Tetramethylthiourea	-546.617	-5.58	-5.39	-0.18	0.38
Tetramethylurea	-225.255	-6.72	-10.55	1.69	6.64
BH_3	-26.612	-9.56	-	-1.78	-
BMe_3	-144.608	-7.99	-7.97	-0.16	-0.16
BBu_3	-498.418		-7.26	-	-0.29

* n.d. = not determined, calculation did not converge

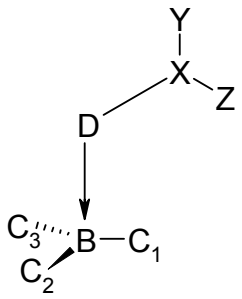

D = atom donating lone pair in Lewis base

Figure 9.1 - Representative labelling of HF/6-31G*-optimised adducts of selected Lewis bases and BMe_3

Table 9.2 - Data for HF/6-31G*-optimised structures of adducts of selected Lewis bases and BMe_3

Lewis Base	$L_{D\rightarrow A}$ (Å)	Bond Angles (°)♣					
		$\angle C_3BC_2$	$\angle C_2BC_1$	$\angle C_1BC_3$	$\angle DBC_1$	$\angle DBC_2$	$\angle DBC_3$
DMF	1.834	115.93	116.15	115.92	99.73	102.67	102.67
DMSO	1.675	113.03	113.03	112.45	101.67	107.91	107.92
HMPA	1.861	115.99	115.93	115.79	99.64	102.25	103.62
HMPT	1.620	106.48	106.83	106.54	112.4	112.31	111.87
Me_3PO	1.818	115.69	115.55	115.25	100.28	104.4	102.59
$(MeO)_3P$	1.601	109.74	109.8	108.79	111.49	109.68	107.28
$(MeO)_3PO$	1.936	117.04	117.07	117.03	99.98	99.99	100.05
NBu_3	1.758	111.96	108.98	107.52	109.67	108.18	110.51
PBu_3	1.581	107.26	108.7	106.63	109.91	112	112.13
Tetramethylthiourea	1.958	110.76	114.44	110.9	110.16	99.62	105.31
Tetramethylurea	1.833	116.86	115.2	114.98	98.55	104.04	103.81

♣ Atom labels described in Error! Reference source not found. above

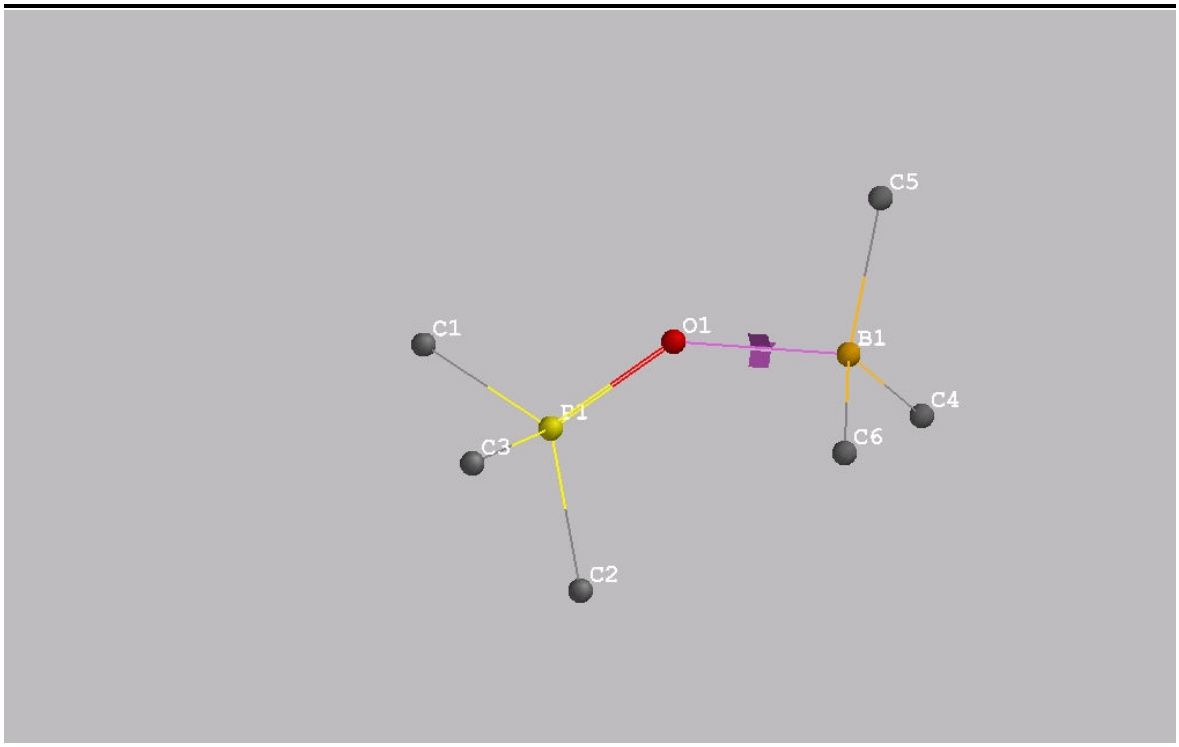

Figure 9.2 - HF/6-31G*-optimised adduct of Me_3PO and BMe_3 for the determination of energetics at the B3LYP/6-31G* level of theory

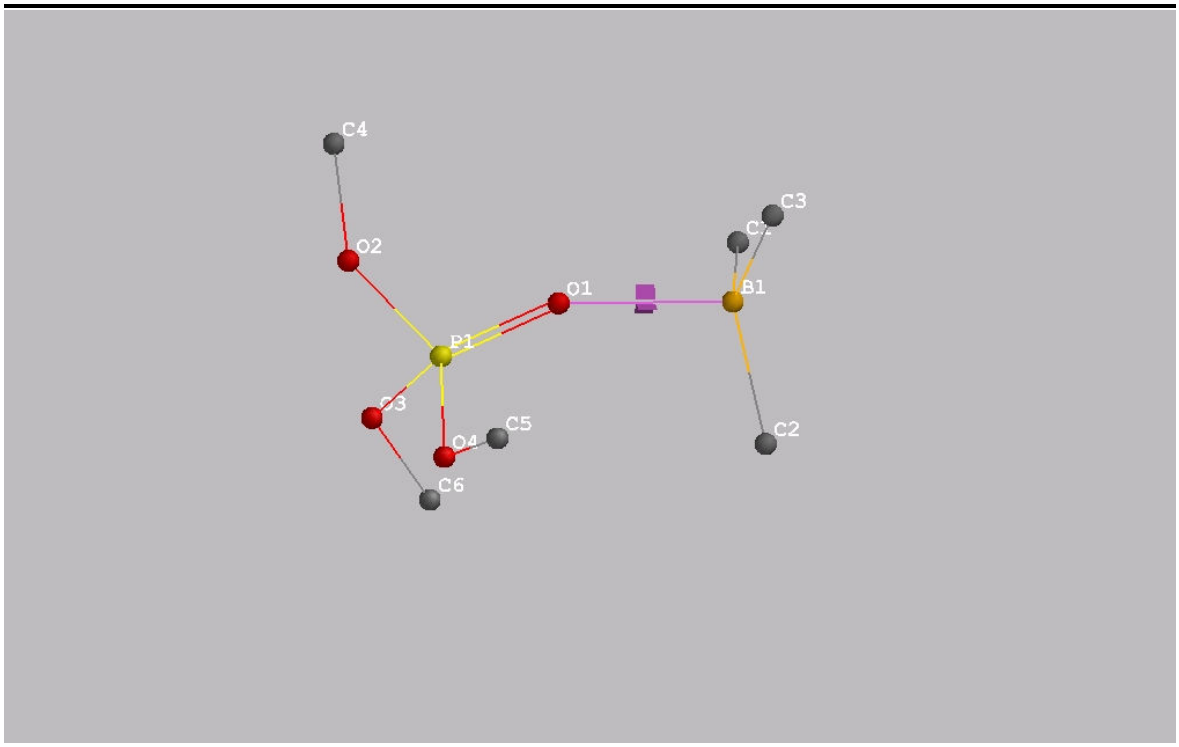

Figure 9.3 - HF/6-31G*-optimised adduct of $(MeO)_3PO$ and BMe_3 for the determination of energetics at the B3LYP/6-31G* level of theory

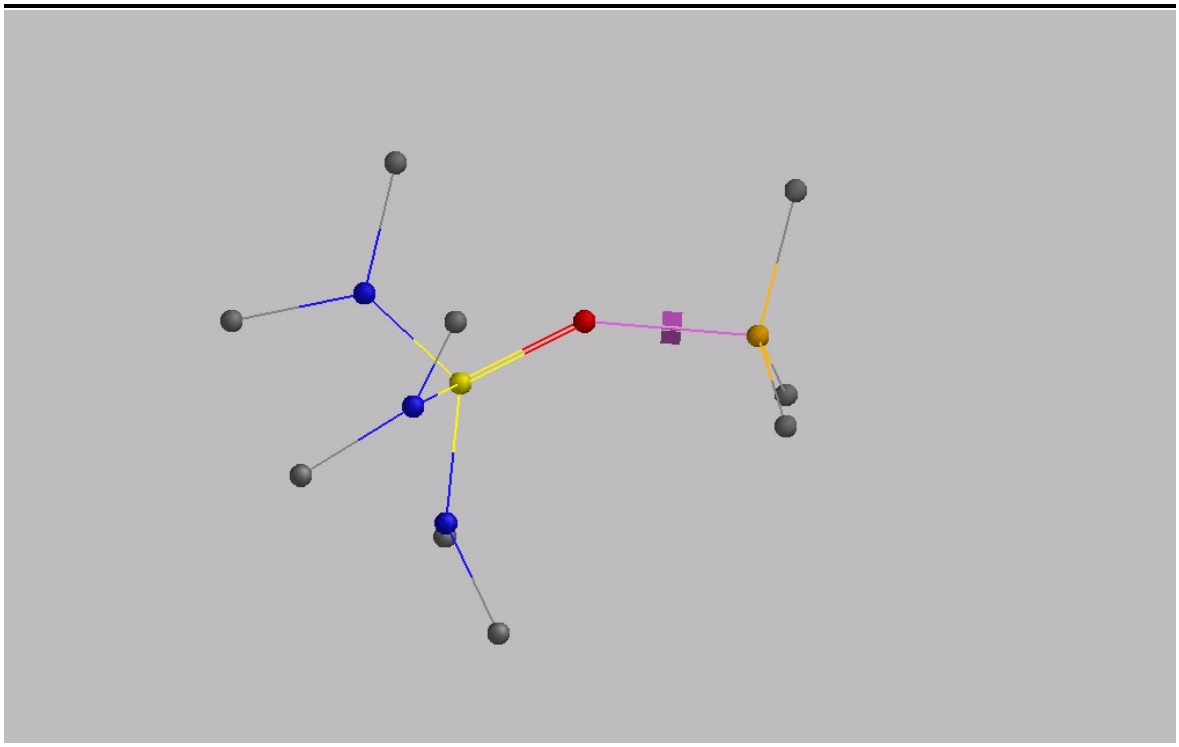

Figure 9.4 - HF/6-31G*-optimised adduct of HMPA and BMe_3 for the determination of energetics at the B3LYP/6-31G* level of theory

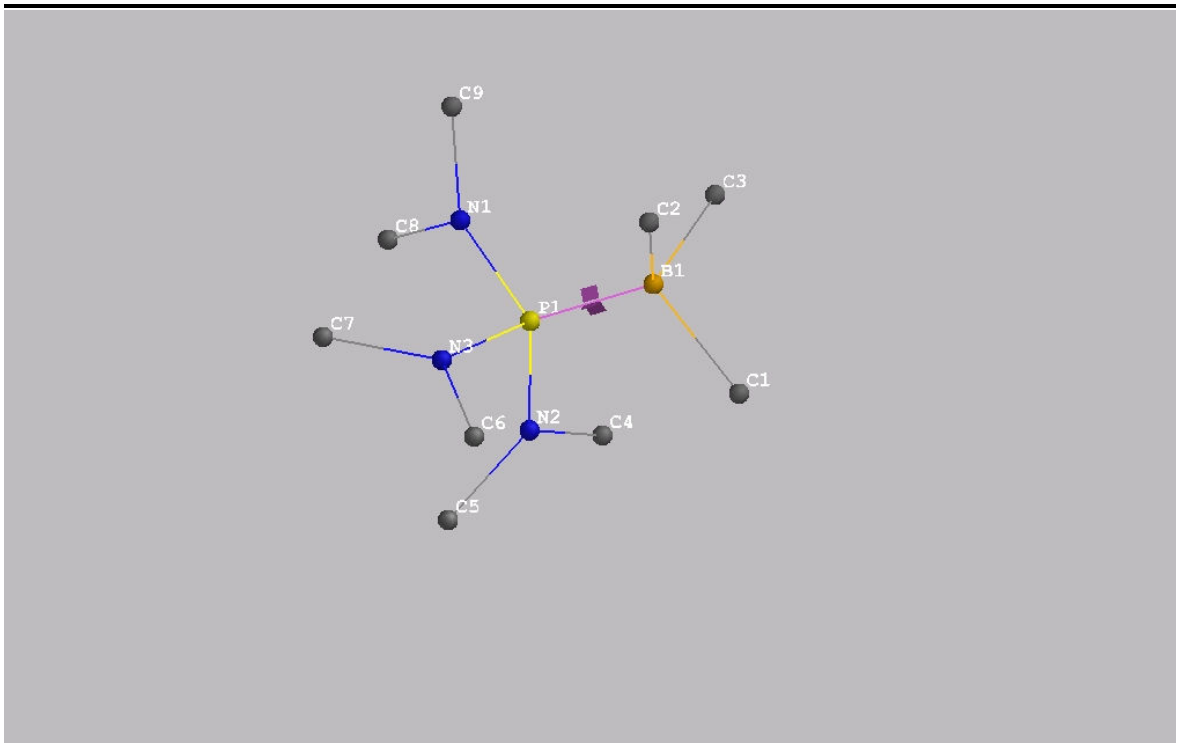

Figure 9.5 - HF/6-31G*-optimised adduct of HMPT and BMe_3 for the determination of energetics at the B3LYP/6-31G* level of theory

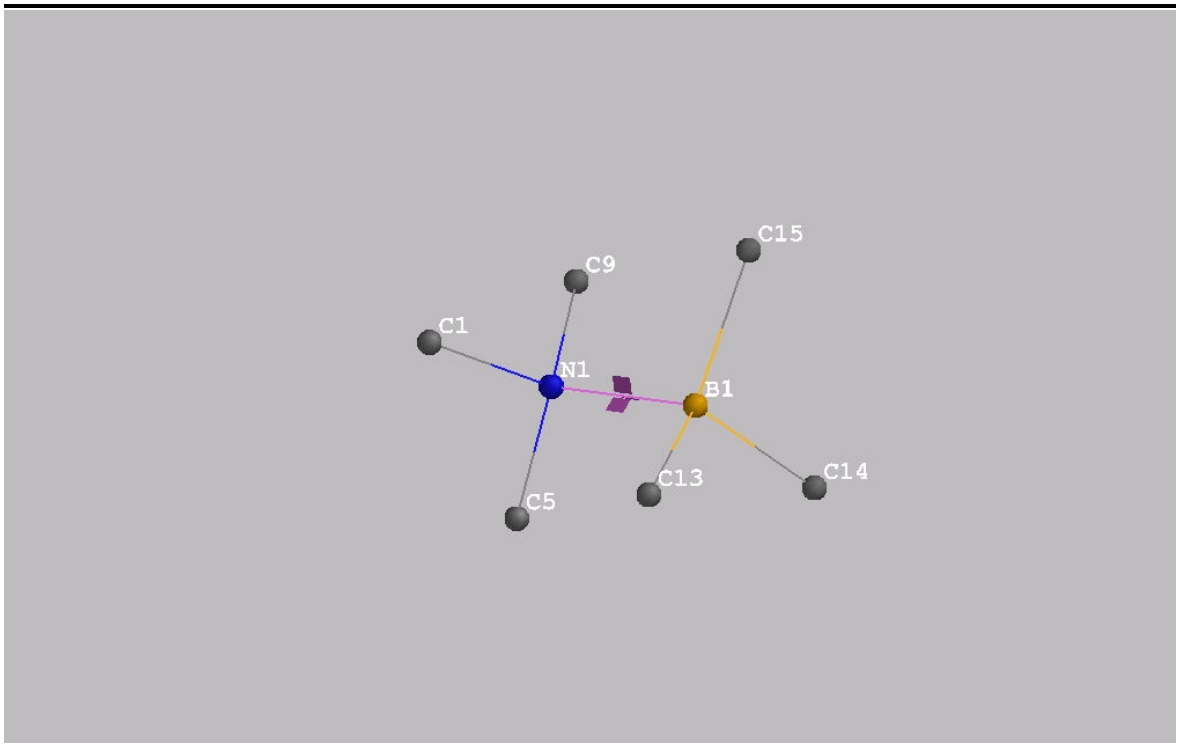

Figure 9.6 - HF/6-31G*-optimised adduct of NMe_3 and BMe_3 for the determination of energetics at the B3LYP/6-31G* level of theory

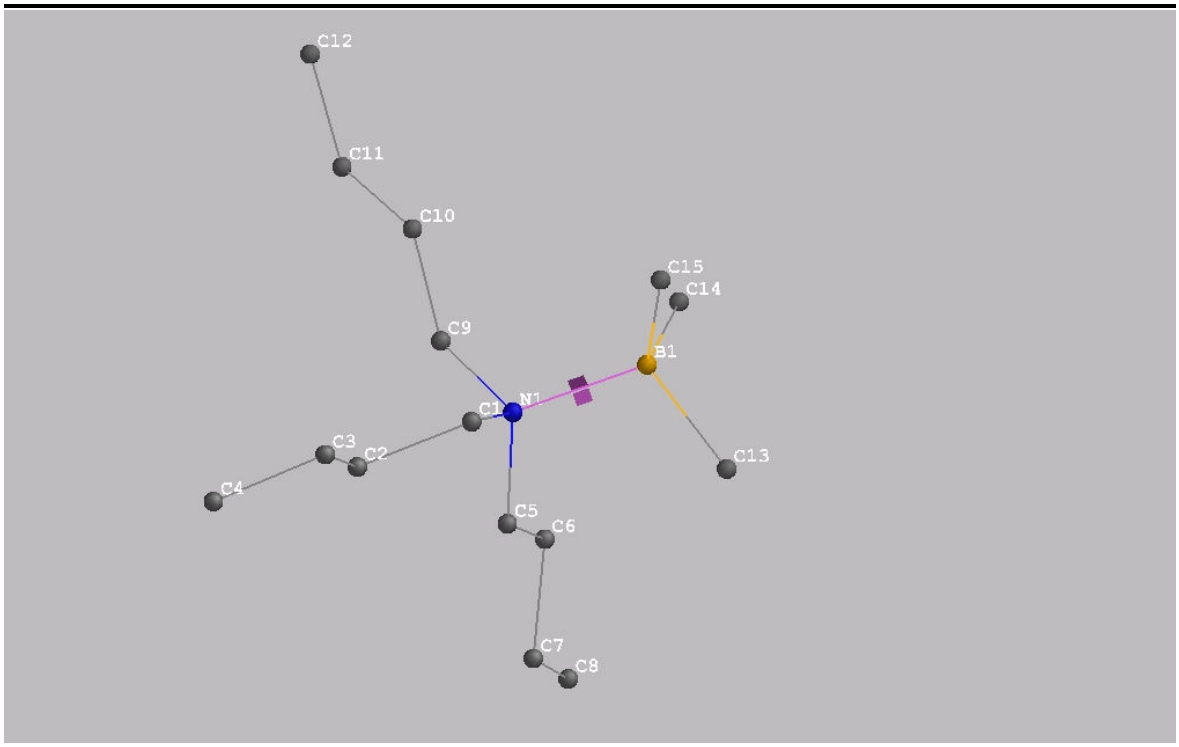

Figure 9.7 - HF/6-31G*-optimised adduct of NBu_3 and BMe_3 for the determination of energetics at the B3LYP/6-31G* level of theory

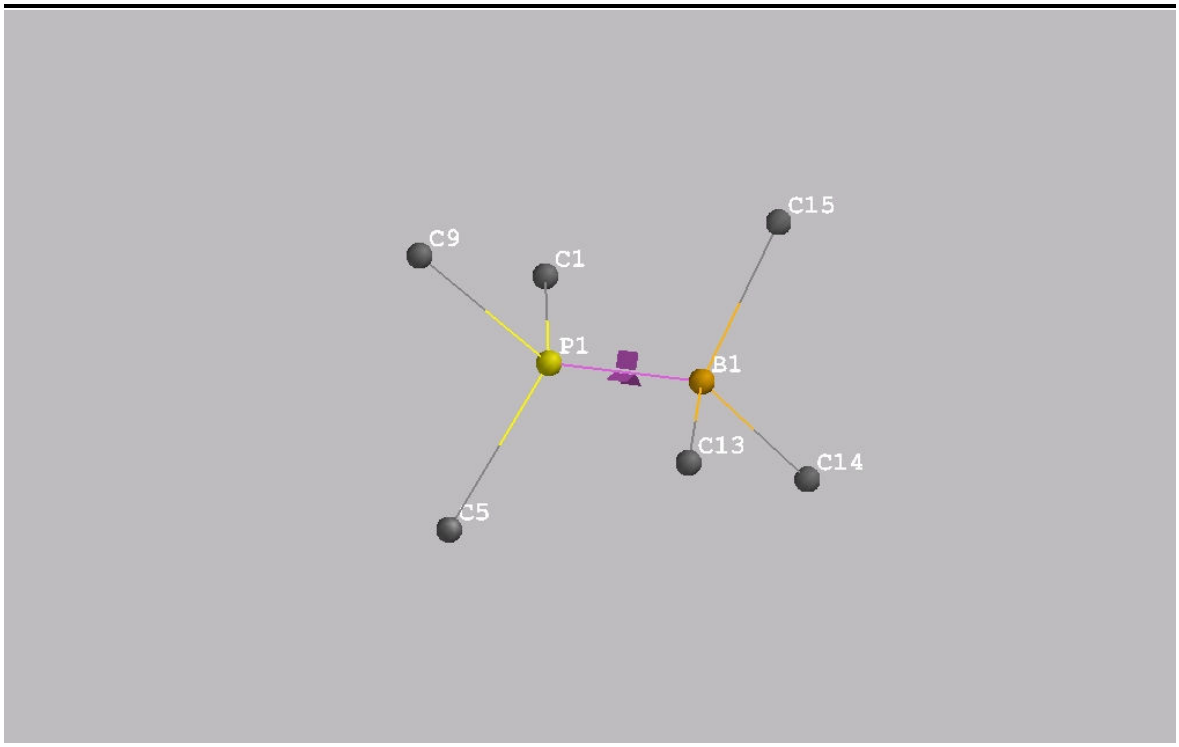

Figure 9.8 - HF/6-31G*-optimised adduct of PMe_3 and BMe_3 for the determination of energetics at the B3LYP/6-31G* level of theory

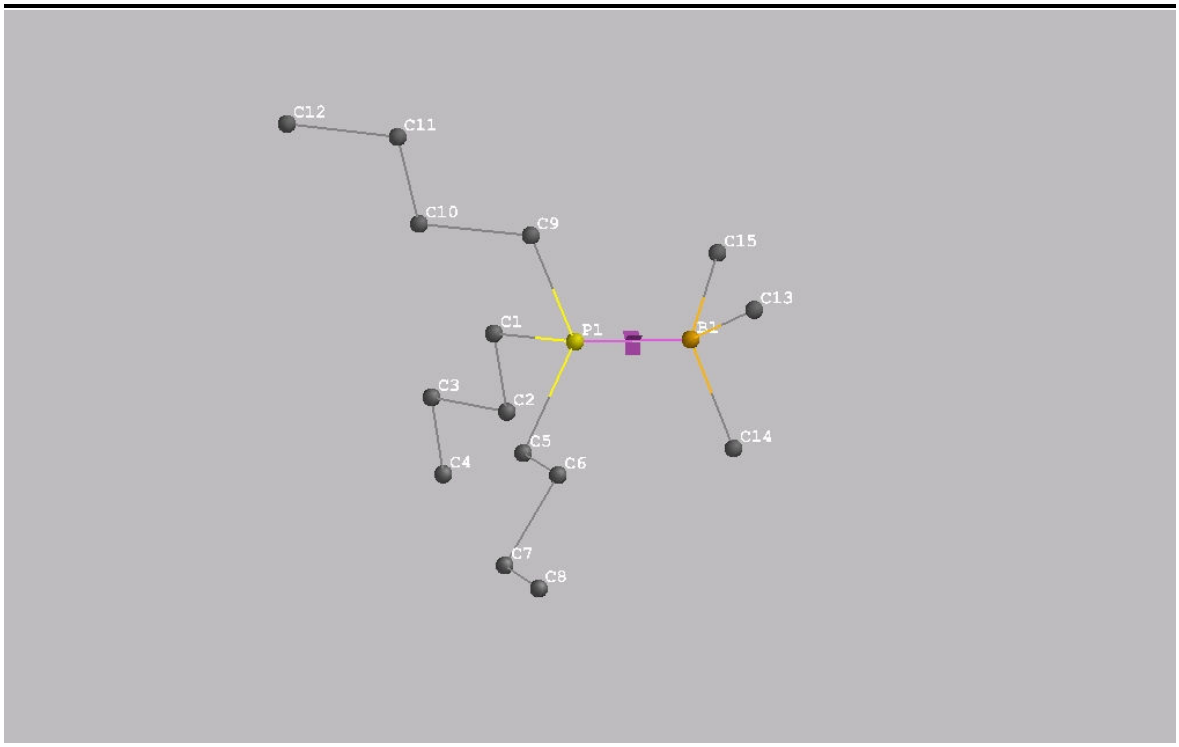

Figure 9.9 - HF/6-31G*-optimised adduct of PBu_3 and BMe_3 for the determination of energetics at the B3LYP/6-31G* level of theory

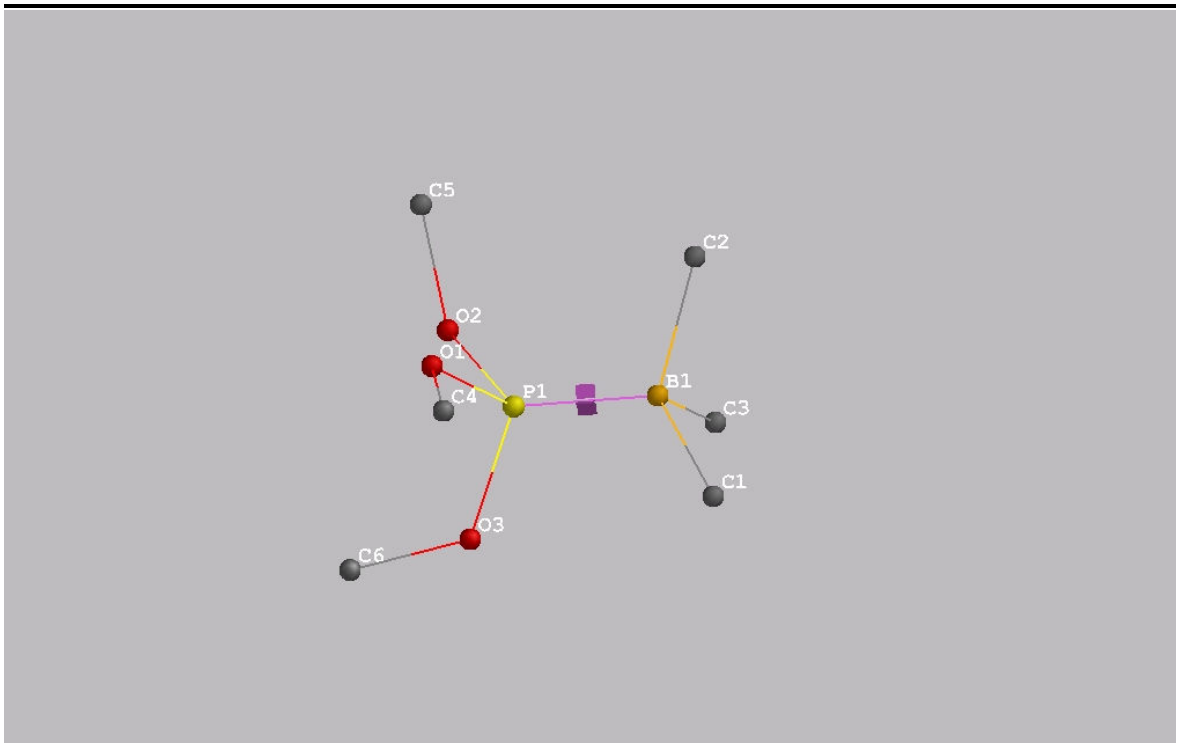

Figure 9.10 - HF/6-31G*-optimised adduct of $POMe_3$ and BMe_3 for the determination of energetics at the B3LYP/6-31G* level of theory

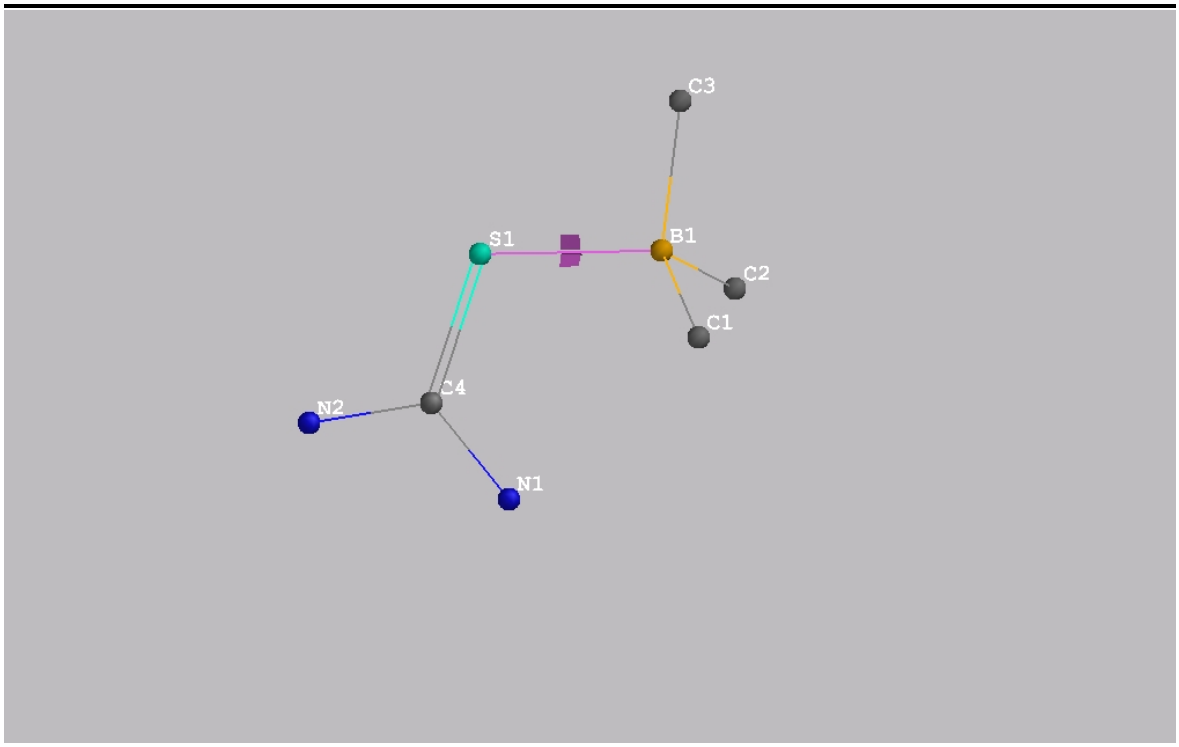

Figure 9.11 - HF/6-31G*-optimised adduct of tetramethylthiourea and BMe_3 for the determination of energetics at the B3LYP/6-31G* level of theory

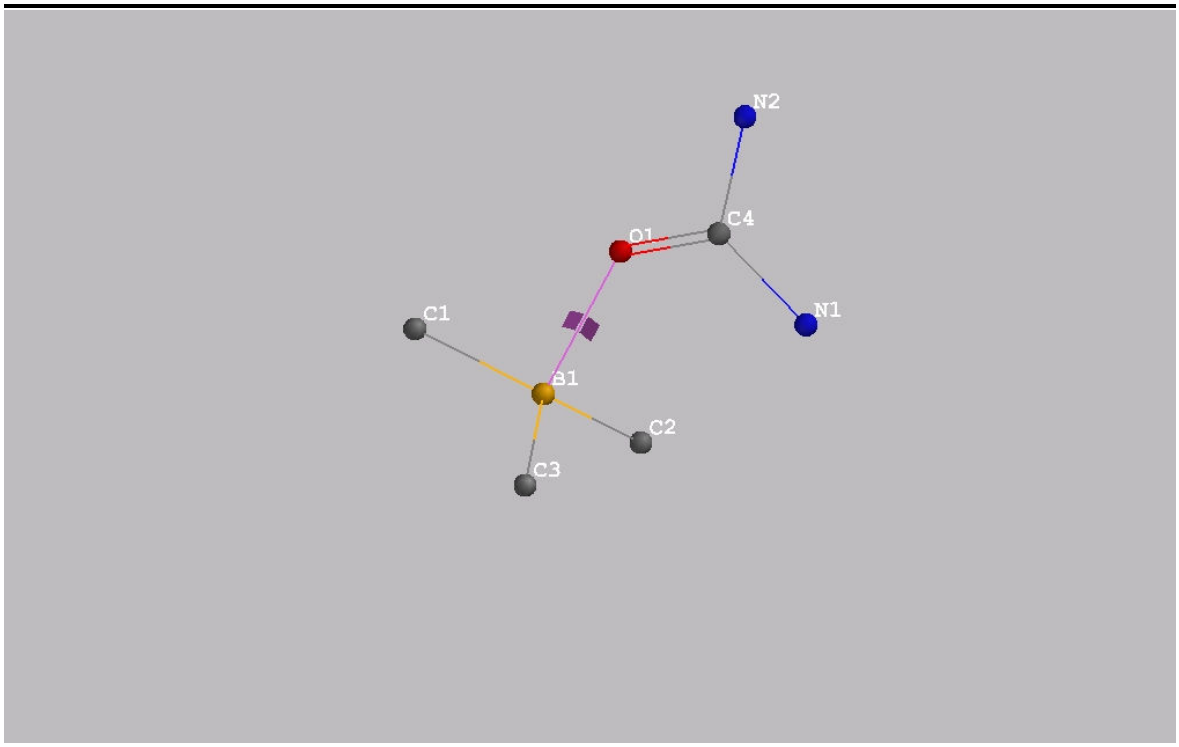

Figure 9.12 - HF/6-31G*-optimised adduct of tetramethylurea and BMe_3 for the determination of energetics at the B3LYP/6-31G* level of theory

[186] W. Janse van Rensburg, PhD Thesis